Math-for-industry
Education & Research Hub

ISSN2188-1200

IMI Workshop of the Joint Usage Research Projects

Mathematics for Innovation in Information and Communication Technology

Editors: Yutaka Jitsumatsu, Masayoshi Ohashi, Akio Hasegawa, Katsutoshi Shinohara, Shintaro Mori

九州大学マス·フォア·インダストリ研究所

MI Lecture Note Vol.100 : Kyushu University

IMI Workshop of the Joint Usage Research Projects

Mathematics for Innovation in Information and Communication Technology

Editors Yutaka Jitsumatsu, Masayoshi Ohashi, Akio Hasegawa,
Katsutoshi Shinohara, Shintaro Mori

About MI Lecture Note Series

The Math-for-Industry (MI) Lecture Note Series is the successor to the COE Lecture Notes, which were published for the 21st COE Program “Development of Dynamic Mathematics with High Functionality,” sponsored by Japan’s Ministry of Education, Culture, Sports, Science and Technology (MEXT) from 2003 to 2007. The MI Lecture Note Series has published the notes of lectures organized under the following two programs: “Training Program for Ph.D. and New Master’s Degree in Mathematics as Required by Industry,” adopted as a Support Program for Improving Graduate School Education by MEXT from 2007 to 2009; and “Education-and-Research Hub for Mathematics-for-Industry,” adopted as a Global COE Program by MEXT from 2008 to 2012.

In accordance with the establishment of the Institute of Mathematics for Industry (IMI) in April 2011 and the authorization of IMI’s Joint Research Center for Advanced and Fundamental Mathematics-for-Industry as a MEXT Joint Usage / Research Center in April 2013, hereafter the MI Lecture Notes Series will publish lecture notes and proceedings by worldwide researchers of MI to contribute to the development of MI.

October 2022
Kenji Kajiwara
Director, Institute of Mathematics for Industry

Mathematics for Innovation in Information and Communication Technology

MI Lecture Note Vol.100, Institute of Mathematics for Industry, Kyushu University
ISSN 2188-1200
Date of issue: March 19, 2025
Editors: Yutaka Jitsumatsu, Masayoshi Ohashi, Akio Hasegawa,
Katsutoshi Shinohara, Shintaro Mori
Publisher:
Institute of Mathematics for Industry, Kyushu University
Graduate School of Mathematics, Kyushu University
Motooka 744, Nishi-ku, Fukuoka, 819-0395, JAPAN
Tel +81-(0)92-802-4402, Fax +81-(0)92-802-4405
URL https://www.imi.kyushu-u.ac.jp/

Preface

This lecture note is a collection of slides presented at the workshop **"Mathematics for Innovation in Information and Communication Technology,"** held in Fukuoka, Japan, from September 25 to 27, 2024. The workshop was sponsored by the Institute of Mathematics for Industry (IMI), Kyushu University, and JSPS KAKENHI Grant Number JP23K26104.

The aim of this workshop was to provide a platform for both academic and industrial researchers to engage in discussions and exchange ideas on cutting-edge research in information and communication technology. Mathematics plays a crucial role in driving innovation by offering abstraction, simplification, and mathematical modeling to address real-world challenges.

The workshop featured 15 presentations.

On the first day, **Professor Shota Saito** discussed the guessing problem in information theory and its relationship with lossy data compression. **Professor Tad Matsumoto** examined decision-making problems in real-world communication systems from the perspective of network information theory, including the Slepian-Wolf coding problem and lossy coding with side information (Wyner-Ziv coding). **Dr. Lei Jiang** presented on Direction of Arrival (DoA) and Doppler frequency estimation. **Professor Christos Masouros, an IEEE ComSoc Lecturer for 2024-2025,** gave a talk on signal processing for Integrated Sensing and Communications (ISAC).

On the second day, **Professor Hidekazu Murata** reported the latest experimental results on collaborative wireless mobile terminals. **Dr. Jun Muramatsu** discussed the channel coding theorem from an information-theoretic perspective, emphasizing the key role of constrained random number generation. **Professor Yutaka Jitsumatsu** explored an ISAC problem and proposed a joint radar and communication system using Orthogonal Time-Frequency Space (OTFS) modulation signals. **Professor Brian Kurkoski** discussed applications of machine learning to communication receiver design. **Professor Hirosuke Yamamoto** presented his research on lossless coding methods, introducing two types of source coding: Almost Instantaneous Fixed-to-Variable (AIFV) codes and the Asymmetric Encoding-Decoding Scheme (AEDS).

On the third day, **Professor Masayoshi Ohashi** reported on the latest advancements in Gabor-Division Spread Spectrum (GDSS) systems. **Professor Osamu Muta** discussed a localization method using channel state information (CSI) from wireless LAN, aided by deep learning. **Professor Keigo Takeuchi** presented a mathematical analysis of efficient algorithms for compressed sensing (CS). **Professor Hamdi Joudeh** shared his recent findings on Joint Communication and Sensing (JCAS) from an information-theoretic perspective. **Dr. Boris Karanov** explored the application of deep learning to optical communication receiver design. Finally, **Professor Teruya Fujii** delivered a lecture on the grand design of a global-scale network connecting terrestrial and non-terrestrial networks while sharing the same frequency bands.

Over the course of three days, various aspects of information and communication technology were extensively discussed. I hope that all attendees will continue to collaborate and communicate, fostering future research advancements.

Organizing Committee Chair: Yutaka Jitsumatsu

Organizing Committee Members

Yutaka Jitsumatsu（Kyushu University/ Associate Professor)

Masayoshi Ohashi（Advanced Telecommunications Research Institute International (ATR)/ Collaborate Researcher）

Akio Hasegawa（Advanced Telecommunications Research Institute International (ATR) / Head）

Katsutoshi Shinohara（Hitotsubashi University / Associate Professor）

Shintaro Mori（Fukuoka University / Assistant Professor）


2024年度九州大学マス・フォア・インダストリ研究所　共同利用・共同研究　一般研究-研究集会(I)
参加無料
事前申込制
講演者
Teruya Fujii (SoftBank Corp.)
Yutaka Jitsumatsu (Kyushu University)
Hamdi Joudeh (Eindhoven University of Technology)
Boris Karanov (Eindhoven Univerisity of Technology)
Brian Kurkoski (JAIST)
Christos Masouros (University College London)
Hidekazu Murata (Yamaguchi University)
Osamu Muta (Kyushu University)
Masayoshi Ohashi (ATR)
Shota Saito (Gunma University)
Hirosuke Yamamoto (The University of Tokyo)
共催
九州大学マス・フォア・インダストリ研究所
科学研究費補助金　基盤研究(B)
「高速移動に伴う二重選択性通信路を介した通信及びセンシングの基礎理論構築」
組織委員
實松 豊 (九州大学)
大橋 正良 国際電気通信基礎技術研究所(ATR)
長谷川 晃朗 国際電気通信基礎技術研究所(ATR)
篠原 克寿 (一橋大学)
森 慎太郎 (福岡大学)
情報通信の技術革新のための基礎数理
Mathematics for Innovation in Information and Communication Technology
2024 9.25 wed → 27 fri
JR博多シティ10階会議室
ハイブリッド開催
E-mail:imikyoten@jimu.kyushu-u.ac.jp
https://joint.imi.kyushu-u.ac.jp/post-14984/
九州大学 KYUSHU UNIVERSITY
Institute of Mathematics for Industry Kyushu University
Joint Research Center for Advanced and Fundamental Mathematics-for-Industry
文部科学大臣認定「産業数学の先進的・基礎的共同研究拠点」
九州大学マス・フォア・インダストリ研究所

Program

Wednesday 25th, September 2024

13:00 Opening

13:10 – 14:10 Shota Saito (Gunma University)

Two Problems Under Logarithmic Loss: Soft Guessing and Lossy Source Coding

14:25 – 15:25 Tad Matsumoto (IMT-Atlantique, JAIST and University of Oulu (Emeritus))

Decision making via End-to-End Lossy Distributed Wireless Cooperative Networks
− A Distributed Hypothesis Testing based Formulation –

16:10 – 16:40 Lei Jiang (Tokyo Institute of Technology)

2D smoothing based recursive subspace and factor graph framework for high mobility geolocation and tracking; − With a duality consideration to joint Delay-Doppler estimation

16:55 – 17:55 Christos Masouros (University College London)

Physical Layer Technologies for Sustainable and Multi-functional Wireless Networks

Thursday 26th, September 2024

9:30-10:30 Hidekazu Murata (Yamaguchi University)

端末連携によって実現する新たな無線通信システム

Novel Wireless Communication System Realized by Mobile Terminal Collaboration (Japanese)

10:45 – 11:25 Jun Muramatsu (NTT Corporation)

Coding Theorems Based on Constrained-Random-Number Generators

13:00 – 14:00 Yutaka Jitsumatsu (Kyushu University)

Delay-Doppler Estimation for Joint Sensing and Communications

14:15 – 15:15 Brian Kurkoski (JAIST)

Designing communication receivers using machine learning techniques

15:30 – 16:30 Hirosuke Yamamoto (The University of Tokyo)

Lossless data compression coding schemes to replace Huffman and arithmetic coding

Friday 27th, September 2024

9:30 – 10:00 Masayoshi Ohashi (ATR)

Detection performance evaluation of Gabor-Division Spread Spectrum signals

10:00 – 10:30 Osamu Muta (Kyushu University)

Experimental Evaluations of Device-Free Localization Using Channel State Information in WLAN Systems

10:45 − 11:25 Keigo Takeuchi (Toyohashi University of Technology)

Comprehensive Comparison of Message-Passing Algorithms for Compressed Sensing

13:30 − 14:30 Hamdi Joudeh (Eindhoven University of Technology)

Some information-theoretic aspects of joint communication and sensing

14:45 – 15:15 Boris Karanov (Eindhoven University of Technology)

Low-complexity machine learning for optimal communication receivers

15:30 − 16:30 Teruya Fujii (SoftBank Corp.)

端末連携によって実現する新たな無線通信システム

―地上セルと上空セルの同一周波数共用―

Three-dimensional spatial cell configuration in mobile communications

― Sharing the same frequency between terrestrial and sky cells ― (Japanese)

Contents

Two Problems Under Logarithmic Loss: Soft Guessing and Lossy Source Coding

Shota Saito

Faculty of Informatics, Gunma University, Japan

Finite blocklength lossy source coding is essential to provide low-latency communications in modern 5G networks and beyond. Some theoretical results for finite blocklength lossy source coding under logarithmic loss are shown. Furthermore, the connection between soft guessing and lossy source coding under logarithmic loss is discussed.

Acknowledgment

This work was supported in part by JSPS KAKENHI Grant Numbers JP22K14254, JP23K11097, and JP23H00468.

References

[1] C. E. Shannon, "A Mathematical Theory of Communication," The Bell System Technical Journal, Vol. 27, pp. 379–423, 623–656, 1948.

[2] T. A. Courtade and R. D. Wesel, "Multiterminal source coding with an entropy-based distortion measure," 2011 IEEE ISIT, St. Petersburg, Russia, 2011, pp. 2040-2044.

[3] T. A. Courtade and T. Weissman, "Multiterminal Source Coding Under Logarithmic Loss," in IEEE Transactions on Information Theory, vol. 60, no. 1, pp. 740-761, Jan. 2014.

[4] Y. Y. Shkel and S. Verdú, "A Single-Shot Approach to Lossy Source Coding Under Logarithmic Loss," in IEEE Transactions on Information Theory, vol. 64, no. 1, pp. 129-147, Jan. 2018.

[5] I. Kontoyiannis and S. Verdú, "Optimal Lossless Data Compression: Non-Asymptotics and Asymptotics," in IEEE Transactions on Information Theory, vol. 60, no. 2, pp. 777-795, Feb. 2014.

[6] L. L. Campbell, "A coding theorem and Rényi's entropy," Information and Control, vol. 8, no. 4, pp. 423-429, Aug. 1965.

[7] S. Saito and T. Matsushima, "Non-Asymptotic Bounds of Cumulant Generating Function of Codeword Lengths in Variable-Length Lossy Compression," in IEEE Transactions on Information Theory, vol. 69, no. 4, pp. 2113-2119, April 2023.

[8] H. Wu and H. Joudeh, "Soft Guessing Under Logarithmic Loss," 2023 IEEE International Symposium on Information Theory (ISIT), Taipei, Taiwan, 2023, pp. 466-471.

[9] S. Saito, "An Upper Bound of Cumulant Generating Function of Codeword Lengths in Variable-Length Lossy Source Coding Under Logarithmic Loss," in 2024 International Symposium on Information Theory and Its Applications (ISITA2024), November 2024.

[10] E. Arikan and N. Merhav, "Guessing subject to distortion," in IEEE Transactions on Information Theory, vol. 44, no. 3, pp. 1041-1056, May 1998.

[11] S. Saito, “Soft guessing under log-loss distortion allowing errors," 2024 IEEE International Symposium on Information Theory (ISIT), Athens, Greece, 2024.

Two Problems Under Logarithmic Loss: Soft Guessing and Lossy Source Coding

Shota Saito
Faculty of Informatics, Gunma University

情報通信の技術革新のための基礎数理@JR博多シティ
25th, September, 2024

PART I

In modern 5G networks and beyond, finite blocklength lossy source coding is important to provide low-latency communications

Title of this workshop

No.3

情報通信の技術革新のための基礎数理

Information and Communication → 情報通信

Fundamental Mathematics → 基礎数理

A mathematical theory of communication

No.4

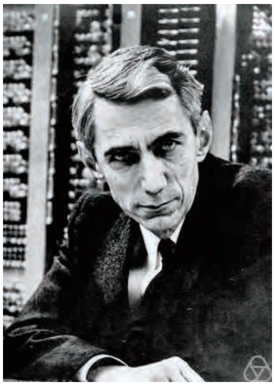

citation :
https://en.wikipedia.org/wiki/Claude_Shannon

In 1948, Shannon [1] proposed
a theoretical framework
that uses **mathematical tools**
to **model and analyze**
digital communication systems.

[1] C. E. Shannon, "A Mathematical Theory of Communication," *The Bell System Technical Journal*, Vol. 27, pp. 379–423, 623–656, 1948.

Schematic diagram of a general communication system

No.5

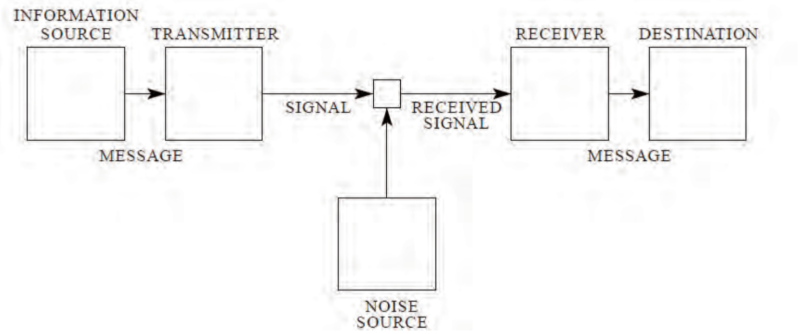

Fig. 1 in [1]

[1] C. E. Shannon, "A Mathematical Theory of Communication," *The Bell System Technical Journal*, Vol. 27, pp. 379–423, 623–656, 1948.

Schematic diagram of a general communication system

No.6

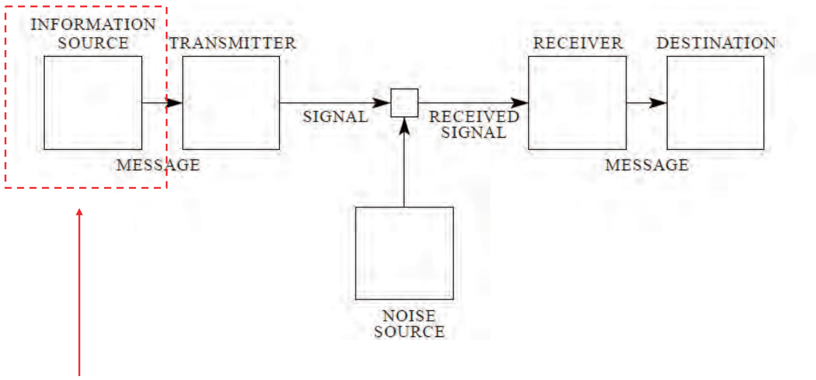

The **information source** produces a message.

Schematic diagram of a general communication system

No.7

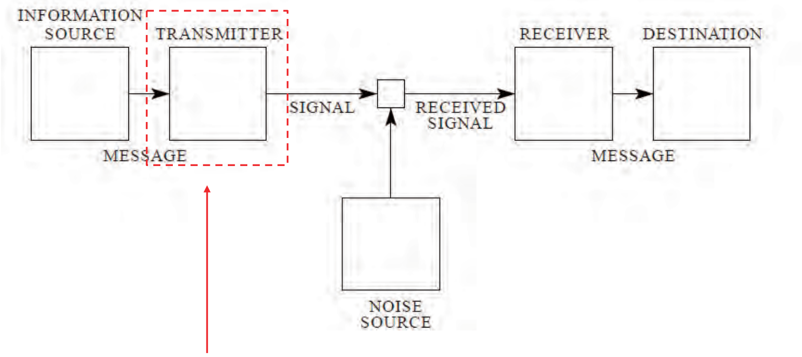

The **transmitter** encodes the message into a form capable of being sent as a signal.

Schematic diagram of a general communication system

No.8

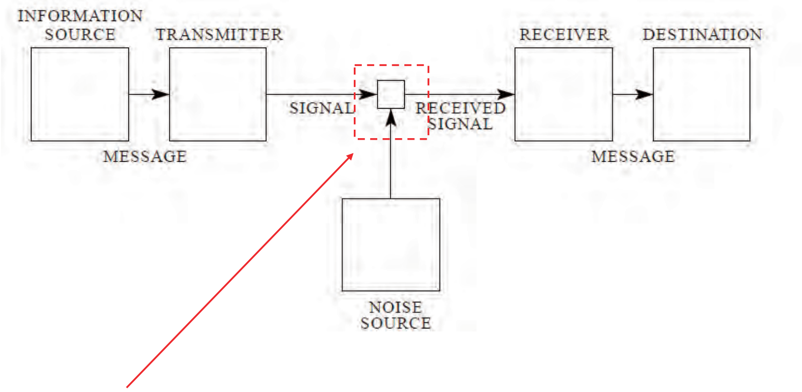

The **channel** is the medium through which the signal passes.

Schematic diagram of a general communication system

No.9

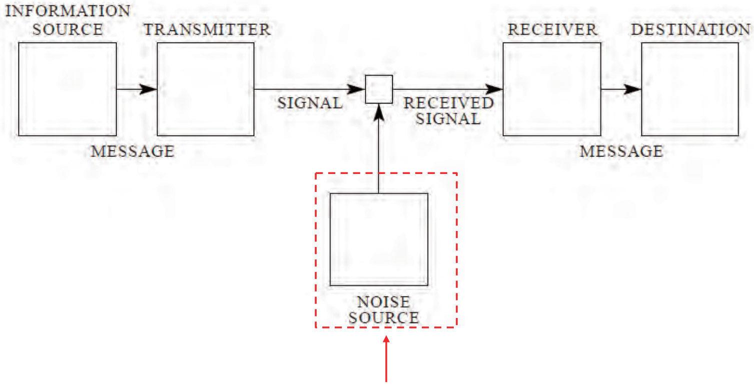

The **noise source** represents the corruptions that afflict the signal on its way to the receiver.

Schematic diagram of a general communication system

No.10

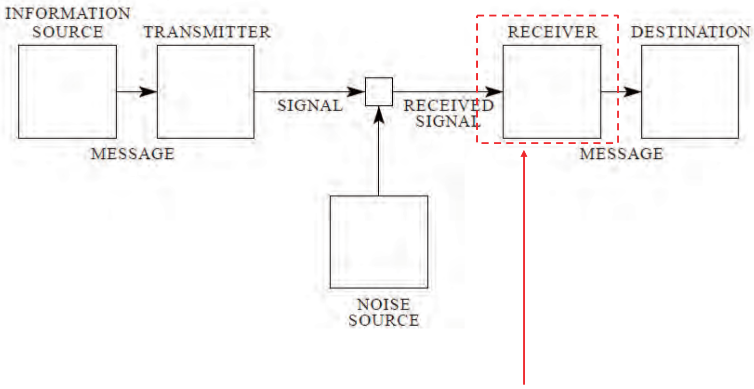

The **receiver** decodes the message.

Schematic diagram of a general communication system

No.11

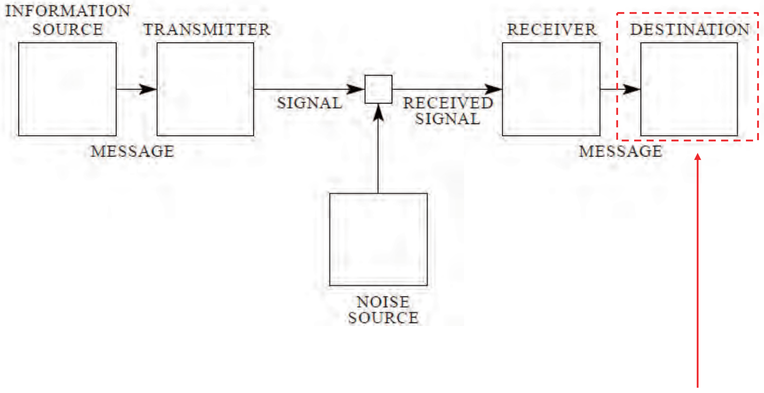

The **destination** is the recipient of the message.

Schematic diagram of a general communication system

No.12

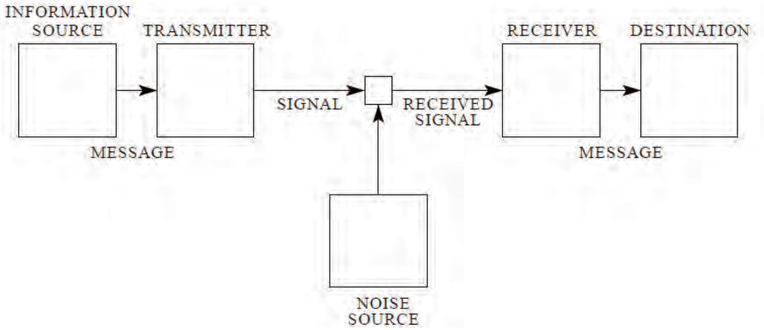

A key component of such a system is **source coding** (also known as **data compression**)

Source coding

No.13

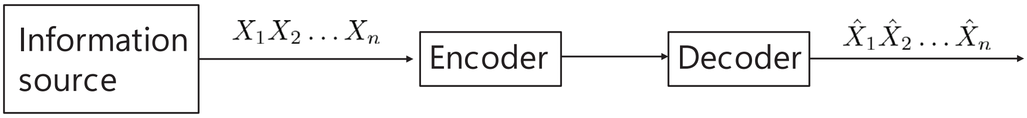

- An information source produces a sequence $X_1X_2\ldots X_n$
- An encoder compresses the data
- A decoder represents $X_1X_2\ldots X_n$ by an estimate $\hat{X}_1\hat{X}_2\ldots\hat{X}_n$

Shannon investigated the case where the **blocklength of the source sequence to be compressed tends to infinity** (i.e., $n \to \infty$).

Finite blocklength source coding

No.14

In modern 5G networks and beyond, **low-latency** is desired.

However, Shannon's coding theorems cannot provide exact theoretical benchmarks for low-latency communication because the assumption that $n \to \infty$ leads to undesired arbitrarily large latency.

To tackle this problem, **finite blocklength source coding** is essential.

Simple notation

No.15

In finite blocklength source coding, n does not play an important role. Hence, we use the following simple notation.

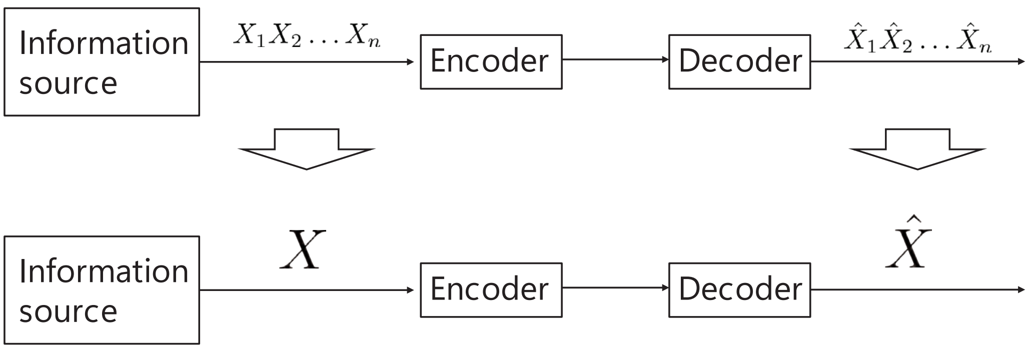

Lossless source coding vs. lossy source coding

No.16

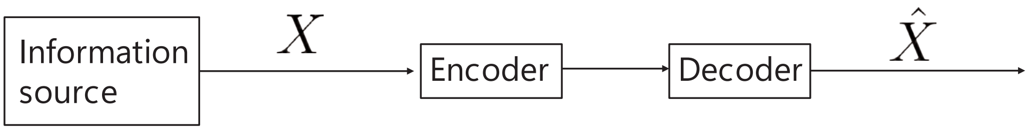

Source coding
- Lossless source coding: $\widehat{X}$ is the same as X
- Lossy source coding: $\widehat{X}$ is **not** the same as X

Practical image and video compression systems usually tolerate some imperfection between $\widehat{X}$ and X.

In this talk, we focus on lossy source coding.

PART II

Logarithmic loss in lossy source coding

Distortion measure

No.18

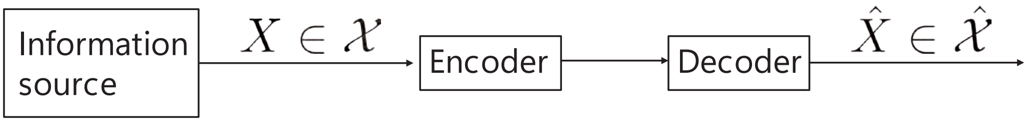

Definition

A **distortion measure**

$$d : \mathcal{X} \times \widehat{\mathcal{X}} \to [0, \infty)$$

evaluates the difference between a source symbol X and a reproduction symbol $\hat{X}$.

Common distortion measures

No.19

Hamming distortion: $$d(x, \hat{x}) = \begin{cases} 1 & (x \neq \hat{x}) \\ 0 & (x = \hat{x}) \end{cases}$$

Squared-error distortion: $$d(x, \hat{x}) = (x - \hat{x})^2$$

For these distortion measures, $\hat{x}$ is a **deterministic value**.

Example

No.20

Estimation: deterministic value

Example

No.21

Estimation: deterministic value

Estimation: **probability distribution**

Rain: 85%

Cloudy: 15%

Sunny: 0%

Soft reconstruction for lossy source coding

No.22

In the following, we assume that $\mathcal{X}$ is a finite set.
The cardinality of $\mathcal{X}$ is denoted by $|\mathcal{X}|$.

Let $\mathcal{P}(\mathcal{X})$ be a set of all probability distributions on $\mathcal{X}$, i.e.,

$$\mathcal{P}(\mathcal{X}) = \left\{ (p_1, \ldots, p_{|\mathcal{X}|}) : p_1 \geq 0, \ldots, p_{|\mathcal{X}|} \geq 0, \sum_{i=1}^{|\mathcal{X}|} p_i = 1 \right\}$$

The reconstruction alphabet is $\mathcal{P}(\mathcal{X})$. In other words,

$$\hat{\mathcal{X}} = \mathcal{P}(\mathcal{X})$$

The reconstructions are allowed to be **soft**.

Logarithmic loss

No.23

Definition

The **logarithmic loss distortion** (log-loss distortion) between $x \in \mathcal{X}$ and its reconstruction $\hat{P} \in \mathcal{P}(\mathcal{X})$ is defined by

$$d(x, \hat{P}) = \log_2 \frac{1}{\hat{P}(x)}$$

Example → next slide

Example

No.24

$$\mathcal{X} = \{1, 2, 3, 4\}$$

$1 \in \mathcal{X}$ → Encoder → Decoder → $\hat{P} \in \hat{\mathcal{X}} = \mathcal{P}(\mathcal{X})$

$\hat{P}$

x	1	2	3	4
Prob.	**1/8**	1/8	1/4	1/2

$$d(1, \hat{P}) = \log_2 \frac{1}{\hat{P}(1)}$$

$$= \log_2 \frac{1}{1/8} = 3$$

Example

No.25

$$\mathcal{X} = \{1, 2, 3, 4\}$$

$1 \in \mathcal{X} \longrightarrow$ Encoder $\longrightarrow$ Decoder $\longrightarrow \hat{P} \in \hat{\mathcal{X}} = \mathcal{P}(\mathcal{X})$

$\hat{P}$

x	1	2	3	4
Prob.	**1/2**	1/4	1/8	1/8

$$d(1, \hat{P}) = \log_2 \frac{1}{\hat{P}(1)}$$

$$= \log_2 \frac{1}{1/2} = 1$$

Example

No.26

$$\mathcal{X} = \{1, 2, 3, 4\}$$

$1 \in \mathcal{X} \longrightarrow$ Encoder $\longrightarrow$ Decoder $\longrightarrow \hat{P} \in \hat{\mathcal{X}} = \mathcal{P}(\mathcal{X})$

$\hat{P}$

x	1	2	3	4
Prob.	**1**	0	0	0

$$d(1, \hat{P}) = \log_2 \frac{1}{\hat{P}(1)}$$

$$= \log_2 1 = 0$$

Some remarks on logarithmic loss

No.27

- The logarithmic loss was introduced in the context of lossy source coding by Courtade and Wesel [2] and Courtade and Weissman [3].

- The logarithmic loss is widely used in machine learning.

[2] T. A. Courtade and R. D. Wesel, "Multiterminal source coding with an entropy-based distortion measure," *2011 IEEE ISIT*, St. Petersburg, Russia, 2011, pp. 2040-2044.

[3] T. A. Courtade and T. Weissman, "Multiterminal Source Coding Under Logarithmic Loss," *in IEEE Transactions on Information Theory*, vol. 60, no. 1, pp. 740-761, Jan. 2014.

PART III

Achievability and converse bounds for finite blocklength lossy source coding under logarithmic loss

Setup

No.29

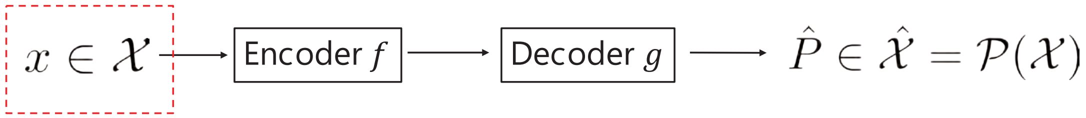

- Let $\mathcal{X} = \{1, 2, \ldots, |\mathcal{X}|\}$
- A random variable X takes values in $\mathcal{X}$
- A probability distribution of X is denoted by P_X
- We assume that $P_X(a) \geq P_X(b)$ for $a \leq b$

Setup

No.30

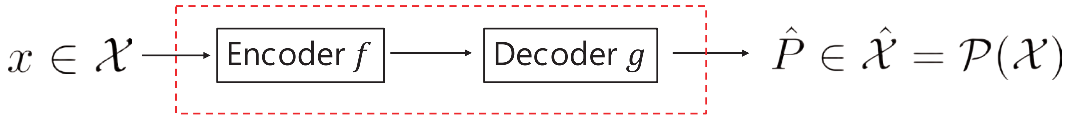

Definition

A variable-length lossy source code is a pair of mappings

$$f : \mathcal{X} \to \{0,1\}^\star, \quad g : f(\mathcal{X}) \to \mathcal{P}(\mathcal{X})$$

where $\{0,1\}^\star$ denotes a finite-length binary strings including an empty string $\varnothing$, i.e.,

$$\{0,1\}^\star = \{\varnothing, 0, 1, 00, 01, 10, 11, 000, \ldots\}$$

Setup

No.31

Definition

If (f, g) is such that no codeword in $f(\mathcal{X})$ is a prefix of any another codeword in $f(\mathcal{X})$, we call (f, g) **prefix free**.

Example

$$\mathcal{X} = \{1, 2, 3, 4\}$$
$$f(1) = 0$$
$$f(2) = 10$$
$$f(3) = 110$$
$$f(4) = 111$$

⇨ $f(\mathcal{X}) = \{0, 10, 110, 111\}$

prefix free

Fundamental limit

No.32

Definition

For $x \in \mathcal{X}$, let $\ell(f(x))$ denote the length of $f(x)$.
A variable-length lossy source code (f, g) is an $(\boldsymbol{L}, \boldsymbol{D})$ **code** if

$$\mathbb{E}[\ell(f(X))] \le L$$

and

$$d(x, g(f(x))) \le D, \quad \forall x \in \mathcal{X}$$

Definition

$$L^*(D) := \inf\{L : \exists \ (L, D) \text{ code}\}$$
$$L_{\mathrm{p}}^*(D) := \inf\{L : \exists \text{ prefix-free } (L, D) \text{ code}\}$$

Converse theorem

No.33

Theorem [4]

$$L^*(D) \geq H(X) - D - \log(\lfloor \log |\mathcal{X}| \rfloor + 1)$$
$$L^*_{\mathrm{p}}(D) \geq H(X) - D$$

where $H(X)$ is the Shannon entropy

$$H(X) = -\sum_{x \in \mathcal{X}} P_X(x) \log P_X(x)$$

[4] Y. Y. Shkel and S. Verdú, "A Single-Shot Approach to Lossy Source Coding Under Logarithmic Loss," in *IEEE Transactions on Information Theory*, vol. 64, no. 1, pp. 129-147, Jan. 2018

Proof of converse theorem

No.34

We only show the proof of $L^*(D)$.

For an arbitrary (L, D) code, we have the following lemma.

Lemma 1

$$\sum_{x \in \mathcal{X}} \exp\{-\ell(f(x)) - d(x, g(f(x)))\} \leq \lfloor \log |\mathcal{X}| \rfloor + 1$$

Remark

Throughout, $\log = \log_2$ and $\exp(a) = 2^a$

Proof of converse theorem

No.35

Proof of Lemma 1:

$$\sum_{x\in\mathcal{X}} \exp\{-\ell(f(x)) - d(x, g(f(x)))\}$$

$$= \sum_{m\in f(\mathcal{X})} \sum_{x:f(x)=m} \exp\{-\ell(m) - d(x, g(m))\}$$

$$= \sum_{m\in f(\mathcal{X})} \exp\{-\ell(m)\} \sum_{x:f(x)=m} \exp\{-d(x, g(m))\}$$

$$= \sum_{m\in f(\mathcal{X})} \exp\{-\ell(m)\} \sum_{x:f(x)=m} \hat{P}_m(x)$$

$$\leq \sum_{m\in f(\mathcal{X})} \exp\{-\ell(m)\} \leq \lfloor \log |\mathcal{X}| \rfloor + 1 \quad \blacksquare$$

Definition of log-loss

$\hat{P}_m(\cdot) = g(m)$

Some calculation

Proof of converse theorem

No.36

Now, consider an arbitrary (L, D) code. We have

$$\exp\{-D\} \sum_{x\in\mathcal{X}} \exp\{-\ell(f(x))\}$$

$$= \sum_{x\in\mathcal{X}} \exp\{-\ell(f(x)) - D\}$$

$$\leq \sum_{x\in\mathcal{X}} \exp\{-\ell(f(x)) - d(x, g(f(x)))\}$$

$$\leq \lfloor \log |\mathcal{X}| \rfloor + 1$$

Lemma 1

Proof of converse theorem

No.37

Let $Q_X(x)$ be defined by $Q_X(x) := \dfrac{\exp\{-\ell(f(x))\}}{\sum_{x'\in\mathcal{X}} \exp\{-\ell(f(x'))\}}$

Then,

$$
\begin{aligned}
&\mathbb{E}[\ell(f(X))] - H(X) \\
&= \sum_{x\in\mathcal{X}} P_X(x) \log \frac{P_X(x)}{\exp\{-\ell(f(x))\}} \\
&= \sum_{x\in\mathcal{X}} P_X(x) \log \frac{P_X(x)}{Q_X(x)} - \log \sum_{x'\in\mathcal{X}} \exp\{-\ell(f(x')\} \\
&\geq \mathrm{KL}(P_X \| Q_X) - \log(\lfloor \log|\mathcal{X}| \rfloor + 1) - D \\
&\geq -\log(\lfloor \log|\mathcal{X}| \rfloor + 1) - D \quad \blacksquare
\end{aligned}
$$

Previous slide

Achievability theorem

No.38

Theorem [4]

$$L^*(D) \leq H(Z)$$

$$L^*_{\mathrm{p}}(D) \leq H(Z) + 1$$

where Z is defined by

$$Z = \left\lceil \frac{X}{\lfloor \exp(D) \rfloor} \right\rceil$$

We explain the proof of this upper bound.

[4] Y. Y. Shkel and S. Verdú, "A Single-Shot Approach to Lossy Source Coding Under Logarithmic Loss," in *IEEE Transactions on Information Theory*, vol. 64, no. 1, pp. 129-147, Jan. 2018

Proof of achievability theorem

First, we introduce the following lemma.

Lemma 2

For any $D \geq 0, \hat{P} \in \mathcal{P}(\mathcal{X})$, we have $|\mathcal{S}_D(\hat{P})| \leq \lfloor \exp(D) \rfloor$,
where

$$\mathcal{S}_D(\hat{P}) := \{x \in \mathcal{X} : d(x, \hat{P}) \leq D\}$$

Proof:
Since $x \in \mathcal{S}_D(\hat{P})$ implies $\hat{P}(x) \geq \exp(-D)$,

$$1 \geq \sum_{x \in \mathcal{S}_D(\hat{P})} \hat{P}(x) \geq \sum_{x \in \mathcal{S}_D(\hat{P})} \exp\{-D\} = |\mathcal{S}_D(\hat{P})| \exp\{-D\} \quad \blacksquare$$

Proof of achievability theorem

Let $L > 0$.
For $x \in \mathcal{X} = \{1, 2, \ldots, |\mathcal{X}|\}$, we define the encoder $f_L^\star$ as follows.

$$f_L^\star(x) = \begin{cases} \varnothing, & \left\lceil \frac{x}{L} \right\rceil = 1, \\ 0, & \left\lceil \frac{x}{L} \right\rceil = 2, \\ 1, & \left\lceil \frac{x}{L} \right\rceil = 3, \\ 00, & \left\lceil \frac{x}{L} \right\rceil = 4, \\ 01, & \left\lceil \frac{x}{L} \right\rceil = 5, \\ \cdots \end{cases}$$

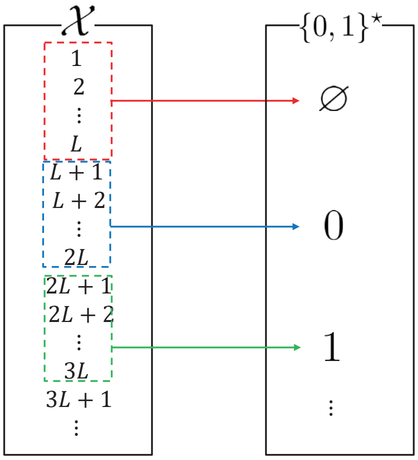

Proof of achievability theorem

No.41

Next, we define the decoder $g_L^\star$ as follows.

$$g_L^\star(m) = \begin{cases} \hat{P}_1, & m = \varnothing, \\ \hat{P}_2, & m = 0, \\ \hat{P}_3, & m = 1, \\ \hat{P}_4, & m = 00, \\ \hat{P}_5, & m = 01, \\ \dots \end{cases} \quad \text{where} \quad \hat{P}_i(x) = \begin{cases} \frac{1}{L}, & (i-1)L+1 \leq x \leq iL, \\ 0, & \text{otherwise} \end{cases}$$

Proof of achievability theorem

No.42

Now, consider the code $\left(f^\star_{\lfloor \exp(D) \rfloor}, g^\star_{\lfloor \exp(D) \rfloor}\right)$

For any $x \in \mathcal{X}$, we have

$$\begin{aligned} d(x, g^\star_{\lfloor \exp(D) \rfloor}(f^\star_{\lfloor \exp(D) \rfloor}(x))) &= \log \lfloor \exp(D) \rfloor \\ &\leq \log \exp(D) \\ &= D \end{aligned}$$

Hence, $\left(f^\star_{\lfloor \exp(D) \rfloor}, g^\star_{\lfloor \exp(D) \rfloor}\right)$ is an (L, D) code for some L.

Proof of achievability theorem

No.43

Moreover, we see that the code $\left(f^\star_{\lfloor \exp(D) \rfloor}, g^\star_{\lfloor \exp(D) \rfloor}\right)$ is optimal in the average codeword length sense because

Lemma 2 implies no codeword can cover more than $\lfloor \exp(D) \rfloor$ elements

and

the encoder $f_L^\star$ assigns shortest strings to the most likely elements.

Proof of achievability theorem

No.44

$$
\begin{aligned}
L^*(D) &= \mathbb{E}[\ell(f^\star_{\lfloor \exp(D) \rfloor}(X))] \\
&= \sum_{x \in \mathcal{X}} P_X(x) \ell(f^\star_{\lfloor \exp(D) \rfloor}(x)) \\
&= (P_X(1) + \cdots + P_X(\lfloor \exp(D) \rfloor))\ell(\varnothing) \\
&\quad + (P_X(\lfloor \exp(D) \rfloor + 1) + \cdots + P_X(2\lfloor \exp(D) \rfloor))\ell(0) \\
&\quad + \cdots \\
&= P_Z(1)\ell(\varnothing) + P_Z(2)\ell(0) + \cdots \\
&\leq H(Z)
\end{aligned}
$$

$$Z = \left\lceil \frac{X}{\lfloor \exp(D) \rfloor} \right\rceil$$

where the final inequality follows from Theorem 2 of [5] ■

[5] I. Kontoyiannis and S. Verdú, "Optimal Lossless Data Compression: Non-Asymptotics and Asymptotics," in *IEEE Transactions on Information Theory*, vol. 60, no. 2, pp. 777-795, Feb. 2014,

Cumulant generating function of codeword lengths

No.45

So far, we have considered the average codeword length:

$$\mathbb{E}[\ell(f(X))]$$

In some applications, we may want to impose more penalty for longer codewords.

For this purpose, we can use a **cumulant generating function of codeword lengths**, which is defied as

$$\frac{1}{\rho} \log \mathbb{E}[\exp\{\rho \ell(f(X))\}]$$

Remarks

No.46

- By using L'Hôpital's theorem, we have

$$\lim_{\rho \to 0} \frac{1}{\rho} \log \mathbb{E}[\exp\{\rho \ell(f(X))\}] = \mathbb{E}[\ell(f(X))]$$

$$\lim_{\rho \to \infty} \frac{1}{\rho} \log \mathbb{E}[\exp\{\rho \ell(f(X))\}] = \max_{x \in \mathcal{X}} \ell(f(x)))$$

- We can control the contribution of the longer codewords via a free parameter ρ in the cumulant generating function; if we increase the value of ρ, we impose a more severe penalty for longer codewords.

Remarks

No.47

- Campbell [6] first proposed the cumulant generating function of codeword lengths for variable-length lossless source coding.
- Summary of variable-length source coding under the cumulant generating function of codeword lengths
  → see, e.g., [7].

[6] L. L. Campbell, "A coding theorem and Rényi's entropy," Information and Control, vol. 8, no. 4, pp. 423-429, Aug. 1965.

[7] S. Saito and T. Matsushima, "Non-Asymptotic Bounds of Cumulant Generating Function of Codeword Lengths in Variable-Length Lossy Compression," in *IEEE Transactions on Information Theory*, vol. 69, no. 4, pp. 2113-2119, April 2023.

Fundamental limit

No.48

Definition

A variable-length lossy source code (f, g) is an $(\boldsymbol{\Lambda}, \boldsymbol{D}, \boldsymbol{\rho})$ **code** if

$$\frac{1}{\rho} \log \mathbb{E}[\exp\{\rho \ell(f(X))\}] \leq \Lambda$$

and

$$d(x, g(f(x))) \leq D, \quad \forall x \in \mathcal{X}$$

Definition

$$\Lambda^*(D, \rho) := \inf\{\Lambda : \exists\ (\Lambda, D, \rho) \text{ code}\}$$

Converse and achievability bounds
No.49

Theorem [8]

$$\Lambda^*(D,\rho) \geq H_{\frac{1}{1+\rho}}(X) - \log\lfloor \exp(D) \rfloor - \log(1+\log|\mathcal{X}|) - 1$$

$$\Lambda^*(D,\rho) \leq \frac{1}{\rho}\log\left[1 + 2^{\rho}\exp\left(\rho H_{\frac{1}{1+\rho}}(X) - \rho\log\lfloor\exp(D)\rfloor\right)\right]$$

where $H_\alpha(X)$ is the Rényi entropy of order α:

$$H_\alpha(X) := \frac{1}{1-\alpha}\log\sum_{x\in\mathcal{X}}[P_X(x)]^\alpha$$

[8] H. Wu and H. Joudeh, "Soft Guessing Under Logarithmic Loss," *2023 IEEE International Symposium on Information Theory (ISIT)*, Taipei, Taiwan, 2023, pp. 466-471

Remarks
No.50

- Saito [9] derived the following achievability bound:

$$\Lambda^*(D,\rho) \leq H_{\frac{1}{1+\rho}}(Z)$$

where Z is defined by $Z = \left\lceil \frac{X}{\lfloor\exp(D)\rfloor} \right\rceil$

- For some cases, the above upper bound is tighter than that in [8].

[9] S. Saito, "An Upper Bound of Cumulant Generating Function of Codeword Lengths in Variable-Length Lossy Source Coding Under Logarithmic Loss," in *2024 International Symposium on Information Theory and Its Applications (ISITA2024)*, November 2024.

PART IV

Soft guessing
under logarithmic loss

Example

No.52

Suppose a malicious person enter the password many times and try to guess the password.

How many time does he enter the password until he correctly guess the password?

Guessing

No.53

In 1994, Massey pioneered the information-theoretic study on the problem of guessing and showed that the **average number of guesses** is characterized by the **Shannon entropy**

Two years later, Arikan proved that the **guessing moment** is characterized by the **Rényi entropy**

Since then, the problem of guessing has been studied in various contexts.

Guessing

No.54

- **guessing subject to distortion**
- guessing allowing errors,
- guessing under source uncertainty,
- joint source-channel coding and guessing,
- guessing via an unreliable oracle,
- guessing with limited memory,
- multi-agent guesswork,
- guesswork of hash functions,
- multi-user guesswork,
- universal randomized guessing,
- guessing individual sequences,
- guesses transmitted via a noisy channel,

and so on.

Arikan & Merhav [10] first proposed.

Recently, Wu & Joudeh [8] and Saito [11] investigated **soft guessing**.

[8] H. Wu and H. Joudeh, "Soft Guessing Under Logarithmic Loss," *2023 IEEE International Symposium on Information Theory (ISIT)*, Taipei, Taiwan, 2023, pp. 466-471
[10] E. Arikan and N. Merhav, "Guessing subject to distortion," in *IEEE Transactions on Information Theory*, vol. 44, no. 3, pp. 1041-1056, May 1998
[11] S. Saito, "Soft guessing under log-loss distortion allowing errors," *2024 IEEE International Symposium on Information Theory (ISIT)*, Athens, Greece, 2024.

Soft guessing

No.55

Suppose Alice has $x \in \mathcal{X}$, which is a realization of a random variable X.

$$X = x$$

Bob, who does not know x and wants to guess it, has his **soft guesses** of x as follows:

$$\hat{P} = (\hat{P}_1, \hat{P}_2, \ldots, \hat{P}_N), \quad \hat{P}_i \in \mathcal{P}(\mathcal{X}) \ (i = 1, 2, \ldots, N)$$

Soft guessing

No.56

Let $D \geq 0$ be a predetermined logarithmic loss level

Bob shows $\hat{P}_1$ to Alice and ask "Is $d(x, \hat{P}_1) \leq D$?"

⇩

Alice calculates $d(x, \hat{P}_1)$, where $d(x, \hat{P}) = \log_2 \dfrac{1}{\hat{P}(x)}$

⇩

If $d(x, \hat{P}_1) > D$, then Alice answers "No."

⇩

continue

⇩

Soft guessing

No.57

Next, Bob shows $\hat{P}_2$ to Alice and ask "Is $d(x, \hat{P}_2) \leq D$?"

⇩

Alice calculates $d(x, \hat{P}_2)$, where $d(x, \hat{P}) = \log_2 \frac{1}{\hat{P}(x)}$

⇩

If $d(x, \hat{P}_2) \leq D$, then Alice answers "Yes!"

⇩

End

Setup

No.58

- We assume $\mathcal{X} = \{1, 2, \ldots, |\mathcal{X}|\}$ and $P_X(1) \geq P_X(2) \geq \cdots \geq P_X(|\mathcal{X}|) > 0$.
- For some integer N, a **guessing strategy** $\mathcal{G}$ is defined by

$$\mathcal{G} = (\hat{P}_1, \hat{P}_2, \ldots, \hat{P}_N), \quad \hat{P}_i \in \mathcal{P}(\mathcal{X}) \ (i = 1, 2, \ldots, N)$$

- $D \geq 0$ is a predetermined logarithmic loss level.
- We consider a ***D*-admissible guessing strategy**:

Definition

If $\mathbb{P}[d(X, \hat{P}_j) \leq D \text{ for some } j] = 1$, then the guessing strategy is called D-admissible. D-admissible guessing strategy is denoted by $\mathcal{G}(D)$.

Setup

No.59

- When $X = x$, for a D-admissible guessing strategy $\mathcal{G}(D)$, the guessing continues until $d(x, \hat{P}_j) \leq D$ at the j-th step ($j = 1, 2, \ldots, N$).
- The **guessing function** $G(x)$ induced by the D-admissible guessing strategy $\mathcal{G}(D)$ is the minimum index j for which $d(x, \hat{P}_j) \leq D$.
- In other words, the guessing function $G(x)$ is the number of guesses required by the D-admissible guessing strategy $\mathcal{G}(D)$ when $X = x$.

Fundamental limit

No.60

Definition

For $D \geq 0$ and $\rho > 0$, the **minimal ρ-th guessing moment** is defined by

$$M^\star(D, \rho) := \min_{\mathcal{G}(D)} \mathbb{E}[G(X)^\rho]$$

Converse and achievability bounds

No.61

Theorem [8]

$$M^\star(D,\rho) \geq (1+\log|\mathcal{X}|)^{-\rho} \exp\left\{\rho H_{\frac{1}{1+\rho}}(X) - \rho \log\lfloor \exp(D)\rfloor\right\}$$

$$M^\star(D,\rho) \leq 1 + 2^{\rho} \exp\left\{\rho H_{\frac{1}{1+\rho}}(X) - \rho \log\lfloor \exp(D)\rfloor\right\}$$

We show only the proof of the achievability bound (upper bound) and consider the connection between guessing and source coding.

[8] H. Wu and H. Joudeh, "Soft Guessing Under Logarithmic Loss," *2023 IEEE International Symposium on Information Theory (ISIT)*, Taipei, Taiwan, 2023, pp. 466-471

Proof of the achievability bound

No.62

Let $N = \left\lceil \frac{|\mathcal{X}|}{\lfloor \exp(D) \rfloor} \right\rceil$ and we construct the guessing strategy $\mathcal{G}^*$ as follows:

$$\mathcal{G}^* = (\hat{P}_1^*, \hat{P}_2^*, \ldots, \hat{P}_N^*), \quad \hat{P}_i^* \in \mathcal{P}(\mathcal{X}) \ (i = 1, 2, \ldots, N)$$

where for $i = 1, 2, \ldots, N-1$,

$$\hat{P}_i^*(x) := \begin{cases} \frac{1}{\lfloor \exp(D) \rfloor}, & (i-1)\lfloor \exp(D) \rfloor + 1 \leq x \leq i\lfloor \exp(D) \rfloor, \\ 0, & \text{otherwise} \end{cases}$$

and

$$\hat{P}_N^*(x) := \begin{cases} \frac{1}{|\mathcal{X}| - (N-1)\lfloor \exp(D) \rfloor}, & (N-1)\lfloor \exp(D) \rfloor + 1 \leq x \leq |\mathcal{X}|, \\ 0, & \text{otherwise} \end{cases}$$

Proof of the achievability bound

No.63

$$\mathcal{X} = \{1, 2, \ldots, |\mathcal{X}|\} \quad L := \lfloor \exp(D) \rfloor \quad N := \lceil |\mathcal{X}|/L \rceil$$

$1\ 2\ \cdots\ L$ | $L+1\ L+2\ \cdots\ 2L$ | $\cdots$ | $(N-1)L+1\ \ (N-1)L+2\ \cdots |\mathcal{X}|$

$i = 1, 2, \ldots, N-1$

$$\hat{P}_i^*(x) = \begin{cases} \frac{1}{L}, & (i-1)L+1 \leq x \leq iL, \\ 0, & \text{otherwise} \end{cases}$$

$$\hat{P}_N^*(x) = \begin{cases} \frac{1}{|\mathcal{X}|-(N-1)L}, & (N-1)L+1 \leq x \leq |\mathcal{X}|, \\ 0, & \text{otherwise} \end{cases}$$

Proof of the achievability bound

No.64

The guessing strategy $\mathcal{G}^*$ is D-admissible because for any $x \in \mathcal{X}$, there exists $\hat{P}^*{}_j$ such that

$$\begin{aligned} d(x, \hat{P}_j^*) &= \log \frac{1}{\hat{P}_j^*(x)} \\ &= \log \lfloor \exp(D) \rfloor \\ &\leq \log \exp(D) \\ &= D \end{aligned}$$

Proof of the achievability bound

No.65

Moreover, the guessing strategy $\mathcal{G}^*$ is optimal soft guessing strategy because

Lemma 2 implies no soft guess can cover more than $\lfloor \exp(D) \rfloor$ elements

and

higher probability elements are assigned shorter guessing orders.

Proof of the achievability bound

No.66

The guessing function $G^*(x)$ induced by the guessing strategy $\mathcal{G}^*$ is given by

$$G^*(x) = \left\lceil \frac{x}{\lfloor \exp(D) \rfloor} \right\rceil$$

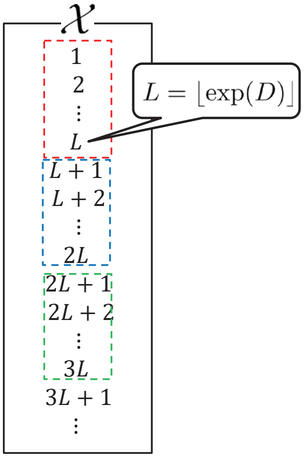

Finally, some calculation yields

$$\mathbb{E}[G^*(X)^\rho] \leq 1 + 2^\rho \exp\left\{\rho H_{\frac{1}{1+\rho}}(X) - \rho \log \lfloor \exp(D) \rfloor \right\}$$

and we complete the proof. ■

Remark

No.67

The soft guessing [8] was recently extended to soft guessing allowing errors by Saito [11].

[8] H. Wu and H. Joudeh, "Soft Guessing Under Logarithmic Loss," *2023 IEEE International Symposium on Information Theory (ISIT)*, Taipei, Taiwan, 2023, pp. 466-471

[11] S. Saito, “Soft guessing under log-loss distortion allowing errors," *2024 IEEE International Symposium on Information Theory (ISIT)*, Athens, Greece, 2024.

Summary

Summary

No.69

Finite blocklength lossy source coding is essential to provide low-latency communications in modern 5G networks and beyond.

Some theoretical results for finite blocklength lossy source coding under logarithmic loss were shown.

Moreover, the connection between soft guessing and lossy source coding under logarithmic loss were discussed.

Decision making via End-to-End Lossy Distributed Wireless Cooperative Networks

- A Distributed Hypothesis Testing based Formulation -

Tad Matsumoto, IEEE Life Fellow

Mathematical and Electrical Engineering, IMT-Atlantique, Brest, invited Professor,

JAIST and UOulu, Professor Emeritus

Project Chair: IoT network Analysis and Design in Chief Executive Officer problem framework (IoTAD-CEO)

E-mail: matumoto@jaist.ac.jp

Abstract

The goal of this tutorial is to provide the course takers with the knowledge on Decision-Making Theory by Distributed Hypothesis Testing (DHT) with Lossy Correlated Sources Observations via End-to-End Distributed Lossy Communications. First of all, this tutorial focuses on Mathematical and Information Theoretic background needed to understand the concept, where important Theorems, Lemmas and their practical meanings are explained. Then, this tutorial introduces analytical methods based on the theorems, and the results of numerical calculations for evaluating their performance represented by their corresponding Rate-Error-Distortion functions and outage probabilities.

This tutorial applies the theoretical framework of DHT for the decision making via lossy networks. *The relationship in the mathematical bases between Wireless Lossy Communications (WLC) and DHT, as well as between WLC and Machine Learning, between WLC and Semantic Communications are investigated.*

We consider the DHT and WLC Toy Scenario, as:

- Two sources, X and Y are correlated, and the correlation is expressed by random bit flipping $Bern(p_0)$ (if p_0=0.0, X and Y are fully correlated).
- X and Y are lossy-compressed with their rates Rx and Ry, respectively. The DHT Center or Network Destination of WLC aim to decode based on the lossy-compressed data. Let the decoded data be denoted by U. Then, U, Y, X form a Markov chain, U→X→Y in both DHT and WLC. Furthermore, in Machine Learning systems, also U→X→Y holds where X is the semantic source, U is the semantic decoding result, and Y can be seen as the training sequence.

This tutorial provides the course takers with theoretical sketch in mathematics for those Toy Scenarios where some example cases are used. To help course takers understand the mathematics, a slide set (roughly 100 pages long) will be distributed beforehand. The curse slide set has the following Sections:

1. End-to-End *Lossless* Relaying: Slepian Wolf Theorem with Source-Channel Separation
   a. EXIT Analysis for Source Bit-Flipped MIMO Transmission with Turbo Equalization
   b. Slepian-Wolf Formulation for Lossless Two-Way Relay Networks
2. End-to-End Lossy Distributed Multi-terminal Networks: Rate Distortion Analysis
   a. Wyner-Ziv Formulation for End-to-End Lossy Two-Way Relay Network
   b. Berger-Tung Formulation for Two Source One Helper Network
   c. End-to-End Lossless and Lossy Multiple Access Networks

   d. Two Stage Wyner-Ziv Network: Distortion Transfer Analysis
3. Wyner-Ziv Formulation for Decision Making Process
   a. Revisit of Helper-aided Lossy Networks
   b. Distributed Hypothesis Testing (DHT)
   c. Semantic Communications
   d. Training Process of Machine Learning

Most of the presentation slides are available at:
https://dspace.jaist.ac.jp/dspace/bitstream/10119/19040/1/Tutorial.pdf

Keywords: Lossy Wireless Communications, Distributed Multi-terminal Source Coding, Distributed Hypothesis Testing, IoT, V2X, Sensor Networks, Decision Making

References

[1] Zhou, Xiaobo, Meng Cheng, Xin He, and Tad Matsumoto, "Exact and approximated outage probability analyses for decode-and-forward relaying system allowing intra-link errors," *IEEE Transactions on Wireless Communications*, vol. 13, no. 12, pp. 7062-7071, Dec. 2014.

[2] Lin Wensheng, Shen Qian, and Tad Matsumoto, "Lossy-Forward Relaying for Lossy Communications: Rate-Distortion and Outage Probability Analyses", *IEEE Transactions on Wireless Communications*, Vol. 18, No. 8, 05 June 2019, pp. pp. 3974-3986, **DoI:** 10.1109/TWC.2019.2919831

[3] Shulin Song, Meng Cheng, Jiguang He , Xiaobo Zhou, and Tad Matsumoto,"Outage Probability of One-Source-with-One-Helper Sensor Systems in Block Rayleigh Fading Multiple Access Channels", IEEE Sensor Journal, Accepted date: Aug. 24, DOI: 10.1109/JSEN.2020.3018787

[4] Amin Zribi, Lin Wensheng, Reza Asvadi, Elsa Dupraz, Tad Matsumoto, "Two-stage Successive Wyner-Ziv Lossy Forward Relaying for Lossy Communications: Rate-distortion and Outage Probability Analyses", Under Review, IEEE Trans. Vehcular Technology.

[5] Gil Katz, Pablo Piantanida, and Merouane Debba, "Distributed Binary Detection With Lossy Data Compression", IEEE TRANS. ON INFORMATION THEORY, VOL. 63, NO. 8, 2017

[6] Elsa Dupraz, Ismaila Salihou Adamou, Reza Asvadi, and Tad Matsumoto, "Practical Short-Length Coding Schemes for Binary Distributed Hypothesis Testing", Conference Record, IEEE ISIT 2024

[7] Fatemeh Khaledian, Reza Asvadi, Elsa Duprazy, and Tad Matsumoto, "Covering Codes as Near Optimal Quantizers for Distributed Hypothesis Testing Against Independence", Conference Record, IEEE ITW 2024

[8] Wensheng Lin, Yuna Yan, Lixin Li, Zhu Han, and Tad Matsumoto, "Semantic-Forward Relaying: A Novel Framework Towards 6G Cooperative Communications", IEEE Communications Letters: 1-1 2024-01-11

[9] Mahdi Nangir, Reza Asvadi, Jun Chen, Mahmoud Ahmadian-Attari, and Tad Matsumoto, "Successive Wyner-Ziv Coding for the Binary CEO Problem under Logarithmic Loss", IEEE Trans. On Communications, 67(11) 7512-7525, 2019

[10]Abbas El Gamal and Young-Han Kim, "Network Information Theory", Cambridge University Press, 2011, ISBN: 978-1-107-00873-1

2D Smoothing based Recursive Subspace and Factor Graph Framework for High Mobility Geolocation and Tracking

- With a duality consideration to joint Delay-Doppler estimation

Lei Jiang*, Nopphon Keerativoranan*, Tad Matsumoto*,※ , Jun-ichi Takada*

*Department of Transdisciplinary Science and Engineering,
Tokyo Institute of Technology, Japan

※Mathematical and Electrical Engineering, IMT-Atlantique, Brest,
invited Professor, JAIST and UOulu, Professor Emeritus

This paper proposes a distributed sensor-based RECursive Subspace and Factor Graph (REC-SaFG) framework for direction-of-arrival (DoA) estimation and geolocation of a fast-moving target. The whole framework includes two recursive processes: (1) DoA estimation and tracking by 2-dimensional (2D) smoothing-based recursive subspace technique using low rank adaptive filter (LORAF); (2) Factor graph (FG)-based geolocation and tracking network utilizing an extended Kalman filter (EKF) which takes into account the target's position and velocity and updates them as well as the acceleration information. In (1), the recursive subspace technique aims to fully utilize sample size insufficiency due to the fast-moving target and to recover the rank deficiency incurred by the coherent signal components. In (2), the estimated DoA and target velocity information obtained by (1) is considered as input to the unified FG implemented by EKF for geolocation and tracking (FG-GE-TR) of the target position. By integrating these two processes, the REC-SaFG framework promises significant improvements in the accuracy and efficiency of geolocation and tracking systems, particularly in environments characterized by a fast-moving target and the need for high-resolution tracking.

Through extensive numerical simulations, the proposed technique demonstrates superior performance in high-mobility applications, including unmanned aerial vehicles (UAVs) and commercial aviation. Furthermore, a duality consideration is explored for joint Delay-Doppler estimation in Orthogonal Time Frequency Space (OTFS) modulation schemes, extending the applicability of the proposed method to next-generation communication systems. This integration lays the groundwork for efficient signal processing in high-mobility scenarios, bridging the gap between theoretical advancements and practical implementations.

References

[1] R. Schmidt, "Multiple emitter location and signal parameter estimation," *IEEE Trans. Anten. and Propa.*, vol. 34, no. 3, pp. 276-280, Mar. 1986.

[2] Tie-Jun Shan, M. Wax and T. Kailath, "On spatial smoothing for direction-of-arrival estimation of coherent signals," *IEEE Trans. Acoust. Speech, Signal Process.* , vol. 33, no. 4, pp. 806-811, Aug. 1985.

[3] M. C. Vanderveen, C. B. Papadias and A. Paulraj, "Joint angle and delay estimation (JADE) for multipath signals arriving at an antenna array," *IEEE Commun. Letters*, vol. 1, no. 1, pp. 12-14, Jan. 1997.
[4] M. Wax and T. Kailath, "Detection of signals by information theoretic criteria," *IEEE Trans. Acoustics, Speech, Signal Process.* , vol. 33, no. 2, pp. 387-392, Apr. 1985.
[5] P. Strobach, "Low-rank adaptive filters," *IEEE Trans. Signal Process.*, vol. 44, no. 12, pp. 2932-2947, Dec. 1996.
[6] L. Jiang, N. Keerativoranan, T. Matsumoto and J. Takada, “Two-dimensional Smoothing in the Presence of Empirical Nonstationarity due to a Fast Moving Target Part I: Blockwise Subspace-based Technique for Coherent Multipath Component Decorrelation,” *TechRxiv.* September 19, 2024.
[7] L. Jiang, N. Keerativoranan, T. Matsumoto and J. Takada, “Two-dimensional Smoothing in the Presence of Empirical Nonstationarity due to a Fast Moving Target Part II: Recursive Subspace Tracking with Low-Rank Adaptive Filter,” *TechRxiv.* September 19, 2024.
[8] Jung-Chieh Chen, Yeong-Cheng Wang, Ching-Shyang Maa and Jiunn-Tsair Chen, "Network-side mobile position location using factor graphs," *IEEE Trans. Wireless Commun*., vol. 5, no. 10, pp. 2696-2704, Oct. 2006.
[9] M. Cheng, M. R. K. Aziz and T. Matsumoto, "Integrated Factor Graph Algorithm for DoA-Based Geolocation and Tracking," *IEEE Access*, vol. 8, pp. 49989-49998, 2020.
[10] L. Jiang, N. Keerativoranan, T. Matsumoto and J. Takada, "A Distributed Sensor-Based Recursive Framework for DoA Estimation and Geolocation," *IEEE Access*, vol. 12, pp. 136073-136087, 2024.
[11] V. S. Bhat, S. G. Dayanand and A. Chockalingam, "Performance Analysis of OTFS Modulation With Receive Antenna Selection," *IEEE Trans. Vehicular Technology*, vol. 70, no. 4, pp. 3382-3395, April 2021.

Physical Layer Technologies for Sustainable and Multi-functional Wireless Networks

Christos Masouros, Fellow IEEE
Professor of Wireless Communications and Signal Processing
Dept. of Electronic & Electrical Engineering
University College London
c.masouros@ucl.ac.uk

Abstract: The future Global cellular infrastructure will underpin smart city applications, urban security, infrastructure monitoring, smart mobility, among an array of emerging applications that require new network functionalities beyond communications. Key network KPIs for 6G involve Gb/s data rates; cm-level localization; µs-level latency; Tb/Joule energy efficiency. Future networks will also need to support the UN's Sustainable Development Goals to ensure sustainability, net-zero emissions, resilience and inclusivity.
The multifunctionality and the net-zero emissions agenda necessitate a redesign of the signals and waveforms for 6G and beyond. In this talk, we first explore a recent research direction involving symbol-level precoding (SLP) approaches that treat interference as a useful resource in multi-access communication systems. These have been shown to offer orders of magnitude savings in power consumption, over a range of communication scenarios. The second part of the talk focuses on enabling the multi-functionality of signals and wireless transmissions, as a means of hardware reuse and carbon footprint reduction. We overview recent research in the area of integrated sensing and communications (ISAC), that is a paradigm shift that enables a both sensing and communication functionalities from a single transmission, a single spectrum use and ultimately a common infrastructure.
With the rising demand for sustainability and resilience from the network infrastructure, the above technologies are becoming essential building blocks of the wireless network.

Acknowledgment

A part of this work was supported by the EU projects 6GMUSICAL and ISLANDS

References

[1] C. Masouros and E. Alsusa, "A Novel Transmitter-Based Selective-Precoding Technique for DS/CDMA systems", IEEE Signal Processing letters, vol. 14, no. 9, pp. 637-640, Sept. 2007

[2] C. Masouros, E. Alsusa, "Dynamic linear precoding for the exploitation of known interference in MIMO broadcast systems," IEEE Trans. Wireless Comms., vol. 8, no. 3, pp. 1396–1404, Mar. 2009.

[3] C. Masouros, "Correlation rotation linear precoding for MIMO broadcast communications", IEEE Trans. Sig. Proc., vol. 59, no. 1, pp. 252–262, Jan. 2011.

[4] A. Li, et al, "A Tutorial on Interference Exploitation via Symbol-Level Precoding: Overview, State-of-the-Art and Future Directions", IEEE Comms. Surveys and tutorials., vol. 22, no. 2, pp. 796-839, 2020

[5] A. Li, C. Masouros, L. Swindlehurst, W. Yu, “1-Bit Massive MIMO Transmission: Embracing Interference with Symbol-Level Precoding”, IEEE Comms. Mag., in press

[6] Z. Wei, C. Masouros, S. Chatzinotas, B. Ottersten, “Energy- and Cost-Efficient Physical Layer Security in the Era of IoT: The Role of Interference”, IEEE Comms. Mag., vol. 58, no. 4, pp. 81-87, April 2020

[7] C. Masouros, T. Ratnarajah, M. Sellathurai, C. Papadias, A. Shukla, “Known interference in the cellular downlink: a limiting factor or a potential source of green signal power?,” IEEE Commun. Mag., vol. 51, no. 10, pp. 162–171, Oct. 2013.

[8] C. Masouros, M. Sellathurai, T. Ratnarajah, “Vector Perturbation Based on Symbol Scaling for Limited Feedback MISO Downlinks”, IEEE Trans. Sig. Proc., vol. 62, no. 3, pp. 562-571, Feb.1, 2014

[9] C. Masouros and G. Zheng, “Exploiting Known Interference as Green Signal Power for Downlink Beamforming Optimization”, IEEE Trans. Sig. Proc., vol.63, no.14, pp.3668-3680, July, 2015.

[10] K. L. Law, C. Masouros, “Symbol Error Rate Minimization Beamforming for Interference Exploitation”, IEEE Trans. Comms., vol. 66, no. 11, pp. 5718-5731, Nov. 2018

[11] F. Liu, Y. Cui, C. Masouros, J. Xu, T. X. Han, A. Hassanien, Y. Eldar, S. Buzzi, “Integrated Sensing and Communications: Towards Future Dual-functional Wireless Networks”, IEEE Journal on Sel. Areas Comms., vol. 40, no. 6, pp. 1728-1767, June 2022

[12] Z. Wei, F. Liu, C. Masouros, N. Su, A. Petropulu, “Towards Multi-Functional 6G Wireless Networks: Integrating Sensing, Communication and Security” IEEE Wireless Comms Mag., vol. 60, no. 4, pp. 65-71, April 2022

[13] J. A. Zhang, F. Liu, C. Masouros, R. W. Heath, Z. Feng, L. Zheng, A. Petropulu, “An Overview of Signal Processing Techniques for Joint Communication and Radar Sensing” IEEE Jour. Selected Topics Sig Proc, vol. 15, no. 6, pp. 1295-1315, Nov. 2021

[14] F. Liu and C. Masouros, "A Tutorial on Joint Radar and Communication Transmission for Vehicular Networks - Parts I - III", IEEE Commun. Lett., vol. 25, no. 2, pp. 322-336, Feb. 2021 - EiC Invited Paper

[15] F. Liu, C. Masouros, H. Griffiths, A. Petropulu, and L. Hanzo, “Joint Radar and Communication Design: Applications, State-of-the-art, and the Road Ahead”, IEEE Trans Commun., vol. 68, no. 6, pp. 3834-3862, June 2020. – EiC invited paper

[16] F. Liu, C. Masouros, Y. Eldar, “Integrated Sensing and Communications”, 2023 edition Springer

[17] F. Liu, A. Garcia, C. Masouros, and G. Geraci, “Interfering Channel Estimation in Radar-Cellular Coexistence: How Much Information Do We Need?”, IEEE Trans. Wireless Comm., vol. 18, no. 9, pp. 4238-4253, Sept. 2019

[18] F. Liu, C. Masouros, A. Li, T. Ratnarajah and J. Zhou, “MIMO Radar and Cellular Coexistence: A Power-Efficient Approach Enabled by Interference Exploitation”, IEEE Trans. Sig Proc, vol. 66, no. 14, pp. 3681-3695, July 2018,

[19] F. Liu, C. Masouros, A. Li, and T. Ratnarajah, "Robust MIMO Beamforming for Cellular and Radar Coexistence," IEEE Wireless Commun. Lett., vol. 6, no. 3, pp. 374-377, June 2017.

[20] F. Liu, L. Zhou, C. Masouros, A. Li, A. Petropulu, “Dual-functional cellular and radar transmission: Beyond co-existence”, IEEE SPAWC 2018

Physical Layer Technologies for Sustainable and Multi-functional Wireless Networks

Christos Masouros, Fellow IEEE
Professor of Wireless Communications and Signal Processing
Dept. of Electronic & Electrical Engineering
University College London
c.masouros@ucl.ac.uk

1

How can Signal Processing help?

UCL

- Multi-access technologies to exploit 'Green' interference power

- Multi-access technologies to enable dual use of hardware - multifunctionality

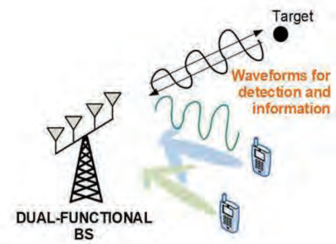

2

Sustainable and Multifunctional Wireless Networks

Part I: Signaling for Sustainability: Re-using Interference

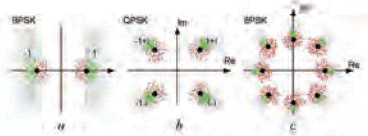

Christos Masouros
Dept. of Electronic & Electrical Eng.
University College London

3

Motivation

ICT: ~2% of global CO_2 emissions

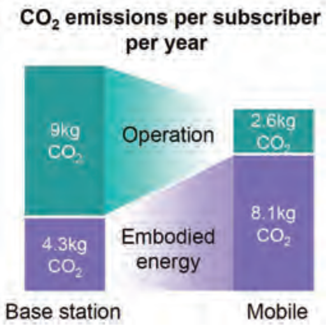

4

Constructive Interference

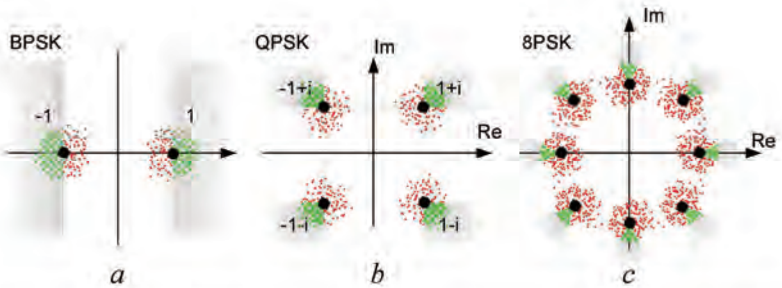

Interference is Constructive when the Distances of the received Symbols from the Decision thresholds are Increased

5

Precoding for the MIMO Downlink

Key Concept: Exploitation of green interference power

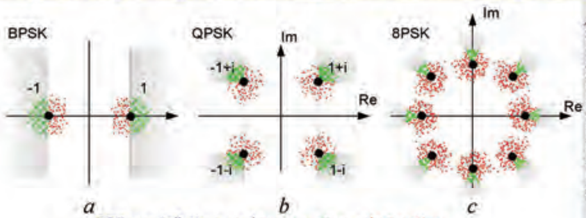

PSK constellations and constructive – destructive interference sectors

Up to 10x Power Reduction

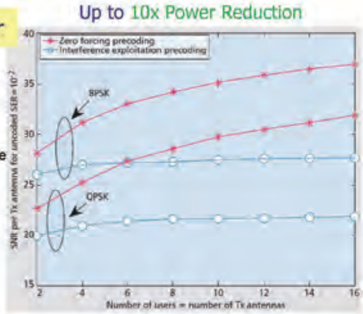

Early Works:

C. Masouros and E. Alsusa, "A Novel Transmitter-Based Selective-Precoding Technique for DS/CDMA systems", IEEE Signal Processing letters, vol. 14, no. 9, pp. 637-640, Sept. 2007

C. Masouros, "Correlation Rotation Linear Precoding for MIMO Broadcast Communications", *IEEE Trans. on Sig. Proc., vol 59, issue 1, pp. 252-262, Jan 2011*

C. Masouros, T. Ratnarajah, M. Sellathurai, C. Papadias, A. Shukla, "Known Interference in Wireless Communications: A Limiting factor or a Potential Source of Green Signal Power?", IEEE Comms. Mag., vol. 51, no. 10, pp. 162-171, Oct. 2013

C. Masouros, M. Sellathurai, T. Ratnarajah, "Interference Optimization for Transmit Power Reduction in Tomlinson-Harashima Precoded MIMO Downlinks", IEEE Trans. Sig. Proc., vol. 60, no. 5, pp. 2470-2481, May 2012

Optimization based Interference Exploitation first introduced in the context of Vector Perturbation:

C. Masouros, M. Sellathurai, T. Ratnarajah, "Vector Perturbation Based on Symbol Scaling for Limited Feedback MIMO Downlinks", IEEE Trans. Sig. Proc., vol. 62, no. 3, pp. 562-571, Feb.1, 2014

6

UCL

Constructive Interference for M-PSK

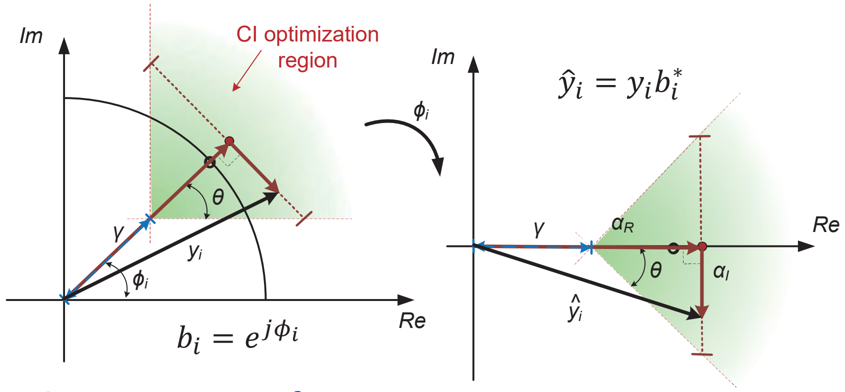

Constructive Interference:

1. $\alpha_R \geq \gamma$
2. $|\alpha_I| \leq (\alpha_R - \gamma)\tan\theta$

$\alpha_R = Re(\hat{y}_i),\ \alpha_I = Im(\hat{y}_i)$

$\theta = \dfrac{\pi}{M}, \gamma = \sqrt{\Gamma_i N_0}$

7

UCL

Constructive Interference for QAM

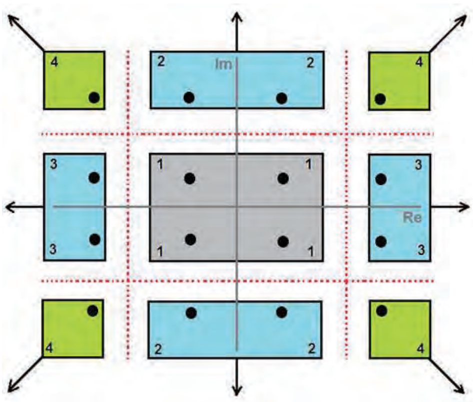

Note: We focus on PSK in the following for analytical simplicity

Section 1: No scope for CI

$C1: Re(y_i) = \sqrt{\Gamma_i^{DL}}\sigma_i Re(d_i)$

$C2: Im(y_i) = \sqrt{\Gamma_i^{DL}}\sigma_i Im(d_i)$

Section 2: CI only on the Im

$C1: Re(y_i) = \sqrt{\Gamma_i^{DL}}\sigma_i Re(d_i)$

$C2: Im(y_i) \gtreqless \sqrt{\Gamma_i^{DL}}\sigma_i Im(d_i)$

Section 3: CI only on the Re

$C1: Re(y_i) \gtreqless \sqrt{\Gamma_i^{DL}}\sigma_i Re(d_i)$

$C2: Im(y_i) = \sqrt{\Gamma_i^{DL}}\sigma_i Im(d_i)$

Section 4: CI similar to QPSK case

A. Li and C. Masouros, "Exploiting Constructive Mutual Coupling in P2P MIMO by Analog-Digital Phase Alignment", IEEE Trans. Wireless Comms., vol. 16, no. 3, pp. 1948-1962, March 2017

8

CI Optimization

UCL

$$|\alpha_I| \le (\alpha_R - \gamma)\tan\theta$$

$$\mathbf{x} = \sum_{i=1}^{K} \mathbf{w}_i b_i$$

$$\min_{\mathbf{w}_i} \sum_{i=1}^{K} \|\mathbf{w}_i\|^2$$

$$s.t. \frac{|\mathbf{h}_i^T \boldsymbol{w}_i|^2}{\sum_{\substack{k=1 \\ k\ne i}}^{K} |\mathbf{h}_i^T \boldsymbol{w}_k|^2 + N_0} \ge \Gamma_i$$

Power minimization

$$\min_{\mathbf{x}} \|\mathbf{x}\|^2$$

$$s.t. \left|Im\left(\mathbf{h}_i^T \mathbf{x} b_i^*\right)\right| \le \left(Re\left(\mathbf{h}_i^T \mathbf{x} b_i^*\right) - \sqrt{\Gamma_i N_0}\right)\tan\theta$$

$$\max_{\boldsymbol{w}_i, \Gamma_t} \Gamma_t$$

$$s.t. \frac{|\mathbf{h}_i^T \boldsymbol{w}_i|^2}{\sum_{\substack{k=1 \\ k\ne i}}^{K} |\mathbf{h}_i^T \boldsymbol{w}_k|^2 + N_0} \ge \Gamma_t$$

$$\sum_{i=1}^{K} \|\boldsymbol{w}_i\|^2 \le P$$

SINR balancing

$$\max_{\mathbf{x}, \Gamma_t} \Gamma_t$$

$$s.t. \left|Im\left(\mathbf{h}_i^T \mathbf{x} b_i^*\right)\right| \le \left(Re\left(\mathbf{h}_i^T \mathbf{x} b_i^*\right) - \sqrt{\Gamma_t N_0}\right)\tan\theta$$

$$\|\mathbf{x}\|^2 \le P$$

9

UCL

Results - Key Benefits

10

Performance Evaluation

Power Minimization

$(N_t \times K)$ 5x4, QPSK 4x4, QPSK

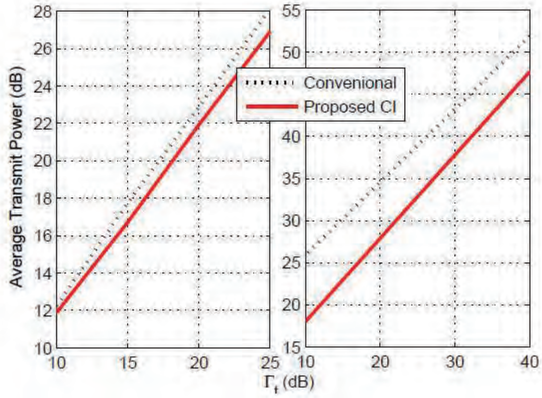

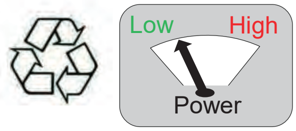

~ 1-2dB SNR gain in 5x4

~ 5-6dB gain in 4x4 MIMO

Just by exploiting interference already existing in the system!!

11

Feasibility Evaluation

$N \times 4$, QPSK

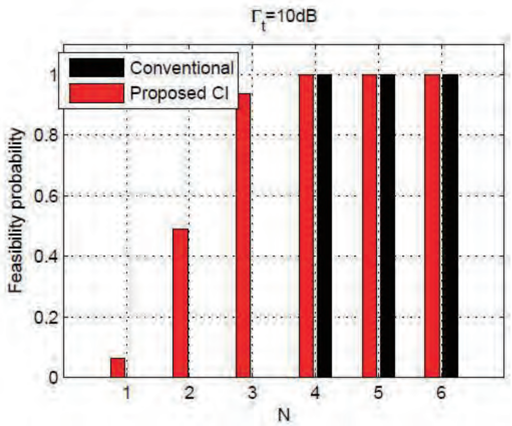

- ✗ Conventional beamforming non-feasible for less than 4 tx antennas
- ✓ CI more relaxed allowing feasibility for less antennas

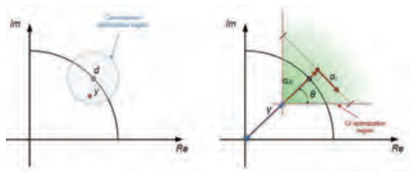

Feasibility: Satisfying the SNR constraint with a 'reasonable' transmit power (below a reasonable threshold)

12

Instantaneous vs Average Constraints

Conventional:
- Statistical constraints → outages
- Instantaneous violation

$$\min_{\mathbf{w}_i} \sum_{i=1}^{K} \|\mathbf{w}_i\|^2 \quad s.t. \quad \frac{\left|\mathbf{h}_i^T \boldsymbol{w}_i\right|^2}{\sum_{k=1, k\neq i}^{K} \left|\mathbf{h}_i^T \boldsymbol{w}_k\right|^2 + N_0} \geq \Gamma_i$$

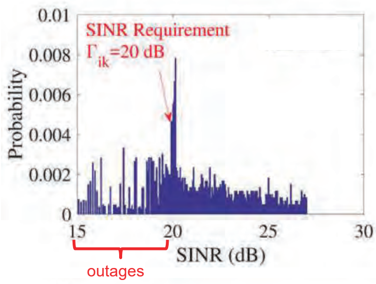

Interference Exploitation:
- Instantaneous constraints
- No outages

$$\min_{\mathbf{x}} \|\mathbf{x}\|^2$$
$$s.t. \left|Im\left(\mathbf{h}_i^T \mathbf{x} b_i^*\right)\right| \leq \left(Re\left(\mathbf{h}_i^T \mathbf{x} b_i^*\right) - \sqrt{\Gamma_i N_0}\right) \tan\theta$$

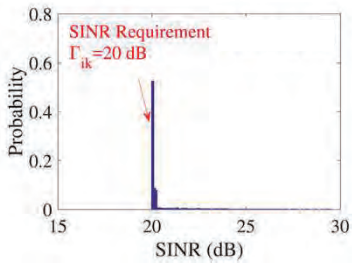

13

How about the Receiver complexity?

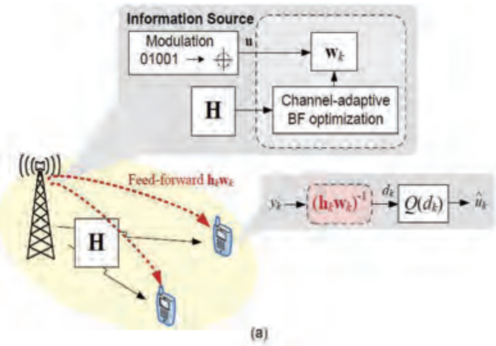

Conventional

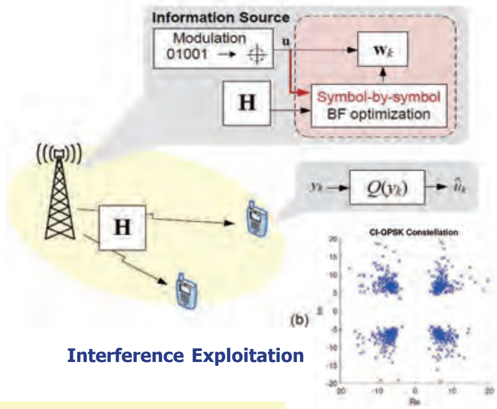

Interference Exploitation

- Lower complexity at the resource-limited MU receiver
- No need for CSI training and overheads at MU receiver
- Immune to such CSI errors

C. Masouros, "Harvesting Signal Power from Constructive Interference in Multiuser Downlinks", in the book "Wireless Energy Harvesting for Future Wireless Communications", Edited by: John Thompson, Symeon Chatzinotas, Salman Durrani, 2018 edition Springer

14

Proof-of-Concept – 6x2 MIMO-OFDM, QPSK

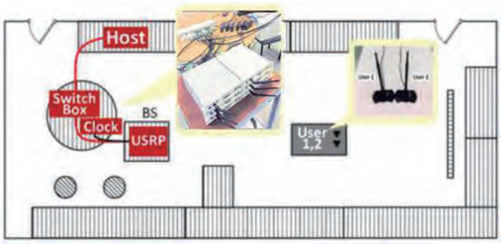

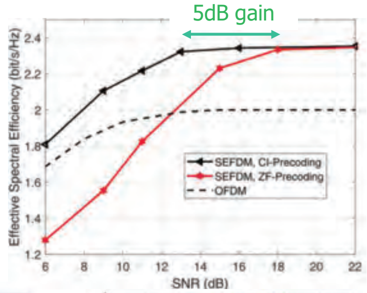

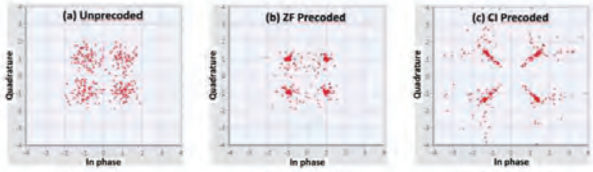

(a) Unprecoded (b) ZF precoded (c) CI precoded

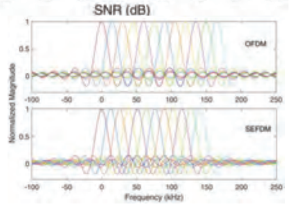

T. Xu, F. Liu, A. Li, C. Masouros, I. Darwazeh, "Constructive Interference Precoding for Reliable Non-Orthogonal IoT Signaling", IEEE INFOCOM2019

A. Li, C. Masouros, "Interference Exploitation Precoding Made Practical: Optimal Closed-Form Solutions for PSK Modulations", IEEE Trans. Wireless Comms., vol. 17, no. 11, pp. 7661-7676, 2018

15

15

Data-Driven CI Precoding (SLP-DNet)

Power Minimization

$$\min_{w} \|\mathbf{w}\|^2$$
$$s.t.\ \left|Im\left(\mathbf{h}_i^T \mathbf{w} e^{j(-\phi_i)}\right)\right| \le \left(Re\left(\mathbf{h}_i^T \mathbf{w} e^{j(-\phi_i)}\right) - \sqrt{\Gamma_i \omega_0}\right) \tan\phi$$

$$\min_{\{\mathbf{w}_1\}} \ \|\mathbf{w}_1\|_2^2$$
$$\text{s.t.} \quad \left|\mathbf{\Lambda}_i^T \mathbf{\Pi} \mathbf{w}_1\right| \le \left(\mathbf{\Lambda}_i^T \mathbf{\Pi} \mathbf{w}_1 - \sqrt{\Gamma_i \omega_0}\right) \tan\phi \ , \ \forall i$$

$$\mathbf{\Lambda} = [\hat{\mathbf{h}}_{Ri} \ ; \ \hat{\mathbf{h}}_{Ii}\ ] \quad \mathbf{w}_1 = [\mathbf{w}_R \quad -\mathbf{w}_I]^T$$
$$\mathbf{\Pi} = \begin{bmatrix} \mathbf{O}_{N_t} & -\mathbf{I}_{N_t} \\ \mathbf{I}_{N_t} & \mathbf{O}_{N_t} \end{bmatrix}$$

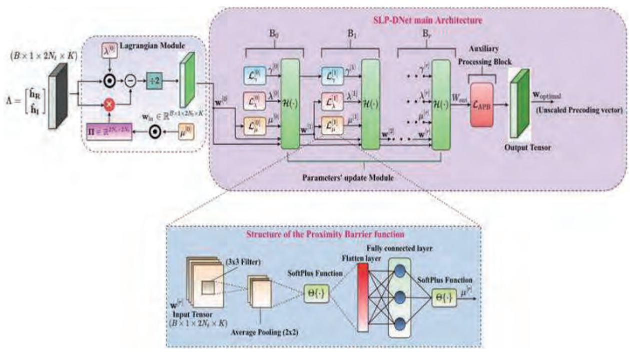

Unfolding using the Lagrangian → regularised loss function:

$$\mathcal{L}_{\text{rl}}(\mathbf{w}_1, \mu_1, \mu_2) = \frac{1}{N}\sum_{i=1} \|\mathbf{w}_1\|_2^2$$
$$+ \frac{1}{N}\sum_{i=1}^{N}\left(\mu_1\left(\mathbf{\Lambda}_i^T\mathbf{\Pi}\mathbf{w}_1 - \mathbf{\Lambda}_i^T\mathbf{w}_1\tan\phi + \sqrt{\Gamma_i w_0}\right)\right)$$
$$- \frac{1}{N}\sum_{i=1}^{N}\left(\mu_2\left(\mathbf{\Lambda}_i^T\mathbf{\Pi}\mathbf{w}_1 + \mathbf{\Lambda}_i^T\mathbf{w}_1\tan\phi - \sqrt{\Gamma_i w_0}\right)\right)$$
$$+ \frac{\vartheta}{NL}\sum_{i=1}^{N}\sum_{i=1}^{L}\|\boldsymbol{\theta}_i\|_2^2,$$

16

Data-Driven CI – NN Quantization

Quantized NN weights

Binary (SLP-DBNet): $\mathbf{B}_w = sign(\mathbf{W}) = \begin{cases} +1 & \text{if } \mathbf{W} \geq 0 \\ -1 & \text{otherwise,} \end{cases}$

Ternary (SLP-DQNet): $\mathbf{B}_w^* = \begin{cases} +1 & \text{, if } \mathbf{W} > \delta \\ 0 & \text{, if } |\mathbf{W}| \leq \delta \\ -1 & \text{, if } \mathbf{W} < -\delta, \end{cases}$

Stochastic quantization (SLP-DQNet): $\mathbf{B}_w = \begin{cases} +1 & \text{with probability } p = \rho(\mathbf{W}) \\ -1 & \text{with probability } 1 - p, \end{cases}$

- ↓ Memory consumption
- ↓ Complexity
- ✓ Hardware Friendly

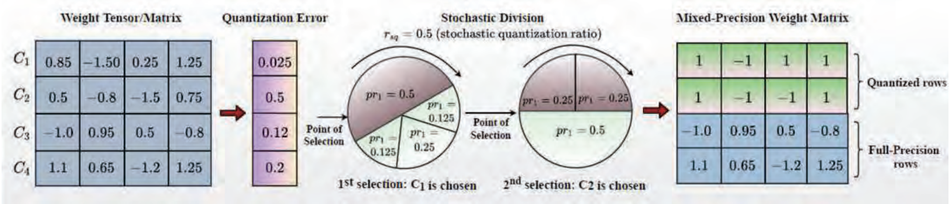

17

Numerical Results – PSK

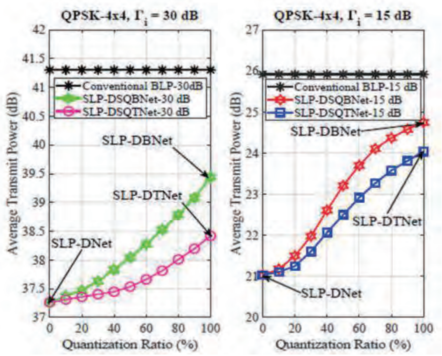

Performance trade-off

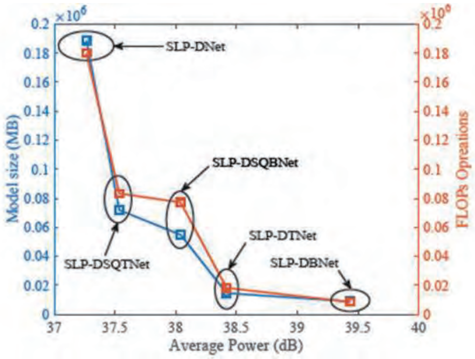

Memory and complexity

- Scalable performance vs quantization trade-off.
- Down to 50% quantization with ~1.5dB loss for Ternary Quantization.
- Scalable memory / complexity vs power trade-off

A. Mohammad, C. Masouros, I. Andreopoulos, “A Memory-Efficient Learning Framework for Symbol Level Precoding with Quantized NN Weights”, IEEE Open Journal ComSoc., vol. 4, pp. 1334-1349, 2023

18

Application to NOMA

CoMA: Constructive Multiple Access

$$y_{k,i} = h_{k,i} \sum_{l=1}^{2} w_{k,l} x_{k,l} + n_{k,i}$$

$$\tilde{y}_1 = h_1^T w_2 x_2 - \hat{h}_1^T \hat{w}_2 \hat{x}_2 + h_1^T w_1 x_1 + n_1$$

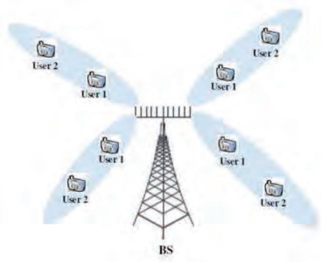

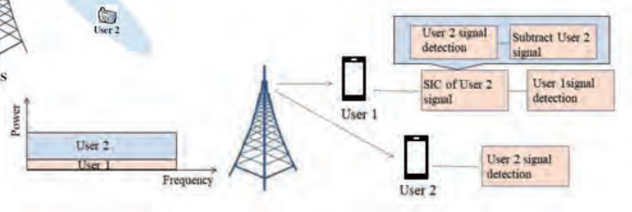

- **Challenge: Symbol-by-symbol (sub msec level) SIC**
- How to remove the detrimental effect of interference + need for SIC?

19

CoMA – Rate Gains

NOMA

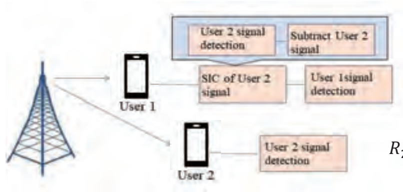

For perfect SIC:

$$R_1 = \log_2\left(1 + |h_1^T w_1|^2\right)$$ Single-user performance

(x_2 must be decodable by both users)

$$R_2 = \min\left(\log_2\left(1 + \frac{|h_1^T w_2|^2}{|h_1^T w_1|^2 + \sigma_1^2}\right), \log_2\left(1 + \frac{|h_2^T w_2|^2}{|h_2^T w_1|^2 + \sigma_2^2}\right)\right)$$

Less than SDMA

CoMA

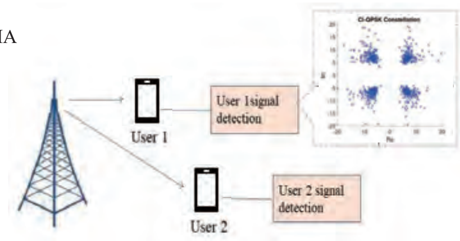

$$R_1 = \log_2\left(1 + |h_1^T w_1|^2 + |h_1^T w_2|^2\right)$$

Better than single-user

$$R_2 = \log_2\left(1 + \frac{|h_2^T w_2|^2}{|h_2^T w_1|^2 + \sigma_2^2}\right)$$

Like SDMA

A. Salem, X. Tong, A. Li and C. Masouros, "NOMA Made Practical: Removing the Receive SIC Processing Through Interference Exploitation," in IEEE Open Journal of the Communications Society, vol. 5, pp. 2723-2734, 2024

20

CoMA vs NOMA - performance

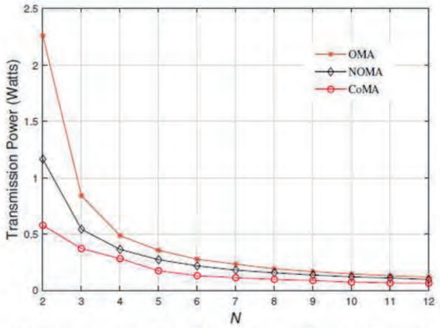

(a) Power consumption versus number of BS antennas when $(r_1, r_2, \sigma_1, \sigma_2) = (1, 1, 2, 1)$.

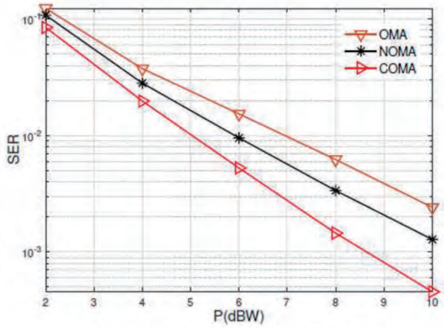

(a) SER versus P for QPSK when $N = 2$.

- CoMA improves Tx power for given SNR target, by exploiting interference power
- CoMA improves SER for given Tx power budget

A. Salem, X. Tong, A. Li and C. Masouros, "NOMA Made Practical: Removing the Receive SIC Processing Through Interference Exploitation," in IEEE Open Journal of the Communications Society, vol. 5, pp. 2723-2734, 2024

21

CoMA vs NOMA – Decoding-only complexity

Decoding-only complexity:

$$\mathcal{C}_{NOMA-pair,k} = \sum_{i=1}^{2} \underbrace{\left(4NM_k + 2M_k^N\right)}_{ML\ \text{detection}} \times (2 - i + 1) + \underbrace{\mathcal{O}\left(M_k^2\right)}_{\text{Subtraction}}$$

(x_1, x_2 @User 1 + x_2 @User 2; User 1)

$$\mathcal{C}_{COMA-pair,k} = \underbrace{\left(4NM_k + 2M_k^N\right)}_{ML\ \text{detection}} + \underbrace{D_k\left(M_k\right)}_{CI\ \text{detection}}$$

(User 2; User 1)

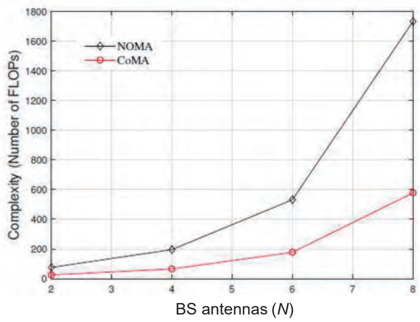

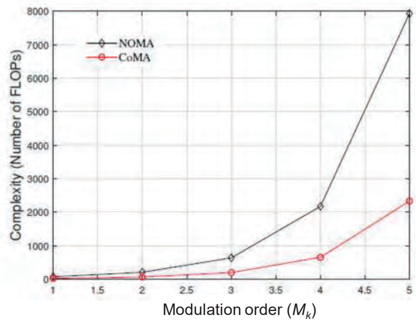

- CoMA reduces decoding complexity w.r.t. NOMA
- **Don't forget CSIR estimation complexity, errors, quantization… !**

A. Salem, X. Tong, A. Li and C. Masouros, "NOMA Made Practical: Removing the Receive SIC Processing Through Interference Exploitation," in IEEE Open Journal of the Communications Society, vol. 5, pp. 2723-2734, 2024

22

References - CI

Constructive Interference

1. C. Masouros and E. Alsusa, "A Novel Transmitter-Based Selective-Precoding Technique for DS/CDMA systems", IEEE Signal Processing letters, vol. 14, no. 9, pp. 637-640, Sept. 2007
2. C. Masouros, E. Alsusa, "Dynamic linear precoding for the exploitation of known interference in MIMO broadcast systems," IEEE Trans. Wireless Comms., vol. 8, no. 3, pp. 1396–1404, Mar. 2009.
3. C. Masouros, "Correlation rotation linear precoding for MIMO broadcast communications", IEEE Trans. Sig. Proc., vol. 59, no. 1, pp. 252–262, Jan. 2011.

Overviews

1. A. Li, et al, "A Tutorial on Interference Exploitation via Symbol-Level Precoding: Overview, State-of-the-Art and Future Directions", IEEE Comms. Surveys and tutorials., vol. 22, no. 2, pp. 796-839, 2020
2. A. Li, C. Masouros, L. Swindlehurst, W. Yu, "1-Bit Massive MIMO Transmission: Embracing Interference with Symbol-Level Precoding", IEEE Comms. Mag., in press
3. Z. Wei, C. Masouros, S. Chatzinotas, B. Ottersten, "Energy- and Cost-Efficient Physical Layer Security in the Era of IoT: The Role of Interference", IEEE Comms. Mag., vol. 58, no. 4, pp. 81-87, April 2020
4. C. Masouros, T. Ratnarajah, M. Sellathurai, C. Papadias, A. Shukla, "Known interference in the cellular downlink: a limiting factor or a potential source of green signal power?," IEEE Commun. Mag., vol. 51, no. 10, pp. 162–171, Oct. 2013.

Beamforming for Constructive Interference

1. C. Masouros, M. Sellathurai, T. Ratnarajah, "Vector Perturbation Based on Symbol Scaling for Limited Feedback MISO Downlinks", IEEE Trans. Sig. Proc., vol. 62, no. 3, pp. 562-571, Feb.1, 2014
2. C. Masouros and G. Zheng, "Exploiting Known Interference as Green Signal Power for Downlink Beamforming Optimization", IEEE Trans. Sig. Proc., vol.63, no.14, pp.3668-3680, July, 2015.
3. K. L. Law, C. Masouros, "Symbol Error Rate Minimization Beamforming for Interference Exploitation", IEEE Trans. Comms., vol. 66, no. 11, pp. 5718-5731, Nov. 2018

23

References – Practical Transmission with CI

Constant Envelope Precoding

1. P. V. Amadori and C. Masouros, "Constant Envelope Precoding by Interference Exploitation in Phase Shift Keying-Modulated Multiuser Transmission", IEEE Trans Wireless Comms., vol. 16, no. 1, Jan. 2017
2. F. Liu, C. Masouros, P. Amadori, H. Sun "An Efficient Manifold Algorithm for Constructive Interference based Constant Envelope Precoding", IEEE Sig. Proc. Let., vol. 24, no. 10, pp. 1542-1546, Oct. 2017

Hybrid Analog-Digital Precoding

1. A. Li, F. Liu, C. Masouros, Y. Li, B. Vucetic, "Interference Exploitation 1-Bit Massive MIMO Precoding: A Partial Branch-and-Bound Solution with Near-Optimal Performance", IEEE Trans. Wireless Comms., vol. 19, no. 5, pp. 3474-3489, May 2020
2. A. Li and C. Masouros, F. Liu, L. Swindlehurst, "Massive MIMO 1-Bit DAC Transmission: A Low-Complexity Symbol Scaling Approach", IEEE Trans. Wireless Comms., vol. 17, no. 11, pp. 7559-7575, Nov. 2018
3. G. Hegde, C. Masouros, M. Pesavento, "Interference Exploitation-based Hybrid Precoding with Robustness Against Phase Errors", IEEE Trans. Wireless Comms., vol. 18, no. 7, July 2019

Massive MIMO

1. P. V. Amadori and C. Masouros, "Interference Driven Antenna Selection for Massive Multi-User MIMO", IEEE Trans Veh Tech., vol. 65, no. 8, pp. 5944-5958, Aug. 2016
2. P. V. Amadori and C. Masouros, "Large Scale Antenna Selection and Precoding for Interference Exploitation", IEEE Trans Comms., *vol. 65, no. 10, pp. 4529-4542, Oct. 2017*

Closed form CI precoding

1. A. Li, C. Masouros, "Interference Exploitation Precoding Made Practical: Optimal Closed-Form Solutions for PSK Modulations", IEEE Trans. Wireless Comms., vol. 17, no. 11, pp. 7661-7676, 2018
2. A. Li, C. Masouros, Y. Li, L. Swindlehurst, "Interference Exploitation Precoding for Multi-Level Modulations: Closed-Form Solutions", IEEE Trans. Comms., vol. 69, no. 1, pp. 291-308, Jan. 2021

Prototyping – Over-the-air Testing

T. Xu, F. Liu, A. Li, C. Masouros, I. Darwazeh, "Constructive Interference Precoding for Reliable Non-Orthogonal IoT Signaling", IEEE INFOCOM2019

24

References - Advanced Scenarios with CI

AI-based SLP

1. A. Mohammad, C. Masouros, I. Andreopoulos, “A Memory-Efficient Learning Framework for Symbol Level Precoding with Quantized NN Weights”, IEEE Open Journal ComSoc., in press
2. A. Mohammad, C. Masouros, I. Andreopoulos, “An Unsupervised Deep Unfolding Framework for Robust Symbol Level Precoding”, IEEE Open Journal ComSoc., in press

Full Duplex Comms

1. M. K. Tukur, C. Masouros, “Delay-Constrained Beamforming and Resource Allocation in Full Duplex Systems”, IEEE Trans. Veh Tech., vol. 69, no. 3, pp. 3476-3480, March 2020
2. M. K. Tukur, M. R. Khandaker, C. Masouros, “Interference Exploitation in Full Duplex Communications: Trading Interference Power for Both Uplink and Downlink Power Savings”, IEEE Trans. Wireless Comms., vol. 17, no. 12, pp. 8314-8329, Dec. 2018

PHY Security

1. M. R. Khandaker, C. Masouros, K. K. Wong, “Constructive Interference Based Secure Precoding: A New Dimension in Physical Layer Security”, IEEE Trans Forensics and Security., vol. 13, no. 9, Sept. 2018
2. Z. Wei, F. Liu, C. Masouros, “Secure Directional Modulation with Few-bit Phase Shifters: Optimal and Closed Form Designs”, IEEE Trans. Comms., vol. 69, no. 1, pp. 486-500, Jan. 2021

Rate Splitting

A. Salem, C. Masouros, “Rate Splitting Approach Under PSK signaling Using Constructive Interference Precoding Technique”, IEEE WCNC 2019, best paper award in Track 1: PHY and Fundamentals

Comms-Radar Transmission

F. Liu, C. Masouros, A. Li., T. Ratnarajah, J. Zhou, “MIMO Radar and Cellular Coexistence: A Power-Efficient Approach Enabled by Interference Exploitation”, IEEE Trans. Sig. Proc., vol. 66, no. 14, July 2018

Multi-Cell Transmission

1. Z. Wei, C. Masouros, K. K. Wong, K. Xin, “Multi-Cell Interference Exploitation: Enhancing the Power Efficiency in Cell Coordination”, IEEE Trans. Wireless Comms., vol. 19, no. 1, pp. 547-562, Jan. 2020
2. Z. Wei, C. Masouros, “Device-Centric Distributed Antenna Transmission: Secure Precoding and Antenna Selection with Interference Exploitation”, IEEE Trans. IoT., vol. 7, no. 3, pp. 2293-2308, March 2020

25

Sustainable and Multifunctional Wireless Networks

Part II: Sustainability Through Hardware Reuse and Multifunctionality

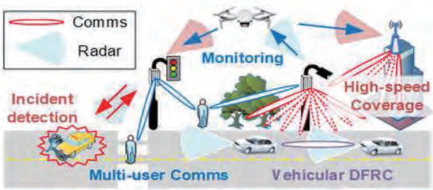

Christos Masouros
Dept. of Electronic & Electrical Eng.
University College London

26

Next Generations of Networks

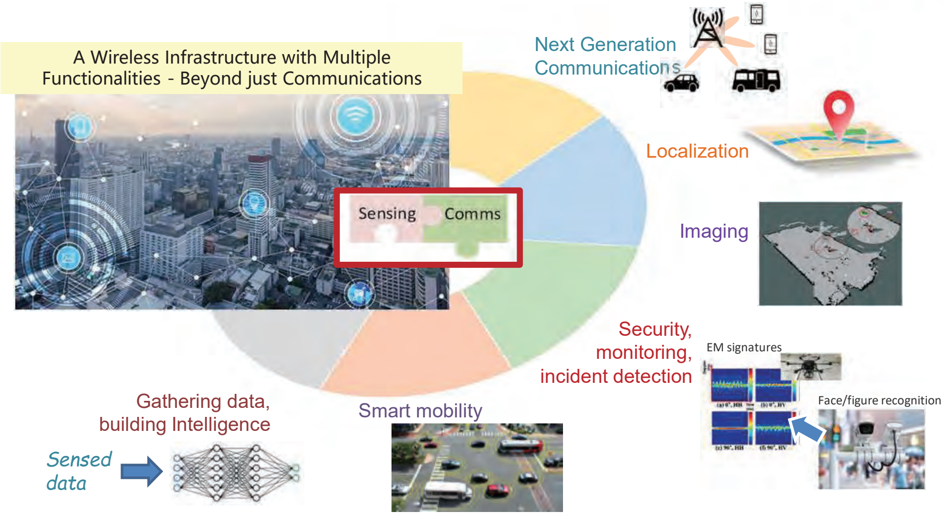

F. Liu, Y. Cui, C. Masouros, J. Xu, T. X. Han, A. Hassanien, Y. Eldar, S. Buzzi, "Integrated Sensing and Communications: Toward Future Dual-functional Wireless Networks", IEEE Journal on Sel. Areas Comms., vol. 40, no. 6, pp. 1728-1767, June 2022

27

ITUs IMT-2030

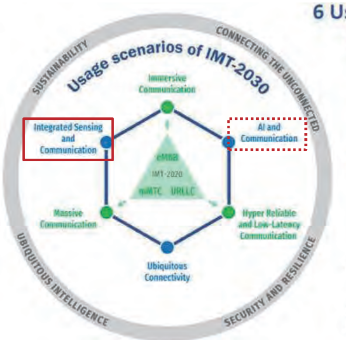

6 Usage scenarios

Extension from IMT-2020 (5G)

- eMBB ➡ Immersive Communication
- mMTC ➡ Massive Communication
- URLLC ➡ HRLLC (Hyper Reliable & Low-Latency Communication)

New

- Ubiquitous Connectivity
- Integrated AI and Communication
- Integrated Sensing and Communication

4 Overarching aspects:

act as design principles commonly applicable to all usage scenarios

Sustainability, Connecting the unconnected,
Ubiquitous intelligence, Security/privacy/resilience

Committed to connecting the world

28

The step change from RCC to DFRC

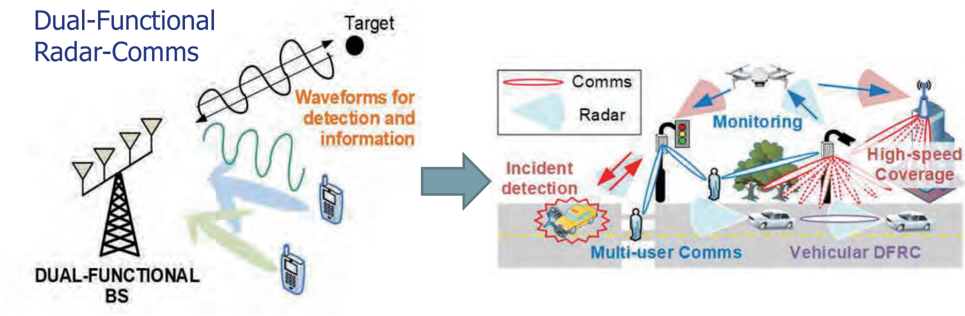

Comms and Radar systems cooperate instead of competing for resources.

- Mutually benefit the real-time performance for both radar and communication systems
- Turn radar applications, which are on the rise with emerging IoT applications such as autonomous cars, into a commodity.

F. Liu, C. Masouros, H. Griffiths, A. Petropulu, L. Hanzo "Joint Radar and Communication Design: Applications, State-of-the-art, and the Road Ahead", IEEE Trans Commun., vol. 68, no. 6, pp. 3834-3862, June 2020.

29

DFRC Signalling Technologies

- Radar-centric design
  - Pulse Interval Modulation (PIM)
  - Radar beampattern sidelobe signalling
  - Index Modulation (IM) using radar waveforms
  - …
- Comms-centric design
  - OFDM based DFRC
  - IEEE 802.11ad based DFRC
  - …
- Jointly optimized design
  - Radar-centric joint design
  - Weighted Comms-Radar optimization
  - …

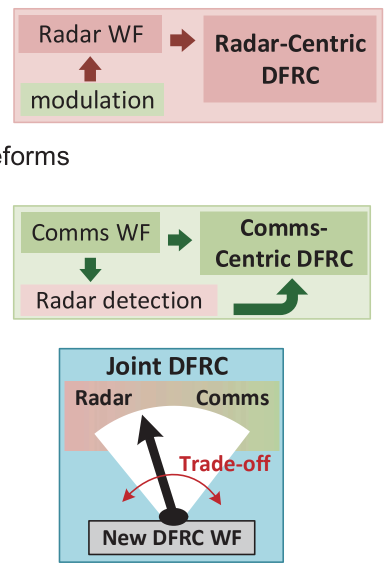

30

Dual-functional Radar-Communication Signals

Joint Design

31

DFRC- Joint Waveform Optimization

Weighted optimization

$$\mathbf{Y} = \mathbf{HX} + \mathbf{Z} = \mathbf{S} + \underbrace{(\mathbf{HX} - \mathbf{S})}_{\text{MUI}} + \mathbf{Z}$$

$$\min_{\mathbf{X}} \rho \left\| \mathbf{HX} - \mathbf{S} \right\|_F^2 + (1-\rho) \left\| \mathbf{X} - \mathbf{X}_0 \right\|_F^2$$

$$s.t. \ \frac{1}{L} \left\| \mathbf{X} \right\|_F^2 = P_T,$$

Ideal radar waveform

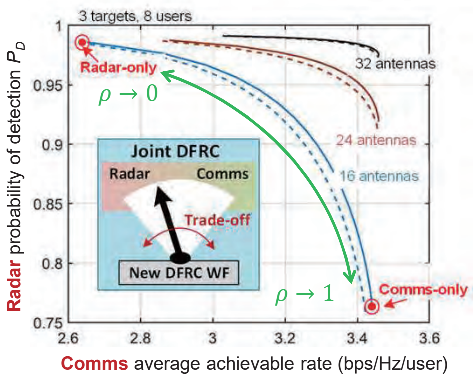

↑ ρ - Comms priority
↓ ρ - Radar priority

F. Liu, L. Zhou, C. Masouros, A. Li, W. Luo, and A. Petropulu, "Toward dual-functional radar-communication systems: Optimal waveform design," IEEE Trans. Signal Process., vol. 66, no. 16, pp. 4264–4279, Aug 2018.

32

Joint DFRC – Over-the-air Proof of concept

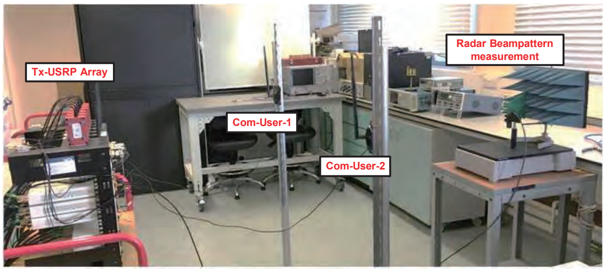

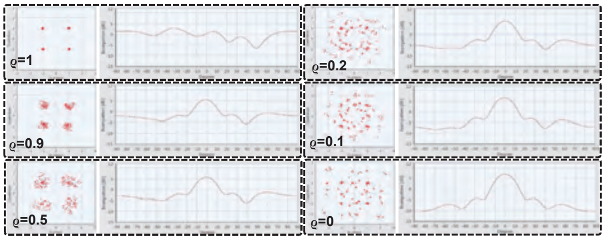

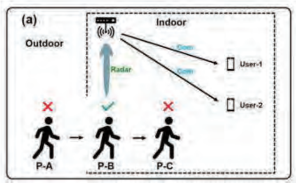

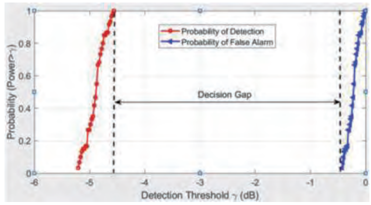

$$P_D = Pr(Power < \gamma \mid obstacle\ present)$$
$$P_{FA} = Pr(Power < \gamma \mid obstacle\ not\ present)$$

T. Xu, F. Liu, C. Masouros, I. Darwazeh, "An Experimental Proof of Concept for Integrated sensing and Communications Waveform Design", IEEE Open Journal of ComSoc, vol. 3, pp. 1643-1655, 2022

33

Dual-functional Radar-Communication Signals

Radar-centric Design

34

Radar-centric DFRC through Index Modulation

Over-The-Air Lab Setup

Radar RFSoC platform

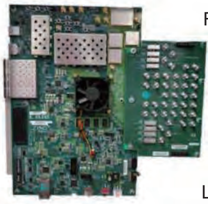

LFM waveform

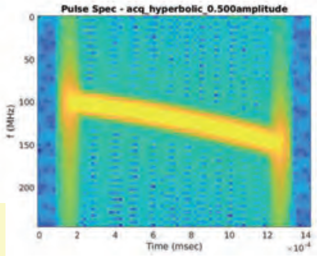

Radar node is situated behind the 'bin' target next to the dual radar Tx and Rx dishes.

The comms Rx ARESTOR node is seen on the bench behind its receiving dish to the right of the image.

Three indices are considered
- centre frequency
- bandwidth
- polarization

M. Temiz, N. Peters, C. Horne, M. Ritchie, C. Masouros, "An Experimental Study of Radar-Centric Transmission for Integrated Sensing and Communications", IEEE Transactions on Microwave Theory and Techniques, in press

35

T_c=50μs

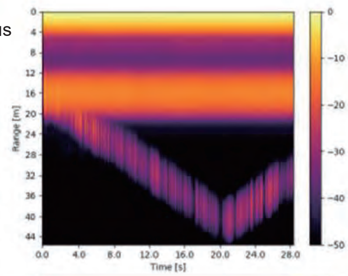

T_c=10μs

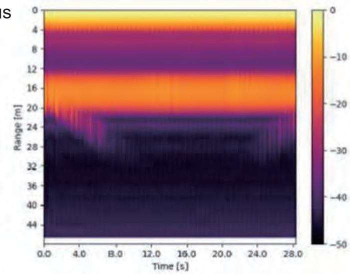

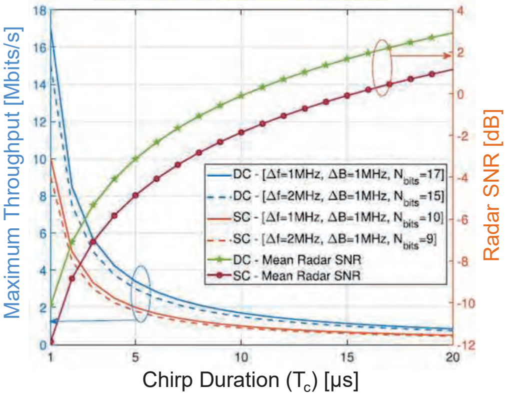

- ↓ Radar pulse duration → ↑ Comms throughput, ↓ Radar integration gain

36

Dual-functional Radar-Communication

Subject to Security threats?

37

Radar + Information: Subject to Security Threats

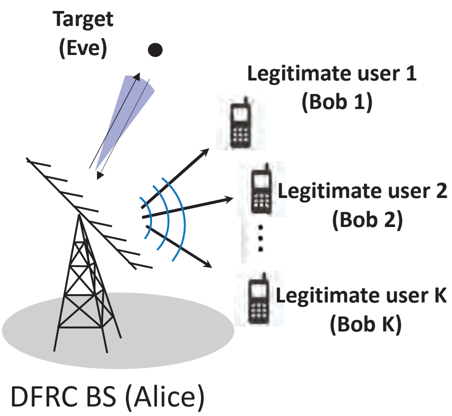

Target can be:

- Enemy aircraft
- Malicious UAV
- Non-cooperative car
- …

Malicious target can:

- Detect Data intended for LUs – unique to DFRC
- Infer critical radar info (location, ID, …, …)

- Need for PHY security guarantees over the Radar beamwidth
- Secure Beamforming / Artificial Noise

38

Secure DFRC Transmission

Unique Sensing Performance vs Security Trade-offs

- ⬆ Power towards the direction of target
- ⬇ Useful signal power ($SINR_E$) towards the target
- ⬆ $SINR_{LU}$ towards the users

Apply PHY Sec approaches
- Secure BF
- AN, Jamming
- Cooperative Security
- …

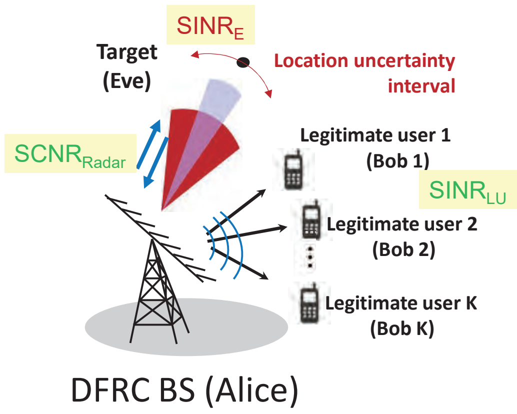

Z. Wei, F. Liu, C. Masouros, N. Su, A. Petropulu, "Towards Multi-Functional 6G Wireless Networks: Integrating Sensing, Communication and Security" IEEE Comms Mag., *vol. 60, no. 4, pp. 65-71, April 2022*

39

Our Work

Secure DFRC Transmission – An Artificial Noise Design

N = 18 antennas, K = 4 legitimate users, one target – LU SNR $\gamma_b = 10\text{dB}$.

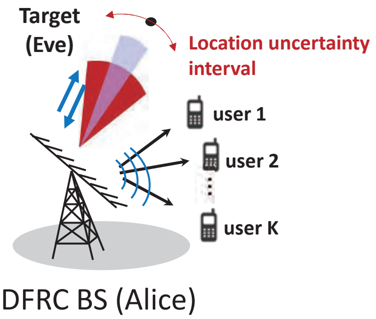

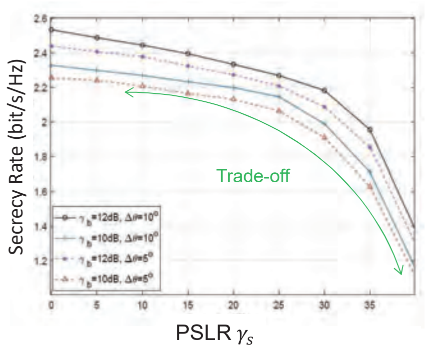

N. Su, F. Liu, C. Masouros, "Secure Radar-Communication Systems with Malicious Targets: Integrating Radar, Communications and Jamming Functionalities", IEEE Trans. Wireless Comms., vol. 20, no. 1, pp. 83-95, Jan. 2021

40

Secure DFRC Communication

Exploiting Subcarrier Interference

Spectrally Efficient FDM

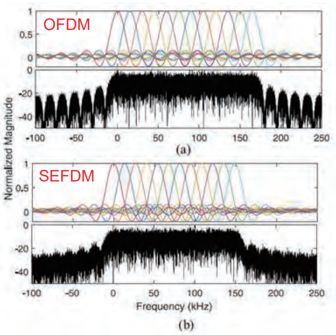

Compression factor $\alpha = \Delta f \cdot T$

$$X_k = \frac{1}{\sqrt{N}} \sum_{n=1}^{N} s_n \exp\left(\frac{j2\pi nk\alpha}{N}\right) = \mathbf{F}S$$

$$R = \mathbf{F}^*(\mathbf{F}S + Z) = \mathbf{C}S + \mathbf{F}^*Z = \mathbf{C}S + Z_{\mathbf{F}^*}$$

$$c_{m,n} = \frac{1}{N} \sum_{k=1}^{N} e^{\frac{j2\pi mk\alpha}{N}} e^{-\frac{j2\pi nk\alpha}{N}} = \left\{ \begin{array}{ll} 1, & m = n \\ \frac{1 - e^{j2\pi\alpha(m-n)}}{N\left(1 - e^{\frac{j2\pi\alpha(m-n)}{N}}\right)}, & m \neq n \end{array} \right\}.$$

$\alpha = 0.9$, QPSK, N_t=6, K=2

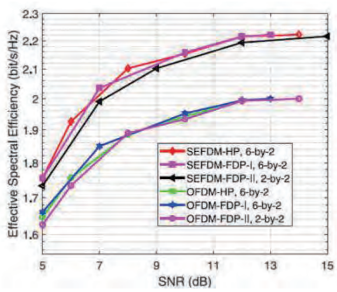

SEFDM: Controllable interference, that can be removed at Rx

T. Xu, C. Masouros, I. Darwazeh "Design and Prototyping of Hybrid Analog Digital Multiuser MIMO Beamforming for Non-Orthogonal Signals", IEEE IoT Journal, vol. 7, no. 3, pp. 1872-1883, March 2020

Non-orthogonal FDM for security

ISAC trade-off for SEFDM

Security by SEFDM:

- Controllable interference, removable at legitimate Rx
- Non-resolvable at Eve

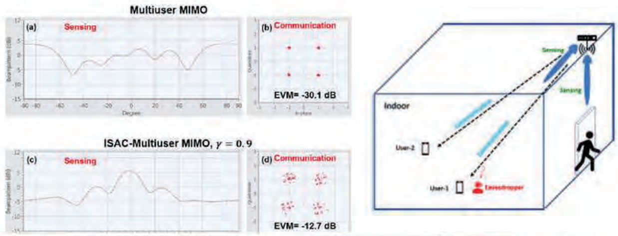

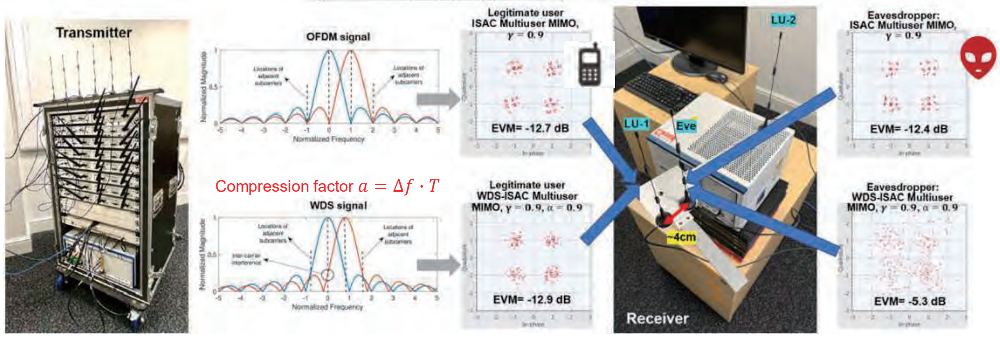

T. Xu, Y. Ye, C. Masouros, “Signal Waveform Design for Resilient Integrated Sensing and Communications” IEEE CSNDSP 2024

43

Secure DFRC Communication

Exploiting Constructive / Destructive Interference

44

Constructive Interference for M-PSK

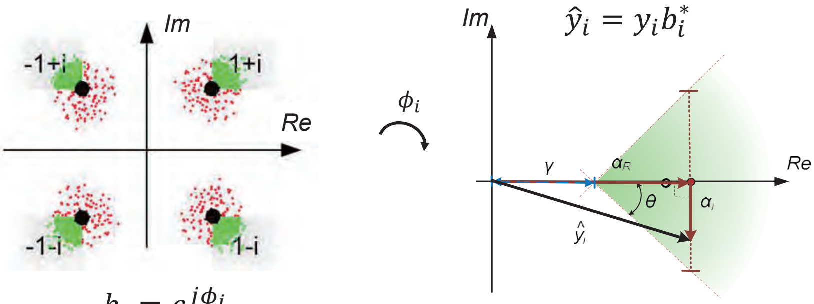

$$b_i = e^{j\phi_i}$$

Constructive Interference:

1. $\alpha_R \geq \gamma$
2. $|\alpha_I| \leq (\alpha_R - \gamma)\tan\theta$

$$\alpha_R = Re(\hat{y}_i),\ \alpha_I = Im(\hat{y}_i)$$

$$\theta = \frac{\pi}{M}, \gamma = \sqrt{\Gamma_i N_0}$$

C. Masouros and G. Zheng, "Exploiting Known Interference as Green Signal Power for Downlink Beamforming Optimization", IEEE Trans. Sig. Proc., vol.63, no.14, pp.3668-3680, July, 2015

A. Li, *et. al*, "A Tutorial on Interference Exploitation via Symbol-Level Precoding: Overview, State-of-the-Art and Future Directions", IEEE Comms. Surveys and tutorials., vol. 22, no. 2, pp. 796-839, 2020

45

Exploiting Interference for Secure DFRC

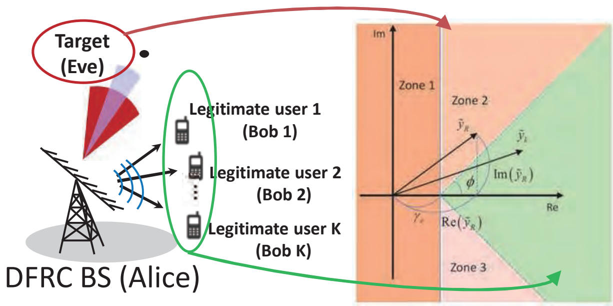

$$\max_{\mathbf{x}} \min_{\theta_p \in \mathrm{card}(\Psi)} \frac{\mu \left|\mathbf{w}^H \mathbf{U}(\theta_p)\mathbf{x}\right|^2}{\mathbf{w}^H(\mathbf{\Sigma}(\mathbf{x}) + \mathbf{I}_{N_R})\mathbf{w}} \quad (38a)$$ ← Radar SNR

$$\text{s.t.} \quad \|\mathbf{x}\|^2 \leq P_0 \quad (38b)$$

$$\left|\mathrm{Im}\left(\tilde{\mathbf{h}}_k^H \mathbf{x}\right)\right| \leq \left(\mathrm{Re}\left(\tilde{\mathbf{h}}_k^H \mathbf{x}\right) - \sqrt{\sigma_{C_k}^2 \Gamma_k}\right)\tan\phi, \forall k \quad (38c)$$ ← Constructive interference to users

$$\left|\mathrm{Im}\left(\alpha_0 \tilde{\mathbf{a}}_t^H(\beta_p)\mathbf{x}\right)\right| \geq \left(\mathrm{Re}\left(\alpha_0 \tilde{\mathbf{a}}_t^H(\beta_p)\mathbf{x}\right) - \sqrt{\sigma_T^2 \Gamma_T}\right)\tan\phi, \forall p, \quad (38d)$$ ← Destructive interference to target (Eve)

N. Su, F. Liu, Z. Wei, Y. Liu, C. Masouros, "Secure Dual-Functional Radar-Communication Transmission: Exploiting Interference for Resilience Against Target Eavesdropping", IEEE Trans. Wireless Comms. *vol. 21, no. 9, pp. 7238-7252, Sept. 2022*

46

Results

N = 10 antennas, K = 5 legitimate users, one target.

Signal Constellations at users / target

Constructive interference

Constructive - Destructive interference

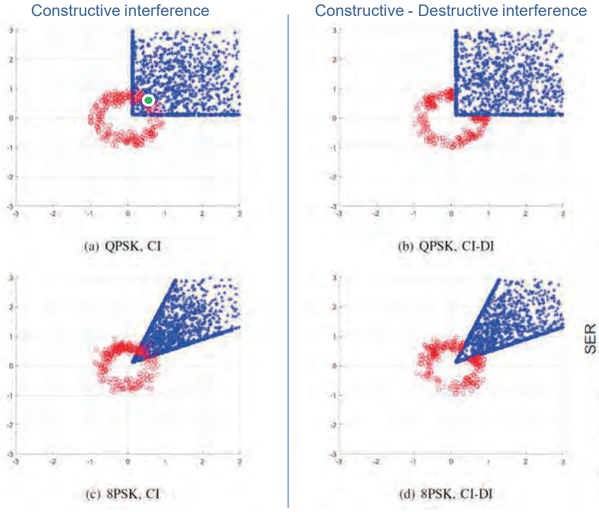

Radar beampattern

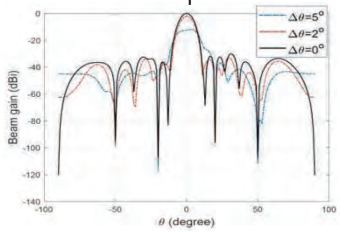

SER at users / target

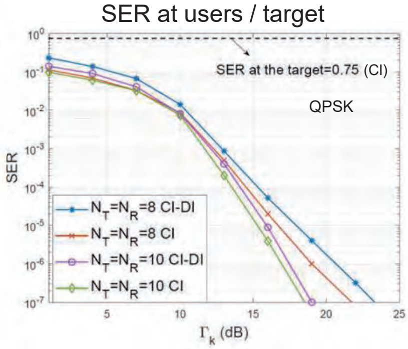

N. Su, F. Liu, Z. Wei, Y. Liu, C. Masouros, "Secure Dual-Functional Radar-Communication Transmission: Exploiting Interference for Resilience Against Target Eavesdropping", IEEE Trans. Wireless Comms. *vol. 21, no. 9, pp. 7238-7252, Sept. 2022*

47

Secure DFRC

Securing the Sensing

48

DFRC Infrastructure: Opportunity for Malicious Sensing

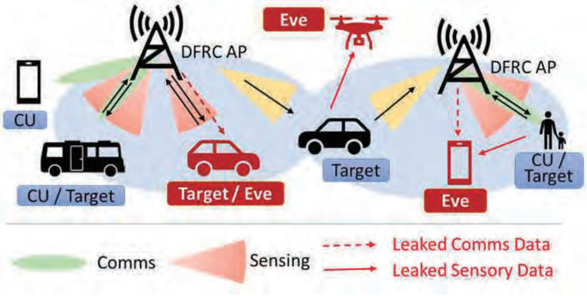

- Need to secure both Communications and Sensing Functionalities
  - Secure DFRC Communication
  - Secure DFRC Sensing

49

Mutual information gap maximization (without artificial noise)

$\mathbf{X} = \mathbf{WS}$ ($\mathbf{W}$: beamforming matrix; $\mathbf{S}$: symbol matrix)

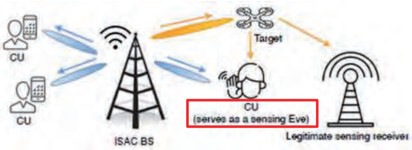

Mutual information with perfectly known reference signal

Legitimate receiver: $I_r(\mathbf{Y}_r;\mathbf{H}_{tr}|\mathbf{X}) = \log\det(\mathbf{I}+\sigma_r^{-2}\mathbf{R}_{h_r}(\mathbf{X}^*\mathbf{X}^T\otimes\mathbf{I}_{N_r}))$

Eavesdropper: $I_e(\mathbf{Y}_e;\mathbf{H}_e|\mathbf{X}) = \log\det(\mathbf{I}+\sigma_e^{-2}L\mathbf{\Lambda}_e\sum_{i=1}^{N_e}\mathbf{Q}_i\mathbf{R}_{\mathbf{X}}^*\mathbf{Q}_i^H)$

$$
\begin{aligned}
\max_{\{\mathbf{W}_k\}_{k=1}^{K}}\ & I_r = \log\det\left(\mathbf{I}+\sigma_r^{-2}L\mathbf{\Lambda}_r\sum_{i=1}^{N_r}\mathbf{P}_i\mathbf{R}_{\mathbf{X}}^*\mathbf{P}_i^H\right)\\
\text{s.t. } & I_e = \log\det\left(\mathbf{I}+\sigma_e^{-2}L\mathbf{\Lambda}_e\sum_{i=1}^{N_e}\mathbf{Q}_i\mathbf{R}_{\mathbf{X}}^*\mathbf{Q}_i^H\right)\le\epsilon,\\
& \operatorname{tr}(\mathbf{R}_{\mathbf{X}})\le P_0,\\
& \frac{\operatorname{tr}(\mathbf{h}_k\mathbf{W}_k\mathbf{h}_k^H)}{\sum_{k=1,k\neq i}^{K}\operatorname{tr}(\mathbf{h}_k\mathbf{W}_i\mathbf{h}_k^H)+\sigma_c^2}\ge\gamma_k,\forall k,\\
& \mathbf{R}_{\mathbf{X}}=\sum_{k=1}^{K}\mathbf{W}_k,\ \mathbf{W}_k\succeq 0,\ \operatorname{rank}(\mathbf{W}_k)=1,\forall k,
\end{aligned}
$$

$\mathbf{\Lambda}_r, \mathbf{P}_i \leftarrow$ *Eigendecomposition of* $\mathbf{R}_{h_r}$

$\mathbf{\Lambda}_e, \mathbf{Q}_i \leftarrow$ *Eigendecomposition of* $\mathbf{R}_{h_e}$

J. Zou, C. Masouros, F. Liu, S. Sun, “Securing the Sensing Functionality in ISAC Networks: An Artificial Noise Design”, IEEE Trans. Veh. Tech., in press

50

Mutual information gap maximization (with artificial noise)

UCL

$\mathbf{X} = \mathbf{WS} + \mathbf{N}$ ($\mathbf{W}$: beamforming matrix; $\mathbf{S}$: symbol matrix; $\mathbf{N}$: artificial noise matrix;)

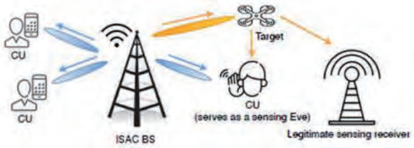

Mutual information with perfectly known reference signal

$$I_r(\mathbf{Y}_r;\mathbf{H}_{tr}|\mathbf{X}) = \log\det\left(\mathbf{I} + \sigma_r^{-2} L \Lambda_r \sum_{i=1}^{N_r} \mathbf{P}_i (\mathbf{R}_{\mathbf{X}}^{*} + \mathbf{R}_{\mathbf{N}}^{*}) \mathbf{P}_i^H\right)$$

$$I_e(\mathbf{Y}_e;\mathbf{H}_e|\mathbf{X}) = \frac{1}{J}\sum_{j=1}^{J} \log\det\left(2\pi e L \mathbf{K}(\mathbf{I}_{N_e} \otimes \mathbf{R}_{\mathbf{N}}^{*})\mathbf{K}^T \mathbf{h}_{e,j}\mathbf{h}_{e,j}^H + \sigma_e^2 \mathbf{I}\right)$$

$$\begin{aligned}
&\max_{\{\mathbf{W}_k\}_{k=1}^{K}, \mathbf{R}_{\mathbf{N}}} \quad I_r(\mathbf{Y}_r;\boldsymbol{\theta}_r|\mathbf{X},\mathbf{N}) \\
&\text{s.t. } \bar{I}_e \le \epsilon, \\
&\quad \frac{\mathrm{tr}(\mathbf{h}_k \mathbf{W}_k \mathbf{h}_k^H)}{\sum_{k=1,k\neq i}^{K} \mathrm{tr}(\mathbf{h}_k \mathbf{W}_i \mathbf{h}_k^H) + \mathbf{h}_k \mathbf{R}_{\mathbf{N}} \mathbf{h}_k^H + \sigma_c^2} \ge \gamma_k, \forall k, \\
&\quad \mathrm{tr}\left(\sum_{k=1}^{K} \mathbf{W}_k + \mathbf{R}_{\mathbf{N}}\right) \le P_0, \\
&\quad \mathbf{R}_{\mathbf{X}} = \sum_{k=1}^{K} \mathbf{W}_k, \mathbf{W}_k \succeq 0, \mathrm{rank}(\mathbf{W}_k) = 1, \forall k,
\end{aligned}$$

J. Zou, C. Masouros, F. Liu, S. Sun, "Securing the Sensing Functionality in ISAC Networks: An Artificial Noise Design", IEEE Trans. Veh. Tech., in press

51

Simulation results

UCL

N_t: 6, SNR_{com}= 28dB, K=3, 1 target

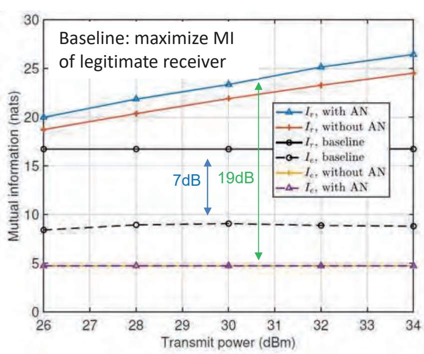

N_t: 6, P_t= 30dBm, K=3, 1 target

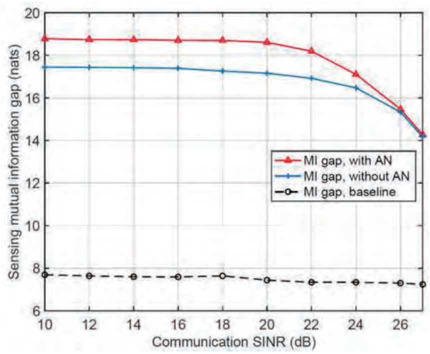

- MI Gap increases with secure sensing transmission
- Trade-off between **Secure Sensing** vs **Comms** performance

52

Secure DFRC Synergies

Sensing-Assisted Data Security

53

Exploiting the Sensing functionality for Secure DFRC

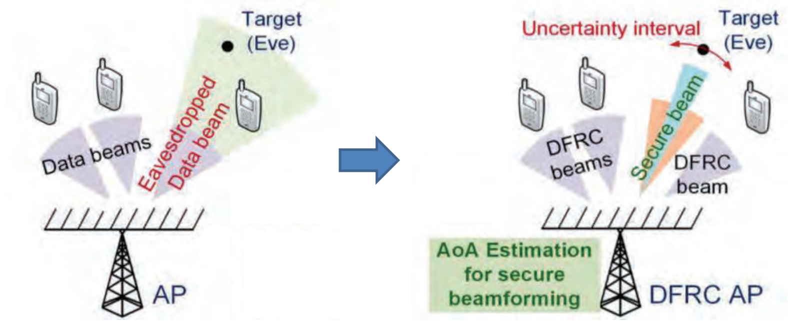

Eve-unaware transmission

Sensing-assisted Secure transmission

- Synergy with One end-goal: Secure Comms – not separate Comms vs Sensing
- New analytical framework where Eve's info is subject to sensing performance (MSE,CRB,…)

N. Su, F. Liu, C. Masouros, "Sensing-Assisted Eavesdropper Estimation: An ISAC Breakthrough in PHY Security", IEEE Trans. Wireless Comms., in press

54

Exploiting the Sensing functionality for Secure DFRC

Stage 1: Initial Eve's estimation (without comms)

$$\max_{\tilde{\mathbf{W}}_i, \mathbf{R}_N} |\mathbf{J}|$$

$$\text{s.t. } \mathbf{R}_N \succeq 0, \tilde{\mathbf{W}}_i \succeq 0, \forall i$$

$$\mathrm{tr}\left(\sum_{i=1}^{I} \tilde{\mathbf{W}}_i + \frac{1}{L}\mathbf{R}_N\right) = P_0.$$

Radar Fisher information matrix

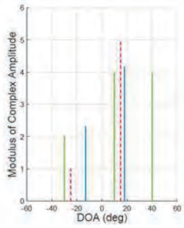

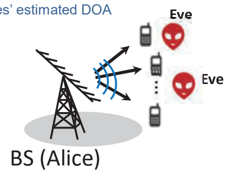

Stage 2 (iterative): DFRC for Eve's estimation refinement + secure comms

$$\max_{\tilde{\mathbf{W}}_i, \mathbf{R}_N} \rho \frac{|\mathbf{J}|}{|\mathbf{J}|_{UB}} + (1-\rho)\frac{\mathrm{SR}}{\mathrm{SR}_{UB}}$$

PSRL

$$\text{s.t. } \mathbf{a}^H(\vartheta_{k,0})\mathbf{R}_X\mathbf{a}(\vartheta_{k,0}) - \mathbf{a}^H(\vartheta_{k,p})\mathbf{R}_X\mathbf{a}(\vartheta_{k,p}) \geq \gamma_s,$$
$$\forall \vartheta_{k,p} \in \mathrm{card}(\Psi_k), \forall k$$

$$\mathrm{SR} = \min_{i,k,n}\left[R_{C_i}\left(\tilde{\mathbf{W}}_i, \mathbf{R}_N\right) - \log\left(1 + \frac{|\alpha_k|^2 \mathbf{a}^H(\vartheta_{k,n})\sum_{i=1}^{I}\tilde{\mathbf{W}}_i\mathbf{a}(\vartheta_{k,n})}{\frac{1}{L}|\alpha_k|^2\mathbf{a}^H(\vartheta_{k,n})\mathbf{R}_N\mathbf{a}(\vartheta_{k,n}) + \sigma_R^2}\right)\right]^+,$$

Function of Eve's uncertainty: $\vartheta_{k,n} \in \mathrm{card}(\Omega_k), \forall k$

Main beam

$$\mathbf{a}^H(\vartheta_{k,n})\mathbf{R}_X\mathbf{a}(\vartheta_{k,n}) \leq (1+\alpha)\mathbf{a}^H(\vartheta_{k,0})\mathbf{R}_X\mathbf{a}(\vartheta_{k,0}), \forall \vartheta_{k,n} \in \mathrm{card}(\Omega_k), \forall k$$

$$\mathbf{a}^H(\vartheta_{k,n})\mathbf{R}_X\mathbf{a}(\vartheta_{k,n}) \geq (1-\alpha)\mathbf{a}^H(\vartheta_{k,0})\mathbf{R}_X\mathbf{a}(\vartheta_{k,0}), \forall \vartheta_{k,n} \in \mathrm{card}(\Omega_k), \forall k$$

$$\mathrm{tr}\left(\sum_{i=1}^{I}\tilde{\mathbf{W}}_i + \frac{1}{L}\mathbf{R}_N\right) = P_0, \quad \mathbf{R}_N \succeq 0, \tilde{\mathbf{W}}_i \succeq 0, \forall i$$

- ↑ Eve's estimation → ↓ uncertainty
- ↑ DoF for secure transmission →
- ↑ Resources for Eve's estimation refinement
- ➢ Iterative estimation that improves performance of secure transmission

N. Su, F. Liu, C. Masouros, "Sensing-Assisted Eavesdropper Estimation: An ISAC Breakthrough in PHY Security", IEEE Trans. Wireless Comms., vol. 23, no. 4, pp. 3162-3174, April 2024

55

Results - K = 3 legitimate users, L = 2 Eves/targets

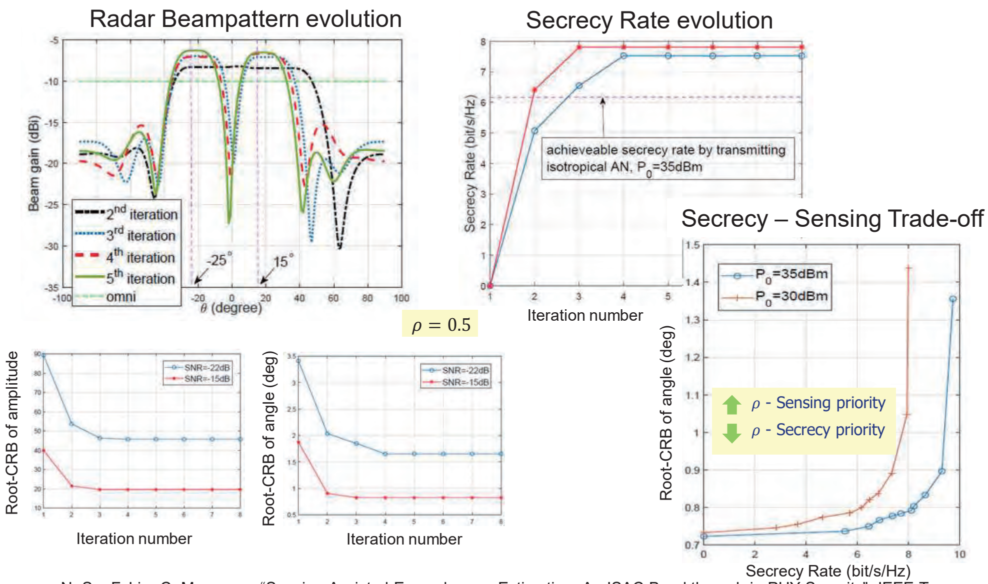

N. Su, F. Liu, C. Masouros, "Sensing-Assisted Eavesdropper Estimation: An ISAC Breakthrough in PHY Security", IEEE Trans. Wireless Comms., vol. 23, no. 4, pp. 3162-3174, April 2024

56

Conclusion

UCL

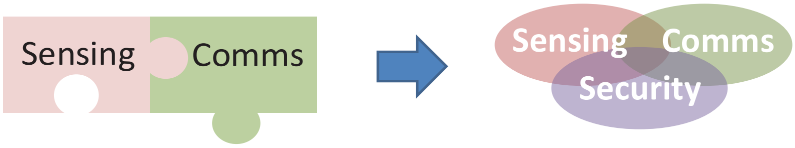

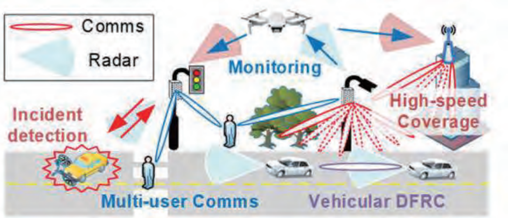

57

UCL

ISAC book

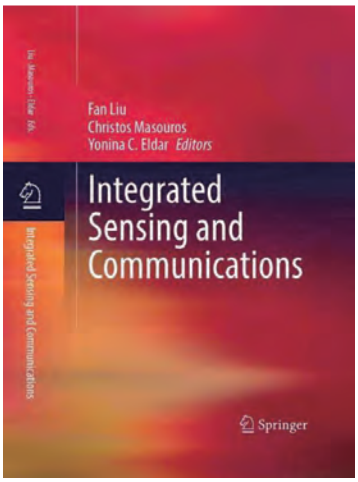

IEEE ComSoc ISAC ETI

ISAC ETSI ISG

ISAC TWG

ISAC ET

58

UCL

Thank you

Fan Liu | Ang Li | Murat Temiz | Kaitao Meng | Iman Vailulahi | Nanchi Su | Abdel Salem | Zhongxiang Wei | Jianjun Zhang | Abdullahi Mohammad | Jiaqi Zhou | Kawon Han | Tongyang Xu | Nial Peters

UDRC Project
Mar 2019 – Dec 2021 (£1m)

Marie Curie Fellowships
Jan 2024 – Jan 2026,
Jun 2023 – Oct 2025 (£650k)

MoD DASA Project
Oct 2023 – Mar 2024 (£100k)

6GMUSICAL
Jan 2024 – Jan 2027 (€4.4m)

ISLANDS Doctoral Network
Jan 2024 – Jan 2028 (€2.7m)

PAINLESS Doctoral Network
Oct 2018 – Sep 2022 (€4.2m)

59

References

UCL

Overviews

1. F. Liu, Y. Cui, C. Masouros, J. Xu, T. X. Han, A. Hassanien, Y. Eldar, S. Buzzi, “Integrated Sensing and Communications: Towards Future Dual-functional Wireless Networks”, IEEE Journal on Sel. Areas Comms., vol. 40, no. 6, pp. 1728-1767, June 2022
2. Z. Wei, F. Liu, C. Masouros, N. Su, A. Petropulu, “Towards Multi-Functional 6G Wireless Networks: Integrating Sensing, Communication and Security” IEEE Wireless Comms Mag., vol. 60, no. 4, pp. 65-71, April 2022
3. J. A. Zhang, F. Liu, C. Masouros, R. W. Heath, Z. Feng, L. Zheng, A. Petropulu, “An Overview of Signal Processing Techniques for Joint Communication and Radar Sensing” IEEE Jour. Selected Topics Sig Proc, vol. 15, no. 6, pp. 1295-1315, Nov. 2021
4. F. Liu and C. Masouros, "A Tutorial on Joint Radar and Communication Transmission for Vehicular Networks - *Parts I - III*", IEEE Commun. Lett., vol. 25, no. 2, pp. 322-336, Feb. 2021 *- EiC Invited Paper*
5. F. Liu, C. Masouros, H. Griffiths, A. Petropulu, and L. Hanzo, “Joint Radar and Communication Design: Applications, State-of-the-art, and the Road Ahead”, IEEE Trans Commun., vol. 68, no. 6, pp. 3834-3862, June 2020. *– EiC invited paper*

Book

6. F. Liu, C. Masouros, Y. Eldar, “Integrated Sensing and Communications”, 2023 edition Springer

Radar-Comms Coexistence

7. F. Liu, A. Garcia, C. Masouros, and G. Geraci, “Interfering Channel Estimation in Radar-Cellular Coexistence: How Much Information Do We Need?”, IEEE Trans. Wireless Comm., vol. 18, no. 9, pp. 4238-4253, Sept. 2019
8. F. Liu, C. Masouros, A. Li, T. Ratnarajah and J. Zhou, “MIMO Radar and Cellular Coexistence: A Power-Efficient Approach Enabled by Interference Exploitation”, IEEE Trans. Sig Proc, vol. 66, no. 14, pp. 3681-3695, July 2018,
9. F. Liu, C. Masouros, A. Li, and T. Ratnarajah, "Robust MIMO Beamforming for Cellular and Radar Coexistence," IEEE Wireless Commun. Lett., vol. 6, no. 3, pp. 374-377, June 2017.
10. F. Liu, L. Zhou, C. Masouros, A. Li, A. Petropulu, “Dual-functional cellular and radar transmission: Beyond co-existence”, IEEE SPAWC 2018

60

References

Dual-functional Radar-Communication

11. I. Valiulahi, A. Salem, C. Masouros, "Net-Zero Energy Dual-Functional Radar and Communication Systems", IEEE Trans. Green Comms. Networks, under review
12. M. Al-Jarrah, E. Alsusa, C. Masouros, "A Uniform Performance Framework for Integrated Sensing-Communications based on KL-Divergence", IEEE Trans. Wireless Comms, under review
13. X. Jing, F. Liu, C. Masouros, Y. Zeng, "ISAC from the Sky: UAV Trajectory Design for Joint Communication and Target Localization", IEEE Trans Wireless Comms, under review
14. A. Salem, C. Masouros, F. Liu, D. Lopez Perez, "Rethinking Dense Cells for Integrated Sensing and Communications: A Stochastic Geometric View" IEEE Trans. Wireless Comms., under review
15. F. Liu, Y. Liu, A. Li, C. Masouros, Y. Eldar, "Cramér-Rao Bound Optimization for Joint Radar-Communication Design", IEEE Trans. Sig. Proc., vol. 70, pp. 240-253, 2022
16. L. Chen, F. Liu, W. Wang, and C. Masouros, "Joint Radar-Communication Transmission: A Generalized Pareto Optimization Framework", IEEE Trans. Signal Process., vol. 69, pp. 2752-2765, 2021.
17. F. Liu, C. Masouros, T. Ratnarajah, and A. Petropulu, "On Range Sidelobe Reduction for Dual-functional Radar-Communication Waveforms", IEEE Wireless Commun. Lett., 2020.
18. F. Liu, C. Masouros, A. Li, H. Sun, and L. Hanzo, "MU-MIMO Communications and MIMO Radar: From Co-existence to Joint Transmission", IEEE Trans. Wireless Commun., vol. 17, no. 4, pp. 2755-2770, April 2018
19. F. Liu, L. Zhou, C. Masouros, A. Li, W. Luo, and A. Petropulu, "Toward Dual-functional Radar-Communication Systems: Optimal Waveform Design," IEEE Trans Signal Process., vol. 66, no. 16, pp. 4264-4279, Aug. 2018.

Hardware-efficient DFRC Transmission

20. I. Valiulahi, A. Salem, C. Masouros, F. Liu "Antenna Selection for Energy-Efficient Dual-Functional Radar-Communication Systems", IEEE Wireless Comms. Let., vol. 11, no. 4, pp. 741-745, April 2022
21. X. Hu, C. Masouros, F. Liu, R. Nissel, "MIMO-OFDM Dual-Functional Radar-Communication Systems: Low-PAPR Waveform Design", IEEE Trans. Comms, under review
22. O. Dizdar, A. Kaushik, B. Clerckx, C. Masouros, "Rate-Splitting Multiple Access for Joint Radar-Communications with Low-Resolution DACs", IEEE Trans. Coms., vol. 15, no. 6, pp. 1332-1347, Nov. 2021

61

References

Secure DFRC Transmission

23. N. Su, F. Liu, C. Masouros, "Sensing-Assisted Eavesdropper Estimation: An ISAC Breakthrough in PHY Security", IEEE Trans. Wireless Comms., under review
24. N. Su, F. Liu, Z. Wei, Y. Liu, C. Masouros, "Secure Dual-Functional Radar-Communication Transmission: Exploiting Interference for Resilience Against Target Eavesdropping", IEEE Trans. Wireless Comms., vol. 21, no. 9, pp. 7238-7252, Sept. 2022
25. N. Su, F. Liu, and C. Masouros, "Secure Radar-Communication Systems with Malicious Targets: Integrating Radar, Communications and Jamming Functionalities", IEEE Trans. Wireless Comm., *vol. 20, no. 1, Jan. 2021*
26. Z. Wei, F. Liu, C. Masouros, N. Su, A. Petropulu, "Towards Multi-Functional 6G Wireless Networks: Integrating Sensing, Communication and Security" IEEE Wireless Comms Mag., vol. 60, no. 4, pp. 65-71, April 2022

Vehicular DFRC Transmission

27. Z. Du, F. Liu, W. Yuan, C. Masouros, Z. Zhang, G. Caire, "Integrated Sensing and Communications for V2I Networks: Dynamic Predictive Beamforming for Extended Vehicle Targets", IEEE Trans. Wireless Comms., in press
28. W. Yuan, F. Liu, C. Masouros, J. Yuan, D. W. K. Ng, and N. G. Prelcic, "Bayesian Predictive Beamforming for Vehicular Networks: A Low-Overhead Joint Radar-Communication Approach", IEEE Trans. Wireless Commun., vol. 20, no. 3, pp. 1442-1456, March 2021
29. F. Liu, W. Yuan, C. Masouros, and J. Yuan, "Radar-assisted Predictive Beam-forming for Vehicular Links: Communication Served by Sensing", IEEE Trans. Wireless Commun., vol. 19, no 11, pp. 7704-7719, Nov. 2020
30. W. Yuan, F. Liu, C. Masouros, J. Yuan, and D. W. K. Ng, "Joint Radar-Communication Based Bayesian Predictive Beamforming for Vehicular Networks", IEEE RadarConf 2020, Special Session on Multi-Function Spectral System Co-Design – *Invited paper*
31. C. Aydogdu, F. Liu, C. Masouros, H. Wymeersch, and M. Rydström, "Distributed Radar-aided Vehicle-to-Vehicle Communication", IEEE RadarConf 2020.
32. F. Liu, W. Yuan, C. Masouros, and J. Yuan, "Radar-assisted Predictive Beamforming for Vehicle-to-Infrastructure Links", IEEE ICC 2020, Workshop on Communication and Radar Spectrum Sharing

DFRC experiments

33. T. Xu, F. Liu, C. Masouros, I. Darwazeh, "An Experimental Proof of Concept for Integrated Sensing and Communications Waveform Design", IEEE Open Journal ComSoc, IEEE Open Journal of Comms. Soc., vol. 3, pp. 1643-1655, 2022
34. M. Temiz, N. Peters, C. Horne, M. Ritchie, C. Masouros, "An Experimental Study of Radar-Centric Transmission for Integrated Sensing and Communications", IEEE Transactions on Microwave Theory and Techniques, vol. 71, no. 7, pp. 3203-3216, July 2023

62

Novel Wireless Communication System Realized by Mobile Terminal Collaboration

Hidekazu Murata
Graduate School of Sciences and Technology for Innovation
Yamaguchi University, Japan
muratahidekazu@yamaguchi-u.ac.jp

This talk introduces a transmission/reception technique based on mobile terminal collaboration that equivalently increases the number of antennas by sharing received signals among mobile terminals. To overcome the shortage of antennas on the mobile terminal side, multi-user multiple-input multiple-output (MIMO) transmission has been studied. However, the accuracy of precoding degrades in mobile environments. On the other hand, terminal collaboration systems, in which terminals collaborate to increase the equivalent number of antennas, eliminate the need for precoding and are therefore suitable for mobile environments. The terminal collaboration system requires high-speed and low-latency communications over short distances, making the use of high-frequency bands suitable. This terminal collaboration system has the potential to effectively expand the number of MIMO signal streams in the so-called platinum band by utilizing the high-frequency bands. In this presentation, we describe recent research results on the terminal collaboration system and its potential application to the uplink.

Acknowledgment

This work was supported in part by JSPS KAKENHI Grant Number JP23H00474.

References

[1] Shunya Morimoto, Hayato Sugai, Hidekazu Murata, Daisuke Murayama, Toshiro Nakahira, Tomoaki Ogawa, "Performance of terminal-collaborated MIMO reception system leveraging multiple decision results," 2024 IEEE 99th Vehicular Technology Conference (VTC2024-Spring), Workshop TPoC6G 2024, Singapore, June 2024.

[2] Hidekazu Murata "[Invited Talk] Mobile terminal collaboration: A spectrum and energy efficient transmission technique for future cellular networks," Proc. 2023 IEEE 97th Vehicular Technology Conference (VTC2023-Spring), Workshop, Florence, Italy, June 2023.

[3] Hokuto Taromaru, Hidekazu Murata, "Performance comparison of error-control schemes in collaborative multiple-input multiple-output systems," Proc. 2022 IEEE 96th Vehicular Technology Conference (VTC2022-Fall), Sept. 2022.

[4] Hokuto Taromaru, Hidekazu Murata, Toshiro Nakahira, Daisuke Murayama, Takatsune Moriyama, "Error control on mobile station sides in collaborative multiple-input multiple-output systems," IEEE Access, Vol. 10, pp. 26493–26500, Mar. 2022.

[5] Hidekazu Murata, "Terminal selection schemes in terminal-collaborated MIMO reception based on subband channel matrices," IEEE Communications Letters, vol. 26, issue 1, pp. 202–206, Jan. 2022.

[6] Fengning Du, Hidekazu Murata, Mampei Kasai, Toshiro Nakahira, Koichi Ishihara, Motoharu Sasaki, Takatsune Moriyama, "Distributed detection of MIMO spatial multiplexed signals in terminal collaborated reception," IEICE Trans. Commun. Vol.E104-B, No.7, pp.884–892, July 2021.

YAMAGUCHI UNIVERSITY

Mathematics for Innovation in Information and Communication Technology

Novel Wireless Communication System Realized by Mobile Terminal Collaboration

Hidekazu Murata

Yamaguchi University

Higher bit rate, more frequency bandwidth

Narrow pulse shape requires more bandwidth

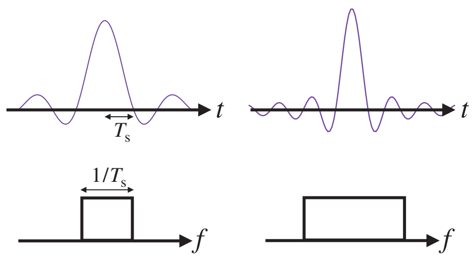

Channel capacity

SISO (Single-Input Single-Output)

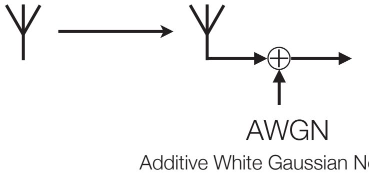

$$C = \log_2(1+\gamma)$$

bits/s/Hz

γ : SNR

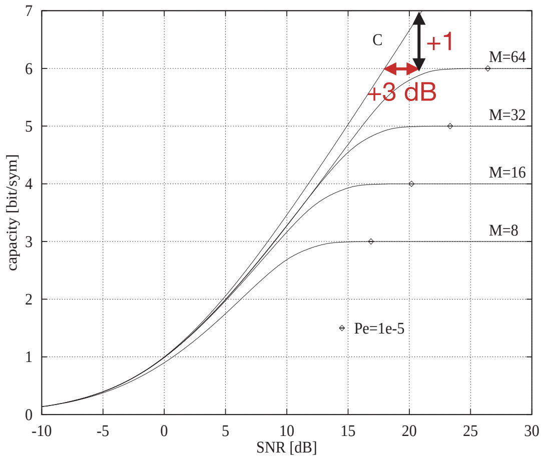

Figure 3.4 Channel capacity for QAM

http://citeseer.ist.psu.edu/viewdoc/download;jsessionid=C3366013A0E7ED3B4F4700A41B6C0DBA?doi=10.1.1.46.186&rep=rep1&type=pdf

Parallel transmission

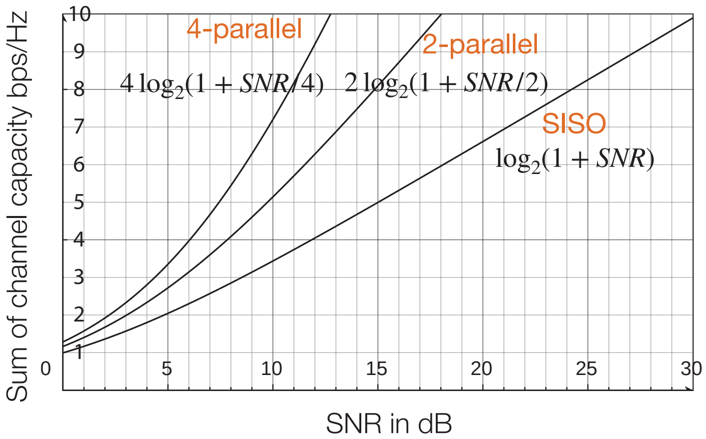

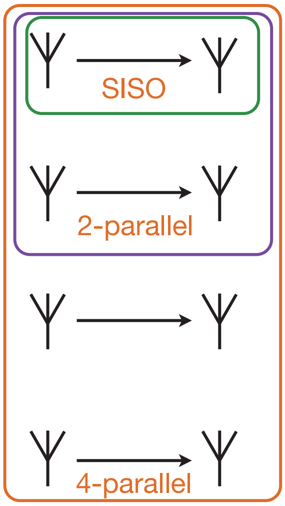

Channel capacity of MIMO

Unknown CSI at transmitter

$$C = \log_2 \det\left(\boldsymbol{I} + \frac{\gamma}{N_{\mathrm{TX}}}\boldsymbol{H}\boldsymbol{H}^{\mathrm{H}}\right)$$

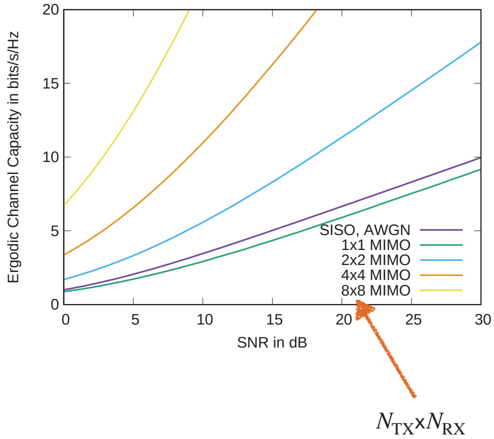

MIMO versus SISO

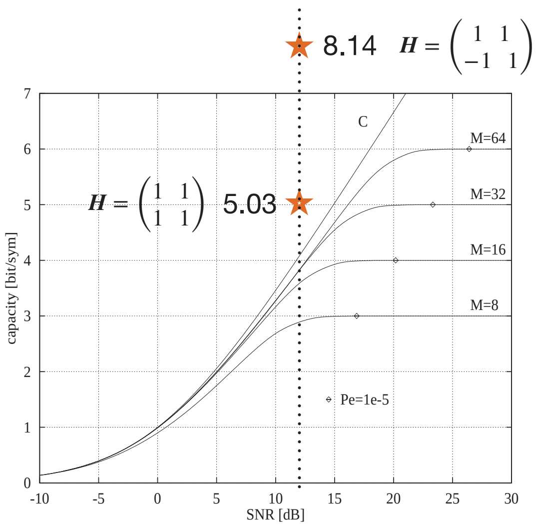

Figure 3.4 Channel capacity for QAM

http://citeseer.ist.psu.edu/viewdoc/download;jsessionid=C3366013A0E7ED3B4F4700A41B6C0DBA?doi=10.1.1.46.186&rep=rep1&type=pdf

Channel capacity of MIMO

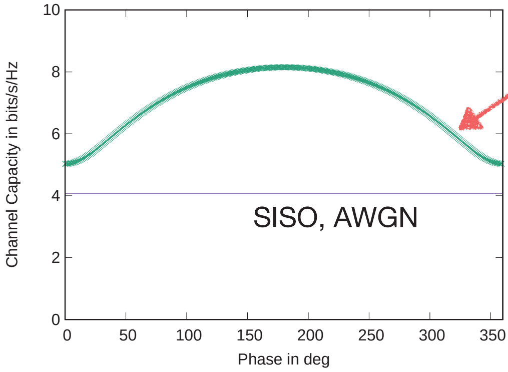

$$\boldsymbol{H} = \begin{pmatrix} 1 & 1 \\ e^{j\theta} & 1 \end{pmatrix}$$

$$\gamma = 12\,\mathrm{dB} = 15.8$$

Channel capacity of MIMO

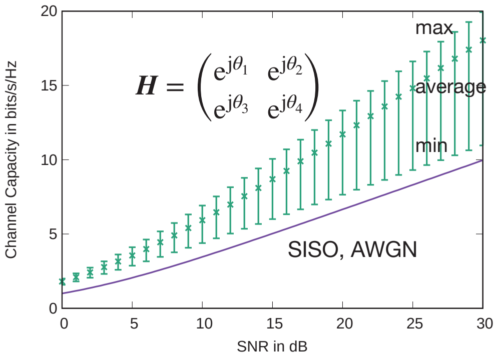

$\theta_1, \theta_2, \theta_3, \theta_4$: independent and uniform

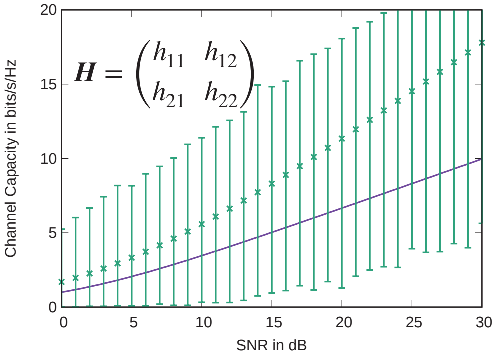

$h_{11}, h_{12}, h_{21}, h_{22}$: i.i.d. Rayleigh

i.i.d. : independent and identically distributed

5G NR and small cell

In 5G, high frequency band is employed.

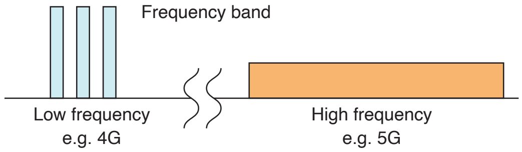

- Low frequency bands: conventional cellular systems
- 5G NR frequency bands: high-speed transmission in small cell

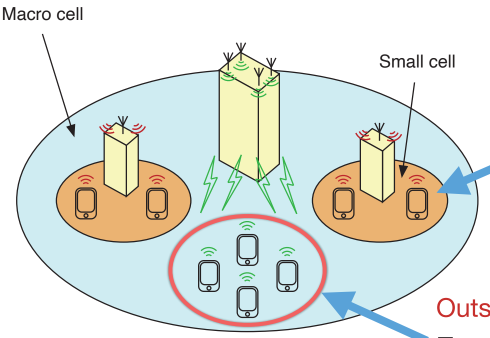

Coverage is limited.

Outside small cell

Transceivers and antennas for 5G NR frequency band are not fully utilized.

9

WIRELESS COMMUNICATION ENGINEERING LABORATORY

Collaborative MIMO reception

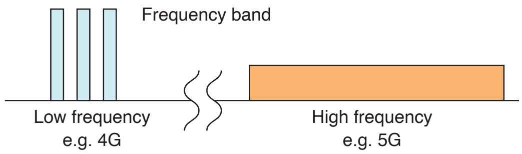

- MSs share own signals with other MSs via higher-frequency bands.
- The number of antennas of each MS can be increased virtually.
- Channel capacity can be increased in proportion to the number of MSs in collaboration.

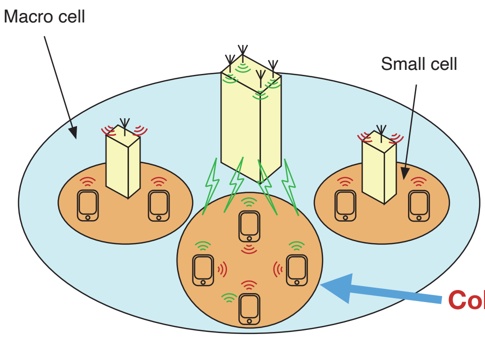

Collaborative MIMO reception

- If MS collaboration is perfect, virtual MS group works as SU-MIMO MS with a number of antennas.

10

Collaborative interference cancellation

Idea: Increase the number of antennas by mobile terminal's collaboration

Technical highlights

- Mobile terminal selection algorithms
- Collaboration techniques via higher frequency band

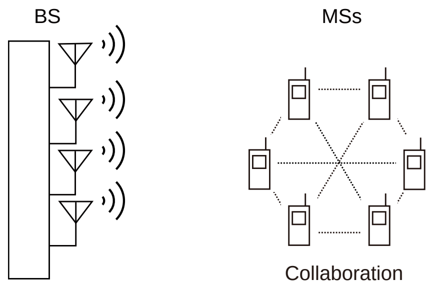

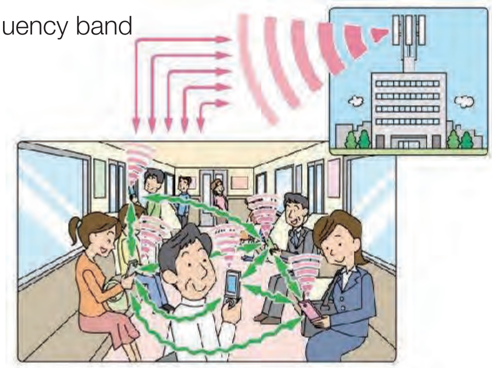

Received signal sharing by high-speed short-range wireless communications

Suitable for bus and train

11

WIRELESS COMMUNICATION ENGINEERING LABORATORY

Collaborative interference cancellation technique

- Collaborative interference cancellation (CIC) can cancel femto/macro interference

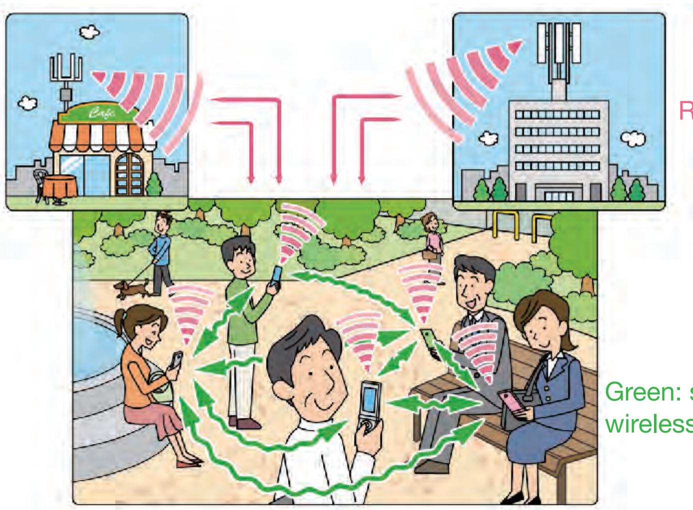

Red: Precious cellular freq.

Green: short-range high-speed wireless communications

12

Field measurements

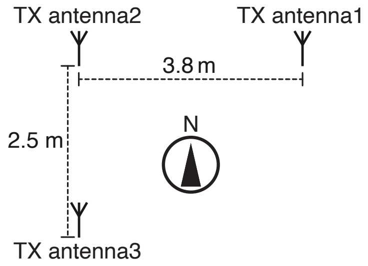

(a) TX antenna setup

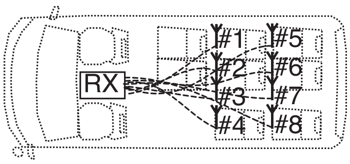

(b) RX antenna setup in vehicle

Hidekazu Murata, Daisuke Umehara, "Collaborative MIMO reception: Measurement campaign and mutual information rate analysis," Proc. 2023 28th Asia Pacific Conference on Communications (APCC), Sydney, New South Wales, Australia, pp. 313-314, Nov. 2023.

WIRELESS COMMUNICATION ENGINEERING LABORATORY

TABLE I
MAJOR PARAMETERS OF MEASUREMENT CAMPAIGN

Parameters	Values
Carrier frequency	427.2 MHz
Number of TX antennas	3
TX antenna	Omnidirectional
TX antenna gain	5.8 dBi
TX antenna height	25.5 m
Cable loss	1.4 dB
Transmit power	1 W per antenna
Packet interval	50 ms
Symbol rate	312.5 ksps
Transmit filter	Square root raised cosine Roll-off factor 0.4
Number of RX antennas	8
RX antenna	Omnidirectional
RX antenna gain	2.15 dBi
RX antenna height	2.1 m

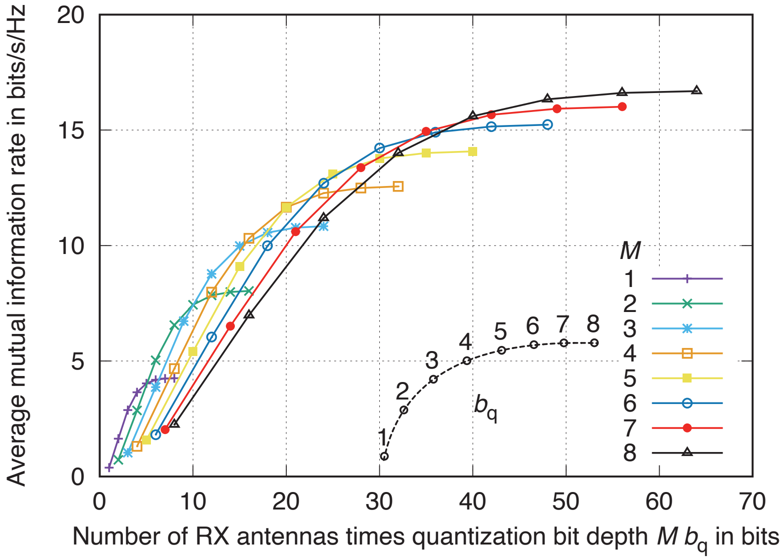

Collaborative MIMO reception

- MS serves as a receive antenna, and/or detector, and/or controller for target MS(s)

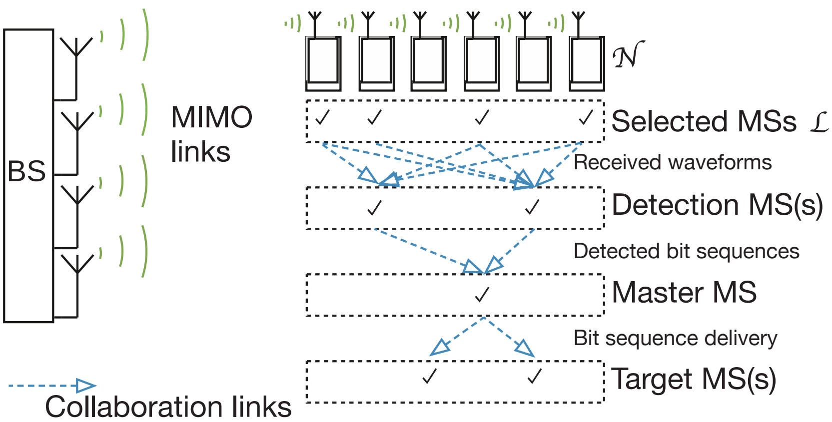

Collaborative MIMO reception

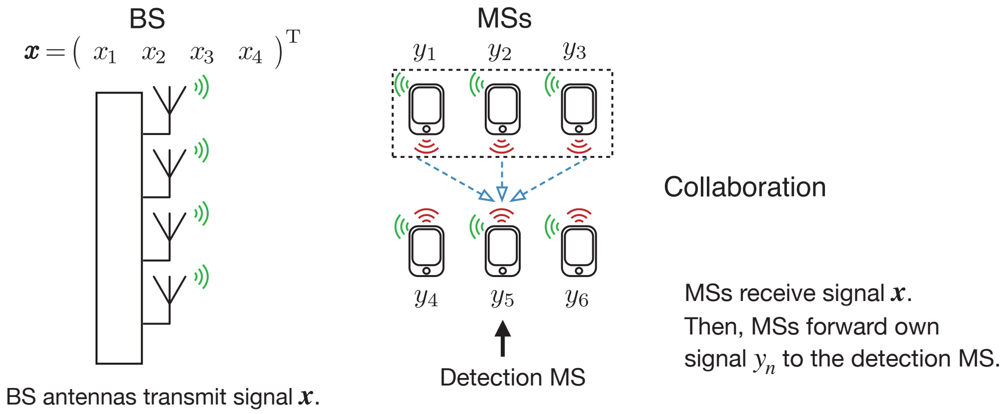

- Detection MS decodes the MIMO signal streams using both the received signals from other MSs y_1, y_2, y_3 and own received signals y_5.

Traffic for collaboration

- Improve the decoding performance while keeping the collaboration traffic as small as possible

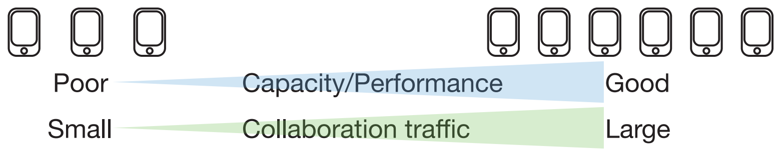

Thanks to broadcast nature of radio signal, other MSs can use y_1, y_2, y_3.

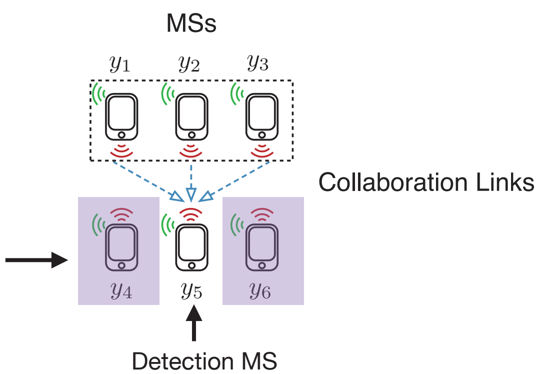

Multiple detection MSs

- If the detected bit sequences at the target MS have low reliability, the target MS requests other detected sequences from other detection MSs.
  - The detected bit sequence with the highest reliability is selected.

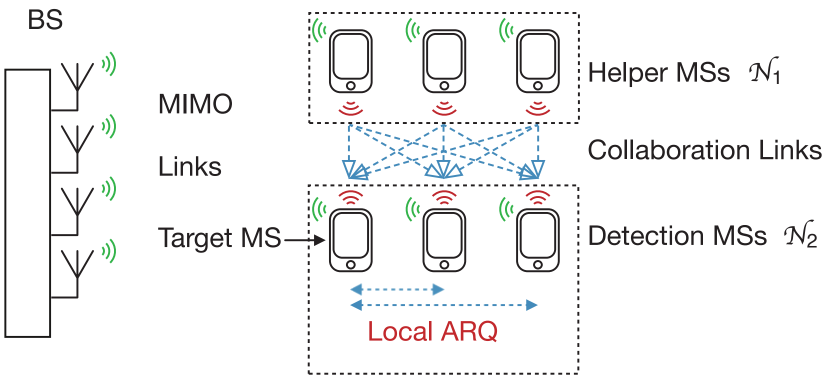

19

WIRELESS COMMUNICATION ENGINEERING LABORATORY

Flow of Local ARQ

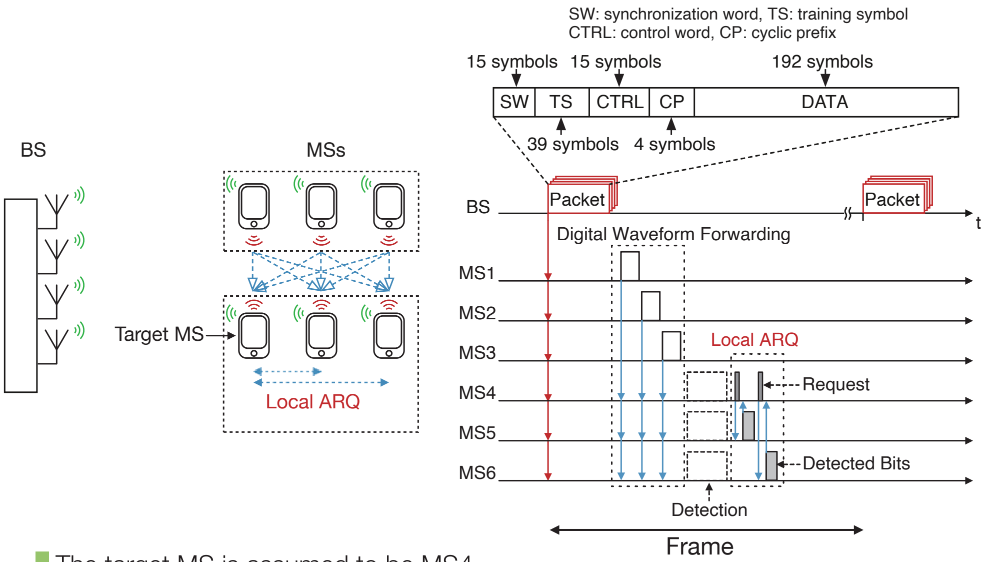

- The target MS is assumed to be MS4.
  - MS5 and MS6 send their detected bit sequences to MS4 upon request.
- The collaboration links are assumed to be error free.

20

Simulation parameters

Parameters	Values
Number of BS antennas	4
Number of MSs	6
Modulation scheme	QPSK
Filter	Square-root Nyquist (roll-off factor = 0.4)
Code	LDPC (rate 1/2)
Code length	384 symbols
Data symbol length	192 symbols
CP length	4 symbols
Equalization	Frequency-domain iterative equalization
Channel model	i.i.d. Rayleigh fading ($f_{\mathrm{D}}T_{\mathrm{s}} = 6.4 \times 10^{-5}$)
Channel estimation	Least-squares

21
21

WIRELESS COMMUNICATION ENGINEERING LABORATORY

Frequency-domain iterative equalization

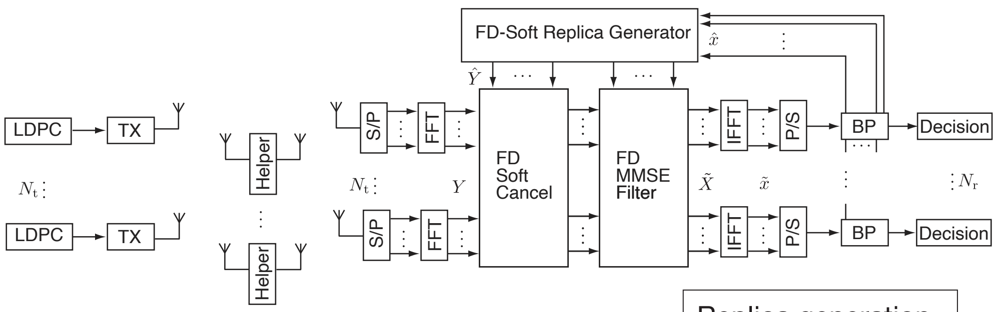

$\boldsymbol{Y}$ Received signal
$\hat{\boldsymbol{Y}}$ Soft-decision replica
$\boldsymbol{g}$ Channel impulse response
$\tilde{X}$ Equalized signal
$\hat{x}$ Soft-decision symbols
β_i Residual interference coefficient

Replica generation

$$\hat{\boldsymbol{Y}}_i(f) = \boldsymbol{g}_i(f)\hat{X}_i(f)$$

MMSE Filter

$$\tilde{X}_n(f) = \boldsymbol{w}_n^{\mathrm{H}}(f)\left\{\boldsymbol{Y}(f) - \sum_{i \neq n} \hat{\boldsymbol{Y}}_i(f)\right\}$$

$$\boldsymbol{w}_n(f) = \left(\boldsymbol{g}_n(f)\boldsymbol{g}_n^{\mathrm{H}}(f) + \sum_{i \neq n} \beta_i \boldsymbol{g}_i(f)\boldsymbol{g}_i^{\mathrm{H}}(f) + \frac{N}{P}\mathbf{I}\right)^{-1} \boldsymbol{g}_n(f)$$

T. Koike, H. Murata, and S. Yoshida, "Frequency-domain SC/MMSE iterative equalizer with MF approximation in LDPC-coded MIMO transmissions," IEEE PIMRC, Sept. 2004.

22

Residual interference coefficients

- Residual interference coefficients
  - Residual interference coefficients indicate the average residual symbol interference after cancellation.

$$\beta_{\mathcal{L},m} = \begin{cases} 0 & \text{Parity-check satisfied} \\ 1 - \underbrace{\frac{1}{K}\sum_k |\hat{x}_m(k)|^2}_{\alpha} & \text{otherwise} \end{cases}$$

$0 \leq |\hat{x}_m(k)| \leq 1$

m : mth stream

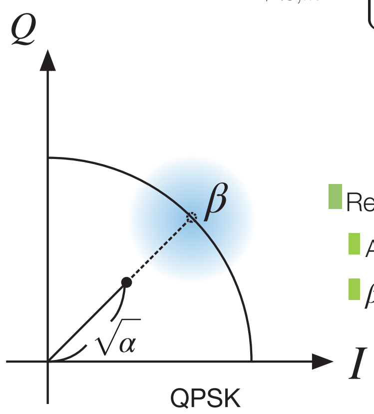

- Residual interference coefficients β
  - Adaptive selection of detected bit sequences based on β.
  - β is utilized in iterative MIMO equalization and detection.

23
23

Two schemes and extra traffic of Local ARQ

4 TDBS

Detected bit sequences

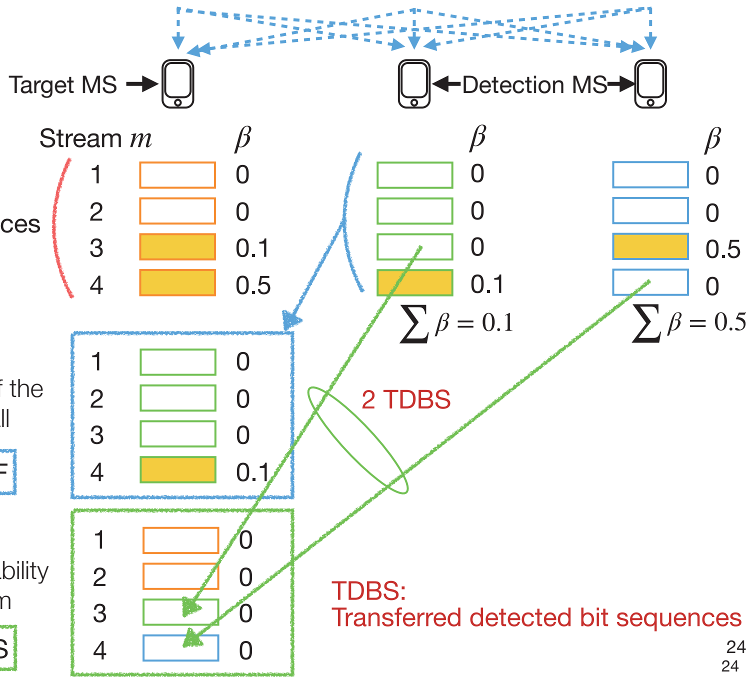

- Per-frame scheme
  - Based on the sum of the reliability metrics of all streams

3DetPF

- Per-stream scheme
  - Based on the reliability metric of each stream

3DetPS

TDBS:
Transferred detected bit sequences

24
24

Best MS subset selection in Local ARQ

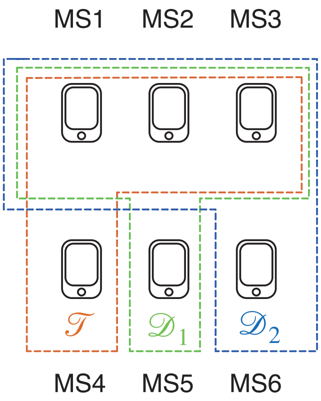

$\mathcal{L}^*$: selected pattern

d-detector per-frame scheme (dDetPF)

$$\mathcal{L}^*_{d\mathrm{DetPF}} = \underset{\mathcal{L} \in \{\mathcal{T}, \mathcal{D}_1, \mathcal{D}_2\}}{\arg\min} \sum_m \beta_{\mathcal{L},m}$$

d-detector per-stream scheme (dDetPS)

$$\mathcal{L}^*_{d\mathrm{DetPS},m} = \underset{\mathcal{L} \in \{\mathcal{T}, \mathcal{D}_1, \mathcal{D}_2\}}{\arg\min} \beta_{\mathcal{L},m}$$

$\mathcal{N}_1$: $N - d$ helper MSs
$\mathcal{N}_2$: $\mathcal{N} \setminus \mathcal{N}_1$ (include d MSs as detection MSs)
m : mth stream at the target MS

25

Average FER and TDBS performance versus SNR

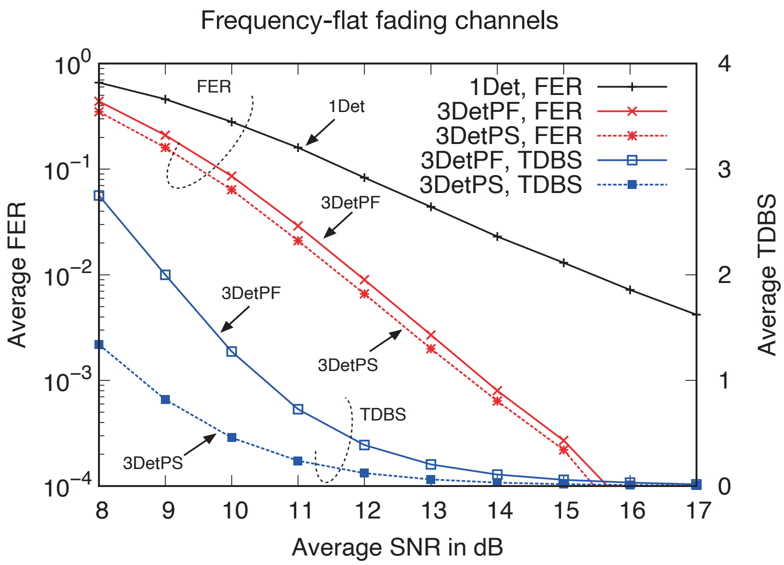

WIRELESS COMMUNICATION ENGINEERING LABORATORY

Average FER and TDBS performance versus SNR

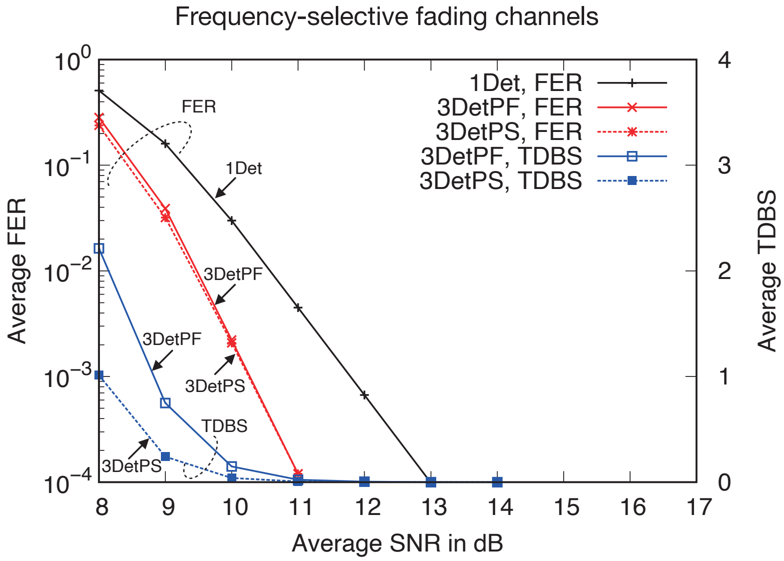

27

WIRELESS COMMUNICATION ENGINEERING LABORATORY

Proof of concept activity

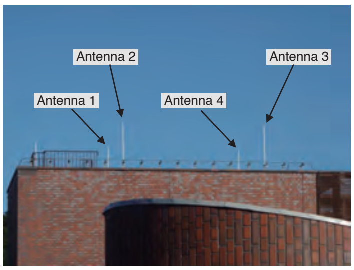

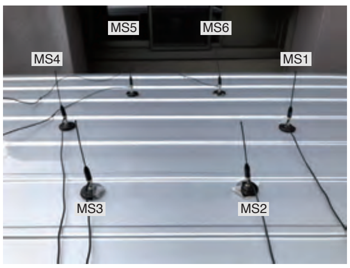

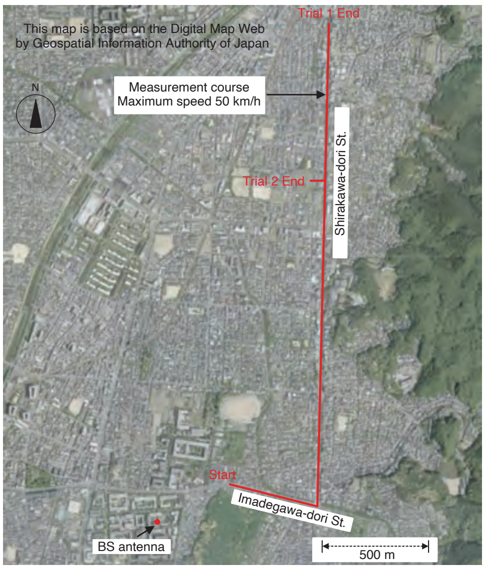

28

Performance comparison

- RIC (Residual interference coefficients)

$$\mathcal{L}^*_{\mathrm{RIC},m} = \underset{\mathcal{L}\in\{\mathcal{T},\mathcal{D}_1,\mathcal{D}_2\}}{\arg\min}\ \beta_{\mathcal{L},m}$$

$\mathcal{L}^*$: selected MS set

m : stream number

- MC (Majority Combining)

- LLR (Log-Likelihood Ratio) combining

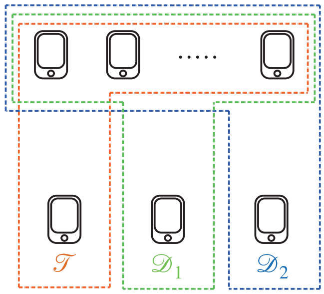

FER performance versus TDBS

Frequency-flat fading channels

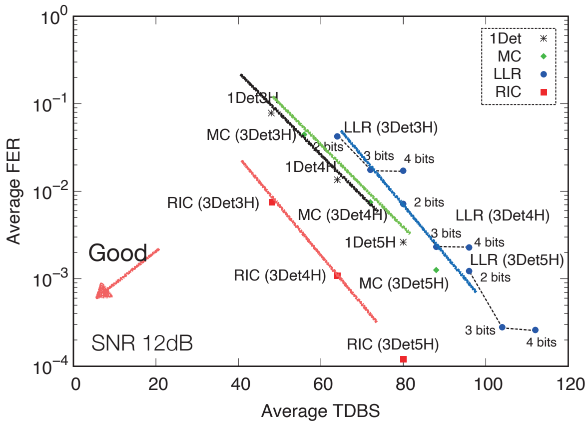

Results of field measurement

- Off-line processing using actual received signals

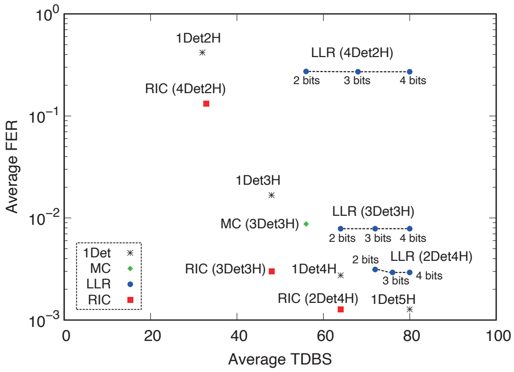

Parameter	Values
Carrier frequency	427.2 MHz
Symbol rate	312.5 ksps
Transmit power of BS	1 W
Number of BS antennas	4
Gain of BS antenna	5.8 dBi
BS antenna height	25.5 m
Cable loss	1.4 dB
Transmit filter	Square root raised cosine Roll-off factor 0.4
Frame interval	50 ms
Number of antennas of each MS	1
Number of MSs	6
Antenna of MS	$\lambda/4$ omnidirectional monopole
MS antenna height	2.1 m

Subband based MS selection

Frequency-selective fading channel, best MS group is not unique.

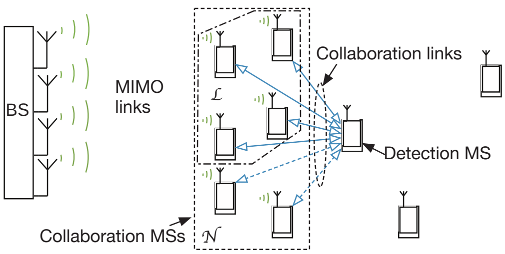

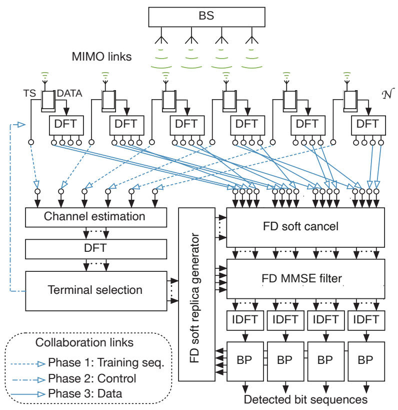

Subband based MS selection

In frequency-selective channel, subband based MS selection improve the performance.

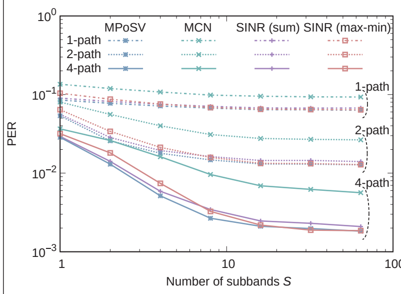

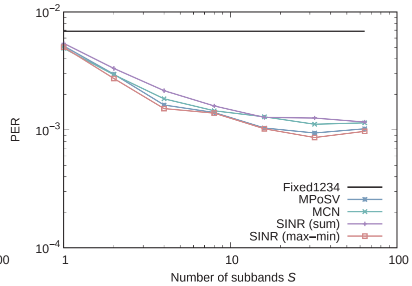

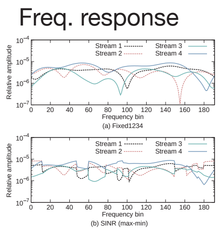

Application to uplink

- Spatial multiplexing (just timing synchronization is required)
- Beam forming, null steering (timing and phase synchronization are required)

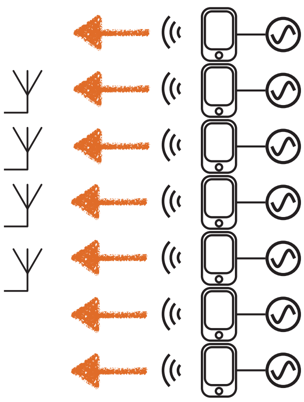

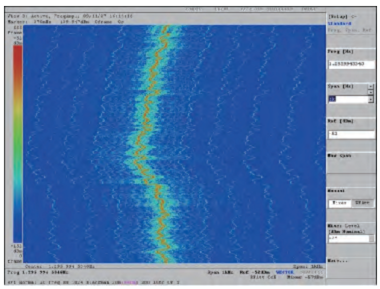

Our current research topic

WIRELESS COMMUNICATION ENGINEERING LABORATORY

12x12 MIMO

12-Stream Spatial Multiplexing Transmitter

12-element ULA

35

WIRELESS COMMUNICATION ENGINEERING LABORATORY

12x12 MIMO transmission

2-antenna terminal

36

Computer simulation

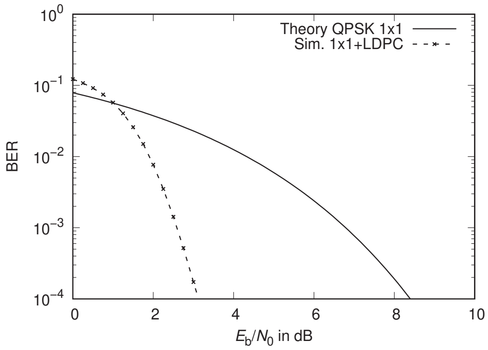

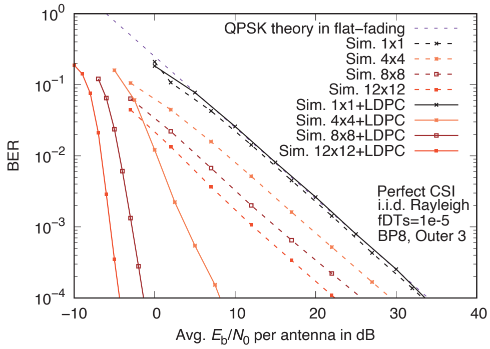

Initial results (fail)

Antenna spacing: 1λ

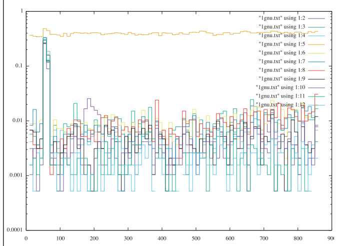

Antenna spacing: 3λ
Trial 1

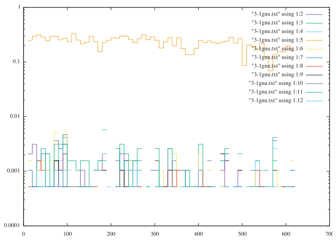

Antenna spacing: 3λ
Trial 2

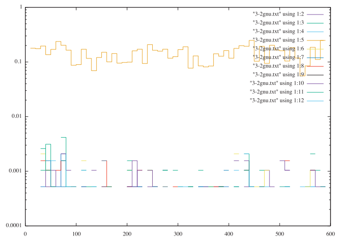

Coding Theorems Based on Constrained-Random-Number Generators

Jun Muramatsu
NTT Communication Science Laboratories, NTT Corporation, Japan
jun.muramatsu@ieee.org
(joint work with Shigeki Miyake)

This talk introduces a channel code constructed by using constrained-random-number generators. The channel capacity is achievable with this type of codes.

References

[1] J. Muramatsu, "Channel coding and lossy source coding using a generator of constrained random numbers," *IEEE Trans. Inform. Theory*, vol. IT-60, no. 5, pp. 2667–2686, May 2014.
[2] J. Muramatsu and S. Miyake, "Concept of CoCoNuTS," *Proceedings of the 10th Asia-Europe Workshop on Information Theory*, Boppard, Germany, Jun. 21–23, 2017, p. 4.
[3] J. Muramatsu and S. Miyake, "Channel code using constrained-random number generator revisited," *IEEE Trans. Inform. Theory*, vol. IT-65, no. 1, pp. 500–510, Jan. 2019.

Coding Theorems Based on Constrained-Random-Number Generators

Jun Muramatsu
NTT Communication Science Laboratories, NTT Corporation, Japan

2024.9.26

joint work with
Sigeki Miyake

Summary of this talk (1)

- Channel code and lossy source code are constructed by using constrained-random-number generators generating a random sequence $\boldsymbol{u}$ subject to the distribution

$$\nu_{\widetilde{U}|C}(\boldsymbol{u}|\boldsymbol{c}) \equiv \begin{cases} \frac{\mu_U(\boldsymbol{u})}{\mu_U(\{\boldsymbol{u}:A\boldsymbol{u}=\boldsymbol{c}\})} & \text{if } A\boldsymbol{u}=\boldsymbol{c}, \\ 0, & \text{otherwise} \end{cases}$$

  for given μ_U, A, and $\boldsymbol{c}$.
- When a channel/source is memoryless, there are tractable approximation algorithms for a constrained-random-number generator by using the Sum-Product algorithm or the Markov Chain Monte Carlo method.
- We call this type of codes CoCoNuTS (Codes based on Constrained Numbers Theoretically-achieving the Shannon limits).

Summary of this talk (2)

- Simple and rigorous proofs are given by using
  - Collision resistance property
  - Balanced coloring property

  of an ensemble satisfying (α, β)-hash property [M.-Miyake,2010,2011].

Outline

- Algorithm of constrained-random-number generator
- (α, β)-hash property
- Construction of channel code (CoCo channel)
- Construction of lossy source code (CoCo lossy)
- Concluding remarks

Algorithm of constrained-random-number generator [M., 2014]

- Assume that U^n is memoryless. Time complexity is $O(n^2w^2\iota)$.

Step 1 Let $k \leftarrow 1$.

Step 2 Calculate the following conditional probability distribution with the Sum-Product algorithm:

$$\nu_{\widetilde{U}_k|\widetilde{U}_1^{k-1}C^l}(u_k|u_1^{k-1},c^l) \equiv \frac{\sum_{u_{k+1}^n}\prod_{j=k}^n \mu_{U_j}(x_j)\prod_{i=1}^l \chi(\boldsymbol{a}_i\cdot\boldsymbol{u}_{\mathcal{S}_i}=c_i)}{\sum_{u_k^n}\prod_{j=k}^n \mu_{U_j}(u_j)\prod_{i=1}^l \chi(\boldsymbol{a}_i\cdot\boldsymbol{u}_{\mathcal{S}_i}=c_i)},$$

where $\chi(\boldsymbol{a}_i\cdot\boldsymbol{u}_{\mathcal{S}_i}=c_i)$ is a parity check function.

Step 3 Generate x_k at random subject to $\nu_{\widetilde{U}_k|\widetilde{U}_1^{k-1}C^l}(\cdot|u_1^{k-1},c^l)$.

Step 4 If $k=n$, then $\boldsymbol{u}\equiv x_1^n$ and exit.

Step 5 Let $k \leftarrow k+1$ and go to Step 2.

Lemma [M., 2014]

- If $\nu_{\widetilde{U}_k|\widetilde{U}_1^{k-1}C^l}(u_k|u_1^{k-1},c^l)$ is computed exactly, then the algorithm outputs a random sequence subject to the distribution

$$\begin{aligned}\nu_{\widetilde{\boldsymbol{U}}|\boldsymbol{C}}(\boldsymbol{u}|\boldsymbol{c}) &= \prod_{k=1}^n \nu_{\widetilde{U}_k|\widetilde{U}_1^{k-1}C^l}(u_k|u_1^{k-1},c^l)\\ &= \frac{\mu_{\boldsymbol{U}}(\boldsymbol{u})\chi(A\boldsymbol{u}=\boldsymbol{c})}{\sum_{\boldsymbol{u}}\mu_{\boldsymbol{U}}(\boldsymbol{u})\chi(A\boldsymbol{u}=\boldsymbol{c})}\\ &= \begin{cases}\frac{\mu_{\boldsymbol{U}}(\boldsymbol{u})}{\mu_{\boldsymbol{U}}(\{\boldsymbol{u}:A\boldsymbol{u}=\boldsymbol{c}\})} & \text{if } A\boldsymbol{u}=\boldsymbol{c}\\ 0 & \text{otherwise,}\end{cases}\end{aligned}$$

where $\chi(\mathsf{S})$ denotes the support funcction ($\chi(\mathsf{S})=1$ iff S is true).

$(\boldsymbol{\alpha}, \boldsymbol{\beta})$-hash property of ensemble $(\mathcal{A}, p_{\mathsf{A}})$ [M.-Miyake,2010]

- $\lim_{n\to\infty} \alpha_A(n) = 1$
- $\lim_{n\to\infty} \beta_A(n) = 0$
- $$\sum_{\substack{\boldsymbol{u}'\in\mathcal{U}^n\setminus\{\boldsymbol{u}\}:\\ p_{\mathsf{A},n}(\{A:A\boldsymbol{u}=A\boldsymbol{u}'\})>\frac{\alpha_{\mathsf{A}}(n)}{|\mathrm{Im}\mathcal{A}_n|}}} p_{\mathsf{A},n}(\{A : A\boldsymbol{u} = A\boldsymbol{u}'\}) \le \beta_{\mathsf{A}}(n) \quad \text{for all } \boldsymbol{u}\in\mathcal{U}^n,$$

  where
  - $\mathcal{A}$: a set of functions $A : \mathcal{U}^n \to \bar{\mathcal{U}}$
  - p_{A} : probability distribution on $\mathcal{A}$

Examples

- 2-universal class of hash functions [Carter-Wegman,1979] with uniform distribution
  - random binning [Cover,1975]
  - random linear functions [Csiszár,1984]
- ensemble of q-ary LDPC matrices (with column weight $O(\log n)$) [M.-M.,2010]

Lemma [M.-Miyake,2010]

- If $(\mathcal{A}, p_{\mathsf{A}})$ satisfies $$\sum_{\substack{\boldsymbol{u}'\in\mathcal{U}^n\setminus\{\boldsymbol{u}\}:\\ p_{\mathsf{A},n}(\{A:A\boldsymbol{u}=A\boldsymbol{u}'\})>\frac{\alpha_{\mathsf{A}}(n)}{|\mathrm{Im}\mathcal{A}_n|}}} p_{\mathsf{A},n}(\{A : A\boldsymbol{u} = A\boldsymbol{u}'\}) \le \beta_{\mathsf{A}}(n)$$ for any $\boldsymbol{u}$, then

  $$p_{\mathsf{A}}(\{A : [\mathcal{T}\setminus\{\boldsymbol{u}\}]\cap\mathcal{C}_A(A\boldsymbol{u})\neq\emptyset\}) \le \frac{|\mathcal{T}|\alpha_{\mathsf{A}}}{|\mathrm{Im}\mathcal{A}|} + \beta_{\mathsf{A}}$$

  for any $\mathcal{T}\subset\mathcal{U}^n$.

Collision-resistance property

- When $|\mathcal{T}| < |\mathrm{Im}\mathcal{A}|$, $\boldsymbol{u}\in\mathcal{T}$ can be specified by $\boldsymbol{c}\equiv A\boldsymbol{u}$.

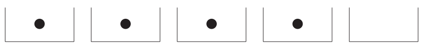

$\bullet \in \mathcal{T}\subset\mathcal{U}^n$

$\mathcal{C}_A(\boldsymbol{c}_1)$ $\mathcal{C}_A(\boldsymbol{c}_2)$ $\mathcal{C}_A(\boldsymbol{c}_3)$ $\cdots$ $\mathcal{C}_A(\boldsymbol{c}_k)$

Coset/Bin determined by $\boldsymbol{c}\in\mathrm{Im}\mathcal{A}$: $\mathcal{C}_A(\boldsymbol{c}) \equiv \{\boldsymbol{u} : A\boldsymbol{u} = \boldsymbol{c}\}$

Lemma [M.-Miyake,2010]

- If $(\mathcal{A}, p_{\mathsf{A}})$ satisfies $\displaystyle\sum_{\substack{\boldsymbol{u}' \in \mathcal{U}^n \setminus \{\boldsymbol{u}\}: \\ p_{\mathsf{A},n}(\{A : A\boldsymbol{u} = A\boldsymbol{u}'\}) > \frac{\alpha_{\mathsf{A}}(n)}{|\mathrm{Im}\mathcal{A}_n|}}} p_{\mathsf{A},n}(\{A : A\boldsymbol{u} = A\boldsymbol{u}'\}) \leq \beta_{\mathsf{A}}(n)$ for any $\boldsymbol{u}$, then

$$E_{\mathsf{A}}\left[\sum_{\boldsymbol{c}}\left|\frac{Q\left(\mathcal{C}_{\mathsf{A}}(\boldsymbol{c}) \cap \mathcal{T}\right)}{Q(\mathcal{T})} - \frac{1}{|\mathrm{Im}\mathcal{A}|}\right|\right] \leq \sqrt{\alpha_{\mathsf{A}} - 1 + \frac{[\beta_{\mathsf{A}} + 1]|\mathrm{Im}\mathcal{A}| \max_{\boldsymbol{u} \in \mathcal{T}} Q(\boldsymbol{u})}{Q(\mathcal{T})}}$$

for any function $Q : \mathcal{U}^n \to [0, \infty)$ and $\mathcal{T} \subset \mathcal{U}^n$, where $Q(\mathcal{T}) \equiv \sum_{\boldsymbol{u} \in \mathcal{T}} Q(\boldsymbol{u})$.

Balanced coloring property

- If $\max_{\boldsymbol{u} \in \mathcal{T}} Q(\boldsymbol{u}) / Q(\mathcal{T}) < 1/|\mathrm{Im}\mathcal{A}|$, then $\mathcal{T}$ can be partitioned equally by A.

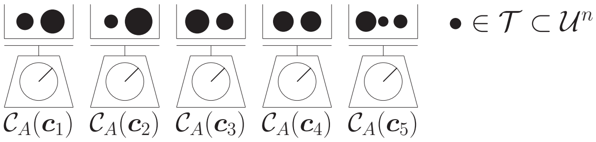

Channel coding

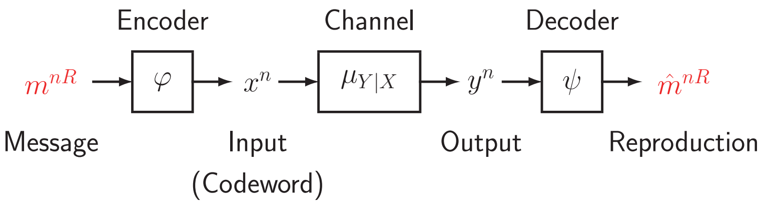

Channel capacity [Shannon, 1948]

$$C(W) = \max_{\mu_X}[H(X) - H(X|Y)] = \max_{\mu_X} I(X;Y)$$

Optimal input distribution μ_X can be obtained by using Arimoto-Blahut algorithm.

Shannon, "A Mathematical Theory of Communication," 1948

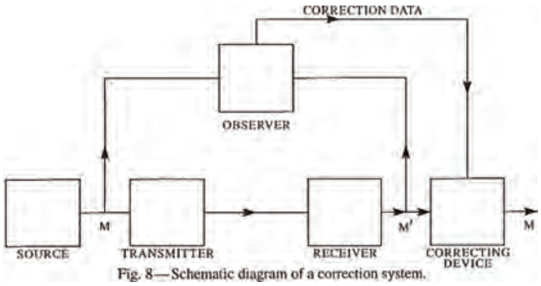

Fig. 8—Schematic diagram of a correction system.

The capacity C of a noisy channel should be the maximum possible rate of transmission, i.e., the rate when the source is properly matched to the channel. We therefore define the channel capacity by

$$C = \mathrm{Max}\big(H(x) - H_y(x)\big)$$

where the maximum is with respect to all possible information sources used as input to the channel.

Shannon, "A Mathematical Theory of Communication," 1948

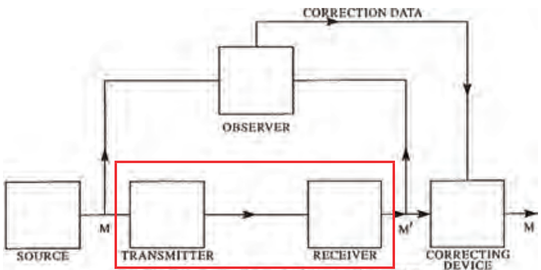

ENCODER

Fig. 8—Schematic diagram of a correction system.

DECODER

The capacity C of a noisy channel should be the maximum possible rate of transmission, i.e., the rate when the source is properly matched to the channel. We therefore define the channel capacity by

$$C = \mathrm{Max}\big(H(x) - H_y(x)\big)$$

where the maximum is with respect to all possible information sources used as input to the channel.

Random codebook generation

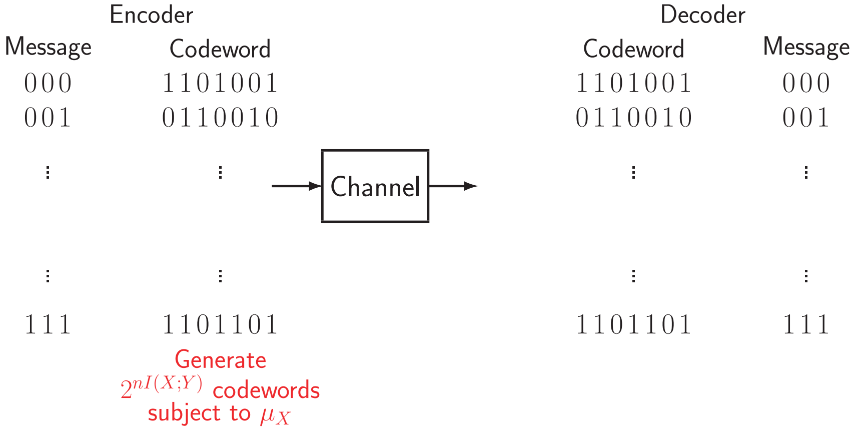

Random codebook generation

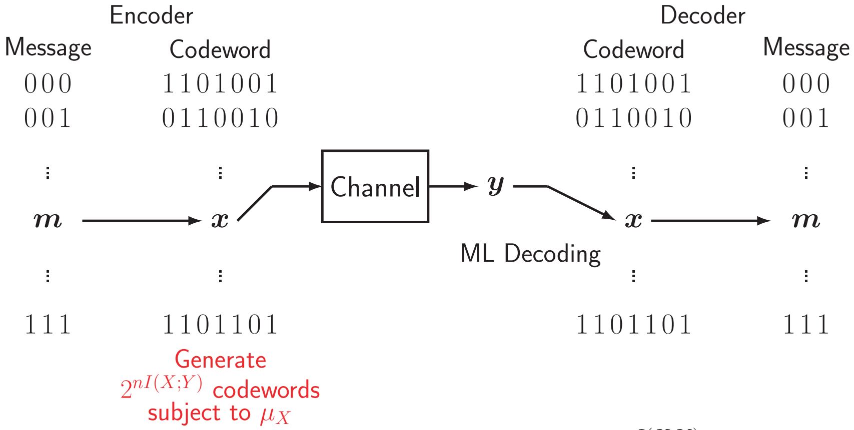

- Decoding error probability $\to 0$ by generating less than $2^{nI(X;Y)}$ codewords.

Random codebook generation [Shannon, 1948]

- Codewords are generated at random.
  - ML decoding is impractical.
  - A large lookup table for $\{(\text{message}, \text{codeword})\}$ is necessary.

LDPC Codes [Gallager, 1963], Polar Codes [Arıkan, 2009]

- Decoding is practical.
- These codes achieve capacity of a symmetric channel.
- An additional technique (e.g. a quantization map) is necessary to achieve capacity of a general (asymmetric) channel.
  - Linear codes cannot achieve capacity of asymmetric channel [Ahlswede, 1971].

Source coding with side information at decoder

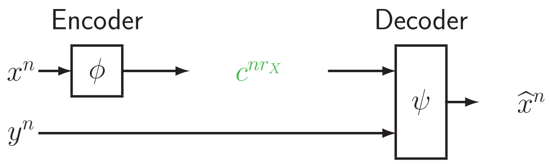

Theorem [Slepian-Wolf, 1973]

- The infimum achievable rate is $H(X|Y)$.

Theorem

- For any (X, Y), the rate $H(X|Y)$ is achievable by using
  - random binning [Cover, 1975]
  - linear codes [Csiszár, 1984]
  - LDPC codes [M.-Uyematsu-Wadayama, 2005].

Shannon, "A Mathematical Theory of Communication," 1948

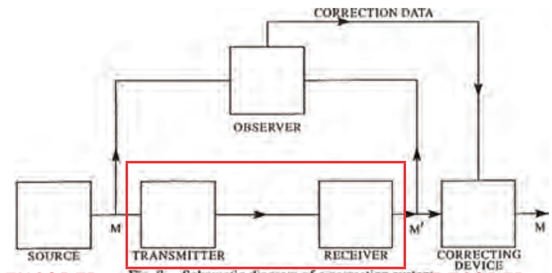

Fig. 8—Schematic diagram of a correction system

- We can interpret 'OBSERVER' as a source encoder and 'CORRECTING DEVICE' as a source decoder with side information.

Shannon, "A Mathematical Theory of Communication," 1948

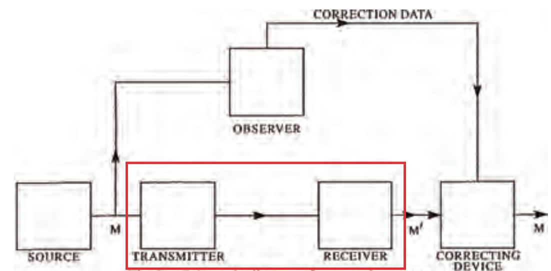

Fig. 8—Schematic diagram of a correction system

- We can interpret 'OBSERVER' as a source encoder and 'CORRECTING DEVICE' as a source decoder with side information.
- From the Slepian-Wolf theorem, the arrow "$M' \to$ OBSERVER" is unnecessary.

Channel code for a general discrete memoryless channel

- A matrix A, a fixed vector $\boldsymbol{c} \in \mathrm{Im}A$, a bijection $\widehat{g}_{A,\boldsymbol{c}} : \mathcal{M} \to \mathcal{T} \cap \{\boldsymbol{x} : A\boldsymbol{x} = \boldsymbol{c}\}$ are shared by an encoder and a decoder.

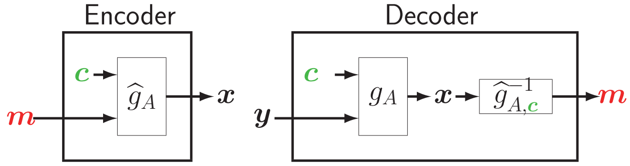

$$g_A(\boldsymbol{c}|\boldsymbol{y}) \equiv \arg \max_{\boldsymbol{x}':A\boldsymbol{x}'=\boldsymbol{c}} \mu_{\boldsymbol{X}|\boldsymbol{Y}}(\boldsymbol{x}'|\boldsymbol{y})$$ Slepian-Wolf decoder

Theorem [M., AEW2004][M.-Uyematsu-Wadayama, 2006]

- When $\dim(\mathrm{Im}A)/n > H(X|Y)$ and $\boldsymbol{x}$ is a typical sequence satisfying $A\boldsymbol{x} = \boldsymbol{c}$, the decoding error $\to 0$ because $\boldsymbol{c}$ is a Slepian-Wolf codeword of $\boldsymbol{x}$
- There are $2^{n[H(X)-H(X|Y)]} = 2^{nI(X;Y)}$ typical sequences satisfying $A\boldsymbol{x} = \boldsymbol{c}$.

Shannon, "A Mathematical Theory of Communication," 1948

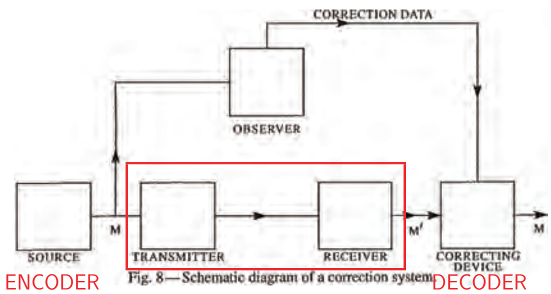

Fig. 8—Schematic diagram of a correction system

- From this theorem,

Shannon, "A Mathematical Theory of Communication," 1948

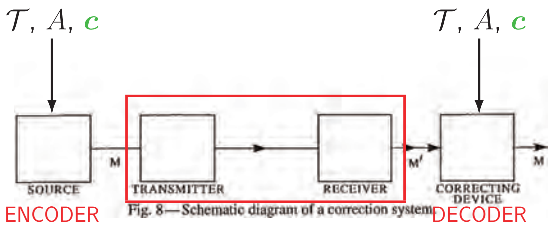

Fig. 8—Schematic diagram of a correction system

- From this theorem, the OBSERVER is unnecessary by sharing $\mathcal{T}$, A, and $\boldsymbol{c}$, and assuming that channel input $\boldsymbol{x}$ always satisfies $\boldsymbol{x} \in \mathcal{T}$ and $A\boldsymbol{x} = \boldsymbol{c}$.

Channel code (CoCo channel) [M.-Miyake,2019]

- Functions A, B, and a fixed vector $\boldsymbol{c} \in \mathrm{Im}A$ are shared by an encoder and a decoder.

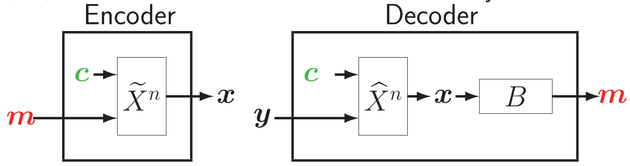

$$r_A \equiv \frac{\log |\mathrm{Im}\mathcal{A}|}{n} \qquad r_A + R_B < H(X)$$

$$R_B \equiv \frac{\log |\mathrm{Im}\mathcal{B}|}{n} \qquad r_A > H(X|Y)$$

$$\nu_{\widetilde{X}^n|C^{l_A}M^{l_B}}(\boldsymbol{x}|\boldsymbol{c},\boldsymbol{m}) \equiv \frac{\mu_{X^n}(\boldsymbol{x})\chi(A\boldsymbol{x}=\boldsymbol{c}, B\boldsymbol{x}=\boldsymbol{m})}{\sum_{\boldsymbol{x}} \mu_{X^n}(\boldsymbol{x})\chi(A\boldsymbol{x}=\boldsymbol{c}, B\boldsymbol{x}=\boldsymbol{m})}$$

$$q_{\widehat{X}^n|Y^nC^{l_A}}(\boldsymbol{x}|\boldsymbol{y},\boldsymbol{c}) \equiv \frac{\mu_{X^n|Y^n}(\boldsymbol{x}|\boldsymbol{y})\chi(A\boldsymbol{x}=\boldsymbol{c})}{\sum_{\boldsymbol{x}} \mu_{X^n|Y^n}(\boldsymbol{x}|\boldsymbol{y})\chi(A\boldsymbol{x}=\boldsymbol{c})}$$ Stochastic decoder

Channel code (CoCo channel) [M.-Miyake,2019]

- Functions A, B, and a fixed vector $\boldsymbol{c} \in \mathrm{Im} A$ are shared by an encoder and a decoder.

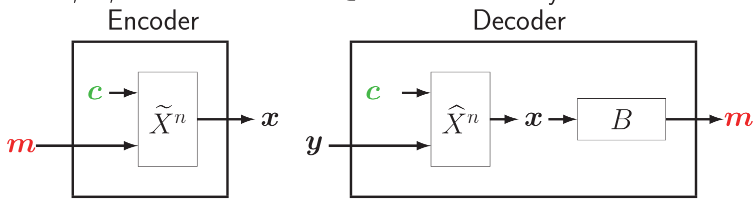

$r_A + R_B < H(X)$ $\qquad$ $r_A > H(X|Y)$

- When $r_A + R_B < H(X)$, we can generate $\boldsymbol{x}$ satisfying $\boldsymbol{c} = A\boldsymbol{x}$ and $\boldsymbol{m} = B\boldsymbol{x}$ from uniformly generated $(\boldsymbol{c}, \boldsymbol{m})$ based on the balanced coloring property.
- When $r_A > H(X|Y)$, the decoder can reproduce $\boldsymbol{x}$ from $\boldsymbol{c}$ and $\boldsymbol{y}$ based on the collision-resistance property.

Theorem [M.-Miyake, 2019]

- For given $r_A, R_B > 0$ satisfying

$$r_A > H(X|Y) \tag{1}$$
$$r_A + R_B < H(X), \tag{2}$$

assume that an ensemble $(\mathcal{A}, p_{\mathsf{A}})$ (resp. $(\mathcal{B}, p_{\mathsf{B}})$) of functions (sparse matrices) satisfies $(\boldsymbol{\alpha}_{\mathsf{A}}, \boldsymbol{\beta}_{\mathsf{A}})$-hash (resp. $(\boldsymbol{\alpha}_{\mathsf{B}}, \boldsymbol{\beta}_{\mathsf{B}})$-hash) property. Then for any $\delta > 0$ and sufficiently large n there are functions $A \in \mathcal{A}$, $B \in \mathcal{B}$, and a vector $\boldsymbol{c} \in \mathrm{Im} A$ such that

$$\mathrm{Error}(A, B, \boldsymbol{c}) \leq \delta.$$

- For any discrete memoryless channel, the capacity

$$\sup_{\mu_X} I(X;Y)$$

is achievable with this code by optimizing μ_X, because for any $R_B < H(X) - H(X|Y) = I(X;Y)$ there is $r_A > 0$ satisfying (1),(2).

Lossy source coding

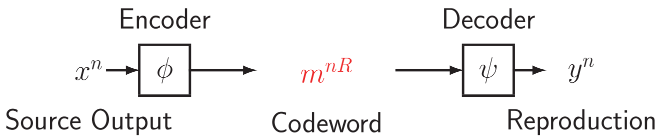

Distortion criterion

$$\mathrm{Prob}\left(d_n(X^n, \psi(\phi(X^n))) > D\right) \leq \delta$$

Random codebook generation [Shannon, 1959]

- Quantization points (reproductions) are generated at random.
  - A large lookup table for $\{(\text{codeword}, \text{quantization point})\}$ is necessary.
  - Encoding (looking for nearest quantization point) is impractical.

Lossy source code (CoCo lossy) [M.,2014]

- An encoder and a decoder share functions (matrices) A, B and a fixed vector $\boldsymbol{c} \in \mathrm{Im}A$.

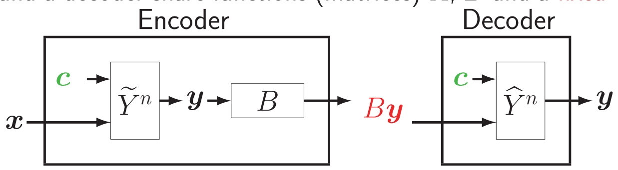

$$r_A \equiv \frac{\log|\mathrm{Im}\mathcal{A}|}{n} \qquad r_A < H(Y|X)$$

$$R_B \equiv \frac{\log|\mathrm{Im}\mathcal{B}|}{n} \qquad r_A + R_B > H(Y)$$

$$\mu_{Y_A^n|X^n C^{l_A}}(\boldsymbol{y}|\boldsymbol{x},\boldsymbol{c}) \equiv \frac{\mu_{Y^n|X^n}(\boldsymbol{y}|\boldsymbol{x})\chi(A\boldsymbol{y}=\boldsymbol{c})}{\sum_{\boldsymbol{y}} \mu_{Y^n|X^n}(\boldsymbol{y}|\boldsymbol{x})\chi(A\boldsymbol{y}=\boldsymbol{c})}$$

$$q_{\widehat{Y}^n|C^{l_A}M^{l_B}}(\boldsymbol{y}|\boldsymbol{c},\boldsymbol{m}) \equiv \frac{\mu_{Y^n}(\boldsymbol{y})\chi(A\boldsymbol{y}=\boldsymbol{c}, B\boldsymbol{y}=\boldsymbol{m})}{\sum_{\boldsymbol{y}} \mu_{Y^n}(\boldsymbol{y})\chi(A\boldsymbol{y}=\boldsymbol{c})}$$

Stochastic decoder

Lossy source code (CoCo lossy) [M.,2014]

- An encoder and a decoder share functions (matrices) A, B and a fixed vector $\boldsymbol{c} \in \mathrm{Im}A$.

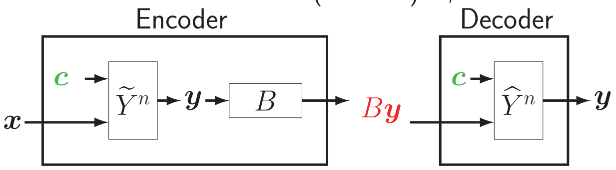

$r_A < H(Y|X)$ $\qquad$ $r_A + R_B > H(Y)$

- When $r_A < H(Y|X)$, we can generate $\boldsymbol{c} \equiv A\boldsymbol{y}$ independent of $\boldsymbol{x}$ based on the balanced coloring property. Then the encoder and the decoder can share a fixed $\boldsymbol{c}$.
- The encoder can generate $\boldsymbol{y}$ satisfying $\boldsymbol{c} = A\boldsymbol{y}$ and $d(\boldsymbol{x},\boldsymbol{y})/n < D$ with high probability.
- When $r_A + R_B > H(Y)$, the decoder can reproduce $\boldsymbol{y}$ from $\boldsymbol{c} = A\boldsymbol{y}$ and $\boldsymbol{m} \equiv B\boldsymbol{y}$ based on the collision-resistance property.

Theorem [M.,2014]+[M.-Miyake,2017], [M.,2024]

- For given $r_A, R_B > 0$ satisfying

$$r_A < H(Y|X) \quad (3)$$

$$r_A + R_B > H(Y) \quad (4)$$

assume that an ensemble $(\mathcal{A}, p_{\mathsf{A}})$ (resp. $(\mathcal{B}, p_{\mathsf{B}})$) has $(\boldsymbol{\alpha}_{\mathsf{A}}, \boldsymbol{\beta}_{\mathsf{A}})$-hash (resp. $(\boldsymbol{\alpha}_{\mathsf{A}}, \boldsymbol{\beta}_{\mathsf{A}})$-hash) property. Then for any $\delta > 0$ and sufficiently large n there are functions A, B and a vector $\boldsymbol{c} \in \mathrm{Im}A$ such that

$$\mathrm{Prob}\left(\rho_n(X^n, \psi(\varphi(X^n))) > D\right) \le \delta.$$

- For any source X, the region

$$\bigcup_{\mu_{Y|X}} \left\{ (R,D) : \begin{array}{c} I(X;Y) \le R \\ E[d(X;Y)] \le D \end{array} \right\}$$

is achievable with the proposed code because for any $R_B > H(Y) - H(Y|X) = I(X;Y)$ there is $r_A > 0$ satisfying (3) and (4).

Concluding remarks

- Channel code and lossy source code are constructed by using constrained-random-number generators.
- Simple and rigorous proof is given by using
  - Balanced coloring property [M.-Miyake,2011]
  - Collision resistance property [M.-Miyake,2010]

  of an ensemble satisfying (α,β)-hash property.
- Codes can be extended intuitively to relayless multi-terminal source/channel coding problems [M.,2023][M.,2024].
  - Random codebook generation can be replaced by random binning.
  - (Goal) Reconstruct all achievability theorems from the above two properties.

 29/32

Multi-terminal channel coding with message access structure [Somekh-Baruch and Verdú,2006][M.-Miyake,2018][M.,2023]

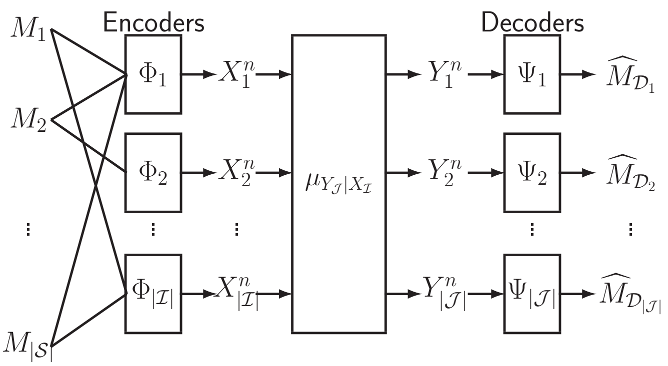

- Optimal muti-letter region is derived in [M.,2023].

 30/32

Distributed source coding [Jana-Blahut,2008][M.,2024]

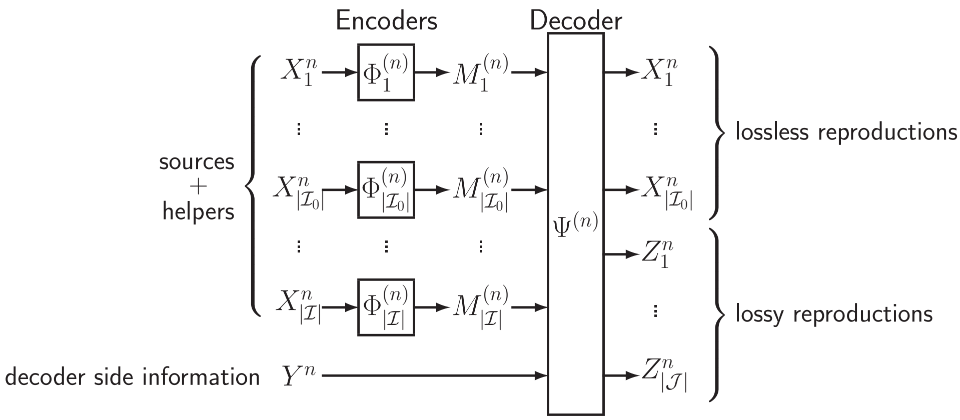

- Optimal muti-letter region is derived in [M.,2024].

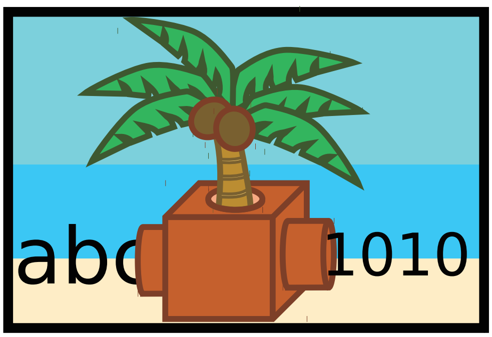

Thank you for your kind attention.

Delay-Doppler Estimation for Joint Sensing and Communications

Yutaka Jitsumatsu
Department of Informatics, Kyushu University, Japan
jitsumatsu@inf.kyushu-u.ac.jp

Recently, the commercial use of millimeter wave wireless communications has become feasible. Millimeter waves have high directivity, which makes them susceptible to obstruction, rendering them less suitable for wireless communication. As a result, they have primarily been used for radar applications. In recent years, attention has shifted to Joint Communications and Sensing (JCAS), which enables simultaneous wireless communication and radar or sensing functions using a single transmission signal. Additionally, Integrated Sensing and Communications (ISAC) has gained attention, as it involves the immediate sharing of sensed data with wireless nodes via communication networks. Orthogonal Time Frequency Space (OTFS) modulation is considered a promising candidate for JCAS.

In this talk, we will describe Frequency Modulated Continuous Wave (FMCW) and pulse radar as typical radar signals. We will compare the delay-Doppler domain in OTFS with that in pulse radar. It is shown that the delay-Doppler domain in OTFS is essentially the same as the delay-Doppler map in pulse radar. Finally, we present the author ’ s proposed method for delay-Doppler estimation.

Acknowledgment

A part of this work was supported by JSPS KAKENHI Grant Numbers JP23H00474 and JP23K26104.

References

[1] M. Kobayashi, G. Caire, and G. Kramer, “Joint State Sensing and Communication: Optimal Tradeoff for a Memoryless Case,” 2018 Int. Symp. Inform. Theory (ISIT2018), 2018.
[2] S.Lu, et al. “Integrated Sensing and Communications: Recent Advances and Ten Open Challenges,” IEEE Internet of Things, June 2024.
[3] Uysal, “Phase-Coded FMCW Automotive Radar: System Design and Interference Mitigation,” IEEE Tran. Veh. Tech. Jan 2020.
[4] R. Hadani, S. Rakib, M. Tsatsanis, A. Monk, A. Goldsmith, A. F. Molisch, and R. Calderbank, “Orthogonal time frequency space modulation,” in Proc. IEEE WCNC, 2017.
[5] P. Raviteja, K. T. Phan, Q. Jin, Y. Hong and E. Viterbo, “Low-complexity iterative detection for orthogonal time frequency space modulation,” WCNC2018.
[6] P. Raviteja, K. T. Phan and Y. Hong, “Embedded Pilot-Aided Channel Estimation for OTFS in Delay-Doppler Channels,” IEEE Trans. Vehicular Technology, 2019
[7] T. Kohda, Y. Jitsumatsu and K. Aihara, “Gabor Division/Spread Spectrum System Is Separable in Time and Frequency Synchronization,” VTC2023 Fall, 2013
[8] L.Gaudio, M.Kobayashi, G.Caire, G.Colavolpe, “On the effectiveness of OTFS for Joint Radar Parameter Estimation and Communication,” IEEE Trans. Wireless Comm.Vol.19, 2020.
[9] K.Zhang et al., “Radar sensing via OTFS signaling: A delay doppler signal processing perspective,” arXiv:2301.09909, 2023.
[10] Y. Jitsumatsu “2D Sinc Interpolation-Based Fractional Delay and Doppler Estimation Using Time and Frequency Shifted Gaussian Pulses,” arXiv:2312.04969

Workshop " Mathematics for Innovation in Information and Communication Technology"

Delay-Doppler Estimation for Joint Sensing and Communications

Yutaka JITSUMATSU, Kyushu University

13:00-14:00

September 26th, 2024, at JR HAKATA CITY

JITSUMATSU LAB.

Outline

- ❑ Introduction
  - Integrated Sensing and Communications (ISAC)
- ❑ Conventional Radar methods
- ❑ OTFS for ISAC
  - Details of OTFS
- ❑ Proposed Delay-Doppler Estimation Method
- ❑ Conclusion
  - Future Research

JITSUMATSU LAB. 2

Introduction

❑ Integrated Sensing and Communications (ISAC)

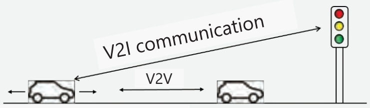

Sensing of environment

- Use of millimeter wave for wireless communications
- V2V, V2I, V2X
- Collision avoidance, congestion mitigation, automated driving
- Instantaneous sharing of sensing information
- Vertical communications (stratosphere, low earth orbit satellites)

JITSUMATSU LAB. 3

Usage scenarios of IMT2030

Usage scenarios

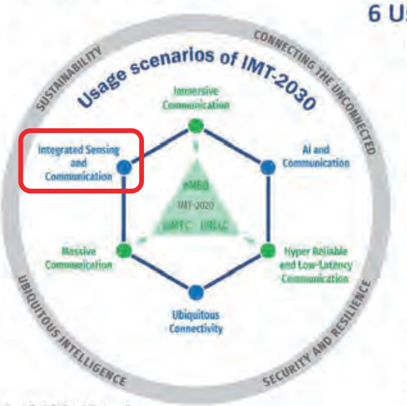

So called "Wheel diagram"

6 Usage scenarios

Extension from IMT-2020 (5G)

eMBB → Immersive Communication

mMTC → Massive Communication

URLLC → HRLLC (Hyper Reliable & Low-Latency Communication)

New

Ubiquitous Connectivity

AI and Communication

Integrated Sensing and Communication

4 Overarching aspects:

act as design principles commonly applicable to all usage scenarios

Sustainability, Connecting the unconnected, Ubiquitous intelligence, Security/resilience

Background of ISAC research

- Joint design of waveforms
  - From split channel use to simultaneous use
  - From a trade-off relationship to a cooperative relationship
- Three theoretical challenges in Ten Open Challenges for ISAC [2]
  1) What are the information-theoretic limits of ISAC systems?
  2) How much channel information can be inferred from the sensory data?
  3) How could we quantify the integration and coordination gains?

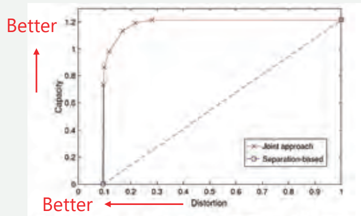

Fig. 3. Capacity-distortion tradeoff of fading AWGN channel $P = 10$ dB.

From [1]

[1] M. Kobayashi, G. Caire, and G. Kramer, "Joint State Sensing and Communication: Optimal Tradeoff for a Memoryless Case," *2018 Int. Symp. Inform. Theory (ISIT2018)*, 2018.
[2] S.Lu, et al. "Integrated Sensing and Communications: Recent Advances and Ten Open Challenges," *IEEE Internet of Things*, June 2024.

Difference between Radar and Communications

- A simple model.

$$Y = H X + Z$$

- RADAR: From X and Y obtain H. From H, we detect
  1) there exists objects or not,
  2) the distance to the objects, (Range)
  3) the moving speed of the objects. (Doppler)
- Communication: From H and Y, obtain X. From X, recover the transmitted symbol.
  Often H is unknown. → Channel estimation is needed.
- NOTE: Channel estimation and radar detection use different methods.

➢How to achieve two objectives simultaneously?

Complex baseband equivalent representation

- Assume that the received signal is expressed by

$$r(t) = \alpha \cdot s(t - t_d)e^{i2\pi f_D t} + \eta(t)$$

$r(t)$: received signal, $s(t)$: transmitted signal, $\eta(t)$: additive noise

Unknown parameters (α, t_d, f_D) = complex attenuation, delay, Doppler frequency, as many as the number of paths

- Prior distribution : α decays with distance, t_d follows uniform distribution, f_D obeys Jakes model

- MIMO radar is an important issue but today's presentation discuss single antena radar.

JITSUMATSU LAB. 7

The conventional methods

- Radar Signal Categories

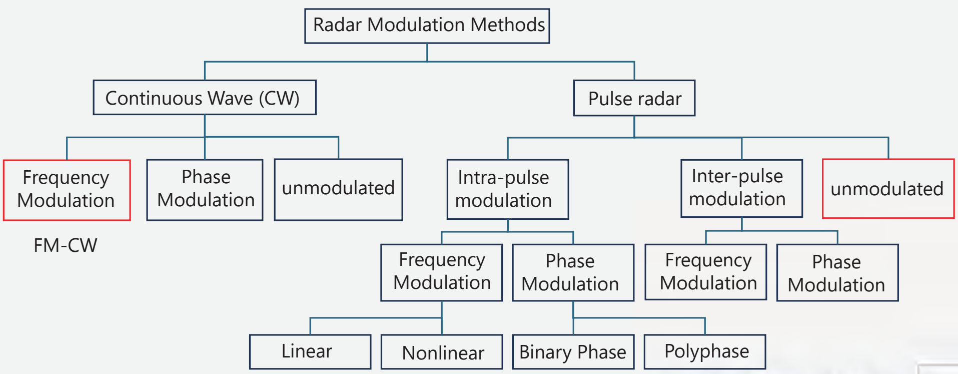

JITSUMATSU LAB. 8

① Frequency Modulated-Continuous Wave (FM-CW)

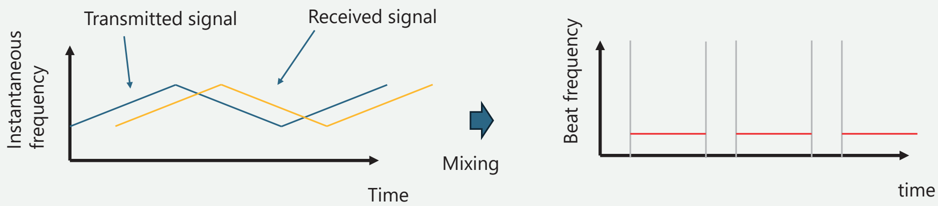

- Widely used in automotive radar and other applications
- Inter-radar interference occurs when two or more FMCW signals are present. Thus, there is a need for interference suppression.
  → Phase-coded FMCW

Detect τ, ν by solving a simultaneous linear equation from the beat frequencies of the up and down chirps

[3] Uysal, "Phase-Coded FMCW Automotive Radar: System Design and Interference Mitigation," IEEE Tran. Veh. Tech. Jan 2020.

JITSUMATSU LAB. 9

②Pulse Radar (1/3)

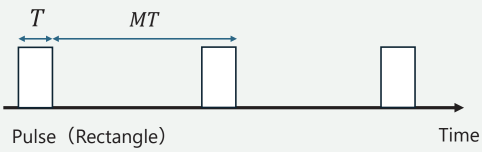

(M: duty ratio)

- Pulses of short time widths are sent repeatedly at regular intervals.
- Detects the reflected wave and calculates the distance to the target from the round-trip time.
- The speed of the target is calculated from the Doppler frequency.

JITSUMATSU LAB. 10

②Pulse Radar (2/3)

- Output of the matched filter

$$Z(t) = \int_0^T p(T-\tau)y(t-\tau)\,d\tau$$

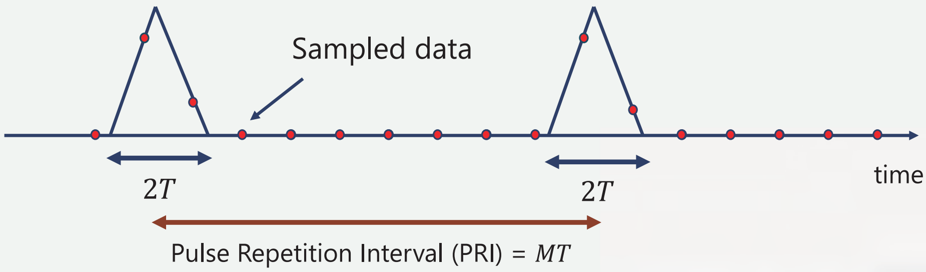

JITSUMATSU LAB.

②Pulse Radar (3/3)

- After placing the signal in two dimensions, the Doppler frequency can be determined by performing a Fourier transform.

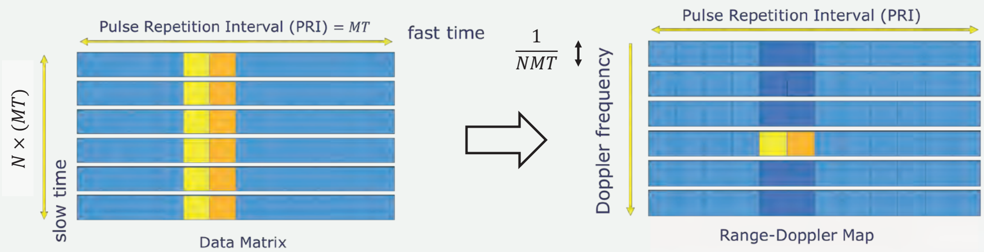

JITSUMATSU LAB.

Orthogonal Time Frequency Space (OTFS) modulation

- ❑ We review the definition of OTFS.
  - Modulation/Demodulation method
  - Channel estimation method
- ❑ We then describe some of the unsatisfactory aspects of OTFS.

JITSUMATSU LAB. 13

OTFS (Orthogonal Time Frequency Space) Modulation

- ❑ Proposed by R. Hadani and S. Rakib [4].
- ❑ Resistant to Doppler-shift
- ❑ Outperforms OFDM in a high-mobility environments
- ❑ Radar applications
- ❑ Candidate waveform for ISAC.
- ❑ Data is allocated in the "Delay-Doppler domain"
  ⇔ In OFDM, data is allocated in the frequency domain.

[4] R. Hadani, S. Rakib, M. Tsatsanis, A. Monk, A. Goldsmith, A. F. Molisch, and R. Calderbank, "Orthogonal time frequency space modulation," in Proc. IEEE WCNC, 2017.

JITSUMATSU LAB. 14

OTFS Signal Configuration

❑ Review of OFDM

- Original definition

$$s(t) = \sum_{m=0}^{M-1} X[m]\, g(t) e^{i2\pi\,\Delta f\, m\, t}$$

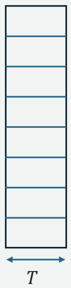

$\Delta f = \frac{1}{T}$: subcarrier spacing

$g(t)$: rectangular waveform with duration T

M subcarriers

- Digital implementation

$$s[\ell] = \sum_{m=0}^{M-1} X[m]\, e^{i\frac{2\pi}{M}m\ell}$$

$$\tilde{s}(t) = \sum_{\ell=0}^{M-1} s[\ell] v\left(t - \ell\frac{T}{M}\right)$$

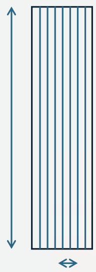

$v(t)$: pulse with duration $T_s = \frac{T}{M}$

$\frac{T}{M}$: sampling interval

- Data symbols $X[m]$ are on frequency domain
- Time domain signal $s[\ell]$ is the IDFT of $X[m]$

JITSUMATSU LAB. 15

OTFS Signal Configuration

- Original definition

$$s(t) = \sum_{m=0}^{M-1} \sum_{n=0}^{N-1} X_{\mathrm{TF}}[m,n] g(t - nT) e^{i2\pi\, m\Delta f t}$$

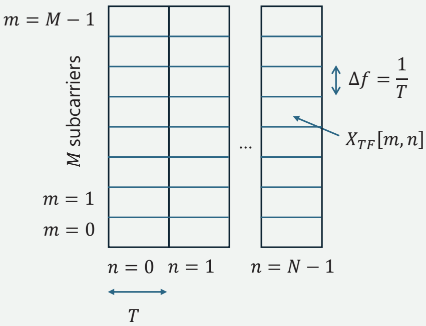

- Digital implementation (if $g(t)$ is rectangular)

$$s[\ell + nM] = \frac{1}{\sqrt{M}} \sum_{m=0}^{M-1} X_{\mathrm{TF}}[m,n] e^{i\frac{2\pi}{M}m\ell}$$

$\ell = 0,1,2,\ldots,M-1$

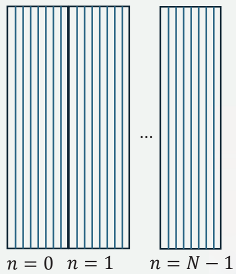

$$\tilde{s}(t) = \sum_{n=0}^{N-1} \sum_{\ell=0}^{M-1} s[\ell + nM] v\left(t - \ell\frac{T}{M} - nT\right)$$

Time index: $\ell + nM$

ℓ: fast time index

n: slow time index

$v(t)$: pulse with duration $T_s = \frac{T}{M}$

$\frac{T}{M}$: sampling interval

JITSUMATSU LAB. 16

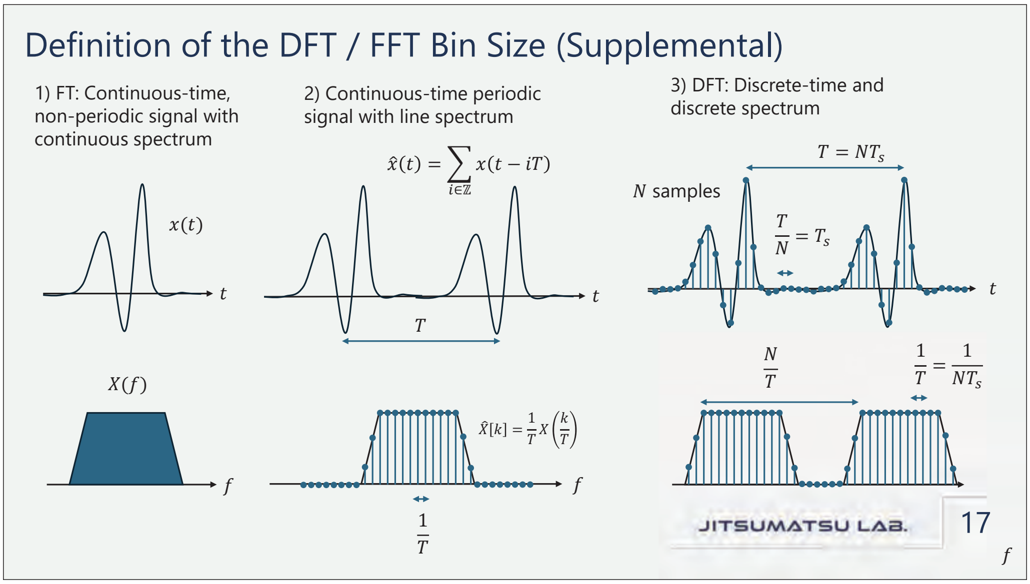
Definition of the DFT / FFT Bin Size (Supplemental)
1) FT: Continuous-time, non-periodic signal with continuous spectrum
2) Continuous-time periodic signal with line spectrum
3) DFT: Discrete-time and discrete spectrum
$\hat{x}(t) = \sum_{i\in\mathbb{Z}} x(t-iT)$
$x(t)$
t
T
$T = NT_s$
N samples
$\frac{T}{N} = T_s$
$X(f)$
f
$\hat{X}[k] = \frac{1}{T}X\left(\frac{k}{T}\right)$
$\frac{1}{T}$
$\frac{N}{T}$
$\frac{1}{T} = \frac{1}{NT_s}$
JITSUMATSU LAB.
17

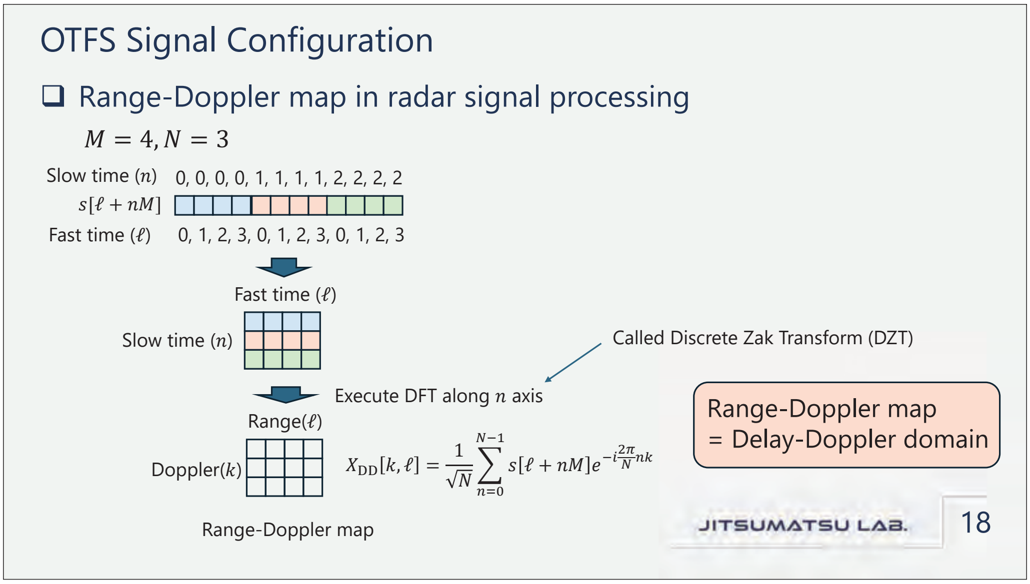
OTFS Signal Configuration
❑ Range-Doppler map in radar signal processing
$M = 4, N = 3$
Slow time (n) 0, 0, 0, 0, 1, 1, 1, 1, 2, 2, 2, 2
$s[\ell + nM]$
Fast time (ℓ) 0, 1, 2, 3, 0, 1, 2, 3, 0, 1, 2, 3
Fast time (ℓ)
Slow time (n)
Called Discrete Zak Transform (DZT)
Execute DFT along n axis
Range(ℓ)
Doppler(k)
$X_{\mathrm{DD}}[k,\ell] = \frac{1}{\sqrt{N}}\sum_{n=0}^{N-1} s[\ell + nM]e^{-i\frac{2\pi}{N}nk}$
Range-Doppler map = Delay-Doppler domain
Range-Doppler map
JITSUMATSU LAB.
18

OTFS Signal Configuration

❑ The OTFS transmit signal is generated in the reverse direction of the previous page.

$M = 4, N = 3$

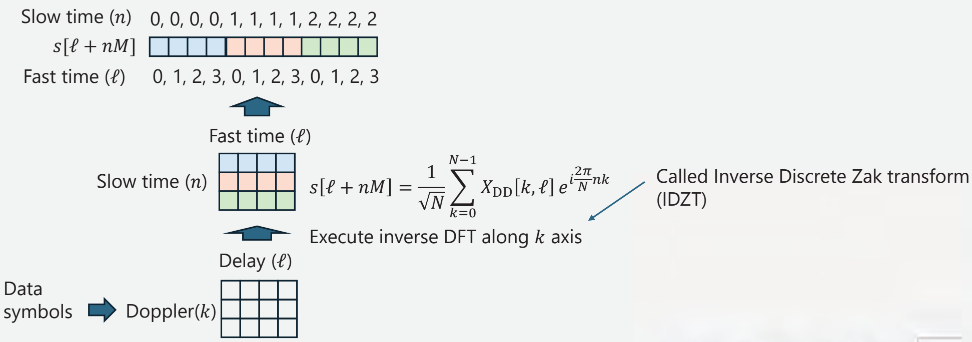

Range-Doppler map = Delay-Doppler Domain

JITSUMATSU LAB. 19

Relation between TF domain and DD domain signals

$$s[\ell + nM] = \frac{1}{\sqrt{M}} \sum_{m=0}^{M-1} X_{\mathrm{TF}}[m, n] e^{i\frac{2\pi}{M}m\ell} \qquad (1)$$

$$X_{\mathrm{DD}}[k, \ell] = \frac{1}{\sqrt{N}} \sum_{n=0}^{N-1} s[\ell + nM] e^{-i\frac{2\pi}{N}nk} \qquad (2)$$

❑ Substituting (1) into (2) yields

$$X_{\mathrm{DD}}[k, \ell] = \frac{1}{\sqrt{NM}} \sum_{m=0}^{M-1} \sum_{n=0}^{N-1} X_{\mathrm{TF}}[m, n] \exp\left(i2\pi \left(\frac{m\ell}{M} - \frac{nk}{N} \right) \right)$$

JITSUMATSU LAB. 20

Time Frequency (TF) domain and Delay Doppler (DD) domain

$$s(t) = \sum_{m=0}^{M-1}\sum_{n=0}^{N-1} X_{\mathrm{TF}}[m,n]\, g(t-nT)\, e^{i2\pi\, m\Delta f t}$$

$$X_{\mathrm{DD}}[k,\ell] = \frac{1}{\sqrt{NM}} \sum_{m=0}^{M-1}\sum_{n=0}^{N-1} X_{\mathrm{TF}}[m,n] \exp\left(i2\pi\left(\frac{m\ell}{M} - \frac{nk}{N}\right)\right)$$

Size of 1 grid on DD domain $(M = 4, N = 3)$

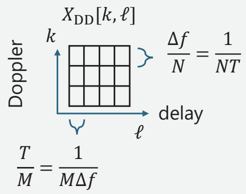

Delay-Doppler domain

Size of 1 grid on TF domain

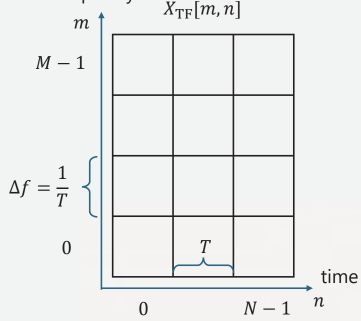

Time-Frequency domain

JITSUMATSU LAB. 21

Frequency domain signal

Continuous-OFDM (Real part) DFT-OFDM $(M = 16)$

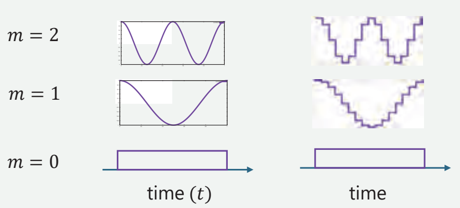

DD domain signal

Zak-OTFS$(N = M - 16)$

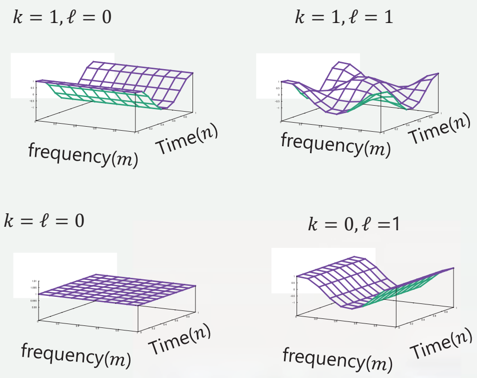

JITSUMATSU LAB. 22

Channel Estimation in OTFS [5]

If delay and Doppler are integers, the received signal is

$$Y_{DD}[k,\ell] = \sum_p h[k_p,\ell_p] e^{-i\frac{2\pi}{NM}k_p \ell} X_{DD}\left[[k-k_p]_N, [\ell-\ell_p]_M\right] + Z_{DD}[k,\ell]$$

$[n]_N$ stands for $n \bmod N$

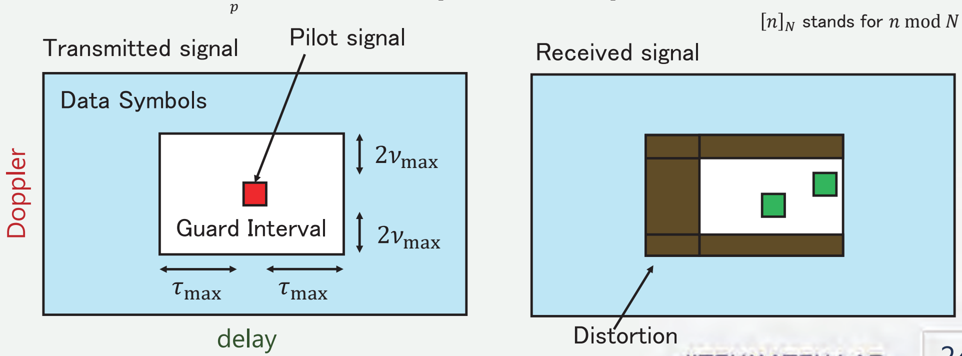

[5] P. Raviteja, K. T. Phan and Y. Hong, "Embedded Pilot-Aided Channel Estimation for OTFS in Delay–Doppler Channels," *IEEE Trans. Vehicular Technology*, 2019

JITSUMATSU LAB.

24

The ambiguity function → DD domain matching

❑ DD domain representation:

Transmitted signal $s[\ell + nM] = \frac{1}{\sqrt{N}} \sum_m X_{\mathrm{DD}}[k,\ell] e^{-i\frac{2\pi}{N}nk}$,

Received signal $r[\ell + nM] = \frac{1}{\sqrt{N}} \sum_n Y_{\mathrm{DD}}[k,\ell] e^{-i\frac{2\pi}{N}nk}$.

❑ Assume $X_{DD}[k-aN, \ell-bM] = X_{DD}[k,\ell]$ holds for any integers a, b.

Proposition[5]: The ambiguity function between s and r is given by

$$A_{rs}[k',\ell'] = \sum_{k=0}^{N-1} \sum_{\ell=0}^{M-1} Y_{DD}[k,\ell] \underbrace{X_{DD}^*[k-k',\ell-\ell'] e^{-i\frac{2\pi}{NM}k'\ell}}_{(k',\ell')\text{-shifted } X_{DD}[k,\ell]}$$

*: complex conjugate

Note.
1. Ambiguity function computation reduces to the matching in DD domain.
2. The TF domain representation does not allow this concise expression.

[5] P. Raviteja, K. T. Phan and Y. Hong, "Embedded Pilot-Aided Channel Estimation for OTFS in Delay–Doppler Channels," *IEEE Trans. Vehicular Technology*, 2019

JITSUMATSU LAB.

25

Proof of Proposition

$$W_N = e^{-i\frac{2\pi}{N}}$$

$$A_{rs}[k',\ell'] = \sum_{n=0}^{N-1}\sum_{\ell=0}^{M-1} r[\ell+nM]s^*[\ell+nM-\ell']\,W_{NM}^{k(\ell+nM)}$$

$$= \sum_{n=0}^{N-1}\sum_{\ell=0}^{M-1}\left(\frac{1}{\sqrt{N}}\sum_{k=0}^{N-1} Y_{DD}[k,\ell]\,W_N^{-nk}\right)\left(\frac{1}{\sqrt{N}}\sum_{k''=0}^{N-1} X_{DD}[k'',\ell-\ell']\,W_N^{-nk''}\right)^* W_{NM}^{k(\ell+nM)}$$

$$= \sum_{\ell=0}^{M-1}\sum_{k=0}^{N-1} Y_{DD}[k,\ell]\sum_{k''=0}^{N-1} X_{DD}[k'',\ell-\ell']\,W_{NM}^{k'\ell}\sum_{n=0}^{N-1}\frac{1}{N}\,W_N^{-n(k-k''-k')}$$

$$= \sum_{\ell=0}^{M-1}\sum_{k=0}^{N-1} Y_{DD}[k,\ell]\,X_{DD}[k-k',\ell-\ell']W_{NM}^{k'\ell}$$

QED

JITSUMATSU LAB. 26

Unsatisfactory aspects of OTFS and my research motivation

1) OTFS's ideal pulse is assumed to satisfy *biorthogonal robust property*, which however cannot be realized.(*)
2) OTFS-based radar transmits NM samples and receives NM samples… How does the receiver find the OTFS frame?
3) OTFS-based Radar often assumes analog-carrier OTFS.
4) Results obtained under the analog-carrier OTFS assumption may not be applied for DZT-based OTFS.

To overcome these drawbacks, consider pulse radar based on DZT

JITSUMATSU LAB. 27

Biorthogonal robust property[3]

$$A_{g_{RX}g_{TX}}(\tau,\nu) = \int g_{RX}(t)g_{TX}^{*}(t-\tau)e^{-i2\pi\nu t}\,dt = 0$$

for $\tau \in (nT - \tau_{\max}, nT + \tau_{\max}), \nu \in (m\Delta f - \nu_{\max}, m\Delta f + \nu_{\max})$

Early studies[6] assumed this equation even though there is no waveform that satisfies it. Today, this assumption is rarely seen.

JITSUMATSU LAB. 28

[6] P. Raviteja, K. T. Phan, Q. Jin, Y. Hong and E. Viterbo, "Low-complexity iterative detection for orthogonal time frequency space modulation," *WCNC2018.*

Our past research and remaining issues

- We have proposed Gabor Division Spread Spectrum (GDSS) [7].
- The transmitted signal is

$$s(t) = \sum_{n=0}^{N-1}\sum_{m=0}^{M-1} X[m,n]\,g(t-nT)e^{j\frac{2\pi}{T}mt} \qquad g(t) \text{ is a Gaussian waveform}$$

- Phase Updating Loop (PUL) algorithm to detect delay and Doppler was proposed. (Details are omitted)
- Digital implementation and radar application was studied by Ohashi. (2018)

Remaining Issues: Convergence proof for PUL. High computational cost of PUL.

JITSUMATSU LAB. 29

[7] T. Kohda, Y. Jitsumatsu and K. Aihara, "Gabor Division/Spread Spectrum System Is Separable in Time and Frequency Synchronization," VTC2023 Fall, 2013

Proposed Method

❑ Pulse radar using DZT-based GDSS signal is considered.

- The transmitted signal is a digital version of GDSS.
- Symbols must be designed (not random) ← under study.
- To be used as a pulse radar, signals are transmitted in pulses at regular intervals.

❑ Delay-Doppler estimation

- Use a discrete ambiguity function.
- Any delay-Doppler estimation is based on the calculation of the ambiguity function.
- Discrete ambiguity function can be efficiently computed by sliding FFT.
  → Avoiding the high computational complexity of PUL

JITSUMATSU LAB. 30

Comparison of OTFS pilot signal and GDSS signal structure

(Omit Guard Interval/Cyclic Prefix)

Assumption: Propagation path is invariant during one block

➢ OTFS one block

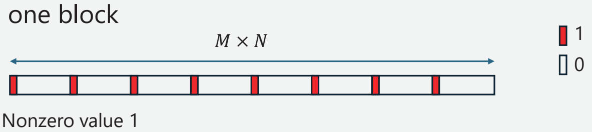

➢ GDSS one block

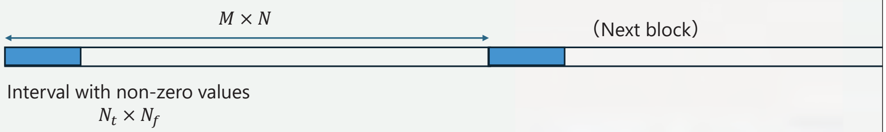

- Processing multiple GDSS blocks together is a future challenge.

JITSUMATSU LAB. 31

TF domain and time domain representation

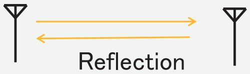

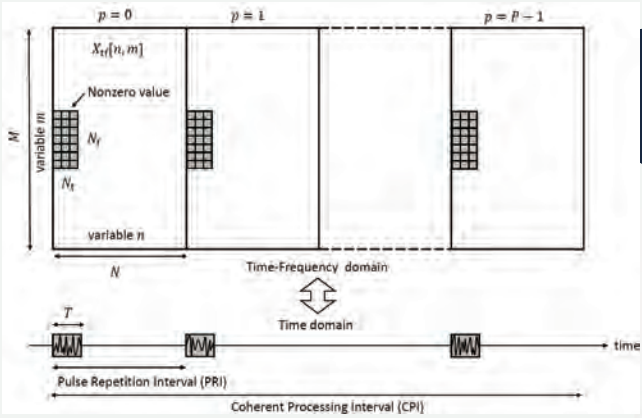

When transmitting radio waves, signals in the same frequency band cannot be received at the same time.

Parameters used in the experiment :

$N_t = N_f = 8, N = 64, M = 16.$

$U_t = \frac{M}{N_f} = 2, U_f = \frac{N}{N_t} = 8$

JITSUMATSU LAB. 32

Delay and Doppler detection for Gabor Division Spread Spectrum

Input $(L = NM)$

Received signal → Calculation of ambiguity function → Output $(L \times L)$ Discrete Ambiguity Function $A[k, \ell]$ → Integer Unit Estimation → Fractional part estimation

Transmitted signal replica → Calculation of ambiguity function

$(L\text{-point FFT}) \times L$

Output L-dimensional vector per unit time

It is a common practice to divide the data into two steps. The fractional part is estimated by completion with a double sinc function.

OTFS

Input $(L = N \times M)$

Received signal $r[nM + \ell]$ → DZT $(n \to k)$ → Output $(N \times M)$ $Y[k, \ell]$ → Integer Unit Estimation → Fractional part estimation

$(M\text{-point IFFT}) \times N$

Transmit signal is fixed to pilot symbols

Output $N \times M$ matrix for each L time

JITSUMATSU LAB. 33

Sliding DFT to compute the discrete ambiguity function

➢ Ambiguity function

$$A_{rs}[k,\ell] = \sum_n r[n]s^*[n-\ell]W_L^{nk} = \mathrm{FFT}\big[r[\cdot]s[\cdot - \ell]\big]$$

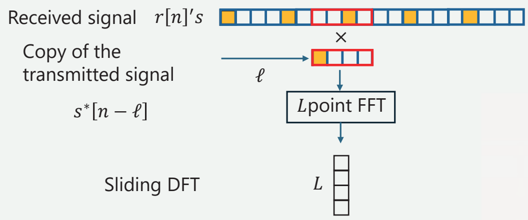

JITSUMATSU LAB. 34

Delay-Doppler Estimation

❑ OTFS-based Method A [8]

- Calculate the ambiguity function $A_{rs}(\tau, \nu)$ on a grid finer than an integer. Disadvantage: increased computational complexity

❑ OTFS-based Method B [9]

- Coarse integer unit estimation of sampling interval and FFT frequency bins. And fractional part estimation (piecewise-linear interpolation)

❑ Our method

- Estimation method: integer unit estimation + fractional part estimation.
- Novelty: use 2-D sinc function for fractional part estimation.
- Simulation evaluation. Greatly improved accuracy. Computational complexity is also small.

[8] L.Gaudio, M.Kobayashi, G.Caire, G.Colavolpe, "On the effectiveness of OTFS for Joint Radar Parameter Estimation and Communication," IEEE Trans. Wireless Comm.Vol.19, 2020.
[9] K.Zhang et al., "Radar sensing via OTFS signaling: A delay doppler signal processing perspective," arXiv:2301.09909, 2023.

JITSUMATSU LAB. 35

Approximation formula for continuous ambiguity function

- Estimation of fractional parts of delay and Doppler

$$(\hat{\alpha}, \hat{\epsilon}_{\mathrm{t}}, \hat{\epsilon}_{\mathrm{f}}) = \operatorname*{argmin}_{\alpha \geq 0, \epsilon_{\mathrm{t}}, \epsilon_{\mathrm{f}}} \sum_{|\ell| \leq U_{\mathrm{t}}} \sum_{|k| \leq U_{\mathrm{f}}} \left\{ |A_{r,s}[\hat{\ell}_{\mathrm{d}} + \ell, \hat{k}_{\mathrm{D}} + k]| - \alpha |\tilde{A}(\ell - \epsilon_{\mathrm{t}}, k - \epsilon_{\mathrm{f}})| \right\}^2$$

- Computing the exact self-ambiguity function $A_{ss}(\tau, \nu)$ is very expensive. → We approximate it.

$$\tilde{A}(\tau, \nu) = \begin{cases} \mathrm{sinc}(U_{\mathrm{t}}\tau) \cdot \mathrm{sinc}(U_{\mathrm{f}}\nu) & \text{if } |U_{\mathrm{t}}\tau| < 1 \text{ and } |U_{\mathrm{f}}\nu| < 1 \\ 0 & \text{otherwise} \end{cases}$$

Pseudorandom Number A

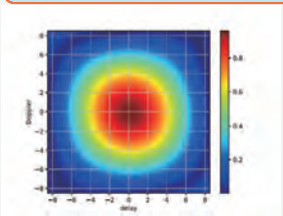

Pseudorandom Number B

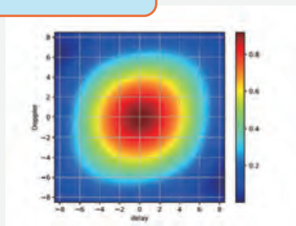

36

Theorem. Let $A_{ss}(\tau, \nu)$ be the symmetric auto-ambiguity function. Let

$$s(t) = \frac{1}{\sqrt{NM}} \sum_{n=0}^{N-1} \sum_{m=0}^{M-1} X_{TF}[m, n] g(t - nT) \, \mathrm{e}^{\mathrm{i}2\pi m \Delta f t}$$

For an i.i.d. $X_{TF}[m, n]$, we have

$$E[A_{ss}(\tau, \nu)] = A_{gg}(\tau, \nu) \mathrm{Diric}_N(\nu T) \mathrm{Diric}_M(\tau \Delta f),$$

where

$$\mathrm{Diric}_N(z) = \frac{1 - \mathrm{e}^{-\mathrm{i}2\pi N z}}{N(1 - e^{-\mathrm{i}2\pi z})}.$$

$|\mathrm{Diric}_N(z)| = \frac{\sin N\pi z}{N \sin \pi z} \approx \mathrm{sinc}(Nz)$ for $|Nz| < 1$ if $N \gg 1$.

Thus, for $|\tau| < \frac{T}{M}, |\nu| < \frac{\Delta f}{N}$, $|E[A_{ss}(\tau, \nu)]| \approx A_{gg}(\tau, \nu) \mathrm{sinc}(\nu N T) \mathrm{sinc}(\tau M \Delta f)$

JITSUMATSU LAB.

37

The discrete version can be proved in a similar way.

Proposed method (delay-Doppler detection algorithm)

- ❑ Choose pseudo-random numbers $X[m,n]$.
- ❑ Select a threshold value $\theta > 0$.

1. Calculate Ambiguity function in discrete time (using FFT)

$$A_{r,s}[\ell,k] = \sum_{j=0}^{NM-1} r[j]s^*[j-\ell]W_{NM}^{kj}$$

2. List up $[\ell,k]$ satisfying $|A_{r,s}[\ell,k]| > \theta$. Denote them as $\hat{\ell}_d$, and $\hat{k}_D$.
3. For each $\hat{\ell}_d$, $\hat{k}_D$ listed in 2., do the following (this time using scipy functions)

$$(\hat{\alpha},\hat{\epsilon}_{\rm t},\hat{\epsilon}_{\rm f}) = \underset{\alpha\geq 0,\epsilon_{\rm t},\epsilon_{\rm f}}{\rm argmin} \sum_{|\ell|\leq U_{\rm t}} \sum_{|k|\leq U_{\rm f}} \left\{ |A_{r,s}[\hat{\ell}_{\rm d}+\ell,\hat{k}_{\rm D}+k]| - \alpha|\tilde{A}(\ell-\epsilon_{\rm t},k-\epsilon_{\rm f})| \right\}^2$$

4. Let $(\hat{\ell}+\epsilon_t,\hat{k}+\epsilon_f)$ be the delay and Doppler estimates.

JITSUMATSU LAB. 38

Performance evaluation

Integer Unit Estimation:
RMSE of uniform distribution on $[-0.5,0.5]$ is 0.288

- ❑ Root Mean Square Error (RMSE)

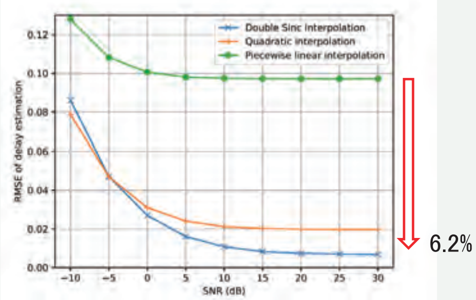

RMSE of delay estimation Unit $\left(\frac{T_s}{U_t}\right)$

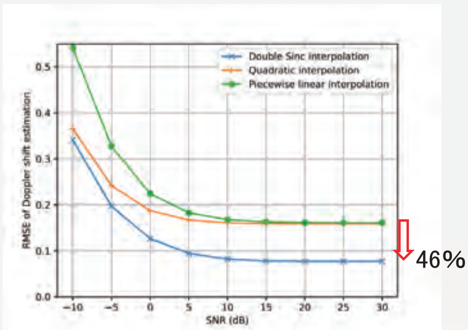

RMSE of Doppler estimation Unit $\left(\frac{f_{\rm bin}}{U_f}\right)$

※ Quadratic approximation around the origin of the Ambiguity function (details omitted)

JITSUMATSU LAB. 39

Comparison of execution times

- ❑ Environment：Intel Core-i9-13900KF 3.0GHz, Memory 128GB Windows + VSCode

  Computation time (average over 1000 runs)

Step1 Computation of discrete Ambiguity function	Step3 Fine estimation via matching with the 2D sinc function	Step3 interpolation by quadratic function	Step3 interpolation by piecewise linear function
1.29 millisecond	2.23millisecond	0.59 microsecond	0.205 microsecond

- ❑ Methods based on approximations by 2D sinc functions take about twice as long as integer unit estimation (first step).
- ❑ The scipy library uses a quasi-Newton method.
- ❑ Evaluation of the computational order is a future work.

JITSUMATSU LAB. 40

Remarks

- ❑ Isn't this a topic that has been well-researched for some time?
  - Yes. However, what we want to claim is the following.
  - The central part of the ambiguity function can be approximated by a two-dimensional sinc function. ➔This is a new finding.
  - We have to choose a good two-dimensional pilot signal.
- ❑ If quadratic interpolation is not sufficient, why not employ a higher-order approximation such as spline interpolation?
  - That's right. We must explore that soon.
- ❑ The simple method of making the grid finer increases the sampling rate and significantly increases the computational complexity.

JITSUMATSU LAB. 41

Conclusions

- ❑ Delay and Doppler estimation for radar.
- ❑ Comparison with existing methods
  - FM-CW
  - Pulse radar
  - OTFS
- ❑ Future research
  - Pilot signal selection method
  - Extension to MIMO
  - Joint Sensing and Communications.

JITSUMATSU LAB. 42

Designing Communication Receivers Using Machine Learning Techniques

Brian Kurkoski

School of Information Science, Japan Advanced Institute of Science and Technology
kurkoski@jaist.ac.jp

Your smartphone has many communications receivers, not only in its various wireless interfaces, but in the flash memory controller as well. In fixed-precision VLSI receivers, reducing the number of bits used to represent messages will reduce power consumption and increase battery life. This presentation describes the design of fixed-precision receivers from an information theory perspective. This can be called "hardware-aware information theory" because the objective is to maximize mutual information (an information theory quantity) while minimizing the number of message bits (in the hardware implementation). Results from machine learning play a key role, because quantization can be seen as classification. Numerical results show that widely-used decoders for low-density parity-check (LDPC) codes based on the proposed max-LUT method can outperform belief-propagation decoders [1] [2] [3] [4] [5].

Acknowledgment

This work was supported by JSPS Kakenhi Grant Number JP 21H04873.

References

[1] Bo-Yu Tseng, Brian M. Kurkoski, Philipp Mohr, and Gerhard Bauch. An FPGA implementation of two-input LUT based information bottleneck LDPC decoders. In *International Conference on Modern Circuits and Systems Technologies (MOCAST)*, 2022.

[2] Brian Michael Kurkoski and Hideki Yagi. Single-bit quantization of binary-input, continuous-output channels. pages 2088–2092, Aachen, Germany, June 2017.

[3] Alan Zhang and Brian M. Kurkoski. Low-complexity quantization of discrete memoryless channels. In *International Symposium on Information Theory and Its Applications*, pages 453–457, October–November 2016.

[4] Francisco Javier Cuadros Romero and Brian M. Kurkoski. LDPC decoding mappings that maximize mutual information. 34(9):2391–2401, August 2016.

[5] Brian M. Kurkoski and Hideki Yagi. Quantization of binary-input discrete memoryless channels. 60(8):4544–4552, August 2014.

Designing Communication Receivers Using Machine Learning Techniques

Brian M. Kurkoski
Japan Advanced Institute of Science and Technology

2024 September 26
Mathematics for Innovation in Information and Communication Technology Workshop

Smartphone Communications Receivers

apple.com

Smartphone has numerous wireless receivers:

- cellular radio (5G, LTE)
- WiFi
- Bluetooth

The data storage also uses a "receiver"

- flash memories

Many other devices have receivers:

- digital video broadcast
- wired ethernet
- SSDs and hard drives

2

Smartphone Communications Receivers

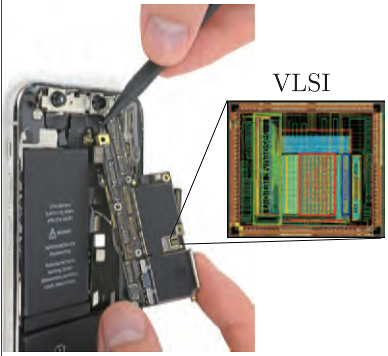

Communication receivers are implemented in VLSI hardware:

- More efficient than CPUs
- VLSI uses integer arithmetic or fixed point
- But, most communications algorithms use real numbers

To implement an algorithm in VLSI, must approximate real numbers with integers.
Tradeoff:

- More bits per integer: better performance
- Fewer bits per integer: more efficient VLSI

ifixit.com

ETH Zurich http://bit.ly/2nTEfCy

3

Smartphone Communications Receivers

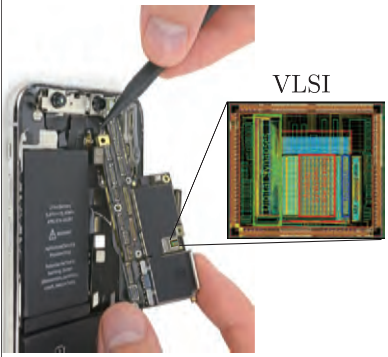

Engineers implement quantization schemes in an “ad hoc” way: try different schemes, choose the best one.

Can we give a theoretical foundation to quantization of communication receivers?

“Communication receiver” includes:

- equalization,
- detection and
- error-correction, particularly LDPC codes

ifixit.com

ETH Zurich http://bit.ly/2nTEfCy

4

Outline

1 Background on Communications and LDPC Codes

- Just enough information theory
- LDPC codes and their decoding

2 Quantization and Classification

- Connections between machine learning on information theory
- Optimal quantization for binary inputs
- “KL-means” algorithm and information bottleneck method

3 Hardware-Aware Information Theory

- Max-LUT method
- Works amazingly well: efficient and good performance
  - LDPC decoding: 4 bits/message “performs like floating point”

5

Just Enough Information Theory

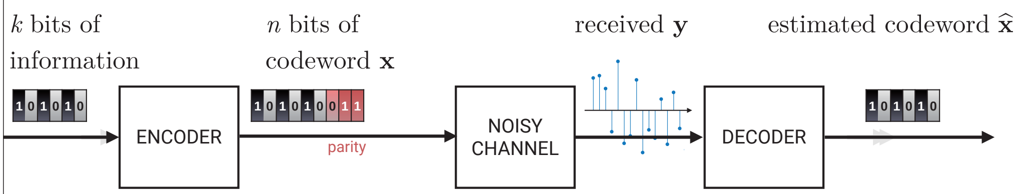

Code rate is $R = k \,/\, n$
Good channel (high SNR) — high code rate R (few parity bits)
Bad channel (low SNR) — low code rate R (many parity bits)

6

Just Enough Information Theory

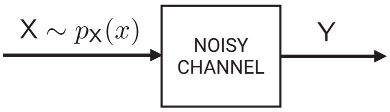

What is the best we can do?

Code rate < Channel Capacity

$$R < C = \max_{p_X(x)} I(X;Y)$$

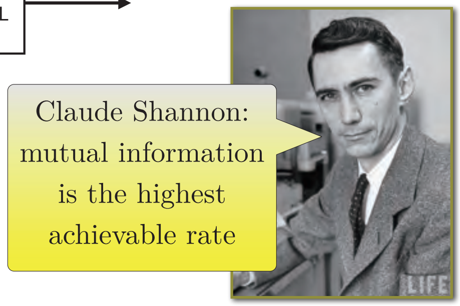

LDPC Codes and Their Success

Low-density parity-check (LDPC) are now a widely-used error-correcting code:

- 5G and 6G cellular data,
- recent WiFi 802.11 standards,
- video broadcasting,
- wired ethernet,
- flash memories, SSD drives, hard drives

Reasons for success of LDPC code:

- LDPC codes are good codes — long codes are close to the Shannon limit, empirically
- Message passing decoding of LDPC codes: complexity is linear in the block length

8

Low-Density Parity-Check (LDPC) Codes

LDPC code is defined by a low-density parity-check matrix H

A codeword $\mathbf{x}$ satisfies $H\mathbf{x} = 0 \bmod 2$

H =

x_0	x_1	x_2	x_3	x_4	x_5	x_6	x_7	x_8	x_9	x_{10}	x_{11}
1	1	1	1	0	0	0	0	0	0	0	0
0	1	1	0	1	0	0	1	0	0	0	0
1	0	1	1	0	0	0	0	1	0	0	0
1	0	0	0	0	0	1	0	1	1	0	0
0	1	0	0	1	0	1	0	0	0	1	0
0	0	0	1	0	1	0	0	0	0	1	1
0	0	0	0	1	0	0	1	1	0	1	0
0	0	0	0	0	1	0	1	0	1	0	1
0	0	0	0	0	1	1	0	0	1	0	1

Parity-Check Matrix

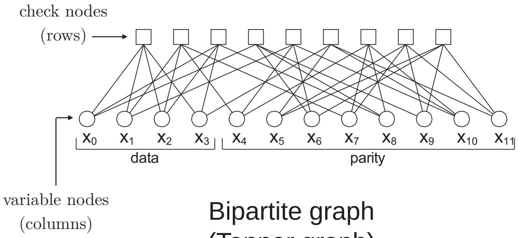

Bipartite graph
(Tanner graph)

9

Decoding LDPC Codes
Input from channel

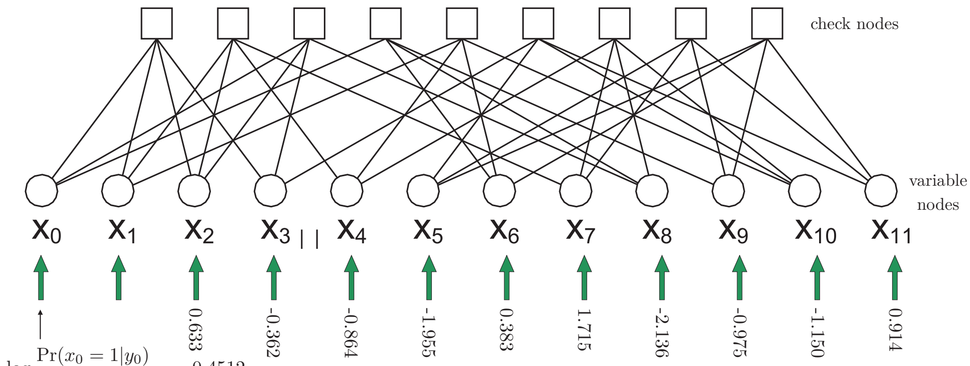

$$\log \frac{\Pr(x_0 = 1|y_0)}{\Pr(x_0 = 0|y_0)} = -0.4512$$

input from channel

Decoding LDPC Codes Iteratively Exchange Messages

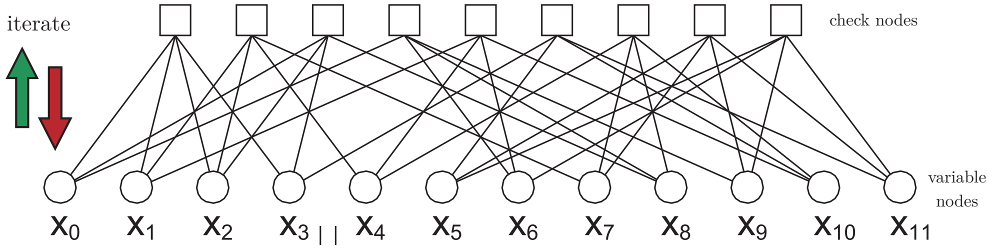

In practice, perform 5 to 50 iterations. Stop when:

- Codeword is detected $H\mathbf{x} = 0$
- maximum number of iterations reached

Nodes are Functions Edges are Messages

check node

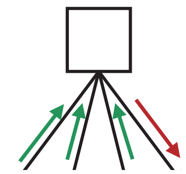

$$-2\tanh^{-1}\Big(\prod_{i\in\mathcal{M}(c)\setminus c}\tanh\big(-\frac{L_i}{2}\big)\Big)$$

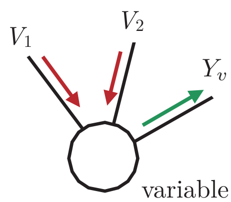

$$Y_v + \sum_{i\in\mathcal{N}(v)\setminus v} V_i$$

variable node

"sum-product rule":
for edge e, do not use incoming message e

final decisions:

$$\widehat{L}_v = Y_v + \sum_{i\in\mathcal{N}(v)} V_i$$

12

Quantization of Message-Passing Decoding

VLSI

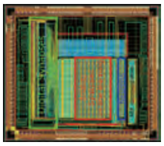

value	two's complement
-1.0	100
-0.75	101
-0.5	110
-0.25	111
0	000
0.25	001
0.5	010
0.75	011

3-bit quantized messages

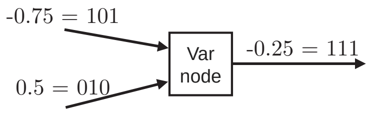

VLSI implementations use fixed point (integer) arithmetic

- How to choose quantization? 7 bits/message for floating-point performance. We want fewer bits/message
- How to implement nonlinear functions?

Instead of ad hoc schemes, can we consider a more theoretical approach?

- **Next: Node function is a lookup table that maximizes mutual information**

13

2 Quantization and Classification

Quantization and Classification

- Key problem is channel quantization to maximize mutual information
- Strong similarities to classification in machine learning
- Optimal, polynomial-time algorithm for binary input
- K-Means algorithm/Lloyd-Max algorithm
- "KL-means" algorithm for non-binary input is suboptimal but efficient

14

Machine Learning: Classification

Example of a simple classification problem:

- X is a fruit
- One-pixel camera takes picture of a fruit, provides sample Y
- A classifier Q should choose one of strawberry, banana or kiwi $\mathsf{Z} = \mathrm{Q}(\mathsf{Y})$

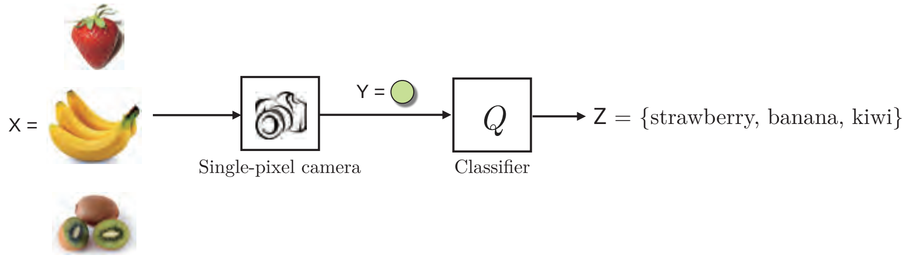

15

Machine Learning: Classification

- Classification is an important machine learning problem
- Connections with information theory

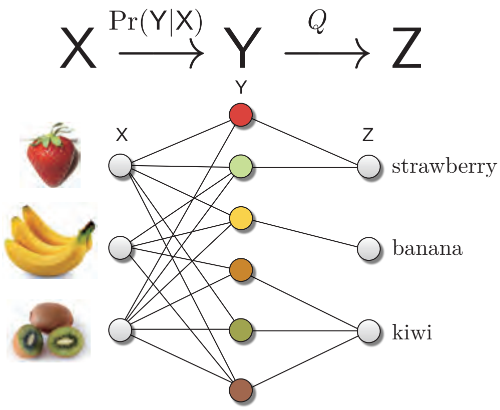

Machine learning
Minimum-entropy optimal classifier Q^*:

$$Q^* = \arg\min_{Q} H(\mathsf{Z}|\mathsf{X})$$

Q is called a classifier

Information Theory

$$\max_{Q} I(\mathsf{X};\mathsf{Z}) = H(\mathsf{X}) - \min_{Q} H(\mathsf{Z}|\mathsf{X})$$

Q is called a quantizer

16

Key Problem — Quantization

$$\mathsf{X} \xrightarrow{\Pr(\mathsf{Y}|\mathsf{X})} \mathsf{Y} \xrightarrow{Q} \mathsf{Z}$$

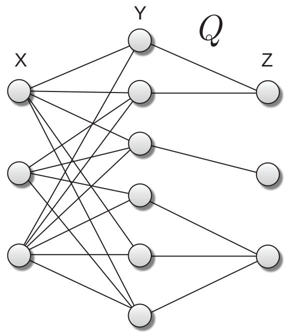

Given a discrete memoryless channel and input distribution $p_{\mathsf{XY}}(x, y)$, find the quantizer Q which maximizes mutual information:

$$Q^* = \arg\max_{Q} I(\mathsf{X}; \mathsf{Z})$$

with $|\mathsf{Z}| < |\mathsf{Y}|$.

$|\mathsf{Z}| \geq |\mathsf{Y}|$ is trivial.

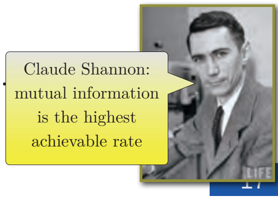

Backward Channel $\Pr(\mathsf{X} \mid \mathsf{Y})$ as a Vector

$$\mathbf{u}_y = \Big[\Pr(\mathsf{X} = 1|\mathsf{Y} = y), \Pr(\mathsf{X} = 2|\mathsf{Y} = y), \ldots, \Pr(\mathsf{X} = J|\mathsf{Y} = y)\Big]$$

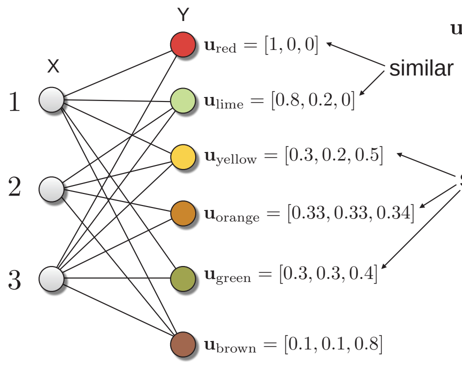

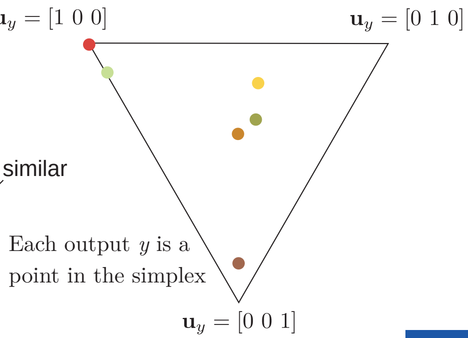

Quantization in Backwards Channel

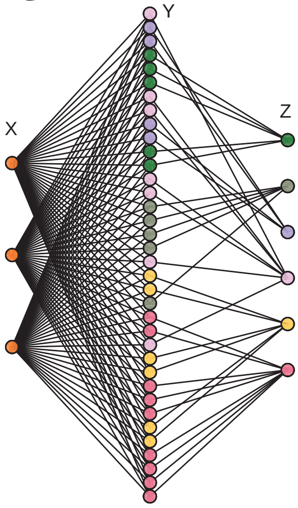

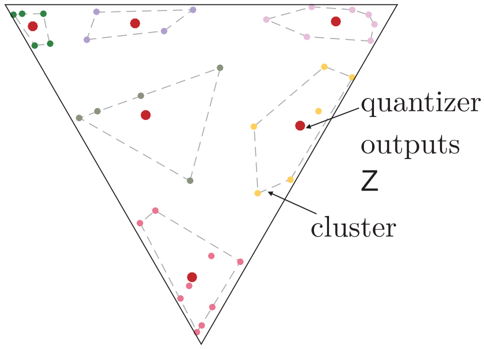

- Cluster shows all y which are mapped to a given z

19

Optimal Quantizer Design Algorithm for Binary Inputs

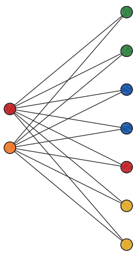

- Cluster (preimage of optimal quantizer) is convex [Burshtein et al, 1992]
- Dynamic programming: Search over all convex quantizers
- Provably optimal — max mutual information
- Complexity is M^3

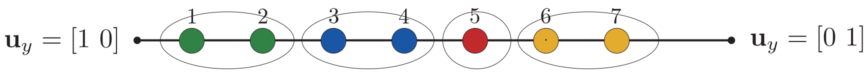

B. Kurkoski and H. Yagi, "Quantization of Binary-Input Discrete Memoryless Channels," IEEE Trans on Information Theory, May 2014.

20

K-Means Algorithm (machine learning) Lloyd-Max Algorithm (information theory)

iterate

1. given n-dimensional data set, randomly choose K means (centroids)
2. **nearest neighbor** K clusters consists of data points closest to its mean in Euclidean distance
3. **centroid step** move the mean to the center of the cluster

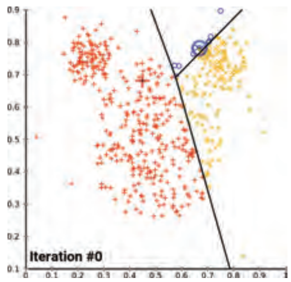

wikipedia

Not optimal but works well in practice.
Hugely successful in machine learning

21

K-Means with Generalized Metrics

"KL-Means algorithm" replace Euclidean distance with Kullback-Leiber Divergence

22

KL-Means Algorithm

"KL-Means algorithm" replace Euclidean distance with KL distance

Min KL divergence = max. mutual information

$$Q^* = \arg\max_Q I(\mathsf{X};\mathsf{Z}) = \arg\min_Q E\big(D(\mathbf{U}||\mathbf{V})\big)$$

Numerical results show tradeoff:

- increasing number of quantizer outputs
- decreases the loss of mutual information

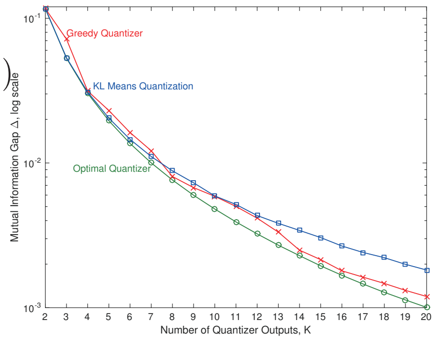

A. Zhang and B. Kurkoski, "Low-Complexity Quantization of Non-Binary Input DMCs" ISITA 2016.

23

KL-Means ≈ Information Bottleneck Method

Information bottleneck method (Tishby, et al., 2000). For the Markov chain:

$$\mathsf{X} \to \mathsf{Y} \to \mathsf{Z}$$

How much information Z provides about X through the "bottleneck" Y:

$$\min_{p_{\mathsf{Z}|\mathsf{Y}}(z|y)} I(\mathsf{Y};\mathsf{Z}) - \beta I(\mathsf{X};\mathsf{Z})$$

The information bottleneck and KL-means algorithms both try to solve:

$$\max_Q I(\mathsf{X};\mathsf{Z})$$

When $\beta \to \infty$ **the two algorithms are equivalent**.

B. M. Kurkoski, "On the relationship between the KL means algorithm and the information bottleneck method," in 11th International ITG Conference on Systems, Communications and Coding (SCC2017).

24

3 Hardware-Aware Information Theory

Hardware-Aware Information Theory

- Max-LUT method — Mutual-information maximizing lookup tables
- Application of Max-LUT to LDPC decoding
- Numerical results: 4 bits/message "performs like floating point"

25

Max-LUT Method

How is it possible to replace mathematical operations with lookup tables?

Max-LUT is a method for implementing the node decoder functions for graph-based decoders, using lookup tables that maximize mutual information.

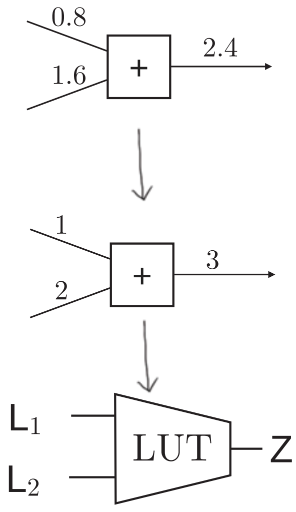

26

Characteristics of the Max-LUT Method

- We need a factor graph
- We need input probability distributions
- Factor graph messages are discrete
- Decoding functions are look up tables (LUT)
- Lookup tables are designed to maximize mutual information

27

Lookup Table (LUT) Implementation

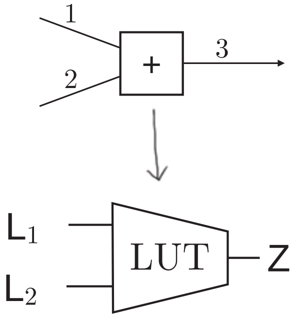

L_1 \ L_2	0	1	2	3
0	0	0	1	2
1	0	1	2	3
2	0	2	2	3
3	2	2	3	3

2-bit lookup table, $0 = 00$, $1 = 01$, etc.

- Assume that LUTs are easy to implement in VLSI hardware
- Do not use quantized LLRs, just labels 0=00, $1 = 01$, etc.

28

Max-LUT Method: Central Idea with Factor Graphs

Encoder Side. Code symbols X

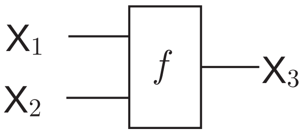

Decoder Side

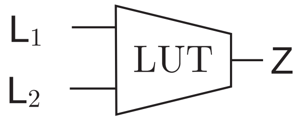

- Check node f : $\mathsf{X}_3 = \mathsf{X}_1 + \mathsf{X}_2$
- Var node f : $\mathsf{X}_1 = \mathsf{X}_2 = \mathsf{X}_3$
- etc.

L_i is a noisy version of X_i ,
Z is a noisy version of X_3

Choose LUT to maximize mutual information

$$\max I\big(\mathsf{X}_3;\mathsf{Z}\big) = \max_{\mathrm{LUT}} I\big(\mathsf{X}_3;\mathrm{LUT}(\mathsf{L}_1,\mathsf{L}_2)\big)$$

Max-LUT Method: Three Steps

- Step 1: Find joint distribution from input distributions
- Step 2: Quantize joint distribution maximize mutual information
- Step 3: Find LUT from the quantizer

Example

- LDPC variable node, two inputs $\mathsf{L}_1, \mathsf{L}_2$ with $\Pr(\mathsf{L}_i|\mathsf{X}_i)$
- local constraint: "$x_1 = x_2 = x_3$"
- Goal: find max-MI lookup table $\mathsf{Z} = \mathrm{LUT}(\mathsf{L}_1, \mathsf{L}_2)$

Max-LUT Step 1: Joint Distribution

- Find joint distribution from input distributions

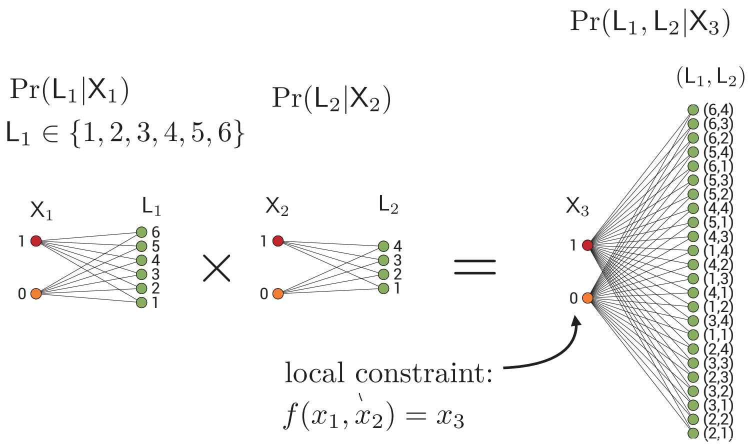

31

Max-LUT Step 2: Quantize

- Too many levels! Reduce to Z with K levels
- Quantizer is a mapping from (L_1,L_2) to Z

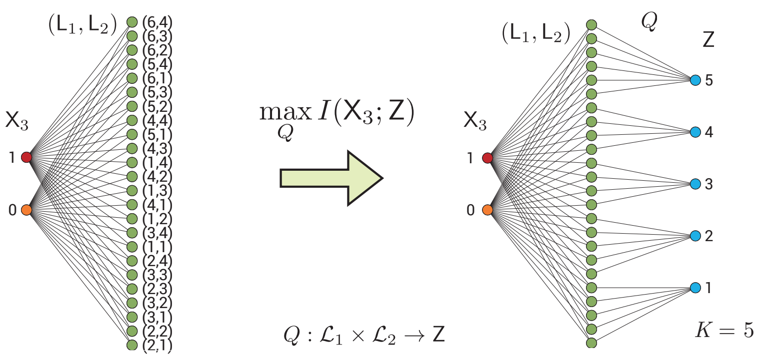

32

Max-LUT Step 3: Lookup Table

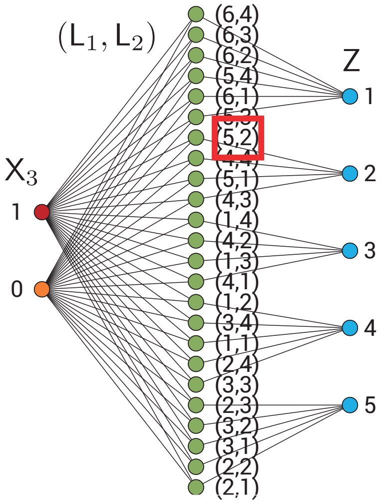

L_1 \ L_2	1	2	3	4
1	4	4	3	3
2	5	5	5	4
3	5	5	4	4
4	3	3	2	2
5	2	2	1	1
6	1	1	1	1

Lookup table:
$Z = \mathrm{LUT}(L_1, L_2)$

33

Application to LDPC Code Decoding

- How to obtain the probability distributions needed by Max-LUT method?

  > Density evolution

- How to keep the lookup table reasonable size?

  > Node decomposition or "opening the node"

- How does it perform numerically?

  > Similar to BP with four bits/message

34

Density Evolution Unwraps the Graph

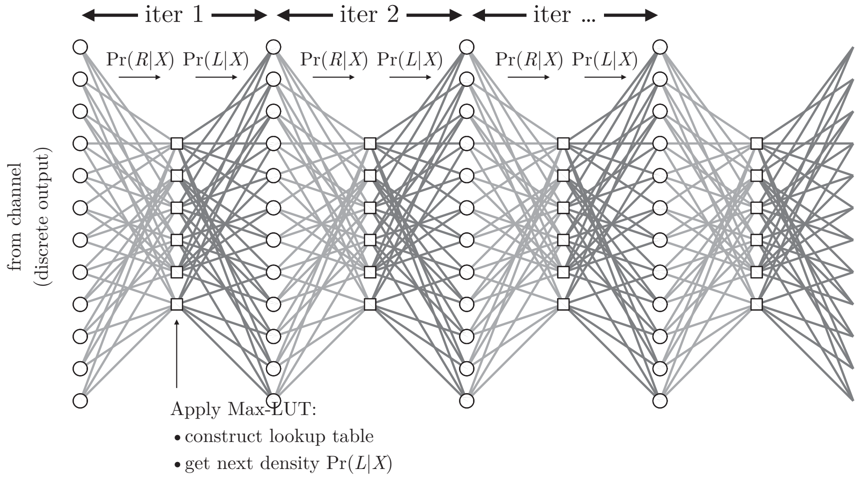

35

Non-Uniform Quantizer: Quantization Points

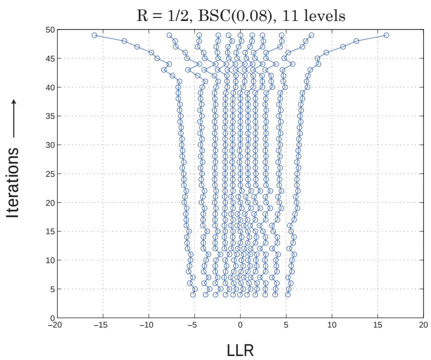

Beyond just LUT labels: We know the probability distributions.

> Use the find LLR values

> These LLR values show non-uniform quantization

36

Noise Thresholds with Quantization

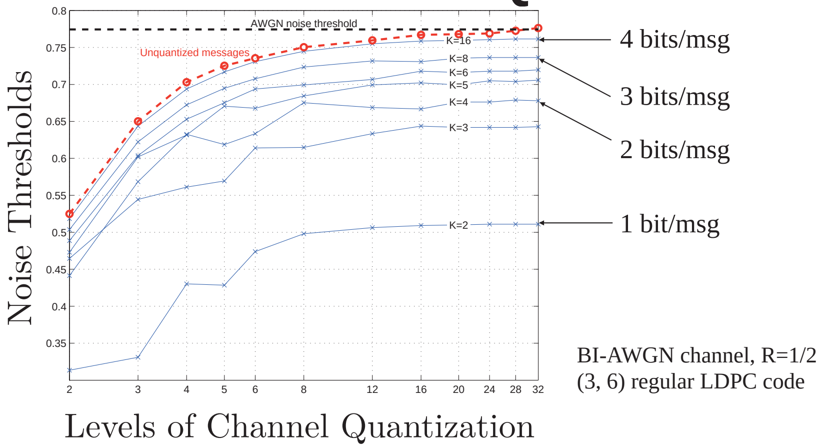

F. J. Cuadros Romero and B. M. Kurkoski, "LDPC decoding mappings that maximize mutual information," IEEE Journal on Selected Areas in Communications, vol. 34, pp. 2391-2401, August 2016

37

4 bits/message close to BP

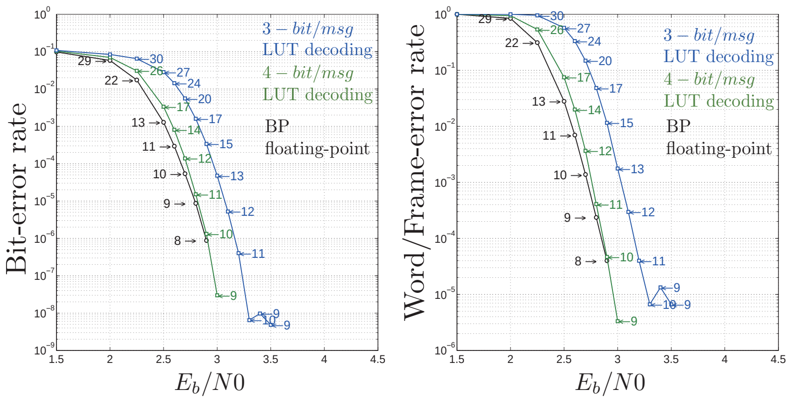

FIGURE 8. BER and WER results for the LUT decoding algorithm. $d_v = 4$, $d_c = 9$, $R = 0.56$, $N = 4113$, Max. Iter.= 30, Array code [2].

F. J. Cuadros Romero and B. M. Kurkoski, "LDPC decoding mappings that maximize mutual information," IEEE Journal on Selected Areas in Communications, vol. 34, pp. 2391-2401, August 2016

38

BSC: Lower Error Floor than Sum-Product But not lower than FAIDs

$N = 2388, (d_v = 3, d_c = 12), R = 0.75$ and Max. iter $= 60$

FAIDs are designed to avoid the effects of harmful subgraphs, lowering the error floor Planjery et al (2013).

The proposed decoding mapping functions can be used in a variety of channels not only in the BSC.

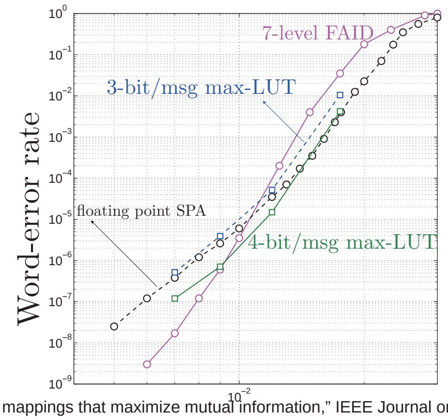

F. J. Cuadros Romero and B. M. Kurkoski, "LDPC decoding mappings that maximize mutual information," IEEE Journal on Selected Areas in Communications, vol. 34, pp. 2391-2401, August 2016

39

FPGA Implementations

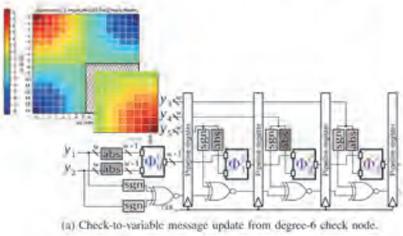

FPGA implementation exploits symmetry in LUT

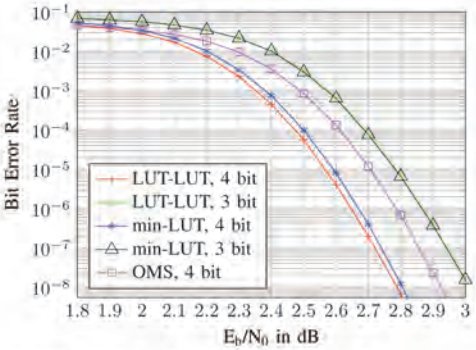

- 4 bit: max-LUT has lower error rates than state-of-the art offset min-sum (OMS)
- 3 bit: max-LUT has higher throughput/area (TAR) than OMS

B.-Y. Tseng, B. M. Kurkoski, P. Mohr, and G. Bauch, "An FPGA implementation of two-input LUT based information bottleneck LDPC decoders," in International Conference on Modern Circuits and Systems Technologies (MOCAST), 2022

40

Conclusion: Hardware-Aware Information Theory

- Overlap between machine learning and information theory
- Max-LUT method can gives floating-point performance using 4-bits/message
- Optimized non-uniform quantization method well-suited for VLSI hardware

Open Questions

- Can these techniques be applied more generally, e.g. to equalization and detection?
- Other decoders: non-binary LDPC or polar codes?
- How to deal with unknown channel distributions?
- What is special about 4-bits/message?

41

Lossless Data Compression Coding Schemes to Replace Huffman and Arithmetic Coding

Yamamoto Hirosuke

School of Frontier Sciences, The University of Tokyo, Japan
hirosuke@ieee.org

(joint work with Ken-ich Iwata)

Abstract: In this talk, we introduce new lossless data compression coding schemes, called the Almost Instantaneous Fixed-to-Variable length code (AIFV code) and the Asymmetric Encoding-Decoding Scheme (AEDS). The AIFV code can attain better compression rate than the Huffman code by using multiple coding trees and allowing a small decoding delay. The AEDS can be considered as a generalization of the ANS (Asymmetric Numeral Systems) proposed by Duda, which can attain almost the same compression rate as the arithmetic code with less arithmetic operations. We explain the encoding and decoding algorithms of the AIFV code and the AEDS, and clarify how and why these codes can beat the Huffman code and the arithmetic code.

Mathematics for Innovation in Information and Communication Technology, Sep. 25-27, 2024

Lossless Data Compression Coding Schemes to Replace Huffman and Arithmetic Coding

Hirosuke Yamamoto
(The University of Tokyo)

Outline

1. Overview of new lossless data compression coding schemes to replace Huffman coding and arithmetic coding.

2. AIFV codes (almost Instantaneous fixed-to-variable length codes) and extended codes, which can attain better compression rate than the Huffman code.

3. ANS (asymmetric numeral systems) and AEDS (asymmetric encoding-decoding schemes), which can attain almost the same compression rate as the arithmetic code with less mathematical operations.

No.3/53

Well-known lossless data compression codes

Huffman code
(Huffman[1] 1952)

Optimal code in the class of prefix−free codes (instantaneous codes).

Arithmetic coding
(Rissanen[2], Pasco[3], 1976)
Range coding
(Nigel-Martin[4], 1979)

Asymptotically optimal code for data sequences.

No.4/53

New lossless data compression coding schemes

Huffman code
(Huffman[1] 1952)

Optimal code in the class of prefix−free codes (instantaneous codes).

→ better compression rate

AIFV code
(Yamamoto-Tsuchihashi-Honda[5], 2015)
AIFV-*m* code
(Hu-Yamamoto-Honda[6], 2017)
N-bit-delay AIFV code
(Sugiura-Kamamoto-Moriya[7], 2023)

Arithmetic coding
(Rissanen[2], Pasco[3], 1976)
Range coding
(Nigel-Martin[4], 1979)

Asymptotically optimal code for data sequences.

→ less mathematical operations

Asymmetric Numeral Systems (ANS)
(Duda[8], 2009)

Asymmetric Encoding-Decoding Scheme (AEDS)
(Yamamoto-Iwata[9], 2024)

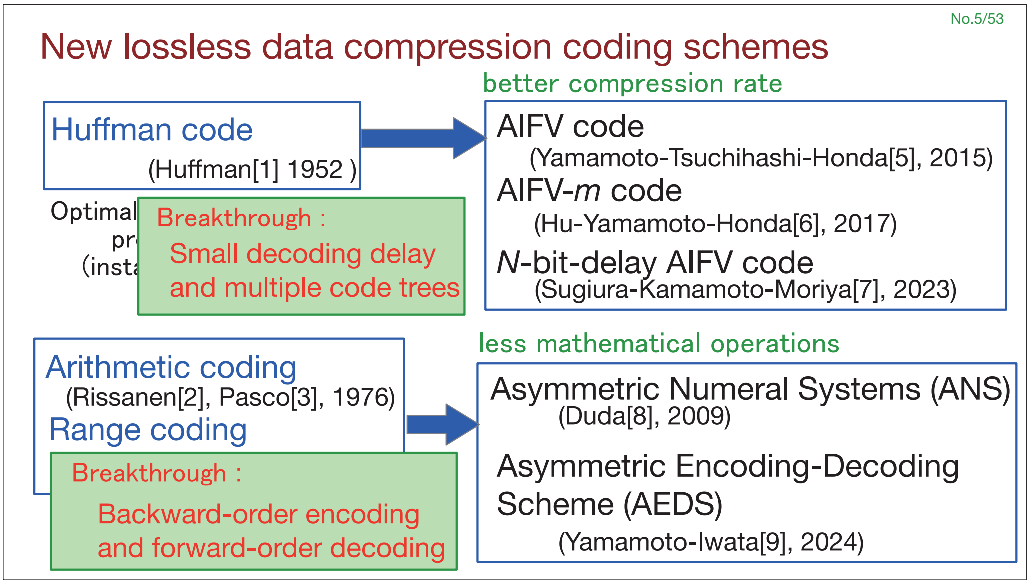

No.6/53

Outline

1. Overview of new lossless data compression coding schemes
   to replace Huffman coding and arithmetic coding.

2. AIFV codes (almost Instantaneous fixed-to-variable length codes)
   and extended codes, which can attain better compression rate
   than the Huffman code.

3. ANS (asymmetric numeral systems) and AEDS (asymmetric
   encoding-decoding schemes), which can attain almost
   the same compression rate as the arithmetic code
   with less mathematical operations.

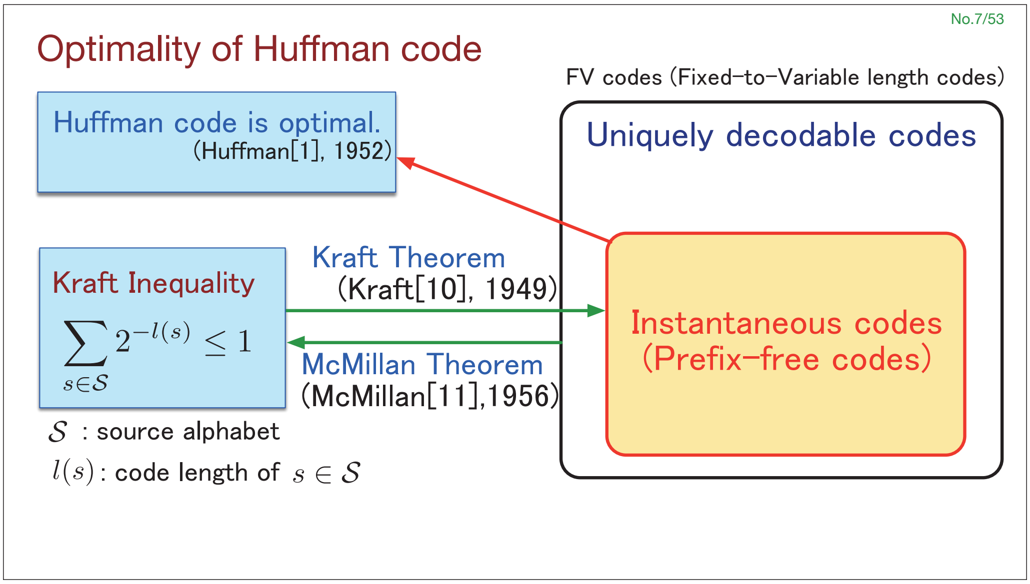
No.7/53
Optimality of Huffman code
Huffman code is optimal.
(Huffman[1], 1952)
FV codes (Fixed–to–Variable length codes)
Uniquely decodable codes
Kraft Inequality
$\sum_{s\in\mathcal{S}} 2^{-l(s)} \leq 1$
Kraft Theorem
(Kraft[10], 1949)
McMillan Theorem
(McMillan[11],1956)
Instantaneous codes
(Prefix–free codes)
$\mathcal{S}$: source alphabet
$l(s)$: code length of $s \in \mathcal{S}$

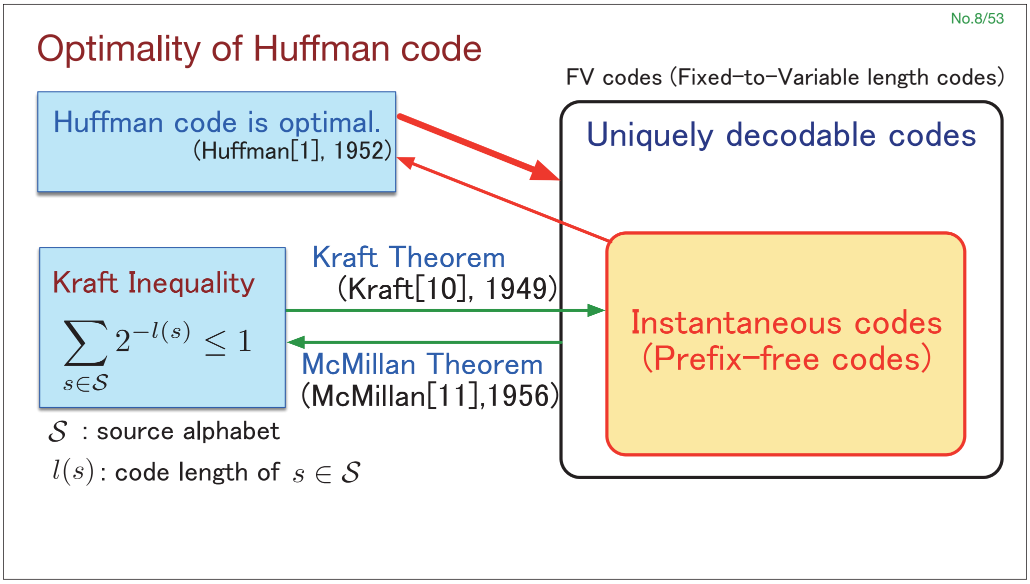
No.8/53
Optimality of Huffman code
Huffman code is optimal.
(Huffman[1], 1952)
FV codes (Fixed–to–Variable length codes)
Uniquely decodable codes
Kraft Inequality
$\sum_{s\in\mathcal{S}} 2^{-l(s)} \leq 1$
Kraft Theorem
(Kraft[10], 1949)
McMillan Theorem
(McMillan[11],1956)
Instantaneous codes
(Prefix–free codes)
$\mathcal{S}$: source alphabet
$l(s)$: code length of $s \in \mathcal{S}$

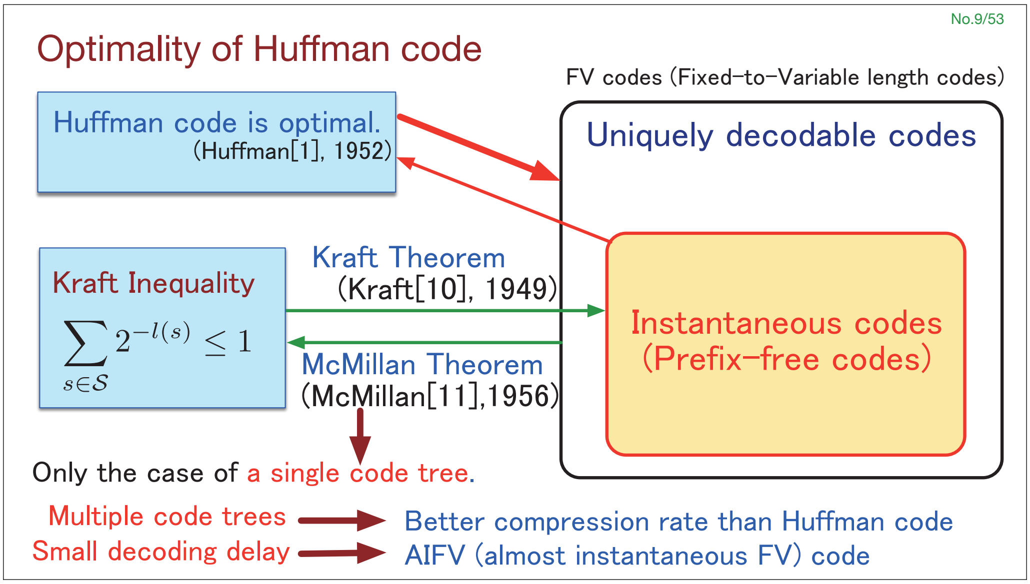

AIFV codes (Almost Instantaneous Fixed-to-Variable length codes)

	Number of code trees	Maximum decoding delay (bits)
AIFV code (Yamamoto-Tsuchihashi -Honda[5], 2015)	2	2
AIFV-m code (Hu-Yamamoto-Honda[6], 2017)	m	m
N-bit-delay AIFV code (Sugiura-Kamamoto-Moriya[7], 2023)	multiple	N

No.11/53

Hierarchy of FV codes

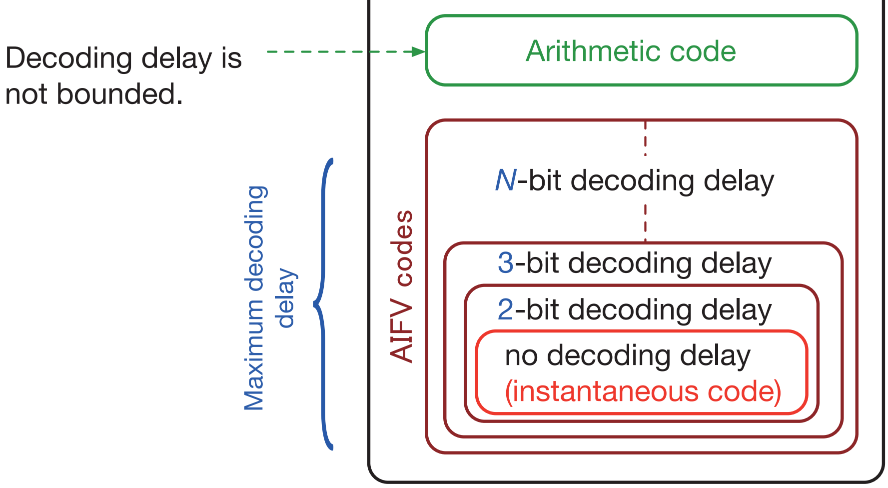

No.12/53

AIFV code (Yamamoto-Tsuchihasi-Honda[5], IEEE IT 2015)

(two code trees and 2-bit decoding delay)

Ex. 1 Source alphabet: $\mathcal{S} = \{a, b, c, d\}$
Code alphabet: $\mathcal{B} = \{0, 1\}$

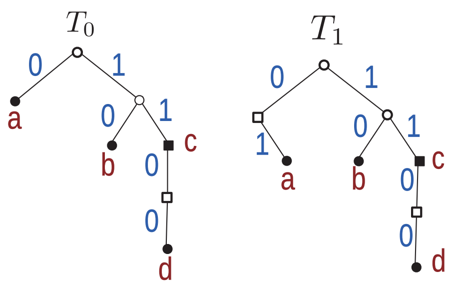

- ● Leaf
- ○ Complete internal node

Incomplete intenal node

- ■ Master node
- □ Slave node

No.13/53

Encoding of AIFV code

Data sequence : c b d c a

Codeword sequence : 11

T_0 : initial tree

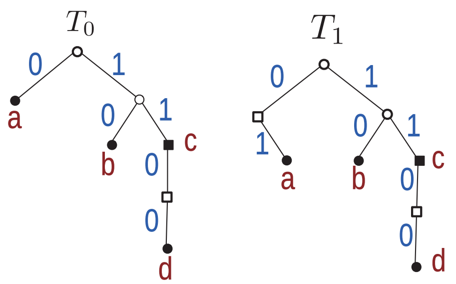

Transition rule of code trees

leaf ⟹ T_0

master node ⟹ T_1

No.14/53

Encoding of AIFV code

Data sequence : c b d c a

Codeword sequence : 11 10 1100 11 01

T_1 T_0 T_0 T_1

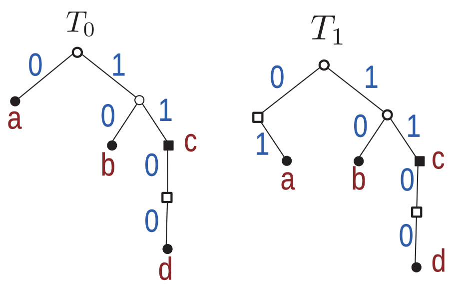

Transition rule of code trees

leaf ⟹ T_0

master node ⟹ T_1

Decoding of AIFV code

Codeword sequence : 111011001101

Data sequence : c

T_0 : initial tree

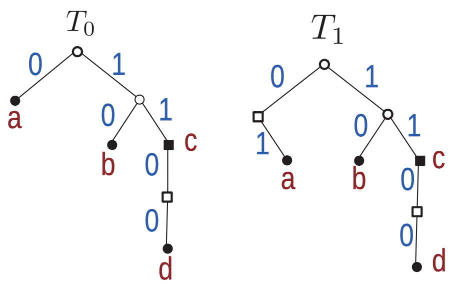

Transition rule of code trees

leaf → T_0

master node → T_1

Decoding of AIFV code

Codeword sequence : 111011001101

Data sequence : c b d c a

T_0 T_1 T_0 T_0 T_1

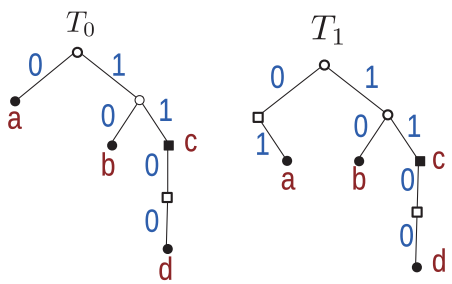

Transition rule of code trees

leaf → T_0

master node → T_1

Decoding of AIFV code

Codeword sequence : 111011001101

Data sequence : c b d c a

T_0 T_1 T_0 T_0 T_1

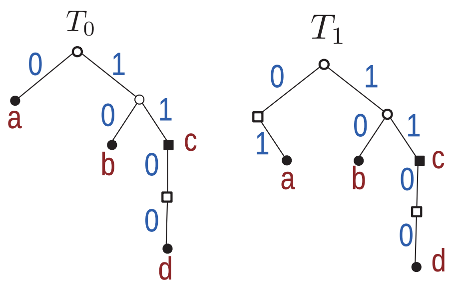

Uniquely decodable code with at most 2-bit decoding delay

Average code length

Ex. 2 $\mathcal{S} = \{a, b, c, d\}$ $\mathcal{B} = \{0, 1\}$

$p(a) = 0.45, p(b) = 0.3,$

$p(c) = 0.2, \quad p(d) = 0.05$

Entropy : $H(S) \approx 1.7200$

Huffman code tree

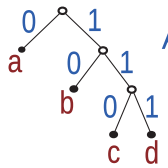

Average code length

$L_H = 1.8$

AIFV code tree

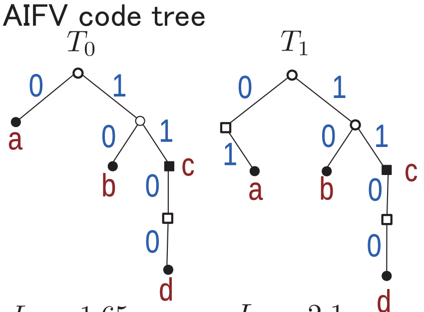

$L_0 = 1.65$ $L_1 = 2.1$

Transition probability of code trees

$Q(T_1|T_0) = p(c) = 0.2$

$Q(T_0|T_1) = p(a) + p(b) + p(d) = 0.8$

Stationary probability of code trees

$Q(T_0) = 0.8, Q(T_1) = 0.2$

Average code length

$$L_{AIFV} = Q(T_0)L_0 + Q(T_1)L_1$$
$$= 0.8 \times 1.65 + 0.2 \times 2.1$$
$$= 1.74$$

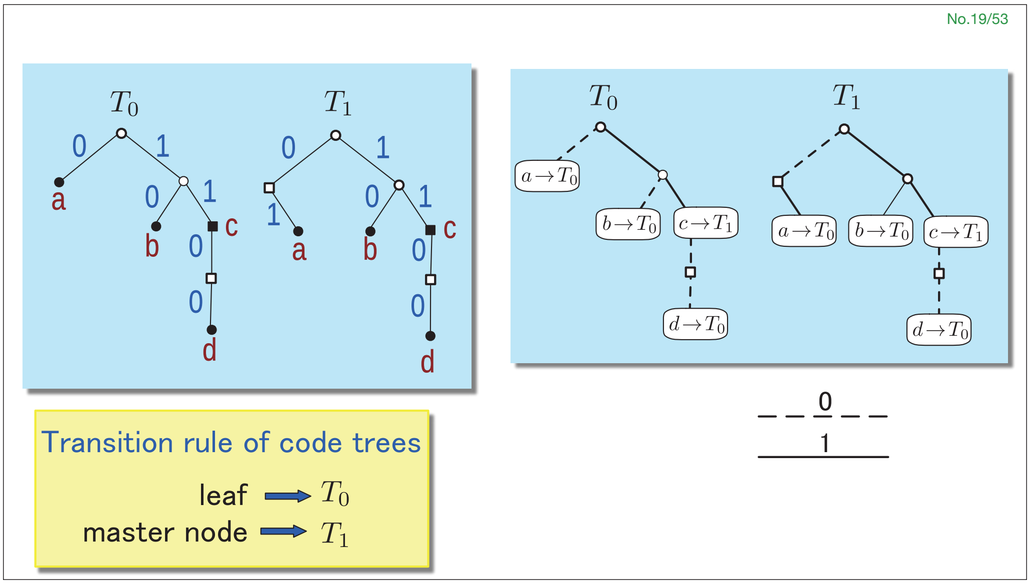
No.19/53
T_0
T_1
0
1
a
b
c
d
$a \to T_0$
$b \to T_0$
$c \to T_1$
$d \to T_0$
$a \to T_0$
$b \to T_0$
$c \to T_1$
$d \to T_0$
Transition rule of code trees
leaf ⟹ T_0
master node ⟹ T_1

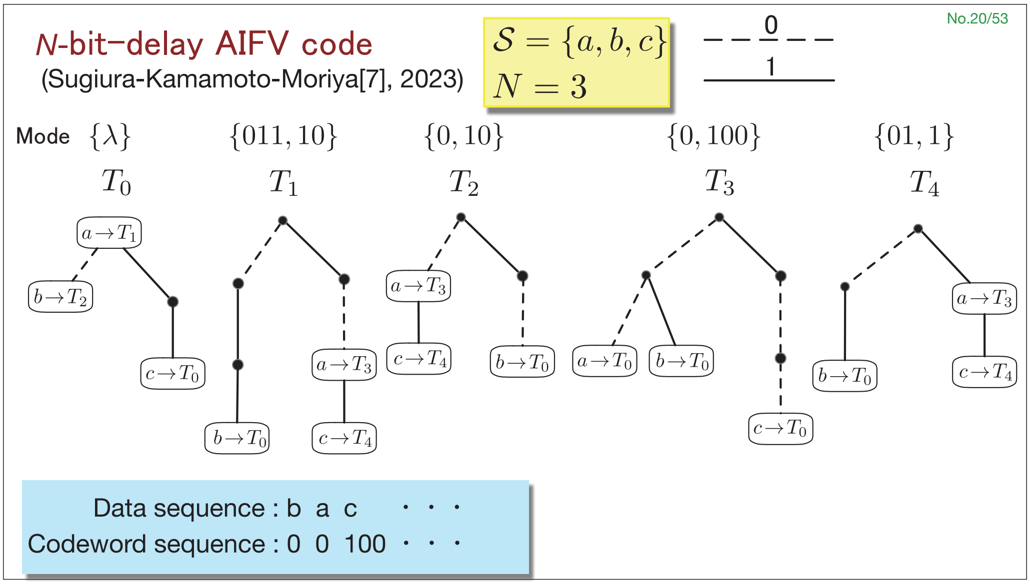
No.20/53
N-bit-delay AIFV code
(Sugiura-Kamamoto-Moriya[7], 2023)
$\mathcal{S} = \{a, b, c\}$
$N = 3$
0
1
Mode $\{\lambda\}$ $\{011, 10\}$ $\{0, 10\}$ $\{0, 100\}$ $\{01, 1\}$
T_0 T_1 T_2 T_3 T_4
$a \to T_1$
$b \to T_2$
$c \to T_0$
$a \to T_3$
$b \to T_0$
$c \to T_4$
$a \to T_3$
$c \to T_4$
$b \to T_0$
$a \to T_0$
$b \to T_0$
$c \to T_0$
$b \to T_0$
$a \to T_3$
$c \to T_4$
Data sequence : b a c · · ·
Codeword sequence : 0 0 100 · · ·

N-bit-delay AIFV code

(Sugiura-Kamamoto-Moriya[7], 2023)

$\mathcal{S} = \{a, b, c\}$
$N = 3$

0 (dashed line), 1 (solid line)

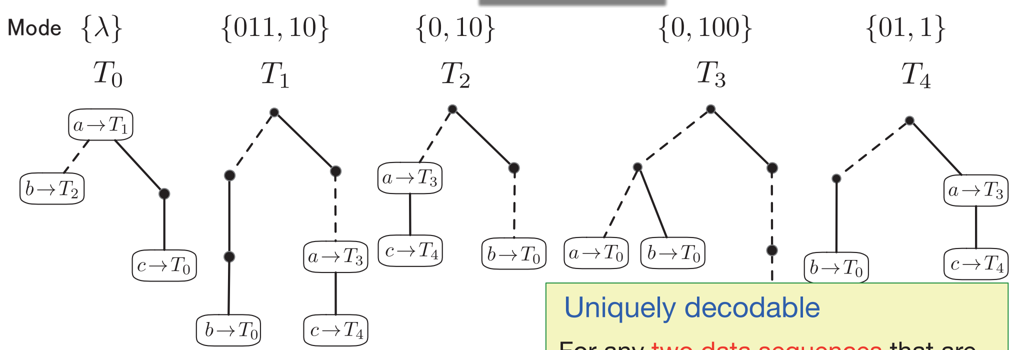

Data sequence : b a c · · ·
Codeword sequence : 0 0 100 · · ·

Uniquely decodable

For any two data sequences that are not a prefix of each other, the corresponding codeword sequences must be not a prefix of each other.

N-bit delay AIFV code

(Sugiura-Kamamoto-Moriya[7], 2023)

$\mathcal{S} = \{a, b, c\}$
$N = 3$

0 (dashed line), 1 (solid line)

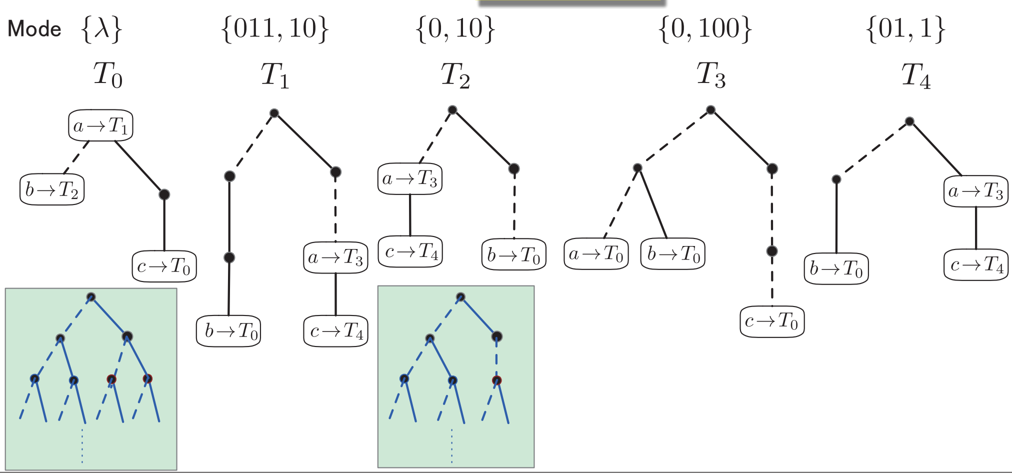

No.23/53

N-bit delay AIFV code
(Sugiura-Kamamoto-Moriya[7], 2023)

$\mathcal{S} = \{a, b, c\}$

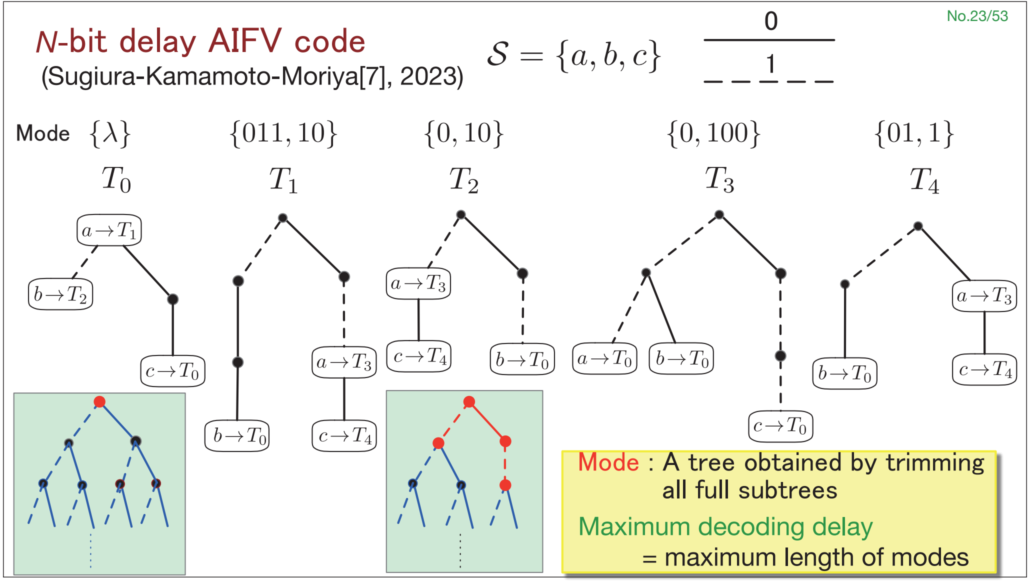

No.24/53

Maximum decoding delay and optimal binary FV code

Maximum decoding delay	(Proved by)	Optimal code
no decoding delay (instantaneous code)	→ (Huffman[1], 1956)	Huffman code — single code tree
1-bit decoding delay	→ (Hashimoto–Iwata[12], 2022)	Huffman code — single code tree
2-bit decoding delay	→ (Hashimoto–Iwata[13], 2023)	AIFV code — two code trees
N-bit decoding delay $N \geq 3$	→	N–bit–delay AIFV code

Construction of optimal AIFV code trees $\boldsymbol{T} = (T_0, T_1, \cdots, T_{m-1})$

Iteration Altorithm (AIFV code : Yamamoto-Tsuchihashi-Honda[5], 2015)
(general case : Fujita-Iwata-Yamamoto[14], 2019)

Parameters: $\boldsymbol{C} = (C_0, C_1, \cdots, C_{m-2})$

→ Local optimization of each $T_j, j = 0, 1, \cdots, m-1$ by IP or DP for a given parameters $\boldsymbol{C}$.

↓

Update $\boldsymbol{C}$ for the newly obtained $\boldsymbol{T}$.

(repeat)

Survey paper

[15] 山本博資,“準瞬時FV符号(AIFV符号)—ハフマン符号に勝る圧縮率を達成する符号—”, 電子情報通信学会誌, vol.104, no.1, pp.35–42, 2021

Topics:

AIFV code, Number of AIFV code trees, AIFV–m code, Dynamic AIFV code, Alphabetic AIFV code, AIVF code, Universal code, Iteration algorithm, etc.

Outline

1. Overview of new lossless data compression coding schemes to replace Huffman coding and arithmetic coding.

2. AIFV codes (almost Instantaneous fixed-to-variable length codes) and extended codes, which can attain better compression rate than the Huffman code.

3. ANS (asymmetric numeral systems) and AEDS (asymmetric encoding-decoding schemes), which can attain almost the same compression rate as the arithmetic code with less mathematical operations.

Arithmetic coding and ANS coding

Arithmetic coding

Data sequence : $s_1 s_2 \cdots\cdots\cdots s_t \cdots\cdots\cdots\cdots$

Encoding direction : $\longrightarrow$

Decoding direction : $\longrightarrow$

Codeword $\boldsymbol{b}$ is determined from the MSB to LSB.

Interval $\boldsymbol{b}(s^t) \in \left[F(\boldsymbol{s}^t), F(\boldsymbol{s}^t) + P(\boldsymbol{s}^t)\right)$ $\quad F(\boldsymbol{s}^t) = \sum_{\tilde{s}^t \prec \boldsymbol{s}^t} P(\tilde{s}^t)$

ANS coding

Data sequence : $s_1 s_2 \cdots\cdots\cdots s_t \cdots\cdots\cdots\cdots$

Encoding direction : $\longleftarrow$

Decoding direction : $\longrightarrow$

Codeword $\boldsymbol{b}$ is determined from the LSB to MSB.

Only one integer variable $\Longrightarrow$ less mathematical operations

No.29/53

ANS (Asymmetric Numeral Systems)

- A noiseless data compression scheme proposed by Jarek Duda, 2009.
  (Duda[8] 2009, Duda[16] 2014, Pieprzyk-Duda-et.al[17] 2022, etc.)
- ANS can attain almost the same compression rate as arithmetic coding with less arithmetic operations.
- ANS is widely used, e.g. Facebook Zstandard (ZSTD) compressor, Apple LZFSE compressor, Google, Dropbox, Microsoft, Pixar, etc.
- Variants
  ABS (Asymmetric Binary Systems), rANS (range variant of ANS)
  tANS (tabled variant of ANS)

No.30/53

Information theoretic analyses for ANS

ABS (Asymmetric Binary Systems), rANS (range variant of ANS)
tANS (tabled variant of ANS)

- Proof of asymptotic optimality for tANS
  (Dubé-Yokoo ISIT2019, Yokoo-Dubé SITA2019)
- Information theoretic analysis of average code length for each variant.
  [18] 山本博資, 岩田賢一, “ANSの符号化・復号アルゴリズムと平均符号長の評価,” 電子情報通信学会和文論文誌A, Nov. 2024, (招待論文)(早期公開: July, 2024)

  (English translation version)
  [19] H.Yamamoto, K.Iwata, “Encoding and Decoding Algorithms of ANS Variants and Evaluation of Their Average Code Lengths,” arXiv: 2408.07322v1, Aug. 2024

tANS

- We treat the encoding and decoding algorithms of tANS, which we refer to tANS as ANS for simplicity.
- We will show how the ANS can be generalized to the AEDS.

Encoding (←)

Data sequence : $s^T = s_1 s_2 \cdots s_{T-1} s_T$

Decoding (→)

$\mathcal{S}$: a finite discrete source alphabet.

s^T : an i.i.d. data sequence, $s_t \in \mathcal{S}$.

$p = \{p(s) | s \in \mathcal{S}\}$: source probability distribution.

ANS

(Duda[8], 2009)
(Pieprzyk-Duda-Pawłowski-Camtepe-Mahboubi-Morawiecki[17], 2022)

$\mathcal{X} = \{N, N+1, \cdots, 2N-1\}$: set of internal states used in ANS.
N is a positive integer, $N = |\mathcal{X}|$.

$\mathcal{X}_s$: subset of $\mathcal{X}$ corresponding to $s \in \mathcal{S}$, $N_s = |\mathcal{X}_s|$.

$$\mathcal{X}_s \cap \mathcal{X}_{s'} = \emptyset \text{ for } s \neq s', \quad \mathcal{X} = \bigcup_{s \in \mathcal{S}} \mathcal{X}_s, \quad N = \sum_{s \in \mathcal{S}} N_s \quad N_s = |\mathcal{Y}_s|$$

$\mathcal{Y}_s = \{N_s, N_s+1, \cdots, 2N_s - 1\}$: another set corresponding to $s \in \mathcal{S}$.

One-to-one correspondence

$$(s, y) \in \mathcal{S} \times \mathcal{Y}_s \Longleftrightarrow x \in \mathcal{X}_s \subset \mathcal{X}$$

$$x = C[s, y] \qquad (s, y) = D[x]$$

$$p(s) \approx \frac{N_s}{N} \text{ for } s \in \mathcal{S}$$

No.33/53

Encoding/decoding algorithms of ANS

$\lg a = \log_2 a$

$\mathcal{X} = \{N, N+1, \cdots, 2N-1\}$

Data sequence : $s^T = s_1 s_2 \cdots s_{T-1} s_T$ (Encoding ←, Decoding →)

Encoding :

1. Select $x_T \in \mathcal{X}$ arbitrarily.
2. Repeat the following from $t = T$ to 1.

$(x_t, s_t) \rightarrow (\beta_t, x_{t-1})$

$$k_t = \lfloor \lg(x_t / N_{s_t}) \rfloor$$
$$\beta_t = x_t \bmod 2^{k_t}$$
$$y_{t-1} = \lfloor x_t / 2^{k_t} \rfloor \in \mathcal{Y}_{s_t}$$
$$x_{t-1} = C[s_t, y_{t-1}] \in \mathcal{X}_{s_t} \subset \mathcal{X}$$

3. Codeword sequence : $(x_0, \beta_1, \beta_2, \cdots, \beta_T)$

Decoding :

1. Codeword sequence : $(x_0, \beta_1, \beta_2, \cdots, \beta_T)$
2. Repeat the following from $t = 1$ to T.

$(\beta_t, x_{t-1}) \rightarrow (x_t, s_t)$

$$(s_t, y_{t-1}) = D[x_{t-1}]$$
$$k_t = \lfloor \lg(N / y_{t-1}) \rfloor$$
$$x_t = 2^{k_t} y_{t-1} + \beta_t$$

3. Decoded sequence : $(s_1, s_2, \cdots, s_T)$

No.34/53

Encoding/decoding algorithms of ANS

$\lg a = \log_2 a$

Data sequence : $s^T = s_1 s_2 \cdots s_{T-1} s_T$ (Encoding ←, Decoding →)

$$p(s) \approx \frac{N_s}{N} \text{ for } s \in \mathcal{S}$$

Encoding :

1. Select $x_T \in \mathcal{X}$ arbitrarily.
2. Repeat the following from $t = T$ to 1.

$(x_t, s_t) \rightarrow (\beta_t, x_{t-1})$

$$k_t = \lfloor \lg(x_t / N_{s_t}) \rfloor$$
$$\beta_t = x_t \bmod 2^{k_t}$$
$$y_{t-1} = \lfloor x_t / 2^{k_t} \rfloor \in \mathcal{Y}_{s_t}$$
$$x_{t-1} = C[s_t, y_{t-1}] \in \mathcal{X}_{s_t} \subset \mathcal{X}$$

3. Codeword sequence : $(x_0, \beta_1, \beta_2, \cdots, \beta_T)$

$$x_t \in \mathcal{X} = \{N, N+1, \cdots, 2N-1\}$$
$$(N \le x_t < 2N)$$

$$\left\lfloor \lg \frac{N}{N_{s_t}} \right\rfloor \le k_t < \left\lfloor \lg \frac{2N}{N_{s_t}} \right\rfloor$$

$$\left\lfloor \lg \frac{1}{p(s_t)} \right\rfloor \lesssim k_t \lesssim \left\lfloor \lg \frac{1}{p(s_t)} \right\rfloor + 1$$

$$\lg \frac{1}{p(s_t)} - 1 \lesssim k_t \lesssim \lg \frac{1}{p(s_t)} + 1$$

AEDS (Asymmetric Encoding–Decoding Scheme)

(Yamamoto-Iwata[9], 2024)

No.35/53

$\lg a = \log_2 a$

$\mathcal{X} = \{\alpha_1, \alpha_2, \cdots, \alpha_N\}$: an arbitrary finite set.

Data sequence : $s^T = s_1 s_2 \cdots s_{T-1} s_T$ (Encoding ←, Decoding →)

Encoding :

1. Select $x_T \in \mathcal{X}$ arbitrarily.
2. Repeat the following from $t = T$ to 1.

$(x_t, s_t) \rightarrow (\beta_t, x_{t-1})$:

$$\beta_t = E^{(1)}_{x_t}(s_t)$$
$$x_{t-1} = E^{(2)}_{x_t}(s_t)$$

3. Codeword sequence : $(x_0, \beta_1, \beta_2, \cdots, \beta_T)$

Decoding :

1. Codeword sequence : $(x_0, \beta_1, \beta_2, \cdots, \beta_T)$
2. Repeat the following from $t = 1$ to T.

$(\beta_t, x_{t-1}) \rightarrow (x_t, s_t)$:

$$s_t = D^{(1)}_{x_t}(\beta_t)$$
$$x_t = D^{(2)}_{x_{t-1}}(\beta_t)$$

3. Decoded sequence : $(s_1, s_2, \cdots, s_T)$

$\{(E^{(1)}_x, E^{(2)}_x, D^{(1)}_x, D^{(2)}_x) \mid x \in \mathcal{X}\}$: AEDS

An example of AEDS

No.36/53

λ : null sequence with length 0.

$\mathcal{S} = \{a, b, c\}$

$\mathcal{X} = \{\alpha_1, \alpha_2, \cdots, \alpha_5\}, \ N = |\mathcal{X}| = 5$

Encoding functions : For each $x \in \mathcal{X}$

$E^{(1)}_x : \mathcal{S} \rightarrow \mathcal{B} = \{0,1\}^*, \quad E^{(2)}_x : \mathcal{S} \rightarrow \mathcal{X}$

Decoding functions : For each $x \in \mathcal{X}$

$D^{(1)}_x : \mathcal{B}^{(D)}_x \rightarrow \mathcal{S}, \ D^{(2)}_x : \mathcal{B}^{(D)}_x \rightarrow \mathcal{X}$

$$\mathcal{B}^{(D)}_x := \{E^{(1)}_{\hat{x}}(s) \mid \hat{x} \in \mathcal{X}, s \in \mathcal{S}\}$$

Uniquely decodable

For each $x \in \mathcal{X}$,

$\mathcal{B}^{(D)}_x$ must satisfy the prefix-free condition.

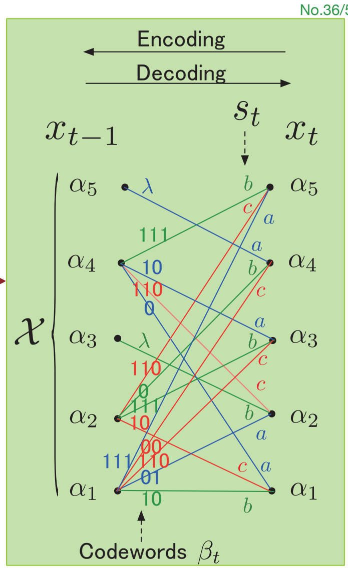

No.37/53

An example of AEDS

λ : null sequence with length 0.

$s^4 = b\ a\ b\ c \qquad x_4 = \alpha_1$

← Encoding

$x_0 = \alpha_2 \quad 0\ 10\ \lambda\ 10$

Decoding → $b\ a\ b\ c$

This can be represented with $\lceil \lg N \rceil$ bits.

In the coding rate of a long s^T, $\lceil \lg N \rceil$ bits can be ignored.

No arithmetic operations are required → fast encoding and decoding

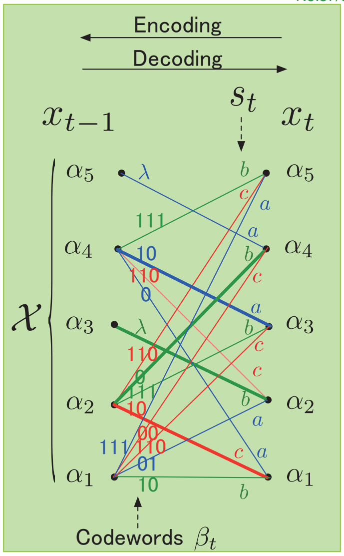

No.38/53

State-divided AEDS (sAEDS)

$$\mathcal{X}_s^{(E)} := \{E_x^{(2)}(s) \mid x \in \mathcal{X}\} \quad \text{for each } s \in \mathcal{S}$$

$$\mathcal{X}_s^{(E)} \cap \mathcal{X}_{s'}^{(E)} = \emptyset \quad \text{for } s \neq s',$$

$$|\mathcal{X}_s^{(E)}| \geq 1 \quad \text{for each } s \in \mathcal{S},$$

$$\mathcal{X} = \bigcup_{s \in \mathcal{S}} \mathcal{X}_s^{(E)}.$$

$$\mathcal{X}_s^{(E)} = \{\mathsf{s}_1, \mathsf{s}_2, \cdots, \mathsf{s}_{N_s}\}$$

$$\mathcal{X}_x^{(D)} = \{D_x^{(2)}(\beta) \mid \beta \in \mathcal{B}_x^{(D)}\}, \quad \text{for each } x \in \mathcal{X}$$

$$\mathcal{X}_x^{(D)} \cap \mathcal{X}_{x'}^{(D)} = \emptyset \quad \text{for } x \neq x',\ x \in \mathcal{X}_s^{(E)}, x' \in \mathcal{X}_s^{(E)},$$

$$|\mathcal{X}_x^{(D)}| \geq 1 \quad \text{for each } x \in \mathcal{X}_s^{(E)},$$

$$\mathcal{X} = \bigcup_{x \in \mathcal{X}_s^{(E)}} \mathcal{X}_x^{(D)} \quad \text{for each } s \in \mathcal{S}$$

$$\mathcal{X}_{\mathsf{a}_1}^{(D)} = \{\mathsf{a}_2, \mathsf{b}_2, \mathsf{b}_1, \mathsf{c}\}, \ \mathcal{X}_{\mathsf{a}_2}^{(D)} = \{\mathsf{a}_1\}$$

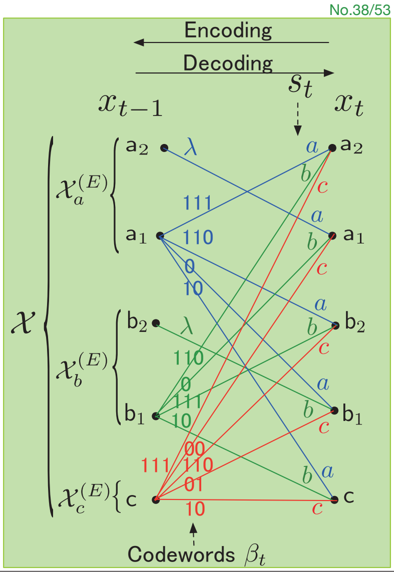

Relation between sAEDS and ANS

ANS is a special case of sAEDS.

ANS: The difference in codeword length of $\bigcup_{x \in \mathcal{X}_s^{(E)}} \mathcal{B}_x^{(D)}$ is within 1 bit.

sAEDS: each $\mathcal{B}_x^{(D)}$ can take any variable-length code satisfying the prefix-free condition.

↓

The class of sAEDS is much wider than ANS.

The optimal sAEDS can attain a compression rate better than (or at worst equal to) the ANS.

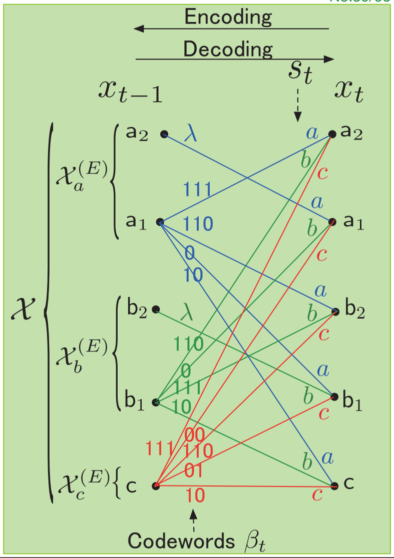

Average code length of sAEDS

$Q(x)$: stationary probability of state $x \in \mathcal{X}$.

The average code length :

$$L = \sum_{\hat{x} \in \mathcal{X}} \sum_{s \in \mathcal{S}} l(E_{\hat{x}}^{(1)}(s)) p(s) Q(\hat{x})$$

$$= \sum_{s \in \mathcal{S}} p(s) \sum_{x \in \mathcal{X}_s^{(E)}} \sum_{\hat{x} \in \mathcal{X}_x^{(D)}} l(E_{\hat{x}}^{(1)}(s)) Q(\hat{x})$$

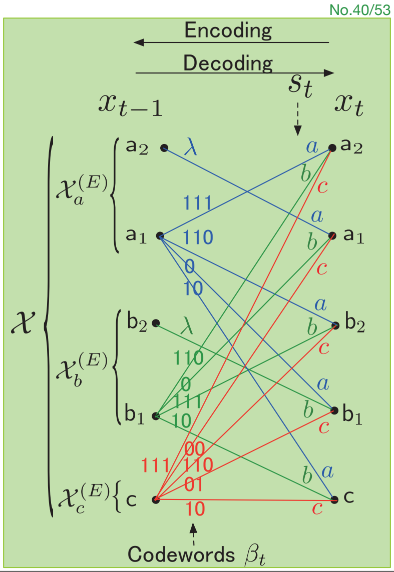

sAEDS with the same average code length as Huffman code.

$\mathcal{S} = \{a, b, c, d\}$

$|\mathcal{X}| = 2^{l_{H,\max}}$

$|\mathcal{X}_s^{(E)}| = 2^{l_{H,\max} - l_H(s)}$

Huffman code tree

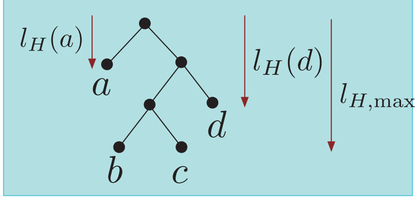

$l_H(s)$: code length of $s \in \mathcal{S}$

$l_{H,\max}$: maximum code length

The optimal sAEDS can attain a compression rate better than (or at worst equal to) the Huffman code.

$|\mathcal{X}_a^{(E)}| = 2^{l_{H,\max} - l_H(a)}$

$|\mathcal{X}_b^{(E)}| = 2^0 = 1$

$|\mathcal{X}_c^{(E)}| = 2^0 = 1$

$|\mathcal{X}_d^{(E)}| = 2^{l_{H,\max} - l_H(d)}$

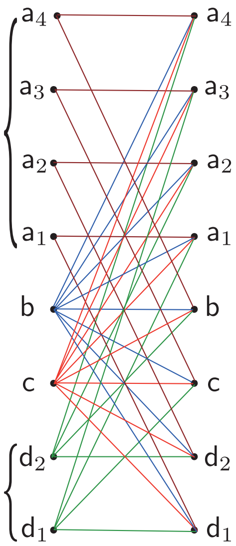

sAEDS for binary sources.

$\mathcal{S} = \{a, b\}$

$p(a) = p,\ p(b) = 1 - p,\ 0.5 \le p < 1$

Stationary prob. : $Q(\mathrm{a}_i) = \dfrac{p^i(1-p)}{1-p^{N_a}},\ Q(\mathrm{b}) = 1 - p$

$N = N_a + 1,\ k = \lceil \lg N \rceil$

Average code length: $L = (1-p)\left(\dfrac{p^{2^k - N_a}}{1 - p^{N_a}} + k\right)$

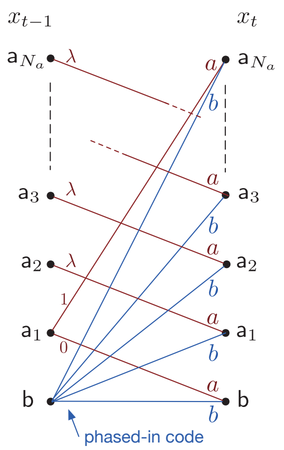

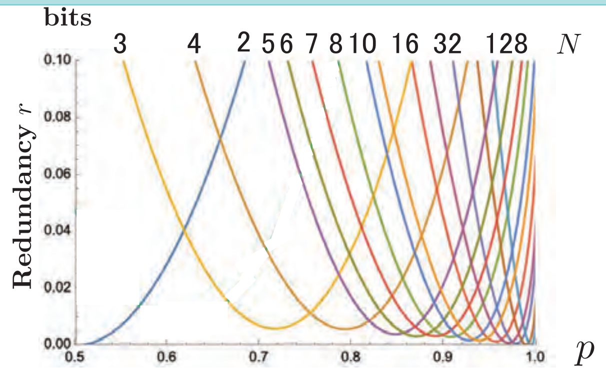

No.43/53

sAEDS for binary sources.

$\mathcal{S} = \{a, b\}$

$p(a) = p,\ p(b) = 1 - p,\ 0.5 \le p < 1$

Stationary prob. : $Q(\mathsf{a}_i) = \dfrac{p^i(1-p)}{1-p^3},\ Q(\mathsf{b}_i) = \dfrac{(1-p)^i}{2-p}$

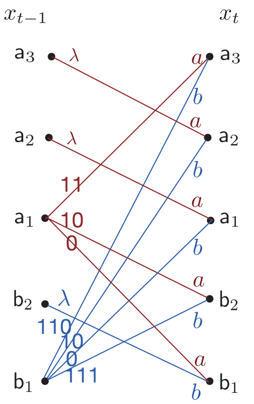

Average code length:

$$L = p[2Q(\mathsf{a}_3) + Q(\mathsf{b}_1) + 2Q(\mathsf{b}_2)] + (1-p)[Q(\mathsf{a}_1) + 2Q(\mathsf{a}_2) + 3Q(\mathsf{a}_3) + 3Q(\mathsf{b}_2)]$$

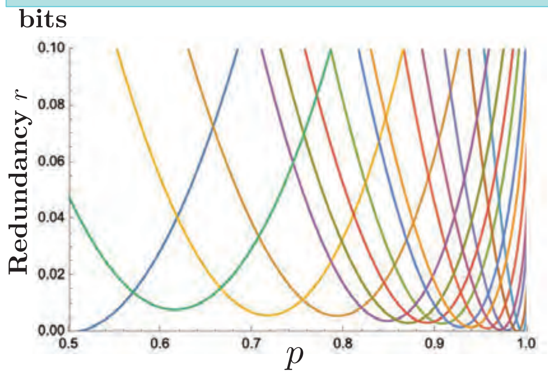

No.44/53

sAEDS for non–binary sources

Source probability distribution : $p = \{p(s) | s \in \mathcal{S}\}$

Number of states : $N = |\mathcal{X}|,\ N_s = |\mathcal{X}_s^{(E)}|$

Case 1: N/N_s is an integer for every $s \in \mathcal{S}$.

$$L \le H(S) + D(p\|q) + \sigma$$

$$q = \{q(s)\,|\,s \in \mathcal{S}\},\quad q(s) = N_s/N$$

$$\sigma = \lg\lg e + 1 - \lg e \approx 0.0860713$$

$$D(p\|q) = \sum_{s \in \mathcal{S}} p(s) \lg(p(s)/q(s))$$

sAEDS for non–binary sources

Source probability distribution : $p = \{p(s) | s \in \mathcal{S}\}$

Number of states : $N = |\mathcal{X}|,\ N_s = |\mathcal{X}_s^{(E)}|$

Case 2: N/N_s may not be integers.

$$L \le H(S) + D(p\|q) + \sigma + \sum_{s\in\mathcal{S}} p(s) \lg \frac{M_s + \tilde{Q}_{M_s+1}}{N/N_s}$$

$$q = \{q(s) \,|\, s \in \mathcal{S}\},\ q(s) = N_s/N,\ M_s = \lfloor N/N_s \rfloor$$

$$\sigma = \lg\lg e + 1 - \lg e \approx 0.0860713$$

$$D(p\|q) = \sum_{s\in\mathcal{S}} p(s) \lg(p(s)/q(s))$$

$$\tilde{Q}_{M_s+1} = \sum_{x:\ x\in\mathcal{X}_s^{(E)},\ |\mathcal{X}_x^{(D)}|=M_s+1} Q(x)$$

sAEDS for non–binary sources

Source probability distribution : $p = \{p(s) | s \in \mathcal{S}\}$

Number of states : $N = |\mathcal{X}|,\ N_s = |\mathcal{X}_s^{(E)}|$

Case 3: N is the power of 2.

$$L \le H(S) + D(p\|q) + \sum_{s\in\mathcal{S}} p(s)\Delta_{N_s,\tilde{Q}_s}$$

$$q = \{q(s) \,|\, s \in \mathcal{S}\},\quad q(s) = N_s/N$$

$$\Delta_{N_s,\tilde{Q}_s} = \sum_{x\in\hat{\mathcal{X}}_s^{(E)}} Q(x) - \frac{2^{k_s} - N_s}{N_s}$$

$\tilde{Q}_s(x) = Q(\mathcal{X}_x^{(D)}) = \sum_{\hat{x}\in\mathcal{X}_x^{(D)}} Q(\hat{x})$ for $x \in \mathcal{X}_s^{(E)}$

$k_s = \lceil \lg N_s \rceil$, $\hat{\mathcal{X}}_s^{(E)}$: subset of $\mathcal{X}_s^{(E)}$ with larger $Q(x)$ and $|\hat{\mathcal{X}}_s^{(E)}| = 2^{k_s} - N_s$.

sAEDS for non-binary sources

Source probability distribution : $p = \{p(s) | s \in \mathcal{S}\}$

Number of states : $N = |\mathcal{X}|, \; N_s = |\mathcal{X}_s^{(E)}|$

Case 3: N is the power of 2.

$$L \le H(S) + D(p\|q) + \sum_{s \in \mathcal{S}} p(s) \Delta_{N_s, \tilde{Q}_s}$$

$$q = \{q(s) \,|\, s \in \mathcal{S}\}, \quad q(s) = N_s / N$$

$$\Delta_{N_s, \tilde{Q}_s} = \sum_{x \in \hat{\mathcal{X}}_s^{(E)}} Q(x) - \frac{2^{k_s} - N_s}{N_s}$$

$\tilde{Q}_s(x) = Q(\mathcal{X}_{\tilde{x}}^{(D)}) = \sum Q(\hat{x})$ for $x \in \mathcal{X}^{(E)}$

[9] H.Yamamoto and K.Iwata, “An asymmetric encoding–decoding scheme for noiseless data compression,” IEEE ISIT2024, pp.50–60, Attens, Grace, July 2024.

Asymptotic optimality of sAEDS

Source probability distribution : $p = \{p(s) | s \in \mathcal{S}\}$ $\qquad q(s) = N_s / N$

Probability distribution of each state: $Q(x_i), \; x_i \in \mathcal{X}, \; i = 1, 2, \cdots, N$

Optimal probability distribution : $Q^*(i) := \lg \dfrac{N+i}{N+i-1}$

If $Q(x_i) = Q^*(i)$ can be realized, we achieve $L = H(S) + D(p\|q)$.

(Dubé-Yokoo[20] 2019, Yokoo-Dubé[21] 2019, Yamamoto-Iwata[22] 2024)

For $\alpha > 0$ and $1 \le i \le N$,

$Q(x_i) - Q^*(i) \le \dfrac{\alpha}{N^2}$ ➡ $L \le H(S) + D(p\|q) + \dfrac{\alpha}{N}$

$Q(x_i) - Q^*(i) \le \dfrac{\alpha}{N \lg N}$ ➡ $L \le H(S) + D(p\|q) + \dfrac{\alpha}{\lg N}$

$Q(x_i) - Q^*(i) \le \dfrac{\alpha}{N}$ ➡ $L \le H(S) + D(p\|q) + \alpha$

(Yamamoto-Iwata[22] 2024)

sAEDS that can satisfy $Q(x_i) - Q^*(i) \le \frac{\alpha}{N^2}$ (Yamamoto-Iwata[22] 2024)

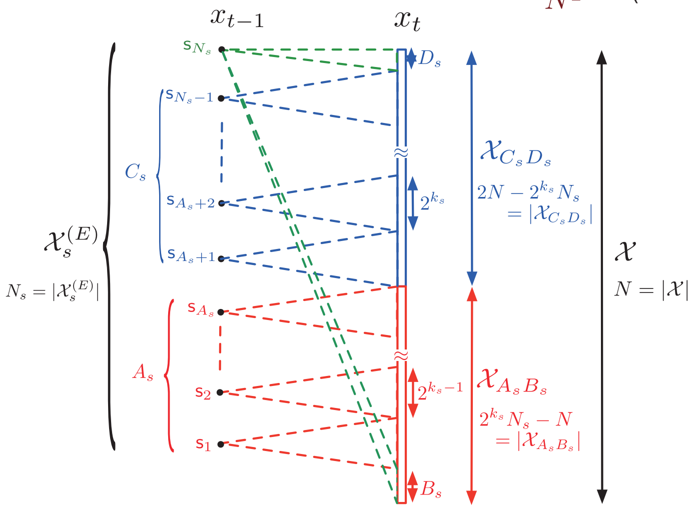

For the case of

$$p(s) = q(s) = \frac{N_s}{N}$$

$$k_s = \left\lceil \lg \frac{N}{N_s} \right\rceil$$

Summary

- AIFV (almost instantaneous fixed-to-variable length) codes and extended codes, which can attain better compression rate than the Huffman code by using multiple code trees and allowing a small decoding delay.

- ANS (asymmetric numeral systems) and AEDS (asymmetric encoding-decoding schemes), which can attain almost the same compression rate as the arithmetic code with less mathematical operations.

Summary

Features of AEDS

- The optimal AEDS can attain a compression rate better than (or at worst equal to) the ANS since the ANS can be considered as a special case of the AEDS.
- The optimal AEDS can attain a compression rate better than (or at worst equal to) the Huffman code.
- The AEDS can realize fast encoding and decoding since the AEDS does not use mathematical operations.
- We showed some examples of AEDS for binary and non-binary sources and we derived several upper bounds of the average code length.

Acknowledgment

A part of this work was supported by JSPS KAKENHI Grant Numbers 18H01436, 20K11674, 24K07487, and 24K14818.

References

[1] D. A. Huffman, "A method for the construction of minimum-redundancy codes", Proc. of the I.R.E., vol. 40, no. 9, pp. 1098-1102, Sept. 1952.

[2] J. J. Rissanen, "Generalized Kraft inequality and arithmetic coding", IBM J. of Research and Development, vol. 20, no. 3, pp. 198-203, May 1976.

[3] R. Pasco, "Source coding algorithms for fast data compression", Ph.D. thesis, Dept. of Electrical Engineering, Stanford Univ., Stanford, Calif., 1976

[4] G. Nigel and N. Martin, "Range encoding: An algorithm for removing redundancy from a digitized message," Proc. of Video and Data Recording Conference, Southampton, UK, July 1979.

[5] H. Yamamoto, M. Tsuchihashi, and J. Honda, "Almost instantaneous fixed-to-variable length codes," *IEEE Trans Inf. Theory*, vol. 61, no. 12, pp. 6432–6443, Dec. 2015.

[6] W. Hu, H. Yamamoto, and J. Honda "Worst-case redundancy of optimal binary AIFV codes and their extended codes," *IEEE Trans Inf. Theory*, vol. 63, no. 8, pp. 5074–5086, Aug. 2017.

[7] R. Sugiura, Y. Kamamoto, and T. Moriya, "General form of almost instantaneous fixed-to-variable-length codes," IEEE Trans. on Inform. Theory, vol. 69, no. 12, pp. 7672-7690, Dec. 2023

[8] J. Duda, "Asymmetric numeral systems," arXiv:0902.0271 v5, May 21, 2009.

[9] H. Yamamoto and K. Iwata, "An asymmetric encoding-eecoding Scheme for lossless data compression," Proc. of IEEE Int. Symp. on Inform. Theory (ISIT2024), pp.55-60, Athens, Greece, July 2024.

[10] L. G. Kraft, "A device for quantizing, grouping, and coding amplitude modulated pulses," MS Thesis, Electrical Engineering Dep. , MIT,1949.

[11] B. McMillan, "Two inequalities implied by unique decipherability," IRE Trans. on Inform. Theory vol.2, no. 4, pp. 115-116, Dec. 1956.

[12] K. Hashimoto and K. Iwata, "Optimality of Huffman code in the class of 1-bit delay decodable codes," IEEE J. of Selected Areas in Inform. Theory, vol. 3, no. 4, pp.616-625, Dec. 2022

[13] K. Hashimoto and K. Iwata, "The optimality of AIFV codes in the class of 2-bit delay decodable codes," arXiv:2306.09671v1, June 2023

[14] R. Fujita, K. Iwata and H. Yamamoto, "An iterative algorithm to optimize the average performance of Markov chains with finite states", Proc. of IEEE Int. Symp. on Inform. Theory (ISIT2019), pp.1902-1906, Paris, France, July 2019.

[15] 山本博資, " 準瞬時 FV 符号 (AIFV 符号)—ハフマン符号に勝る圧縮率を達成する符号—", 電子情報通信学会誌, vol. 104, no. 1, pp. 35-42, Jan. 2021.

[16] J. Duda, "Asymmetric numeral systems: entropy coding combining speed of Huffman coding with compression rate of arithmetic coding," arXiv:1311.2540v2, Jan. 6, 2014.

[17] J. Pieprzyk, J. Duda, M. Pawlowski, S. Camtepe, A. Mahboubi, P. Morawiecki, "Compression optimality of asymmetric numeral systems," arXiv:2209. 02228v1, Sep 6, 2022.

[18] 山本博資, 岩田賢一, " ANS の符号化・復号アルゴリズムと平均符号長の評価, " 電子情報通信学会和文論文誌 A, Nov.2024, (招待論文) (早期公開: July, 2024)

[19] H.Yamamoto and K.Iwata, " Encoding and decoding algorithms of ANS variants and evaluation of their average code lengths, " arXiv: 2408.07322v1, Aug. 2024

[20] D. Dubé and H. Yokoo, "Fast construction of almost optimal symbol distributions for asymmetric numeral systems," Proc. of 2019 IEEE Int. Sym. of Inform. Theory (ISIT2019), pp. 1682–1686, July 2019.

[21] H. Yokoo and D. Dubé, "Asymptotic optimality of asymmetric numeral systems," Proc. of 42th Sym. on Inform. Theory and its Appli. (SITA2019), 4.2.3, pp. 289–294, Nov. 2019.

[22] H. Yamamoto and K. Iwata, "Asymptotic optimality of the asymmetric encoding-decoding scheme," Proc. of 2024 Int. Sym. of Inform. Theory and its Appli., pp.354-359, Nov., 2024.

Detection performance evaluation of Gabor-Division Spread Spectrum signals

Masayoshi Ohashi

Adaptive Communications Research Laboratories, ATR, Japan
ohashi@ieee.org

For delay and Doppler estimation using Gabor GDSS(Gabor Division Spread Spectrum) , we propose a simple method for estimation of sparse GDSS signals in the time and frequency domains. Instead of PUL(Phase Updating Loop) search in the time and frequency domains, the estimation is performed via matched filters in both domains. Although it is a simple method, it is computationally inexpensive, and estimation can be performed with fairly good accuracy with relatively high signal-to-noise ratio.

Acknowledgment

A part of this work was supported by Grant-in-Aid for Scientific Research JP23744396.

References

[1] D. Gabor, "Theory of Communication", in *Proc. Inst. Elect. Engr,*, pt. III, **93**, 429-41, 1946.
[2] T.Kohda, Y.Jitsumatsu, and K.Aihara,"Signals that can be easily time-frequency synchronized from their ambiguity function," *Proc.ITW2013*, Sept.2013.
[3] T. Kohda, Y. Jitsumatsu, and K. Aihara, "2D Markovian SS codes flatten time-frequency distribution of signals in asynchronous Gabor division CDMA systems," *2011 IEEE International Conference on Acoustics, Speech, and Signal Processing*, 2011.
[4] 大橋正良，香田徹, "離散ガウス波形による 2 元 BPSK 信号の時間周波数対称性について"，第 41 回情報理論とその応用シンポジウム,8.2.2, いわき, Dec. 2018.
[5] 大橋正良，香田徹, "離散ガウス波形による 2 元 BPSK 信号の基本復調特性"，第 42 回情報理論とその応用シンポジウム, 5.4.2, 霧島. Nov. 2019.
[6] T. Kohda, Y. Jitsumatsu, and K. Aihara, "Frequency synchronisation using SS technique," *Proc. The ninth Int. Sympo. on Wireless Communication Systems*, Aug. 2012, pp. 855-859.
[7] T. Kohda, Y. Jitsumatsu, and K. Aihara, "Frequency-division spread spectrum makes frequency synchronisation easy," *Proc. IEEE Globecom 2012*, Dec. 2012, pp. 3976-3982.
[8] Y. Jitsumatsu, T. Kohda, and K. Aihara, "Delay-Doppler Space Division-based Multiple-Access Solves Multiple-Target Detection," 6th International Workshop on Multiple Access Communication, MACOM2013, Eds. by M.Jonsson, LNCS 8310, 39-53, (2013).
[9] Y. Jitsumatsu, and T. Kohda, "Digital Phase updating Loop and Delay-Doppler Space Division Multiplexing for Higher Order MPSK," MACOM2014,LNCS 8715,ed.by M.Jonnson, et al. pp.1-15,2014.
[10] J.von Neumann,*The Geometry of Operators*, vol.II (*Ann.Math.Studies*, no.22),1950.
[11] 香田徹, 大橋正良，櫻井幸一，篠原克寿，長谷川晃朗，森　慎太郎, "２次元位相変調ガウス波によるレーダ信号の DFT-,IDFT-変調 Transmultiplexers"，第 42 回情報理論とその応用シンポジウム,5.4.3, 霧島, Nov. 2019.
[12] 香田徹, 大橋正良，櫻井幸一，篠原克寿，長谷川晃朗，森　慎太郎, "２次元位相変調ガウス波によるレーダ信号のツイン-マルチキャリアフィルタバンク"，第 34 回信号処理シンポジウム,B6-3, 鳥取, Nov. 2019.
[13] 大橋正良，" 離散ガウス波形による２次元 BPSK 信号の信号復調に関する検討"，IEICE NLP 研究会, NLP2019-112, 宮古,2020 年 1 月.

[14] Masayoshi Ohashi,”Study on a delay and Doppler estimation using discrete gaussian wave,” ISITA2020, Hawaii(online), October, 2020.
[15] 森 慎太郎, 長谷川晃朗, 大橋正良, ”ガウス波形による 2 次元 BPSK を用いた最尤推定レーダ実証に向けた検討,”IEICE RCS 研究会, RCS-8, 2020 年 3 月.
[16] 大橋正良,’ 離散ガウス波形による 2 次元 BPSK 信号の性能評価”’,IEICE IT 研究会,T2020-24, 2020 年 12 月.
[17] 甘利俊一, ”情報理論”，ちくま学芸文庫,2011 年 4 月.

DETECTION PERFORMANCE EVALUATION OF GABOR-DIVISION SPREAD SPECTRUM SIGNALS

Masayoshi Ohashi

ATR

Outline

- History of study
- Issues to be solved
- Proposal for simplified method
- Performance evaluation
- Conclusion

Radar basics

- Radar system transmits a radar signal (radio pulse).
- It is reached to the target object and reflected.
- Radar RX system receive a weak reflected pulse energy.
- From the observed time delay and Doppler shift, distance and speed of the object can be measured.

Precise detection and identification of Δt and Δf is the key

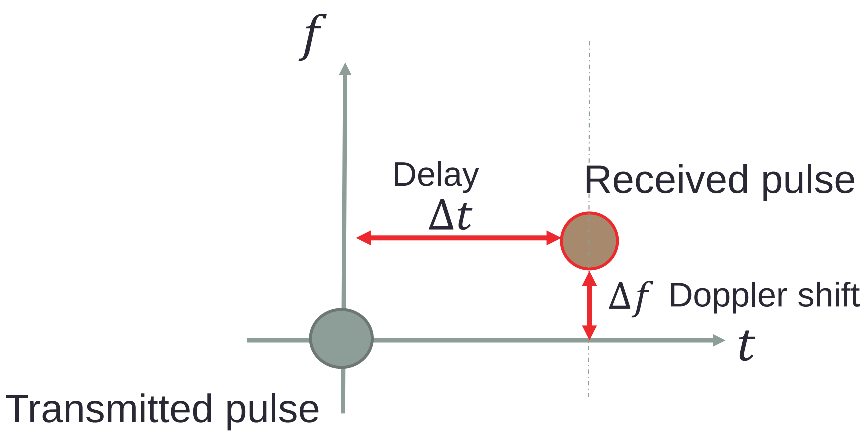

Conventional method

- FMCW

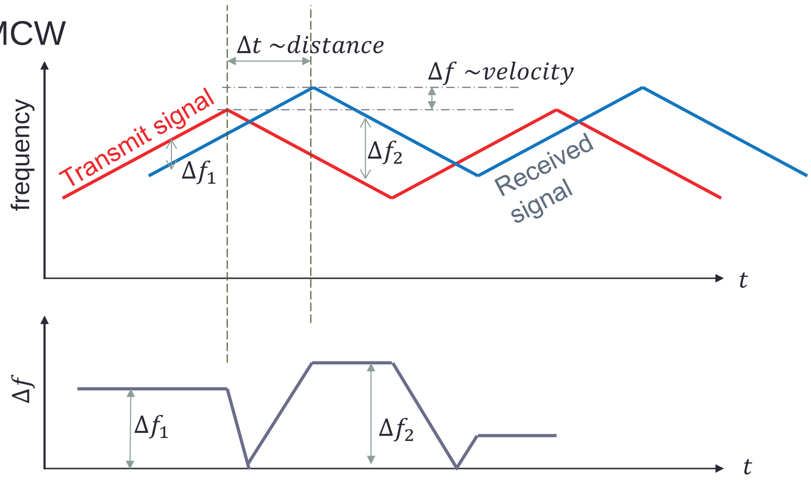

$$distance = \frac{c}{4a}(\Delta f_1 + \Delta f_2),\ \ velocity = \frac{c}{4f_0}(\Delta f_2 - \Delta f_1)$$

$c = light\ speed, f_0 = TX\ freq,\qquad a = \frac{df}{dt}\ of\ TX\ signal.$

UWB radar

- Very short impulse is used

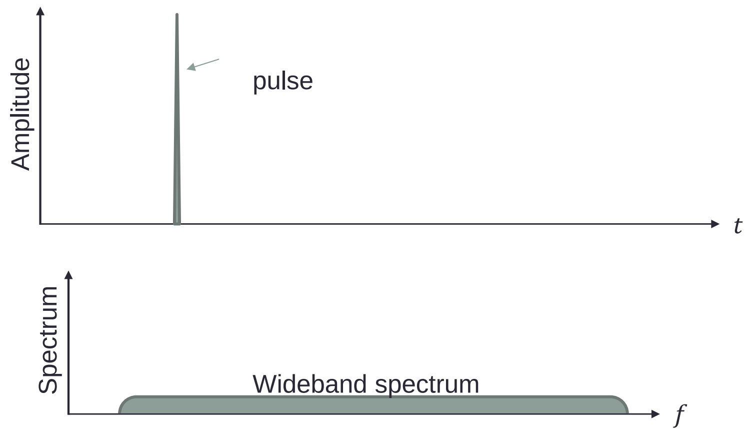

Problems of Δt and Δf ML estimation

- Basically, it is 2-dimensional estimation
- ML (maximum likelihood) estimation requires time space × frequency space 2D-search.
- If we take exhaustive approach using conventional matched filter on both TD and FD, N^2 order computation is inevitable.

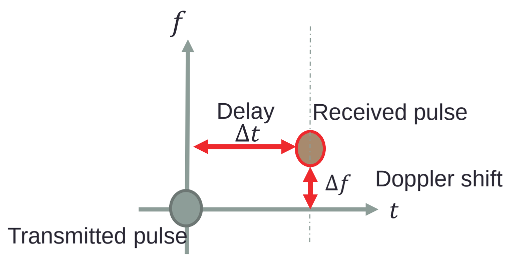

Study by Jitsumatsu, Kohda and Aihara -1

[1] T. Kohda, Y. Jitsumatsu, and K. Aihara, " 2D Markovian SS codes flatten time-frequency distribution of signals in asynchronous Gabor division CDMA systems, "*2011 IEEE ICASSP* , 2011.

[2] T. Kohda, Y. Jitsumatsu, and K. Aihara,"Frequency synchronisation using SS technique, "*Proc. ISWCS*, Aug. 2012, pp.855-859.

[3] T. Kohda, Y. Jitsumatsu, and K. Aihara," Frequency-division spread spectrum makes frequency synchronisation easy, "*Proc. IEEE Globecom 2012*, Dec. 2012, pp. 3976-3982.

[4] T. Kohda, Y. Jitsumatsu, and K. Aihara, " Separability of time-frequency synchronization, "*Proc. International Radar Symposium 2013*, June, 2013, pp.964-969.

[5] T. Kohda, Y. Jitsumatsu, and K. Aihara, " Gabor division/spread spectrum system is separable in time and frequency synchronization, "in *Proc. Vehicular Technology Conference 2013 Fall*, 2013.

Study by Jitsumatsu, Kohda and Aihara - 2

[6] Y. Jitsumatsu, T. Kohda, and K. Aihara, “ Spread Spectrum-based Cooperative and individual time-frequency synchronization, ”*Proc.ISWS 2013*, 2013,pp.497-501.

[7] T.Kohda, Y.Jitsumatsu, and K.Aihara, ”Signals that can be easily time frequency synchronized from their ambiguity function,” *Proc.ITW2013*, Sept.2013.

[8] T. Kohda, Y. Jitsumatsu, and K. Aihara, “ PLL-free Receiver for Gabor Division/Spread Spectrum System, ”*Proc. WiMob2013*, Oct. 2013.

[9] Y. Jitsumatsu, T. Kohda, and K. Aihara, ”Delay-Doppler Space Division based Multiple-Access Solves Multiple-Target Detection,” MACOM2013, Eds. by M.Jonsson, LNCS **8310**, 39-53, (2013).

[10] Y. Jitsumatsu, and T. Kohda, ”Digital Phase updating Loop and Delay-Doppler Space Division Multiplexing for Higher Order MPSK,” MACOM2014, LNCS **8715**,ed.by M.Jonsson, et al. pp.1-15,2014.

Delay and Doppler is not commutative

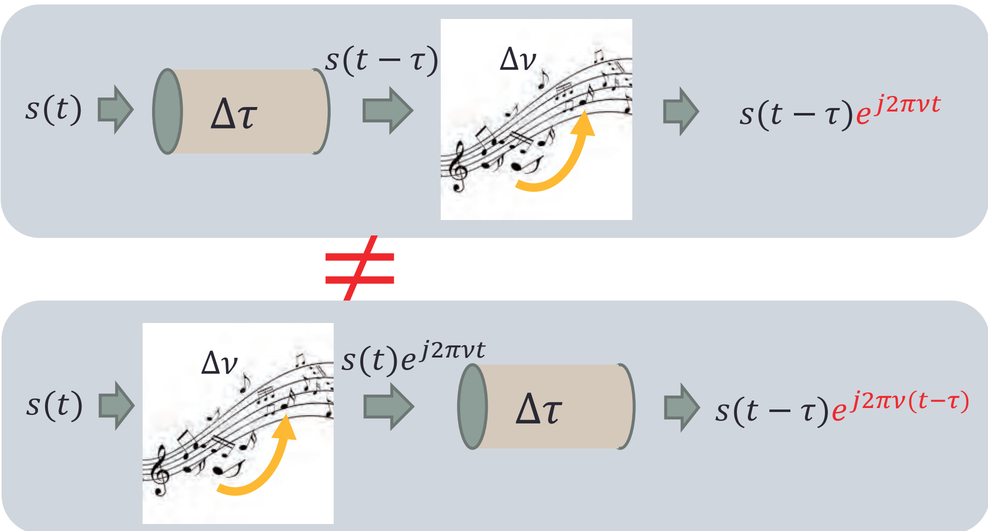

[7]Kohda et al, ITW2013

Time shift and frequency shift operator

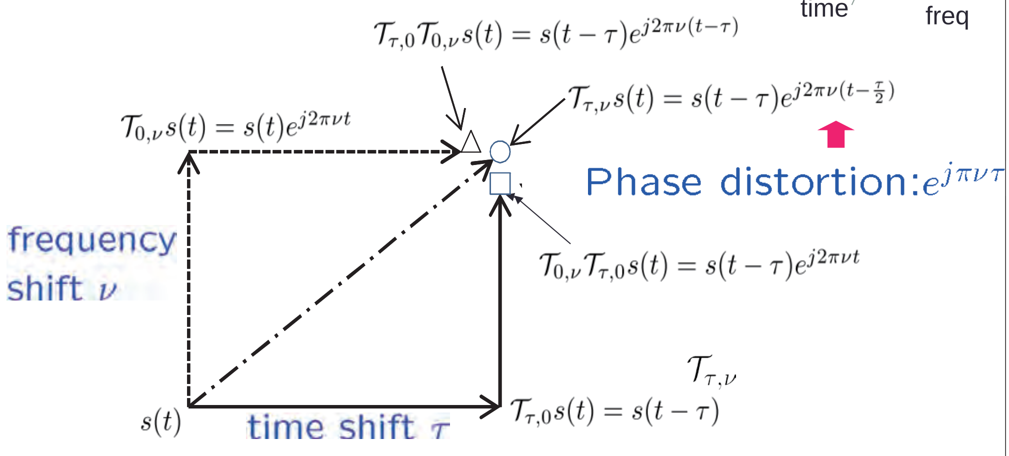

time shift $\mathcal{T}_{\tau,0}$ **frequency shift** $\mathcal{T}_{0,\nu}$

Non-commutativity of operators: $\mathcal{T}_{\tau,0}\cdot\mathcal{T}_{0,\nu} = e^{-j2\pi\nu\tau}\cdot\mathcal{T}_{0,\nu}\cdot\mathcal{T}_{\tau,0}$

Symmetric delay-shift operator

[7]Kohda et al, ITW2013

- $\mathcal{T}_{\tau,\nu}s(t) \overset{\text{def}}{=} s(t-\tau)e^{j2\pi\nu\left(t-\frac{\tau}{2}\right)}$
- $\mathcal{T}^{(f)}_{-\tau,\nu}S(f) \overset{\text{def}}{=} S(f-\nu)e^{-j2\pi\tau\left(f-\frac{\nu}{2}\right)}$

FD operation

such that

$$\mathcal{T}^{f}_{f_D,-t_d} = \mathcal{F}\,\mathcal{T}_{t_d,f_D}\mathcal{F}^{-1}$$

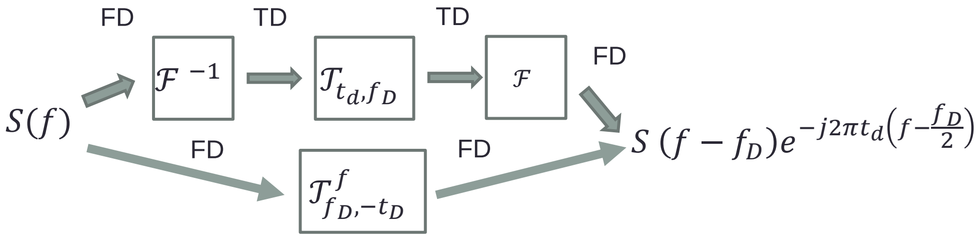

This operator makes manipulation on TD and FD plane equivale

DEFINING 2D SS SIGNAL WITH TFS PROPERTY

Application of gaussian wave

- Gaussian wave is applied for constructing Gabor Division / spread spectrum system
- Equivalent waveform is kept between TD and FD plane

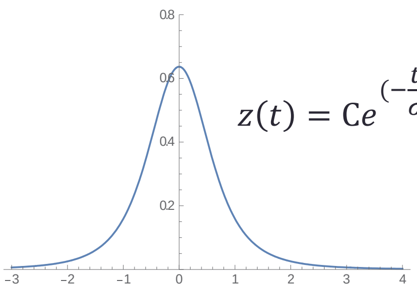

$$z(t) = Ce^{\left(-\frac{t^2}{\sigma_t^2}\right)}$$

[1] T. Kohda, Y. Jitsumatsu, and K. Aihara, “ 2D Markovian SS codes flatten time-frequency distribution of signals in asynchronous Gabor division CDMA systems, ”2011 IEEE ICASSP , 2011.

Template on TD (1st level 2D SS code)

(1) Define TD template (in case of N=4)

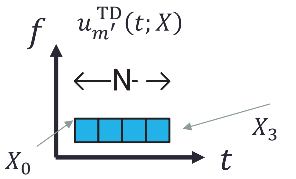

template TD signal

$$u^{TD}_{m'}(t;X) = \frac{1}{\sqrt{N}} \sum_{m=0}^{N-1} X_m \, e^{-j\pi m m' T_c F_c} \mathcal{T}_{mT_c,0} z(t),$$

$$0 \le m' \le N' - 1$$

Signature on TD (1st level 2D SS code)

(2) Define TD signature(In case of N=4)

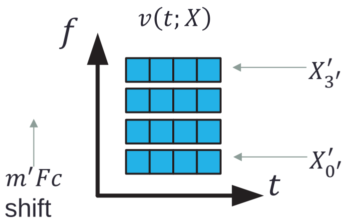

$$v(t;X) = \frac{1}{\sqrt{N'}} \sum_{m'=0}^{N'-1} X'_{m'} \mathcal{T}_{0,m'F_c} \, u^{TD}_{m'}(t;X)$$

Template on FD (1st level 2D SS code)

(3) Define FD template (in case of N'=4)

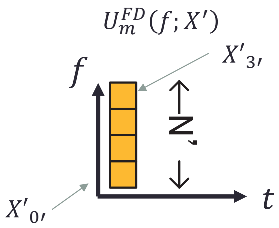

$$U_m^{FD}(f;X') = \frac{1}{\sqrt{N'}} \sum_{m'=0}^{N'-1} X'_{m'} e^{j\pi m m' T_c F_c} \mathcal{T}^f_{0,m' F_c} Z(f),$$

$$0 \leq m \leq N-1$$

Signature on FD (1st level 2D SS code)

(4) Define FD template (in case of N'=4)

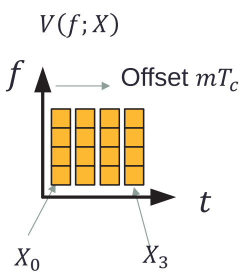

$$V(f;X) = \frac{1}{\sqrt{N}} \sum_{m=0}^{N-1} X_m T^f_{-mT_c,0} U_m^{\mathrm{FD}}(f;X)$$

These signatures are perfectly symmetrical

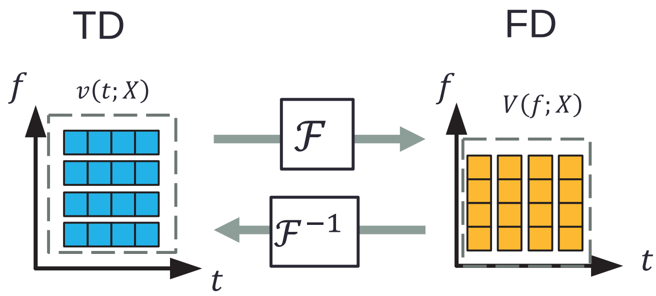

Gabor Division/Spread Spectrum System (2nd level SS signal)

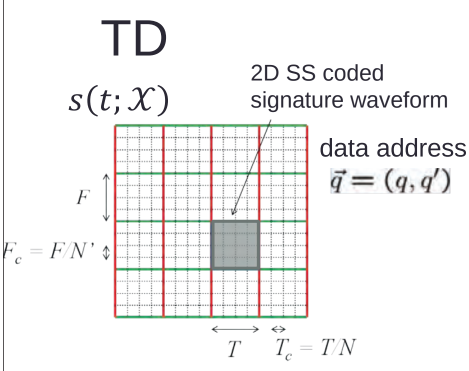

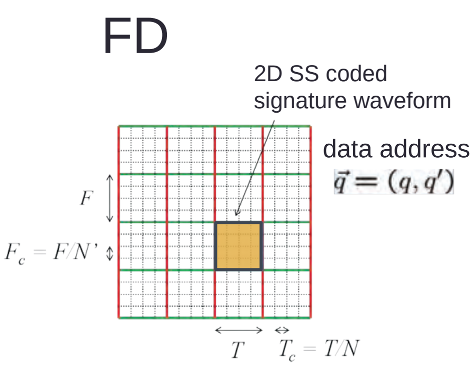

$$s(t;\mathcal{X}) = \sum_{\vec{q}} d_{\vec{q}} \cdot \mathcal{T}_{qT,q'F}\, v(t;X)$$

$$S(f;\mathcal{X}) = \sum_{\vec{q}} d_{\vec{q}} \cdot \mathcal{T}^{f}_{q'F,qT}\, V(f;X)$$

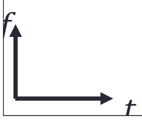

Transmitted and received signal

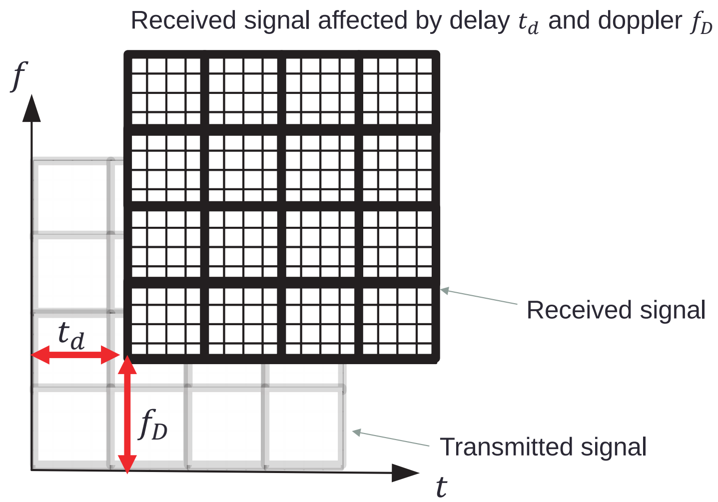

t_d and f_D 2D estimation

Receiver design

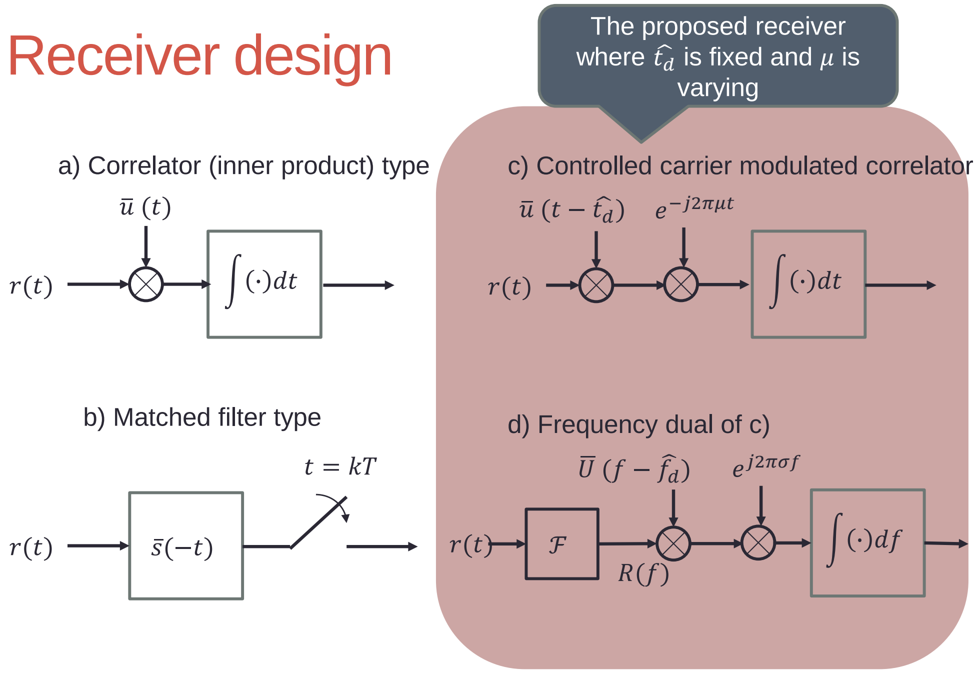

Correlation calculation

[5]Kohda et al, VTC2013 (modified)

- $c^{\mathrm{TD}}_{\vec{p},n}\ (\mu;\hat{t}_d)$
  $$=< r(t;\mathcal{X}), \mathcal{T}_{\hat{t}_d,\mu}\mathcal{T}_{pT,p'F}\mathcal{T}_{nT_c,0}Y_n\ \ u^{\mathrm{FD}}_n(t;\mathbf{Y})\ >_t$$
- $C^{\mathrm{FD}}_{\vec{p},n'}(\sigma;\hat{f}_D)$
  $$=< R(f;\mathcal{X}), \mathcal{T}^{\mathrm{f}}_{\hat{f}_D,-\sigma}\mathcal{T}^{\mathrm{f}}_{p'F,-pT}\mathcal{T}^{\mathrm{f}}_{n'F_c,0}Y_{n'}U^{\mathrm{TD}}_{n'}\ (f;\mathbf{Y}')\ >_f$$

- In $c^{\mathrm{TD}}_{\vec{p},n}\ (\mu;\hat{t}_d),\mu$: a controlled parameter for estimating f_D
- In $C^{\mathrm{FD}}_{\vec{p},n'}(\sigma;\hat{f}_D)$, σ : a controlled parameter for estimating t_d

Phase Updating Loop (PUL)

$$(\mu^*, n^*) = \arg\max_{\mu,n} \mathcal{R}[c^{\mathrm{TD}}_{\vec{p},n}\ (\mu;\hat{t}_d)]$$
$$(\sigma^*, n'^*) = \arg\max_{\sigma,n'} \mathcal{R}[C^{\mathrm{FD}}_{\vec{p},n'}(\sigma;\hat{f}_D)]$$

$$\hat{f}_D \leftarrow \mu^*,\ \hat{t}_d \leftarrow \sigma^*$$

$\hat{t}_d$ and $\hat{f}_D$ are updated alternatively and iteratively.

Phase Updating Loop process

$$(\mu^*, n^*) = \arg\max_{\mu,n} \mathcal{R}[c^{\mathrm{TD}}_{\vec{p},n}(\mu; \hat{t}_d)]$$

$$\hat{f}_D \leftarrow \mu^*$$

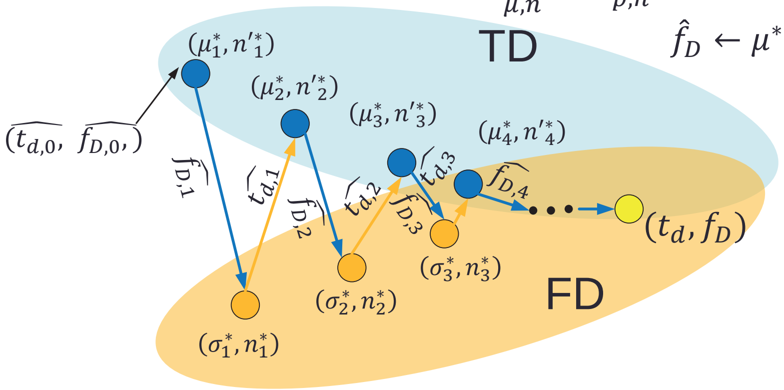

$$(\sigma^*, n'^*) = \arg\max_{\sigma,n'} \mathcal{R}[C^{\mathrm{FD}}_{\vec{p},n'}(\sigma; \hat{f}_D)]$$

$$\hat{t}_d \leftarrow \sigma^*$$

Von Neumann's APT (Alternative Projection Theorem) guarantees the conversion to target (t_d, f_D)

History of our study

- Verification of TFS property and performance evaluation(SITA2018,2019,NLP2020/01,ISITA2020).
  - Good estimation performance is observed under low noise condition
  - False locks sometimes happen depends on templates assignment
- GDSS RF waves are generated using software radio BladeRF(RCS2020).
- Test trial using other type of templates (e.g., Frequency Hopping type)(SITA2021)
- Feasible parameter study（IT2020）

Issues to be considered

- Large computational efforts required for for GDSS correlation
- Measurable Doppler and delay unit would be rather large

	Time Domain	Freq. Domain
Number of window samples	4096	4096
Number of samples between pulses	64	64
Number of Gauss waves	16	16
Signal duration	34μsec	-
Sampling period	33nsec	
Required bandwidth	-	30MHz
Range resolution	10m	
Velocity resolution	3.9m/s	
Frequency band	80GHz	

M. IT(2020/12)

Proposed idea

- GDSS Gauss pulses are sparsely placed onto TD and FD domain.(like pulse radar type approach was taken by Y. Jitsumatsu)
- 2-dimensional conventional GDSS PUL is used if necessary

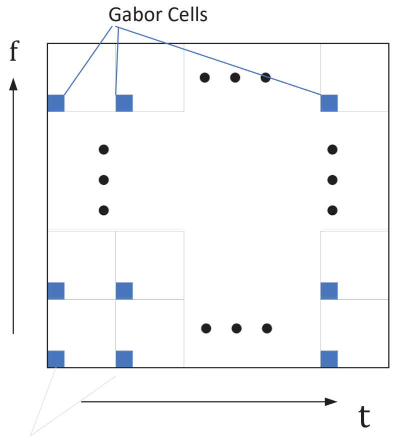

Possible advantages

- Only sparse Gauss signals may be observed both on TD and FD
- Because Gauss wave is used, no sidelobe is seen both on TD and FD (unlike OFDM), simultaneous measurements of delay and Doppler may be possible.

Model

- Total cell size: 16x16 cells
- GDSS gauss pulse is placed on every 4cells on TD and FD. No signal is generated at other cells

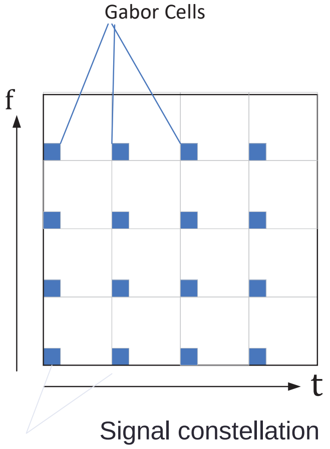

Signal constellation

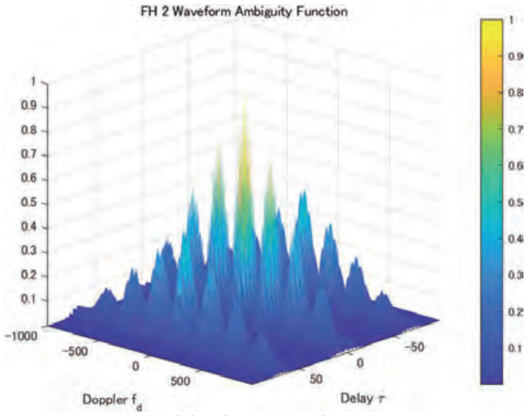

Ambiguity Function

Generated signals on TD/FD domain

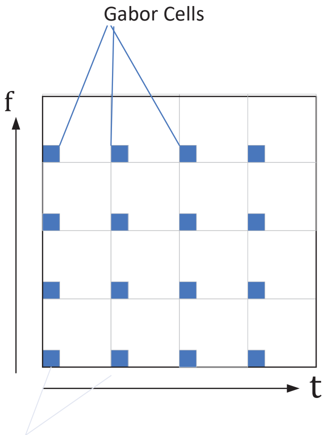

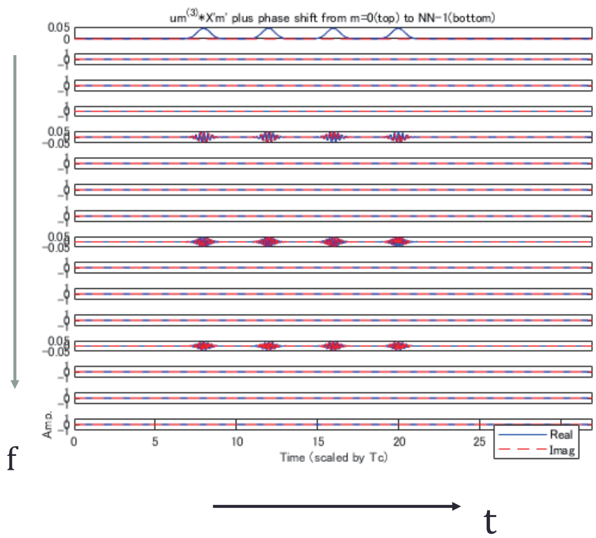

Signals on TD and FD domain

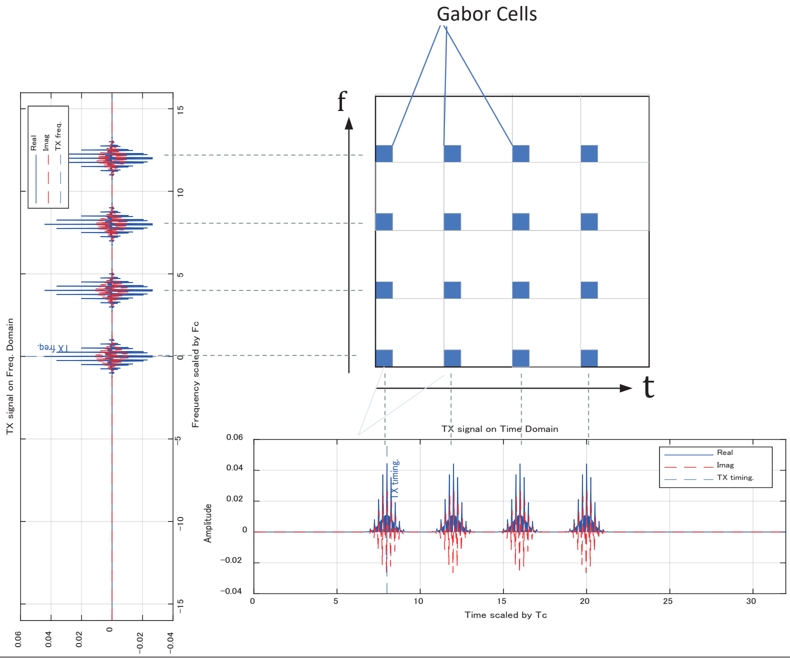

Basic search result with PUL

- Under no noise, delay search follow by Doppler search gives a correct search result

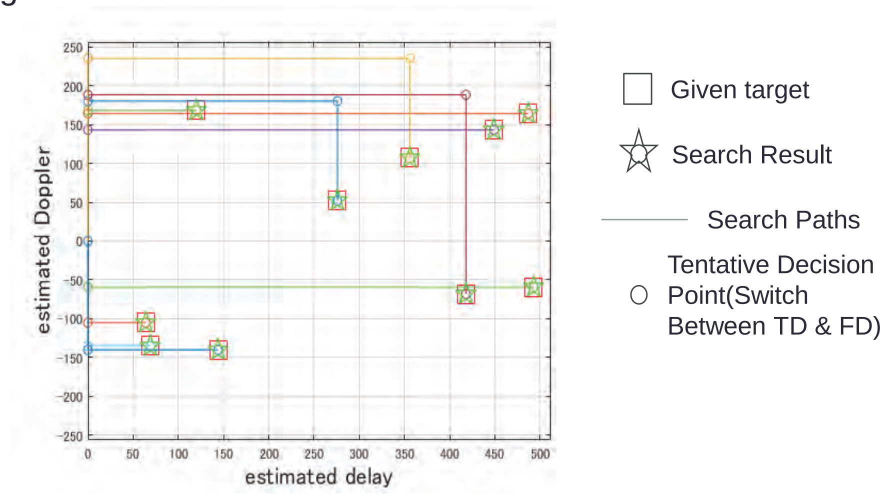

Example of RX signal

S/N=5dB

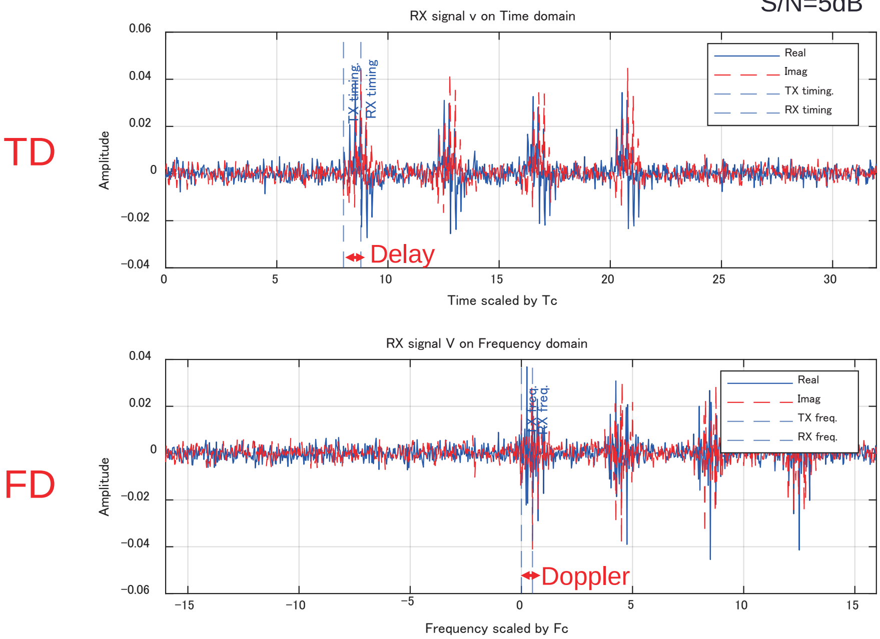

Matched filter output on Time Domain

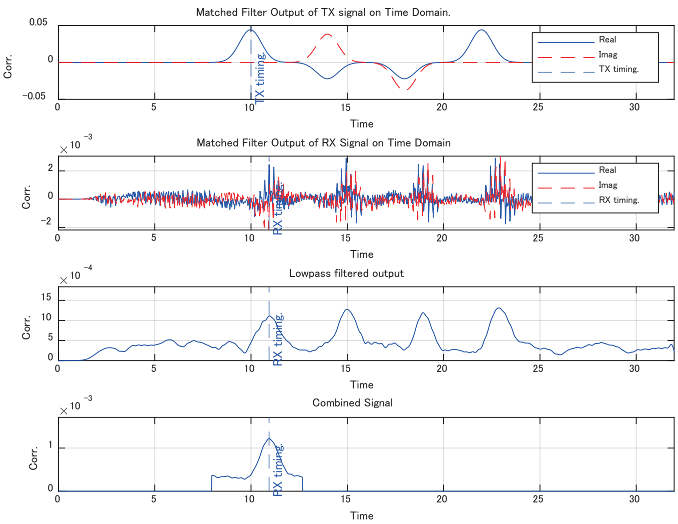

Matched filter output on Freq. Domain

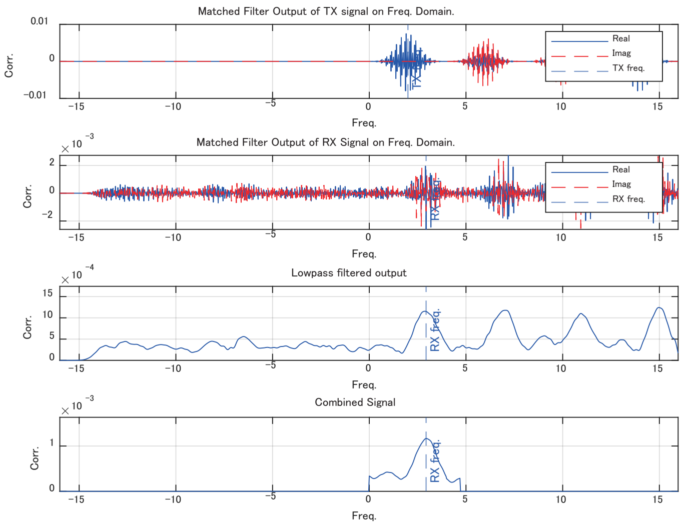

Conclusion

- Under relatively high S/N condition(up to S/N=5dB), Delay and Doppler may be well estimated.
- However, sometimes there are cases that causes wrong estimation, we need to investigate further.

Experimental Evaluations of Device-Free Localization Using Channel State Information in WLAN Systems

Osamu Muta

Kyushu University, Japan

Abstract: Wireless sensing technologies integrated with wireless communication systems are key technologies for the development of 6G systems. Specifically, future wireless networks are expected to provide not only data transmission services but also additional functions to support new application services such as object detection or localization by radio signals. The basic principle of object detection using radio signals and channel state information (CSI) is to capture the target object's behavior by monitoring the fluctuations that it causes in the wireless channel. In this talk, an indoor localization approach that utilizes radio signals is presented. We introduce a real-time device-free indoor machine learning-based localization scheme utilizing feedback beam-forming weights for IEEE802.11-based wireless local area networks (WLANs), where feedback beam-forming weights from stations to the access point are utilized as feature information for machine learning. Both simulation and experimental results prove the effectiveness of the proposed WLAN-based localization approaches in indoor environments.

Acknowledgement:
This research was conducted as a collaborative research project with NTT access network service systems laboratories.

References:

[1] NTT DOCOMO White Paper Ver. 5.0, “5G Evolution and 6G,” Jan. 2023.
[2] T. Murakami, M. Miyazaki, M. Ishida, and A. Fukuda, "Wireless LAN-Based CSI Monitoring System for Object Detection," MDPI Electronics, pp. 1–11, Nov. 2018.
[3] O. Muta, K. Takata, K. Noguchi, T. Murakami, and S. Ohtsuki, "Device-free WLAN Based Indoor Localization Scheme with Spatially Concatenated CSI and Distributed Antennas," IEEE Transactions on Vehicular Technology, Jan. 2023.
[4] O. Muta, K. Noguchi, J. Izumi, S. Shimizu, T. Murakami, and S. Ohtsuki, "Device-free Indoor WLAN Localization with Distributed Antenna Placement Optimization and Spatially Localized Regression," IEEE Transactions on Wireless Communications, Vol. 23, Issue 8, pp.9869 - 9883, Aug. 2024.
[5] O. Muta, J. Izumi, S. Shimizu, T. Murakami, and S. Otsuki, "Experimental Evaluation of Device-free Indoor Localization Using Channel State Information in WLAN Systems with Distributed Antennas," IEICE Transactions on Communications, Vol.E107-B, No.12, pp.890-898, Dec. 2024.
[6] IEEE Computer Society, IEEE 802.11-2016, “IEEE Standard for Information Technology – Telecommunications and information exchange between systems Part 11: Wireless LAN Medium Access Control (MAC) and Physical Layer (PHY) Specifications”, LAN/MAN Standards Committee, 2016.

Experimental Evaluations of Device-Free Localization Using Channel State Information in WLAN Systems

Osamu MUTA

Kyushu University

Background (1/2)

1

Wireless signals are used not only for wireless communications but also sensing for new application services.

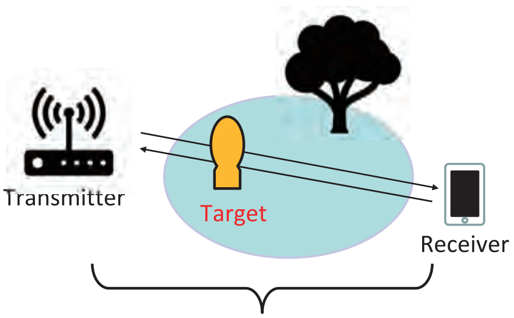

- Wireless sensing is a key technology that supports the evolution of wireless communications for beyond-5G and 6G networks[1]

[1] NTT DOCOMO White Paper Ver. 5.0, "5G Evolution and 6G," Jan. 2023.

Background (2/2)

2

- Wireless sensing techniques can be categorized into two main directions:

Device-base

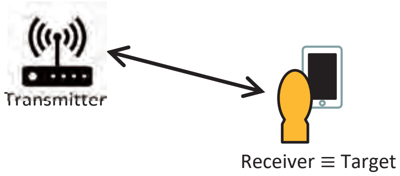

- Target object has a wireless device.
- Distance to target can be estimated. Simple triangulation-based localization is possible.

Device-free

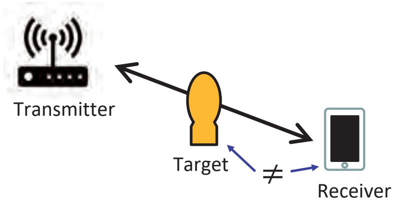

- Target object has NO wireless device.
- The system can detect targets who have no wireless devices. Various applications such as intrusion detection are expected.

Objective of this presentation

3

- In this talk, we will introduce our recent study on **a device-free indoor localization** utilizing channel state information (CSI) for IEEE802.11-based WLANs.

This research was conducted as a collaborative research project with NTT (Nippon Telegraph and Telephone Corporation) access network service systems laboratories.

O. Muta, K. Takata, K. Noguchi, T. Murakami, and S. Otsuki, "Device-free WLAN Based Indoor Localization Scheme with Spatially Concatenated CSI and Distributed Antennas," IEEE Transactions on Vehicular Technology, Jan. 2023.

Principles of device-free localization

- Characterize target object behaviors as fluctuations of wireless channels.

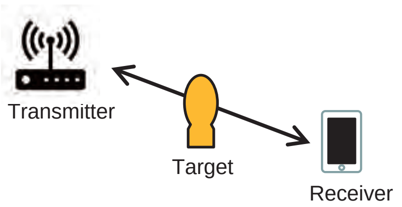

- The target's existence and behaviors can be estimated by learning the relationship between target status and channel status (CSI: channel state information).

Example of impulse response
(simulation results)

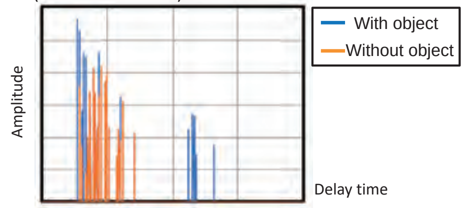

Example of frequency response
(simulation results)

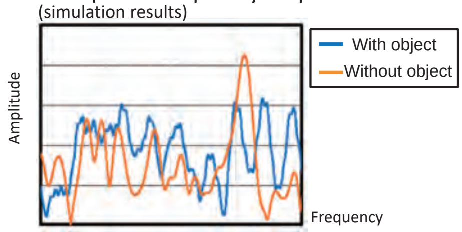

Difference between **H** and **V** (4x4 MU-MIMO)

Using **H**

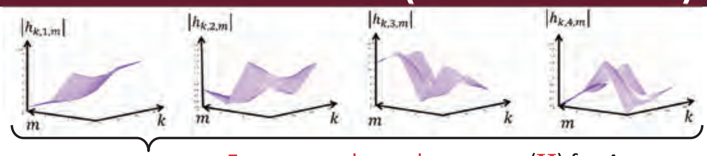

Frequency channel response (**H**) for 4 users

Extract right singular matrix of **H**

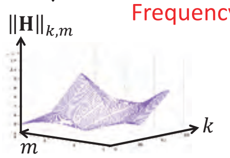

m: Antenna index
K: subcarrier index

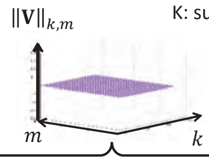

Beam-forming weight (**V**) for 4 users

Using **V**

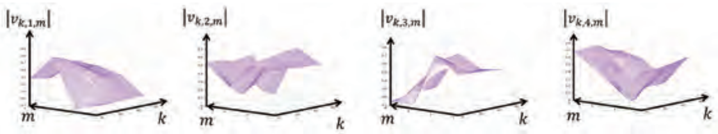

CSI concatenation for CSI-based WLAN localization [3]

- We aim to design a lightweight object detection algorithm with a small dataset.

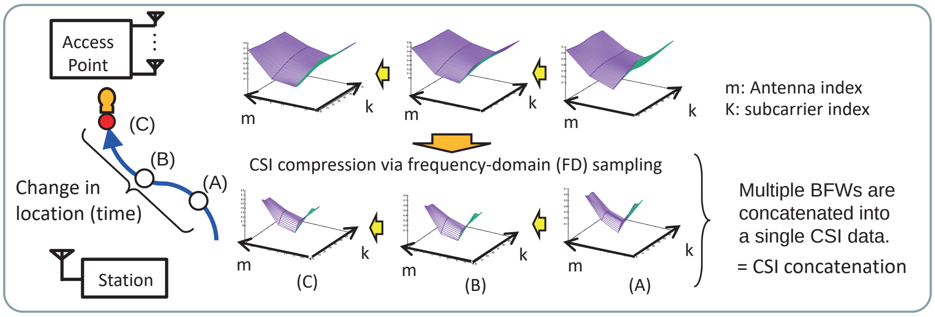

Frequency-domain CSI sampling is adopted to reduce the data size and the required complexity

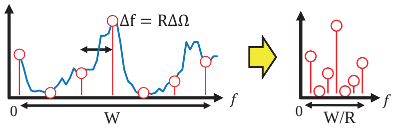

[3] O. Muta, K. Takata, K. Noguchi, T. Murakami, and S. Ohtsuki, "Device-free WLAN Based Indoor Localization Scheme with Spatially Concatenated CSI and Distributed Antennas," IEEE Transactions on Vehicular Technology, Jan. 2023.

Overall system configuration [2][3]

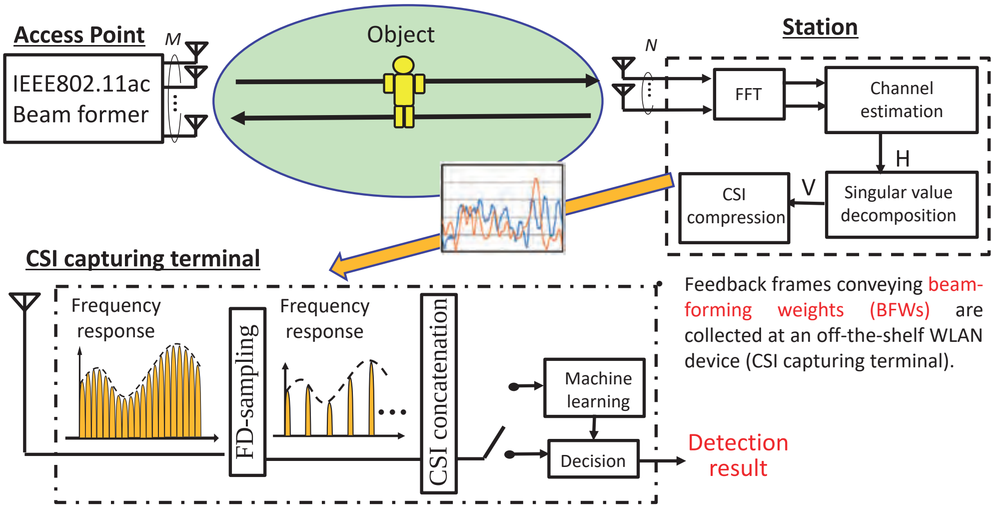

Experiment Scenario #1

- The machine learning (ML) model is trained on measured CSI during the offline training phase.
- Object localization is carried out using the trained ML model in the online testing phase.

AP

CSI capturing terminal

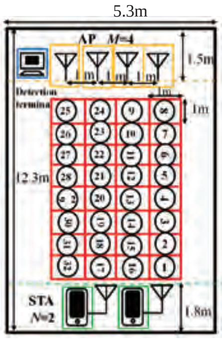

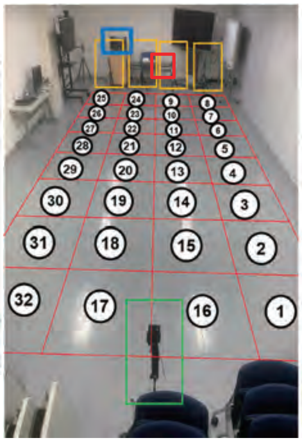

Experiment Setup	
Number of antennas at AP	$M = 4$
System bandwidth	20 MHz
Center frequency	5.18 GHz
Number of subcarriers	52
Machine learning model	Random Forest

Measured CSI in Experiment

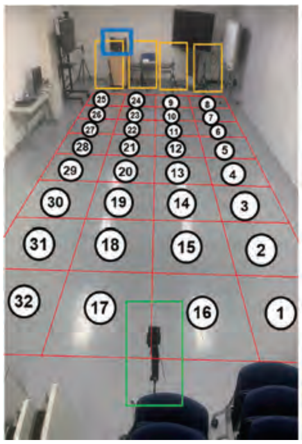

CSI (beam-forming weight) at AP

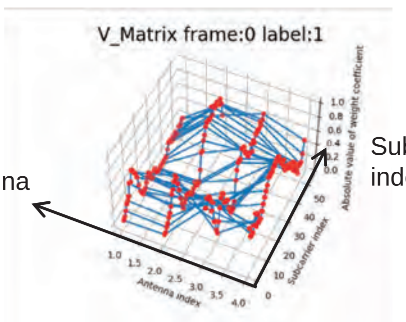

Antenna index

Subcarrier index

Experiment results : Area-wise detection probability 10

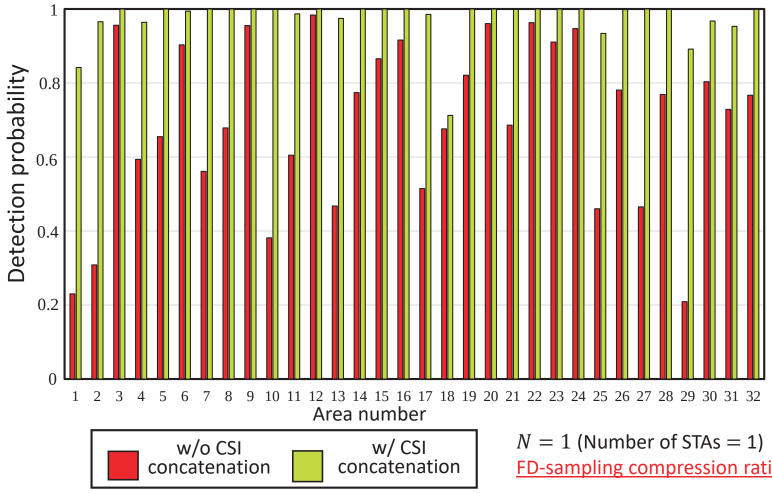

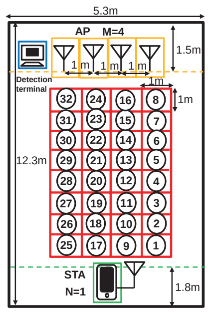

$N = 1$ (Number of STAs = 1)

FD-sampling compression ratio : 1/13

Impact of antenna spacing on detection performance 11

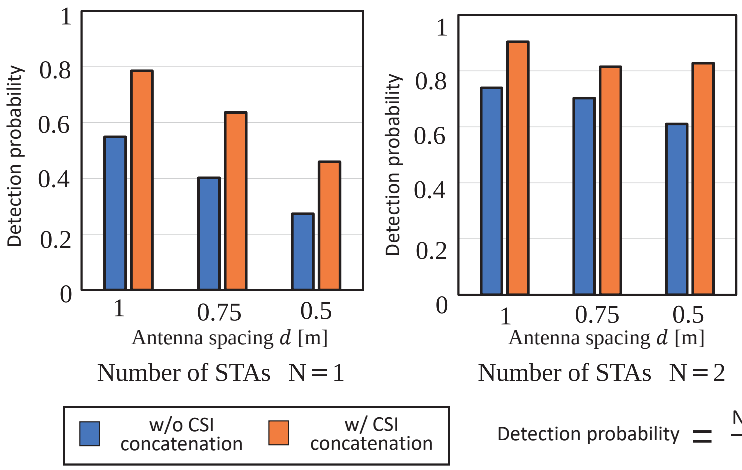

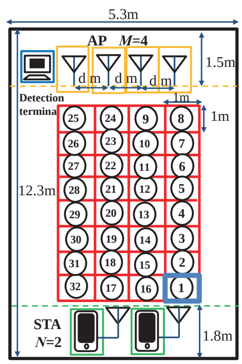

$$\text{Detection probability} = \frac{\text{Number of correct results}}{\text{Number of tests}}$$

Experiment scenario #2

12

- We consider the following two experiment scenarios. Offline training is used by using measured CSI samples.

Experiment scenario at a gymnasium

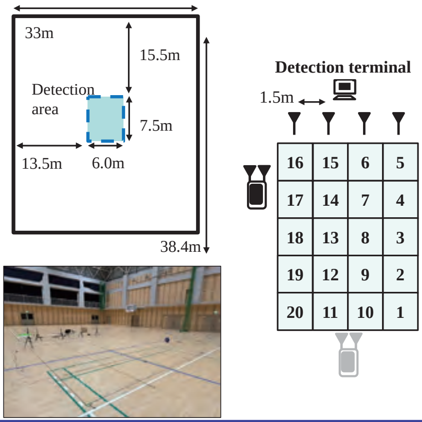

Experiment scenario in an outdoor environment

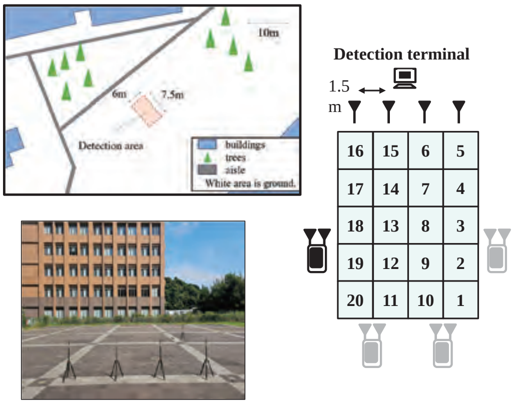

Experiment results for scenario #2

13

Gymnasium

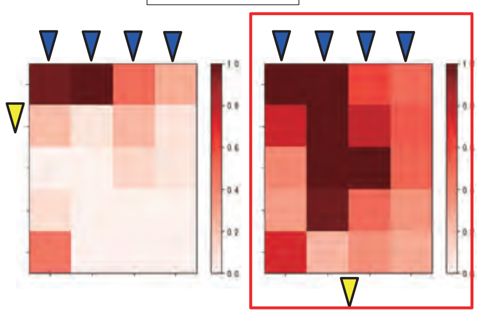

Outdoor

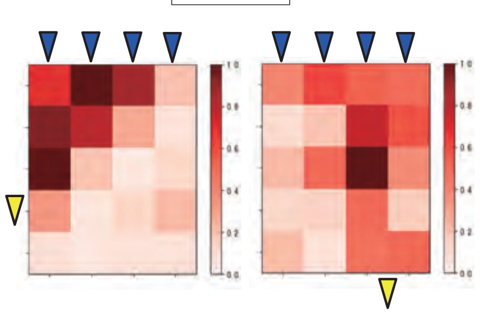

- When the target is located in areas directly facing the AP antennas and STAs, it results in higher detection probabilities unlike other areas that experience a marked drop in detection probabilities.
- This result suggests the detection probability can be enhanced in specific areas by properly determining the AP antenna and STA positions.

Average detection probability vs. compression ratio R 14

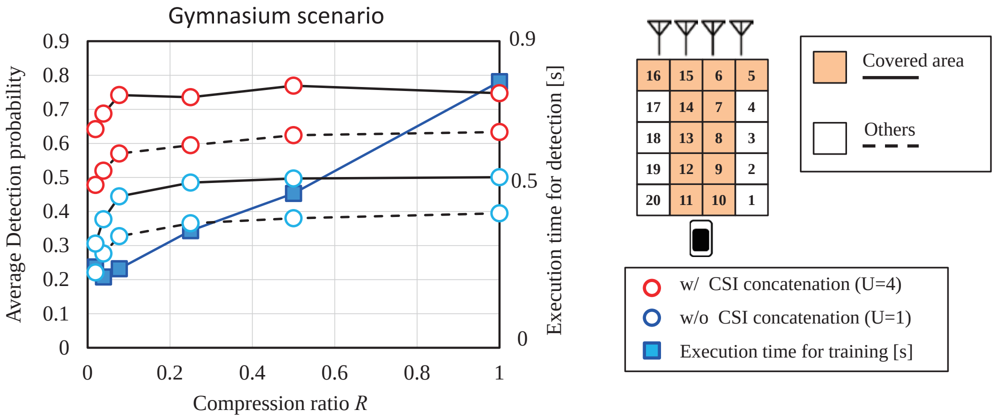

Almost the same detection probability can be obtained even when frequency-domain sampling rate is about $R = 0.1$, while the execution time is reduced to 1/10.

Conclusion and Future work 15

- We briefly introduced our recent studies on a device-free CSI based WLAN indoor localization with a small dataset, and demonstrated the achieved performance of our developed scheme in various environments.

- Future work:
  - The concept is applicable to other wireless communication systems if the acquisition of CSI between transceivers is possible.
  - Advanced sensing with more powerful ML models under various scenarios.

Comprehensive Comparison of Message-Passing Algorithms for Compressed Sensing

Keigo Takeuchi

Dept. Electrical and Electronic Inf. Eng., Toyohashi University of Technology, Japan
takeuchi@ee.tut.ac.jp

The purpose of compressed sensing is recovery of sparse signals from compressed linear measurements. This lecture note reviews four message-passing algorithms for signal recovery: approximate message-passing (AMP) [1], orthogonal/vector AMP [2, 3], convolutional AMP [4], and memory AMP [5].

AMP is a low-complexity and Bayes-optimal algorithm for zero-mean independent and identically distributed (i.i.d.) Gaussian sensing matrices. The main feature of AMP is the so-called Onsager correction to realize asymptotic Gaussianity for the estimation errors. A disadvantage of AMP is that AMP fails to converge when the sensing matrix has non-zero mean or dependent elements.

Orthogonal/vector AMP solves the disadvantage of AMP: It achieves the Bayes-optimal performance for all right-orthogonally invariant sensing matrices. However, orthogonal/vector AMP requires high-complexity linear minimum mean-square error (LMMSE) estimation.

Convolutional AMP is a message-passing algorithm with long-term memory to realize the advantages of AMP and orthogonal/vector AMP. The current messages are updated with messages in all previous iterations. Convolutional AMP can achieve the Bayes-optimal performance for right-orthogonally invariant sensing matrices if it converges to a fixed point. However, it fails to converge for ill-conditioned sensing matrices.

Memory AMP approximates the LMMSE estimation in orthogonal/vector AMP with gradient descent. Memory AMP is in a similar situation to that in convolutional AMP. When long-memory damping [5, 6] is utilized, however, memory AMP is guaranteed to converge asymptotically.

In the end of this lecture note, these four algorithms are numerically compared. Numerical simulations were originally presented in [7].

References

[1] D. L. Donoho, A. Maleki, and A. Montanari, "Message-passing algorithms for compressed sensing," *Proc. Nat. Acad. Sci.*, vol. 106, no. 45, pp. 18914–18919, Nov. 2009.

[2] J. Ma and L. Ping, "Orthogonal AMP," *IEEE Access*, vol. 5, pp. 2020–2033, Jan. 2017.

[3] S. Rangan, P. Schniter, and A. K. Fletcher, "Vector approximate message passing," *IEEE Trans. Inf. Theory*, vol. 65, no. 10, pp. 6664–6684, Oct. 2019.

[4] K. Takeuchi, "Bayes-optimal convolutional AMP," *IEEE Trans. Inf. Theory*, vol. 67, no. 7, pp. 4405–4428, Jul. 2021.

[5] L. Liu, S. Huang, and B. M. Kurkoski, "Memory AMP," *IEEE Trans. Inf. Theory*, vol. 68, no. 12, pp. 8015–8039, Dec. 2022.

[6] K. Takeuchi, "On the convergence of orthogonal/vector AMP: Long-memory message-passing strategy," *IEEE Trans. Inf. Theory*, vol. 68, no. 12, pp. 8121–8138, Dec. 2022.

[7] K. Takeuchi, "Challenges and future direction in message-passing demodulation," *IEICE Tech. Rep.*, vol. 123, no. 439, CS2023-114, pp. 58–63, Mar. 2024. (in Japanese)

Comprehensive Comparison of Message-Passing Algorithms for Compressed Sensing

Mathematics for Innovation in Information and Communication Technology
Fukuoka, Japan
September 27, 2024

Keigo Takeuchi
Toyohashi University of Technology, Japan

1

Signal Recovery from Linear Measurements

Linear Measurement Model

$$\boldsymbol{y} = \boldsymbol{A}\boldsymbol{x} + \boldsymbol{w}, \qquad \boldsymbol{w} \sim \mathcal{N}(\boldsymbol{0}, \sigma^2 \boldsymbol{I}_M).$$

$\boldsymbol{x} \in \mathbb{R}^N$: N-dimensional unknown sparse signal vector with i.i.d. elements

$\boldsymbol{y} \in \mathbb{R}^M$: M-dimensional compressed measurement vector ($M \leq N$)

$\boldsymbol{A} \in \mathbb{R}^{M \times N}$: Known sensing matrix

Ultimate Goal in Signal Recovery

Construct an estimator $\hat{\boldsymbol{x}}(\boldsymbol{y}, \boldsymbol{A})$ of $\boldsymbol{x}$ that satisfies

- Bayes-optimal performance in the sense of mean-square error (MSE)
- Minimum (optimal) complexity in the order of M and N

2

Summary of Message-Passing Algorithms

Algorithms	Complexity	Matrices	Performance
Approximate message-passing (AMP) [1]	$\mathcal{O}(tMN)$ t: #iterations	i.i.d. Gaussian	Optimum
Orthogonal/Vector AMP (OAMP/VAMP) [2, 3]	$\mathcal{O}(tMN + M^3 + M^2N)$	Right-orthogonal invariant	Optimum
Convolutional AMP (CAMP) [4]	$\mathcal{O}(tMN)$	Right-orthogonal invariant	Optimum?
Memory AMP (MAMP) [5]	$\mathcal{O}(tMN)$	Right-orthogonal invariant	Optimum?

[1] D. L. Donoho, A. Maleki, and A. Montanari, “Message-passing algorithms for compressed sensing,” *Proc. Nat. Acad. Sci.*, vol. 106, no. 45, pp. 18914–18919, Nov. 2009.

[2] J. Ma and L. Ping, “Orthogonal AMP,” *IEEE Access*, vol. 5, pp. 2020–2033, Jan. 2017.

[3] S. Rangan, P. Schniter, and A. K. Fletcher, “Vector approximate message passing,” *IEEE Trans. Inf. Theory*, vol. 65, no. 10, pp. 6664–6684, Oct. 2019.

[4] K. Takeuchi, “Bayes-optimal convolutional AMP,” *IEEE Trans. Inf. Theory*, vol. 67, no. 7, pp. 4405–4428, Jul. 2021.

[5] L. Liu, S. Huang, and B. M. Kurkoski, “Memory AMP,” *IEEE Trans. Inf. Theory*, vol. 68, no. 12, pp. 8015–8039, Dec. 2022.

Memoryless Message-Passing

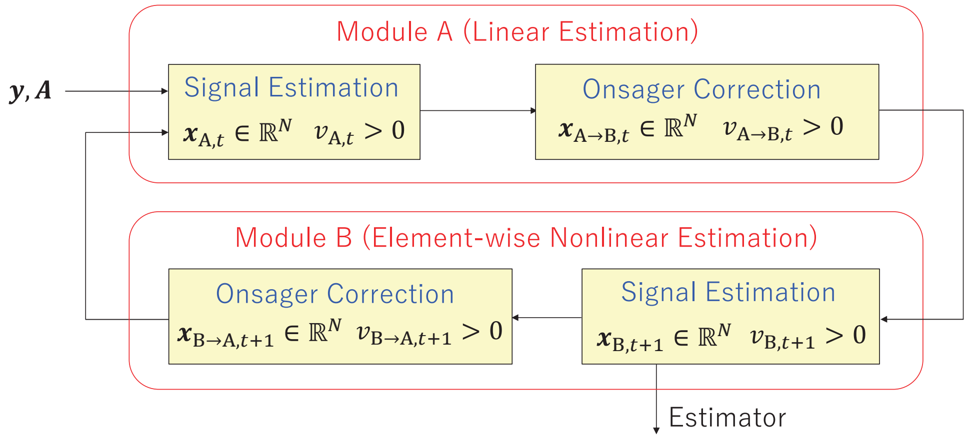

Approximate Message-Passing (AMP)

Module A (Matched-Filter Estimation)

$$\boldsymbol{x}_{\mathrm{A}\to\mathrm{B},t} = \boldsymbol{x}_{\mathrm{B},t} + \boldsymbol{A}^{\mathrm{T}}\boldsymbol{z}_t, \qquad \boldsymbol{z}_t = \boldsymbol{y} - \boldsymbol{A}\boldsymbol{x}_{\mathrm{B},t} + \frac{N v_{\mathrm{B},t}}{M v_{\mathrm{A}\to\mathrm{B},t-1}}\boldsymbol{z}_{t-1}.$$

$$v_{\mathrm{A}\to\mathrm{B},t} = \sigma^2 + \frac{N}{M}v_{\mathrm{B},t},$$

Onsager correction

Module B (Element-wise Denoiser)

$$\boldsymbol{x}_{\mathrm{B},t+1} = \mathbb{E}[\boldsymbol{x}|\boldsymbol{x}_{\mathrm{A}\to\mathrm{B},t}, v_{\mathrm{A}\to\mathrm{B},t}], \qquad v_{\mathrm{B},t+1} = \frac{1}{N}\mathbb{E}\left[\|\boldsymbol{x} - \boldsymbol{x}_{\mathrm{B},t+1}\|^2 | \boldsymbol{x}_{\mathrm{A}\to\mathrm{B},t}, v_{\mathrm{A}\to\mathrm{B},t}\right]$$

Virtual Gaussian Measurement

$$\boldsymbol{x}_{\mathrm{A}\to\mathrm{B},t} = \boldsymbol{x} + \boldsymbol{h}_t, \qquad \boldsymbol{h}_t \sim \mathcal{N}(\boldsymbol{0}, v_{\mathrm{A}\to\mathrm{B},t}\boldsymbol{I}_N).$$

Postulate asymptotic Gaussianity of the estimation error $\boldsymbol{x}_{\mathrm{A}\to\mathrm{B},t} - \boldsymbol{x}$.

5

Effect of the Onsager Correction

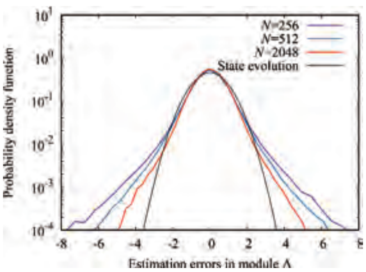

Without correction

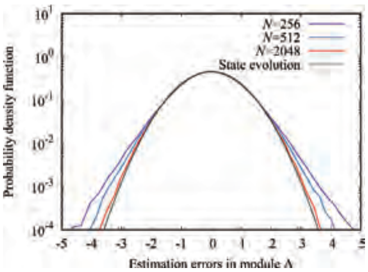

With correction

Compression rate	$M/N = 0.5$
Signals	Bernoulli-Gaussian with signal density $\rho = 0.1$
Sensing matrices	i.i.d. Gaussian matrices
Signal-to-noise ratio (SNR)	30 dB
Number of iterations	2

6

Orthogonal/Vector AMP (OAMP/VAMP)

Module A (LMMSE Estimation)

$$\boldsymbol{x}_{\mathrm{A},t} = \boldsymbol{x}_{\mathrm{B}\to\mathrm{A},t} + \boldsymbol{A}^{\mathrm{T}}\boldsymbol{\Xi}_t^{-1}(\boldsymbol{y} - \boldsymbol{A}\boldsymbol{x}_{\mathrm{B}\to\mathrm{A},t}), \quad \boldsymbol{\Xi}_t = \frac{\sigma^2}{v_{\mathrm{B}\to\mathrm{A},t}}\boldsymbol{I}_M + \boldsymbol{A}\boldsymbol{A}^{\mathrm{T}},$$

$$v_{\mathrm{A},t} = \frac{v_{\mathrm{B}\to\mathrm{A},t}}{N}\mathrm{Tr}\left(\boldsymbol{I}_N - \boldsymbol{A}^{\mathrm{T}}\boldsymbol{\Xi}_t^{-1}\boldsymbol{A}\right),$$

$$\boldsymbol{x}_{\mathrm{A}\to\mathrm{B},t} = \frac{\boldsymbol{x}_{\mathrm{A},t} - \xi_{\mathrm{A},t}\boldsymbol{x}_{\mathrm{B}\to\mathrm{A},t}}{1 - \xi_{\mathrm{A},t}}, \quad v_{\mathrm{A}\to\mathrm{B},t} = \frac{\xi_{\mathrm{A},t}v_{\mathrm{B}\to\mathrm{A},t}}{1 - \xi_{\mathrm{A},t}}, \quad \xi_{\mathrm{A},t} = \frac{v_{\mathrm{A},t}}{v_{\mathrm{B}\to\mathrm{A},t}}.$$

Module B (Element-wise Denoiser)

Onsager correction

$$\boldsymbol{x}_{\mathrm{B},t+1} = \mathbb{E}[\boldsymbol{x}|\boldsymbol{x}_{\mathrm{A}\to\mathrm{B},t}, v_{\mathrm{A}\to\mathrm{B},t}],$$

$$v_{\mathrm{B},t+1} = \frac{1}{N}\mathbb{E}\left[\|\boldsymbol{x} - \boldsymbol{x}_{\mathrm{B},t+1}\|^2 | \boldsymbol{x}_{\mathrm{A}\to\mathrm{B},t}, v_{\mathrm{A}\to\mathrm{B},t}\right]$$

Equivalent to AMP

$$\boldsymbol{x}_{\mathrm{B}\to\mathrm{A},t} = \frac{\boldsymbol{x}_{\mathrm{B},t+1} - \xi_{\mathrm{B},t}\boldsymbol{x}_{\mathrm{A}\to\mathrm{B},t}}{1 - \xi_{\mathrm{B},t}}, \quad v_{\mathrm{B}\to\mathrm{A},t} = \frac{\xi_{\mathrm{B},t}v_{\mathrm{A}\to\mathrm{B},t}}{1 - \xi_{\mathrm{B},t}}, \quad \xi_{\mathrm{B},t} = \frac{v_{\mathrm{B},t+1}}{v_{\mathrm{A}\to\mathrm{B},t}}.$$

7

Long-Memory Message-Passing

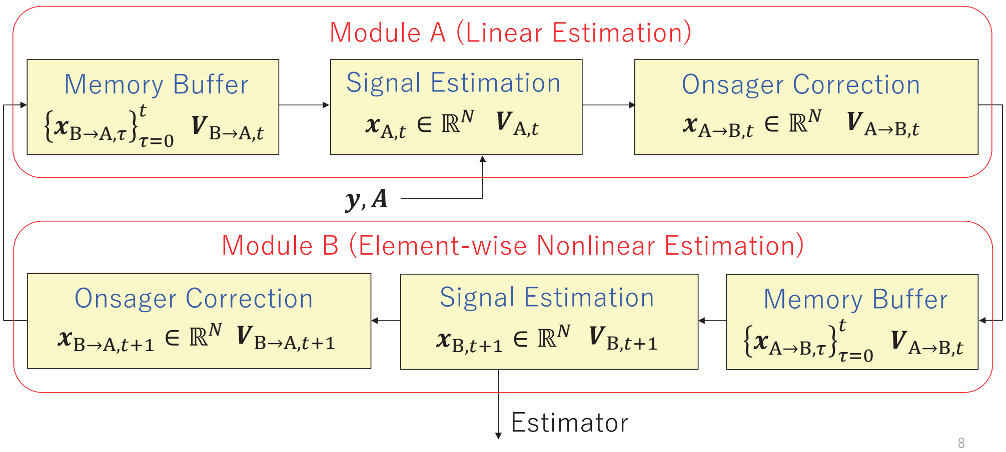

8

Convolutional AMP (CAMP)

Module A (Matched-Filter Estimation) $\rho_{\boldsymbol{A}^{\mathrm{T}}\boldsymbol{A}}$: Asymptotic eigenvalue distribution of $\boldsymbol{A}^{\mathrm{T}}\boldsymbol{A}$

$$\boldsymbol{z}_t = \boldsymbol{y} - \boldsymbol{A}\boldsymbol{x}_{\mathrm{B},t} + \sum_{\tau=0}^{t-1} \xi_\tau^{(t-1)} g_{t-\tau} \boldsymbol{z}_\tau, \quad \xi_\tau^{(t-1)} = \prod_{t'=\tau}^{t-1} \frac{v_{\mathrm{B},t'+1,t'+1}}{v_{\mathrm{A}\to\mathrm{B},t',t'}},$$

$$\boldsymbol{x}_{\mathrm{A}\to\mathrm{B},t} = \boldsymbol{x}_{\mathrm{B},t} + \boldsymbol{A}^{\mathrm{T}}\boldsymbol{z}_t, \quad \boldsymbol{V}_{\mathrm{A}\to\mathrm{B},t} = \boldsymbol{\Phi}_t^{\mathrm{CAMP}}(\boldsymbol{V}_{\mathrm{A}\to\mathrm{B},t-1}, \boldsymbol{V}_{\mathrm{B},t}; \rho_{\boldsymbol{A}^{\mathrm{T}}\boldsymbol{A}}).$$

The tap coefficient $g_\tau \in \mathbb{R}$ and covariance matrix $\boldsymbol{V}_{\mathrm{A}\to\mathrm{B},t}$ are designed via state evolution.

Module B (Element-wise Denoiser)

$$\boldsymbol{x}_{\mathrm{B},t+1} = \mathbb{E}[\boldsymbol{x}|\boldsymbol{x}_{\mathrm{A}\to\mathrm{B},t}, v_{\mathrm{A}\to\mathrm{B},t}], \; v_{\mathrm{B},t+1,t'+1} = \frac{1}{N}\mathbb{E}\left[(\boldsymbol{x} - \boldsymbol{x}_{\mathrm{B},t+1})^{\mathrm{T}}(\boldsymbol{x} - \boldsymbol{x}_{\mathrm{B},t'+1})|\boldsymbol{x}_{\mathrm{A}\to\mathrm{B},t}, \boldsymbol{x}_{\mathrm{A}\to\mathrm{B},t'}\right]$$

$$\boldsymbol{x}_{\mathrm{A}\to\mathrm{B},t} = \boldsymbol{x} + \boldsymbol{h}_t, \quad (\boldsymbol{h}_t, \boldsymbol{h}_{t'}) \sim \mathcal{N}\left(\boldsymbol{0}, \begin{bmatrix} v_{\mathrm{A}\to\mathrm{B},t,t}\boldsymbol{I} & v_{\mathrm{A}\to\mathrm{B},t,t'}\boldsymbol{I} \\ v_{\mathrm{A}\to\mathrm{B},t',t}\boldsymbol{I} & v_{\mathrm{A}\to\mathrm{B},t',t'}\boldsymbol{I} \end{bmatrix}\right)$$

Contour of Joint pdf for Estimation Errors

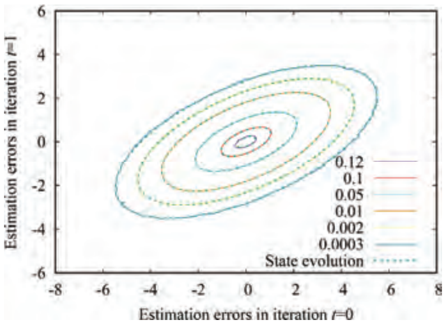

System size	$M = 8192$, $N = 16384$
Signals	Bernoulli-Gaussian with signal density $\rho = 0.1$
Sensing matrices	Right-orthogonally invariant (Condition number $\kappa = 5$)
Signal-to-noise ratio (SNR)	30 dB

Matrix-Inversion Approx. via Gradient Descent

Matrix Inversion in OAMP/VAMP

$$\boldsymbol{z}_t = c_t \boldsymbol{\Xi}_t^{-1}(\boldsymbol{y} - \boldsymbol{A}\boldsymbol{x}_{\mathrm{B}\to\mathrm{A},t}) \quad \Leftrightarrow \quad \boldsymbol{\Xi}_t \boldsymbol{z}_t = c_t(\boldsymbol{y} - \boldsymbol{A}\boldsymbol{x}_{\mathrm{B}\to\mathrm{A},t})$$

$c_t \in \mathbb{R}$: any constant

Quadratic-Programming Formulation

$$\boldsymbol{z}_t = \underset{\boldsymbol{z}\in\mathbb{R}^M}{\operatorname{argmin}} f_t(\boldsymbol{z}), \quad f_t(\boldsymbol{z}) = \frac{1}{2}\boldsymbol{z}^{\mathrm{T}}\boldsymbol{\Xi}_t\boldsymbol{z} - c_t(\boldsymbol{y} - \boldsymbol{A}\boldsymbol{x}_{\mathrm{B}\to\mathrm{A},t})^{\mathrm{T}}\boldsymbol{z}.$$

Approximation via Gradient Descent

$$\boldsymbol{z}_t^{(i+1)} = \boldsymbol{z}_t^{(i)} - \epsilon_t \nabla f_t\left(\boldsymbol{z}_t^{(i)}\right) = (\boldsymbol{I} - \epsilon_t\boldsymbol{\Xi}_t)\boldsymbol{z}_t^{(i)} + \epsilon_t c_t(\boldsymbol{y} - \boldsymbol{A}\boldsymbol{x}_{\mathrm{B}\to\mathrm{A},t})$$

Optimizing $\epsilon_t > 0$ ⇒

$$\boldsymbol{z}_t^{(i+1)} = \epsilon_t(\bar{\lambda}\boldsymbol{I} - \boldsymbol{A}\boldsymbol{A}^{\mathrm{T}})\boldsymbol{z}_t^{(i)} + \underbrace{\epsilon_t c_t}_{=\zeta_t}(\boldsymbol{y} - \boldsymbol{A}\boldsymbol{x}_{\mathrm{B}\to\mathrm{A},t})$$

11

Memory AMP (MAMP)

Design Idea

Perform one update of gradient descent in each MAMP iteration.

Module A (Matched-Filter Estimation)

$$\boldsymbol{z}_t = \epsilon_t(\bar{\lambda}\boldsymbol{I} - \boldsymbol{A}\boldsymbol{A}^{\mathrm{T}})\boldsymbol{z}_{t-1} + \zeta_t(\boldsymbol{y} - \boldsymbol{A}\boldsymbol{x}_{\mathrm{B}\to\mathrm{A},t}),$$

$$\boldsymbol{x}_{\mathrm{A}\to\mathrm{B},t} = \frac{\boldsymbol{A}^{\mathrm{T}}\boldsymbol{z}_t + \sum_{\tau=0}^{t}\zeta_\tau\epsilon_{\tau+1}^{(t)}\xi_{\mathrm{A},t-\tau}\boldsymbol{x}_{\mathrm{B}\to\mathrm{A},\tau}}{\sum_{\tau=0}^{t}\zeta_\tau\epsilon_{\tau+1}^{(t)}\xi_{\mathrm{A},t-\tau}}, \quad \epsilon_{\tau+1}^{(t)} = \prod_{t'=\tau}^{t-1}\epsilon_{t'},$$

$$\boldsymbol{V}_{\mathrm{A}\to\mathrm{B},t} = \boldsymbol{\Phi}_t^{\mathrm{MAMP}}(\boldsymbol{V}_{\mathrm{B},t}; \rho_{\boldsymbol{A}^{\mathrm{T}}\boldsymbol{A}}).$$

Design $\xi_{\mathrm{A},\tau}$, $\zeta_t \in \mathbb{R}$ and covariance matrix $\boldsymbol{V}_{\mathrm{A}\to\mathrm{B},t}$ via state evolution.

12

Memory AMP (MAMP)

Module B (Element-wise Denoiser)

$$\boldsymbol{x}_{\mathrm{B},t+1} = \mathbb{E}[\boldsymbol{x}|\boldsymbol{x}_{\mathrm{A}\to\mathrm{B},t}, v_{\mathrm{A}\to\mathrm{B},t}],$$

Equivalent to CAMP

$$v_{\mathrm{B},t+1,t'+1} = \frac{1}{N}\mathbb{E}\left[(\boldsymbol{x}-\boldsymbol{x}_{\mathrm{B},t+1})^{\mathrm{T}}(\boldsymbol{x}-\boldsymbol{x}_{\mathrm{B},t'+1})|\boldsymbol{x}_{\mathrm{A}\to\mathrm{B},t}, \boldsymbol{x}_{\mathrm{A}\to\mathrm{B},t'}\right]$$

$$\boldsymbol{x}_{\mathrm{B}\to\mathrm{A},t} = \frac{\boldsymbol{x}_{\mathrm{B},t+1} - \xi_{\mathrm{B},t}\boldsymbol{x}_{\mathrm{A}\to\mathrm{B},t}}{1-\xi_{\mathrm{B},t}}, \quad \xi_{\mathrm{B},t} = \frac{v_{\mathrm{B},t+1,t+1}}{v_{\mathrm{A}\to\mathrm{B},t,t}},$$

Equivalent to OAMP/VAMP

$$v_{\mathrm{B}\to\mathrm{A},t+1,t'+1} = \frac{v_{\mathrm{B},t+1,t'+1} - \xi_{\mathrm{B},t}\xi_{\mathrm{B},t'}v_{\mathrm{A}\to\mathrm{B},t,t'}}{(1-\xi_{\mathrm{B},t})(1-\xi_{\mathrm{B},t'})} \quad [6]$$

[6] has used to define $v_{\mathrm{B}\to\mathrm{A},t+1,t'+1}$, instead of the original paper [5].

[6] K. Takeuchi, "On the convergence of orthogonal/vector AMP: Long-memory message-passing strategy," *IEEE Trans. Inf. Theory*, vol. 68, no. 12, pp. 8121–8138, Dec. 2022.

Convergence Guarantee

Long-Memory (LM) Damping [5, 6, 7]

For all $t' \in \{0, \dots, t\}$

$$\boldsymbol{x}_{\mathrm{A}\to\mathrm{B},t} := \sum_{\tau=0}^{t} \theta_{t,\tau}\boldsymbol{x}_{\mathrm{A}\to\mathrm{B},\tau}, \quad v_{\mathrm{A}\to\mathrm{B},t,t'} := \frac{1}{\mathbf{1}^{\mathrm{T}}\boldsymbol{V}_{\mathrm{A}\to\mathrm{B},t}^{-1}\mathbf{1}}, \qquad \begin{bmatrix}\theta_{t,0}\\ \vdots \\ \theta_{t,t}\end{bmatrix} = \frac{\boldsymbol{V}_{\mathrm{A}\to\mathrm{B},t}^{-1}\mathbf{1}}{\mathbf{1}^{\mathrm{T}}\boldsymbol{V}_{\mathrm{A}\to\mathrm{B},t}^{-1}\mathbf{1}}.$$

Effect of LM Damping [6, 7]

In general, the MSE $N^{-1}\mathbb{E}\left[\|\boldsymbol{x}-\boldsymbol{x}_{\mathrm{A}\to\mathrm{B},t}\|^2\right]$ after LM damping is monotonically decreasing in the large system limit as t increases.

⇒ LM damping guarantees the convergence of MAMP.

[7] L. Liu, S. Huang, and B. M. Kurkoski, "Sufficient statistic memory approximate message passing," in *Proc. 2022 IEEE Int. Symp. Inf. Theory*, Espoo, Finland, Jun.-Jul. 2022, pp.1378–1383.

Numerical Conditions

System size	$M = 8192$, $N = 16384$
Signals	Bernoulli-Gaussian with signal density $\rho = 0.1$
Sensing matrices	Right-orthogonally invariant
Condition number	$\kappa = 10$
SNR	30 dB

15

Numerical Simulation (Copyright©2024 IEICE, [8] Fig. 2)

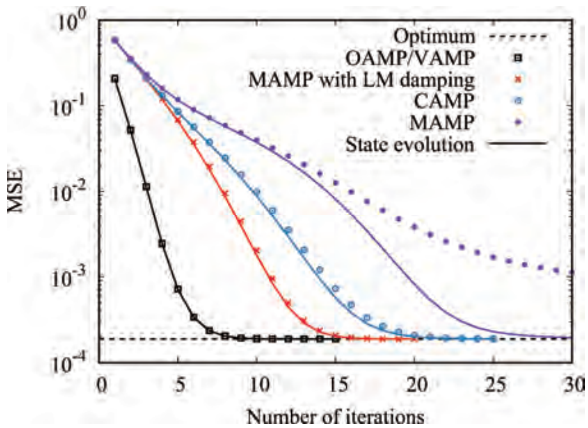

[8] K. Takeuchi, "Challenges and Future Direction in Message-Passing Demodulation," *IEICE Tech. Rep.*, vol. 123, no. 439, CS2023-114, pp. 58-63, Mar. 2024.

16

Numerical Simulation (Copyright©2024 IEICE, [8] Fig. 1)

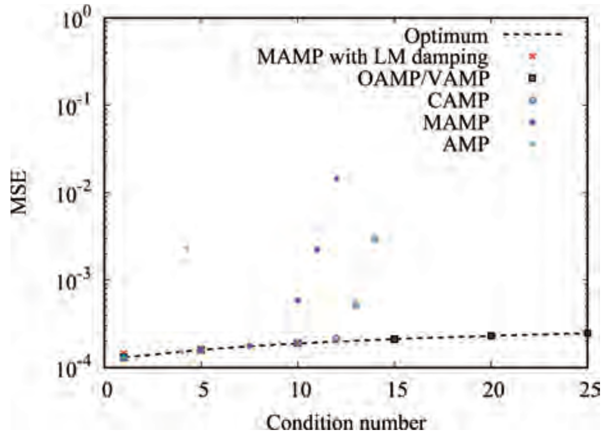

[8] K. Takeuchi, “Challenges and Future Direction in Message-Passing Demodulation,” *IEICE Tech. Rep.*, vol. 123, no. 439, CS2023-114, pp. 58-63, Mar. 2024.

17

Conclusions

Summary

The advantages (complexity, flexibility, and performance) of both AMP and OAMP/VAMP can be realized in part via LM damping.

Direction in Future Research

- Performance of current LM message-passing (Condition number < 30)

  ≪ Performance of OAMP/VAMP (Condition number < 10^4)
- LM message-passing requires a huge system ($N > 10^4$)
- LM message-passing cannot treat non-zero mean sensing matrices.

⇨ Much room for improvement in LM message-passing

18

Some information-theoretic aspects of joint communication and sensing

Joudeh Hamdi

Department of Electrical Engineering
Eindhoven University of Technology
The Netherlands
h.joudeh@tue.nl

Abstract: In this talk, I will discuss a basic model for joint communication and sensing, where a transmitter simultaneously communicates with a receiver over a state-dependent discrete memoryless channel and senses the channel state through a generalized feedback channel. First, I will discuss a list estimation approach to the sensing problem and establish a suitable notion of sensing capacity. Then, I will focus on reliability and discuss error exponents for sensing and communication.

Acknowledgment

This work was supported in part by the European Research Council (ERC) through the ERC Starting Grant N. 101116550 (IT-JCAS).

References

[1] M. Kobayashi, G. Caire and G. Kramer, "Joint state sensing and communication: Optimal tradeoff for a memoryless case," IEEE International Symposium on Information Theory, 2018.

[2] H. Joudeh and G. Caire, "Joint communication and state sensing under logarithmic loss," IEEE International Symposium on Joint Communications & Sensing, 2024.

[3] Y. Shkel and S. Verdú, "A single-shot approach to lossy source coding under logarithmic loss," IEEE Transactions on Information Theory, vol. 64, no. 1, 2018.

[4] E. Arikan, "An inequality on guessing and its application to sequential decoding," in IEEE Transactions on Information Theory, vol. 42, no. 1, 1996.

Some information-theoretic aspects of joint communication and sensing

Hamdi Joudeh

ICT Lab, EE Department
Eindhoven University of Technology

Mathematics for Innovation in Information and Communication Technology
Fukuoka, September 2024

Joint Communication and Sensing (JCAS)

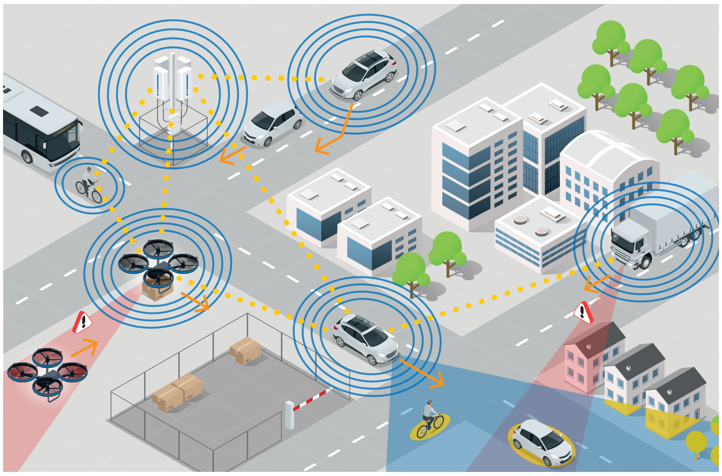

Source: VDE-ITG position paper on JCAS

- a.k.a. Integrated Sensing and Communication (ISAC)
- Major challenge: IT framework and limits

2 / 27

Talk Outline

1. **Sensing (and JCAS) Capacity**
2. Sensing (and JCAS) Reliability

Communication Channel

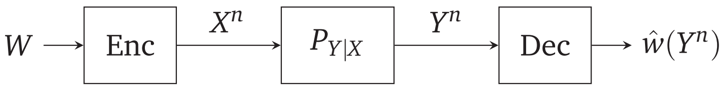

- R achievable if there exists (n, M, ϵ)-codes with

$$\frac{1}{n}\log M \to R \quad \text{and} \quad \epsilon \to 0$$

- Capacity: $C \triangleq$ maximum achievable rate

(Shannon'48)

$$C = \max_{P_X} I(X;Y)$$

- Concise and insightful. Can we do similar for JCAS?

Sensing Channel

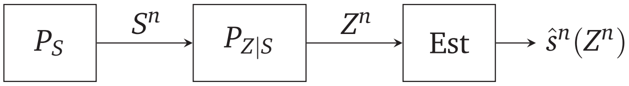

Models:

- Fixed random state: $S_i = \Theta$, for all i
- i.i.d. state: $S_i \sim S_j$ and $S_i \perp S_j$, for all $i \neq j$ **(this talk)**

i.i.d. state estimation:

- Point (sequence) estimate $\hat{s}^n = (\hat{s}_1, \hat{s}_2, \ldots, \hat{s}_n)$
- Additive (separable) distortion measure

$$d_n(s^n, \hat{s}^n) = \frac{1}{n}\sum_{i=1}^{n} d(s_i, \hat{s}_i)$$

- Excess or expected distortion criteria

$$\mathbb{P}\left[d_n\left(S^n, \hat{s}^n(Z^n)\right) \geq D\right] \quad \text{or} \quad \mathbb{E}\left[d_n\left(S^n, \hat{s}^n(Z^n)\right)\right]$$

5 / 27

Sensing Channel: List Estimation

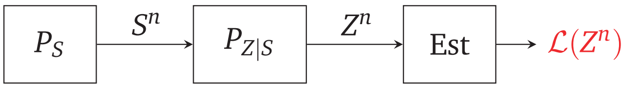

- L-list estimation: $\mathcal{L}(Z^n) \subseteq \mathcal{S}^n$ with $|\mathcal{L}(Z^n)| = L$
- Sensing error: state sequence not in list

$$\delta = \mathbb{P}\left[S^n \notin \mathcal{L}(Z^n)\right]$$

- Δ achievable if there exists (n, L, δ)-schemes with

$$\frac{1}{n}\log L \to \Delta \quad \text{and} \quad \delta \to 0$$

- Sensing Equivocation: $\Delta^\star \triangleq$ minimum achievable list rate

Theorem

$$\Delta^\star = H(S|Z)$$

6 / 27

Proof: Achievability

- Given that sensor observes z^n, select list as

$$\mathcal{L}(z^n) = \left\{ s^n : \frac{1}{n} \log \frac{1}{P(s^n|z^n)} \le H(S|Z) + \varepsilon \right\}$$

  List size

$$\begin{aligned} 1 &= \sum_{s^n \in \mathcal{S}^n} P(s^n|z^n) \\ &\ge \sum_{s^n \in \mathcal{L}(z^n)} P(s^n|z^n) \\ &\ge |\mathcal{L}(z^n)| \exp\{-n(H(S|Z) + \varepsilon)\} \end{aligned}$$

- Error probability: By the WLLN

$$\mathbb{P}\left[S^n \notin \mathcal{L}(Z^n)\right] = \mathbb{P}\left\{ \frac{1}{n} \log \frac{1}{P(S^n|Z^n)} > H(S|Z) + \varepsilon \right\} \to 0$$

7 / 27

Typical Set Intuition

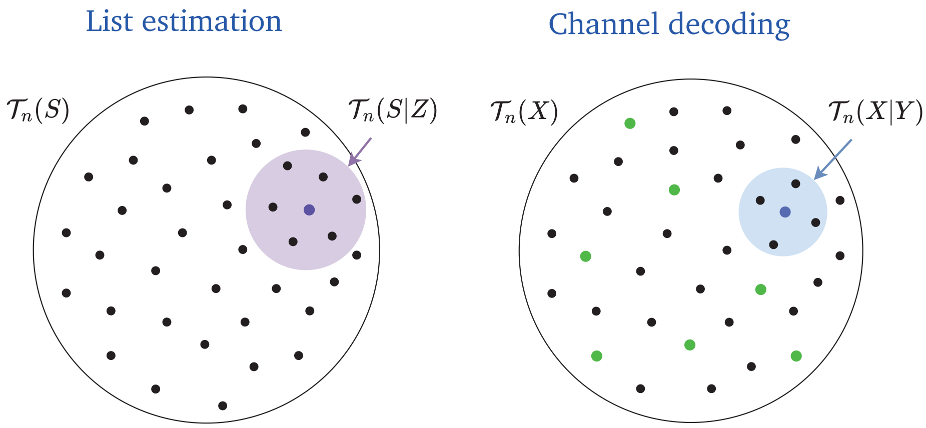

8 / 27

Proof: Converse

- Recall that $\delta = \mathbb{P}\left[S^n \notin \mathcal{L}(Z^n)\right]$
- Fano's inequality for lists (Kim et al.'08)

$$H(S^n|Z^n) \leq \log|\mathcal{L}(Z^n)| + h_b(\delta) + \delta \log \frac{|\mathcal{S}|^n}{|\mathcal{L}(Z^n)|}$$

- For small δ, the above implies

$$\begin{aligned} \log|\mathcal{L}(Z^n)| &\geq H(S^n|Z^n) - \varepsilon \\ &= H(S|Z) - \varepsilon \text{ (i.i.d. and DMC)} \end{aligned}$$

Sensing Channel: Active Probing

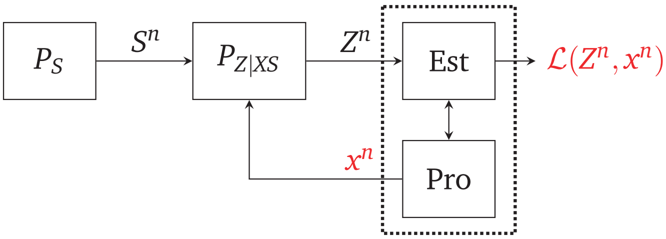

- Input cost constraint:

$$\frac{1}{n}\sum_{i=1}^{n} b(x_i) \leq B$$

- Type (empirical distribution) of x^n:

$$Q_{x^n}(a) = \frac{1}{n}\sum_{i=1} \mathbb{1}\left[x_i = a\right], \text{ for all } a \in \mathcal{X}$$

e.g. cost constraint: $\sum_{a\in\mathcal{X}} Q_{x^n}(a)b(a) \leq B$

Sensing Channel: Active Probing

- Achievable list rate:

$$\begin{aligned}\Delta(x^n) - \varepsilon &\le H(S^n|Z^n, X^n = x^n)\\ &= \frac{1}{n}\sum_{i=1}^{n} H(S_i|Z_i, X_i = x_i)\\ &= \sum_{x\in\mathcal{X}} Q_{x^n}(x) H(S|Z, X = x)\end{aligned}$$

- minimize w.r.t. Q_{x^n}, subject to $\sum_{x\in\mathcal{X}} Q_{x^n}(x) b(x) \le B$

$$\Delta^\star = \min_{P_X:\mathbb{E}[b(X)]\le B} H(S|Z, X)$$

No cost constraint:

$$\Delta^\star = \min_{x\in\mathcal{X}} H(S|Z, X = x)$$

11 / 27

Sensing Channel: Further Remarks

- Sensing Capacity: Define sensing rate as

$$\Gamma \triangleq H(S) - \Delta$$

Then sensing capacity given by

$$C_s = \max_{P_X:\mathbb{E}[b(X)]\le B} I(S; Z|X)$$

- Same results obtained under excess log-loss distortion

$$\delta = \mathbb{P}\left[\ell\left(S^n, \hat{P}(\cdot|Z^n)\right) \ge n\Delta\right]$$

where $\ell\left(s^n, \hat{P}(\cdot|z^n)\right) = -\log \hat{P}(s^n|z^n)$

- List est. $\iff$ Soft est. under log-loss (Shkel-Verdú'18)

12 / 27

JCAS Channel

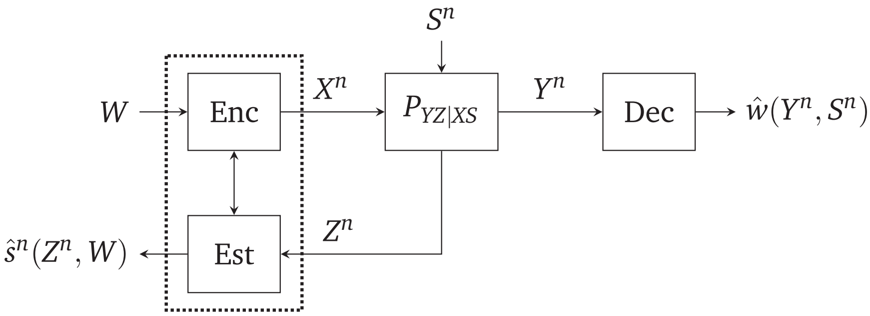

- State dependent channel
- Feed-forward: communication; and feedback: sensing
- Coupled by the same input (dual function)
- Introduce by (Kobayashi-Caire-Kramer'18)

13 / 27

JCAS Channel: List Estimation

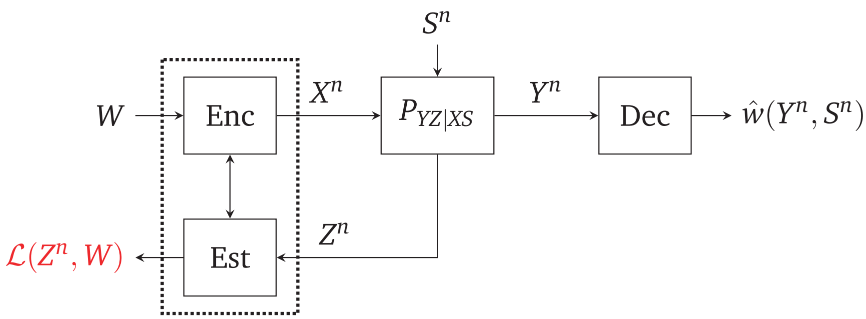

Theorem (H.J-Caire'24)

$$R \le I(X;Y|S) \quad \text{and} \quad \Delta \ge H(S|Z,X)$$

for some P_X s.t. $\mathbb{E}[b(X)] \le B$

Equivalently, $\Gamma \triangleq H(S) - \Delta$ leads to

$$R \le I(X;Y|S) \quad \text{and} \quad \Gamma \le I(S;Z|X)$$

14 / 27

Talk Outline

1. Sensing (and JCAS) Capacity
2. **Sensing (and JCAS) Reliability**

Reliability Function

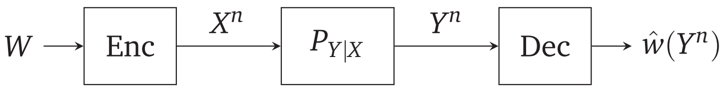

- (R, E) achievable if (as $n \to \infty$)

$$\frac{1}{n} \log M \to R \quad \text{and} \quad \frac{1}{n} \log \frac{1}{\epsilon} \to E$$

- Reliability function: maximum E for fixed R

$$E^\star(R) \triangleq \sup\{E : (R, E) \text{ is achievable}\}$$

(Fano'61, Gallager'65, Shannon et al.'67)

$$E_{\mathrm{r}}(R) \le E^\star(R) \le E_{\mathrm{sp}}(R)$$

Reliability Function: BSC

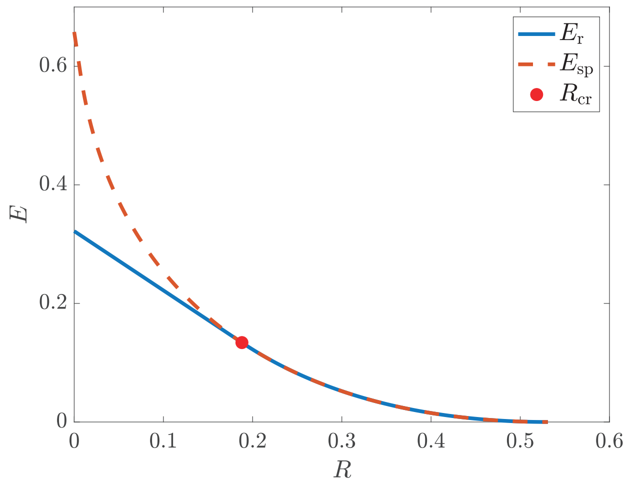

E.g. URLLC vs. Broadband

Next: do something similar for sensing and JCAS!

17 / 27

Sensing Reliability Function

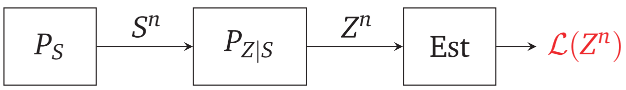

- (Δ, E_s) achievable if (as $n \to \infty$)

$$\frac{1}{n}\log L \to \Delta \quad \text{and} \quad \frac{1}{n}\log\frac{1}{\delta} \to E_s$$

- Sensing reliability function: maximum E_s for fixed Δ

$$E_s^\star(\Delta) \triangleq \sup\{E_s : (\Delta, E_s) \text{ is achievable}\}$$

To find $E_s^\star(\Delta)$, we'll take a small digression

18 / 27

Guessing Digression

- Determine S through sequence of inquiries

$$\text{“is } S = s_1\text{?”}$$
$$\text{“is } S = s_2\text{?”}$$
$$\vdots$$

  until answer is “yes”
- Guessing number (rank): $G(S)$
- Optimal guessing: $G^\star$ according to decreasing probability

(Arikan’96)

$$\mathbb{E}\left[G^\star(S)^\rho\right] \leq \exp\left(\rho H_{\frac{1}{1+\rho}}(S)\right)$$

Converse: $\mathbb{E}\left[G^\star(S)^\rho\right] \geq \exp\left(\rho H_{\frac{1}{1+\rho}}(S) - \rho \log(1 + \log|\mathcal{S}|)\right)$

19 / 27

Guessing Proof

$$G^\star(s) = \sum_{s' \in \mathcal{S}} \mathbb{1}\left[P(s') \geq P(s)\right] \leq \sum_{s' \in \mathcal{S}} \left(\frac{P(s')}{P(s)}\right)^\alpha$$

where $\alpha \geq 0$. Set $\alpha = \frac{1}{1+\rho}$, where $\rho \geq 0$

$$\begin{aligned}\mathbb{E}\left[G^\star(S)^\rho\right] &\leq \sum_{s \in \mathcal{S}} P(s) \left(\sum_{s' \in \mathcal{S}} \left(\frac{P(s')}{P(s)}\right)^\alpha\right)^\rho \\ &= \left(\sum_{s \in \mathcal{S}} P(s)^{\frac{1}{1+\rho}}\right)^{1+\rho} \\ &\triangleq \exp\left(\rho H_{\frac{1}{1+\rho}}(S)\right)\end{aligned}$$

Corollary (i.i.d.)

$$\mathbb{E}\left[G^\star(S^n)^\rho\right] \leq \exp\left(n\rho H_{\frac{1}{1+\rho}}(S)\right)$$

20 / 27

Guessing with side information

- Guess S given that Z is available
- Given $Z = z$, guess $G^\star(s|z)$ according to $P(s|z)$

$$\mathbb{E}\left[G^\star(S|Z)^\rho\right] = \sum_{z\in\mathcal{Z}} P(z)\mathbb{E}\left[G^\star(S|z)^\rho\right]$$
$$\leq \sum_{z\in\mathcal{Z}} P(z)\left(\sum_{s\in\mathcal{S}} P(s|z)^{\frac{1}{1+\rho}}\right)^{1+\rho}$$
$$\triangleq \exp\left(\rho H_{\frac{1}{1+\rho}}(S|Z)\right)$$

(Arimoto's cond. Rényi entropy)

Corollary (i.i.d.)

$$\mathbb{E}\left[G^\star(S^n|Z^n)^\rho\right] \leq \exp\left(n\rho H_{\frac{1}{1+\rho}}(S|Z)\right)$$

21 / 27

Back to sensing

- Optimal list: L-MAP list

$$\text{Given } Z = z,\ \mathcal{L}^\star(z) = \{L \text{ highest posterior realizations}\}$$
$$\iff \mathcal{L}^\star(z) = \{s' \in \mathcal{S} : G^\star(s'|z) \leq L\}$$

- Error probability bound:

$$\mathbb{P}\left[S \notin \mathcal{L}^\star(Z)\right] = \mathbb{P}\left[G^\star(S|Z) > L\right]$$
$$\text{(tilting+Markov)} \quad \leq \frac{1}{L^\rho}\mathbb{E}\left[G^\star(S|Z)^\rho\right]$$
$$\text{(Arikan'96)} \quad \leq \frac{1}{L^\rho}\exp\left(\rho H_{\frac{1}{1+\rho}}(S|Z)\right)$$

Achievability

$$\frac{1}{n}\log\frac{1}{\mathbb{P}\left[S^n \notin \mathcal{L}^\star(Z^n)\right]} \geq \sup_{\rho\geq 0}\rho\left(\Delta - H_{\frac{1}{1+\rho}}(S|Z)\right)$$

22 / 27

Sensing Reliability Function

Converse (through method of types)

$$\limsup_{n\to\infty} \frac{1}{n} \log \frac{1}{\mathbb{P}\left[S^n \notin \mathcal{L}(Z^n)\right]} \leq \min_{Q_{\tilde{S}\tilde{Z}}:H(\tilde{S}|\tilde{Z})\geq\Delta} D(Q_{\tilde{S}\tilde{Z}}\|P_{SZ})$$

$$\text{(Bunte-Lapidoth'13)} = \sup_{\rho\geq 0} \rho\left(\Delta - H_{\frac{1}{1+\rho}}(S|Z)\right)$$

Theorem

$$E_s^\star(\Delta) = \sup_{\rho\geq 0} \rho\left(\Delta - H_{\frac{1}{1+\rho}}(S|Z)\right)$$

With Probing:

$$E_s^\star(\Delta) = \sup_{\rho\geq 0} \max_{P_X} \rho\left(\Delta - H_{\frac{1}{1+\rho}}(S|Z,X)\right)$$

23 / 27

Sensing Reliability Function: BS-BSC

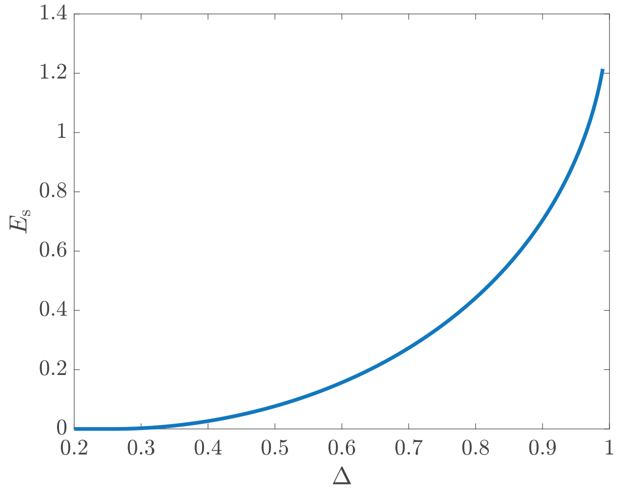

Bernoulli-q i.i.d. state sequence observed through BSC-p

24 / 27

JCAS: Rate-Reliability Trade-Off

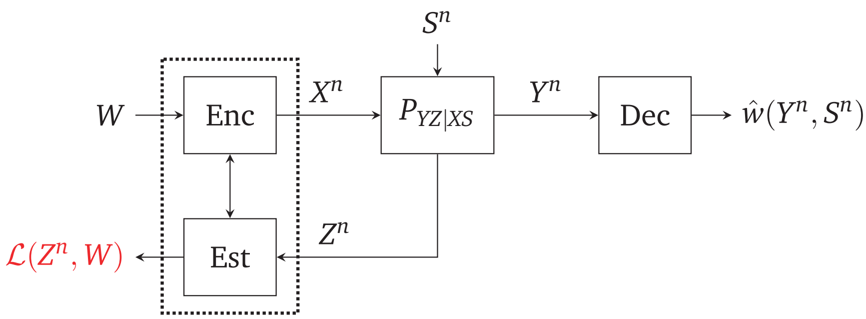

Corollary: All non-negative (R, E, Δ, E_s) satisfying

$$E \leq E_0(\varrho, P_X) - \varrho R$$
$$E_s \leq \rho\Delta - E_{0,s}(\rho, P_X)$$

for some P_X, $\rho \geq 0$ and $\varrho \in [0, 1]$, are achievable

25 / 27

Summery and Remarks

- Basic Shannon-theoretic framework for sensing and JCAS
- Sensing capacity and JCAS rate trade-offs
- Sensing reliability and JCAS rate-reliability trade-offs
- Method of types for achievability: universal estimation

Food for thought:

- Clean results but not (perhaps at all!) practical
- **States with memory?!**
- Continuous alphabets
- Distributed models and Networks

26 / 27

Thank you!

h.joudeh@tue.nl

Supported by the ERC Starting Grant IT-JCAS

Neural Networks in Communication Transceivers

Boris Karanov

Department of Electrical Engineering, Eindhoven University of Technology, Netherlands

Recently, end-to-end deep learning-based autoencoder systems where the complete transceiver is implemented as a single neural network (NN) were demonstrated, both numerically and on experimental test-beds, as a viable alternative to conventional DSP for both the optical and wireless communication links. In particular, it has been shown that carefully chosen autoencoder architectures have the potential to provide performance improvement as well as complexity reduction. Nevertheless, one of the challenges in designing NN-based transceivers for economical communication links lies in developing simple yet efficient neural network architectures and optimization procedures, thus circumventing a substantial computational complexity overhead.

References

[1] O. Simeone, “A very brief introduction to machine learning with applications to communication systems,” IEEE Trans. Cogn. Commun. Netw., vol. 4, no. 4, pp. 648-664.

[2] T. O’Shea and J. Hoydis, “An introduction to deep learning for the physical layer,” IEEE Trans. Cogn. Commun. Netw., vol. 3, no. 4, pp. 563-575, 2017.

[3] S. Dörner, S. Cammerer, J. Hoydis and S. ten Brink, “Deep learning based communication over the air,” IEEE J. Sel. Topics Signal Process., vol. 12, no. 1, pp. 132-143, 2018.

[4] B. Karanov, M. Chagnon, F. Thouin, T. A. Eriksson, H. Bülow, D. Lavery, P. Bayvel and L. Schmalen, “End-to-end deep learning of optical fiber communications,” IEEE/Optica J. Lightw. Technol., vol. 36, no. 20, pp. 4843-4855, 2018.

[5] F. A. Aoudia and J. Hoydis, “Model-free training of end-to-end communication systems,” IEEE J. Sel. Areas Commun., vol. 37, no. 11, pp. 2503-2516, 2019.

[6] B. Karanov, M. Chagnon, V. Aref, D. Lavery, P. Bayvel and L. Schmalen, “Concept and Experimental demonstration of optical IM/DD end-to-end system optimization using a generative model,” in Proc. Optical Fiber Communications Conference and Exhibition (OFC), 2020, pp. 1-3.

Neural Networks in Communication Transceivers

27TH SEPTEMBER 2024, MATHEMATICS FOR INNOVATION IN INFORMATION AND COMMUNICATION TECHNOLOGY, FUKUOKA, JAPAN

Boris Karanov

Eindhoven University of Technology

Recent success of neural networks

https://www.cs.toronto.edu/~kriz/cifar.html

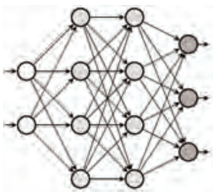

Recent success of neural networks

https://benchmarks.ai/cifar-10

- Neural networks surpass human capabilities in fields such as image processing
- Almost perfect recognition

1 Neural Networks in Communication Transceivers

TU/e

Communication system design

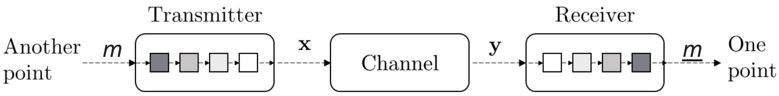

- "Reproduce reliably at one point a message selected at another point" [Shannon, 1948]
- Design transmitter and receiver to reliably transmit a message over the channel

2 Neural Networks in Communication Transceivers

TU/e

Communication system design

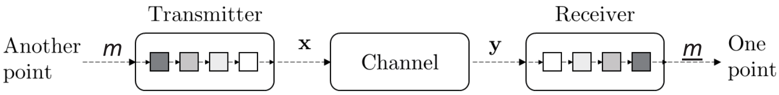

- "Reproduce reliably at one point a message selected at another point" [Shannon, 1948]
- Design transmitter and receiver to reliably transmit a message over the channel
- **Conventional:** separate processing blocks responsible for individual transceiver tasks (coding, modulation, pulse-shaping, equalization, etc.)

Communication system design

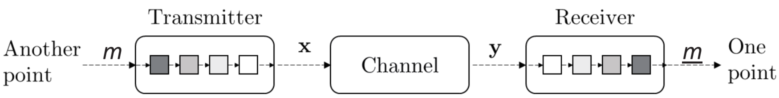

- "Reproduce reliably at one point a message selected at another point" [Shannon, 1948]
- Design transmitter and receiver to reliably transmit a message over the channel
- **Conventional:** separate processing blocks responsible for individual transceiver tasks (coding, modulation, pulse-shaping, equalization, etc.)
  - Model-based – relies on full channel knowledge
  - Absence of optimal computationally feasible algorithms for some practically relevant nonlinear channels

End-to-end neural network-based transceiver

- Fundamentally reconsider communication system design
- Optimization of transmitter and receiver in a single process
- Idea of learnable communication systems*
- **Deep learning** for **transceiver optimization** over the channel constraints
- **Auto-encoder** which minimizes the end-to-end error

* T. O'Shea and J. Hoydis, ``An introduction to deep learning for the physical layer,'' IEEE Trans. Cogn. Commun. Netw., vol. 3, no. 4, pp. 563-575, 2017.

TU/e

End-to-end neural network-based transceiver

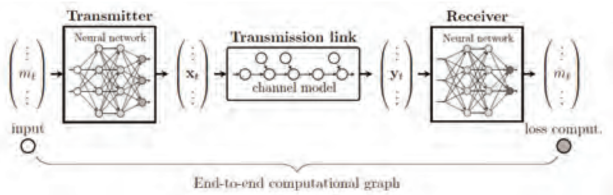

- Complete chain of transmitter, channel model and receiver implemented as an **end-to-end computational graph**
- Achieved by using differentiable transmission model and NN-based transceiver

TU/e

End-to-end neural network-based transceiver

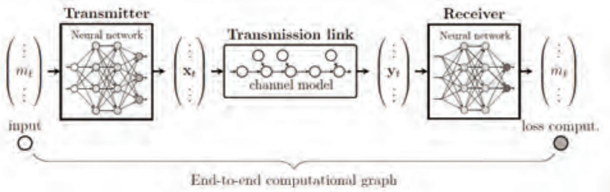

- Complete chain of transmitter, channel model and receiver implemented as an **end-to-end computational graph**
- Achieved by using differentiable transmission model and NN-based transceiver
- Message sequences encoded by Tx NN and decoded by Rx NN

TU/e

End-to-end neural network-based transceiver

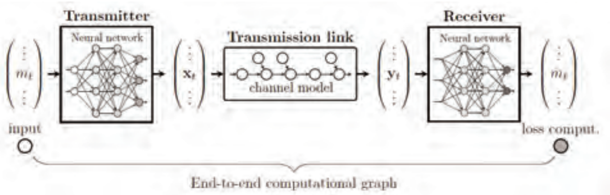

- Complete chain of transmitter, channel model and receiver implemented as an **end-to-end computational graph**
- Achieved by using differentiable transmission model and NN-based transceiver
- Message sequences encoded by Tx NN and decoded by Rx NN
- Cross-entropy loss computed between the transmitted and received messages
- Optimization via **backpropagation** and **gradient descent** for minimizing the loss, e.g. the message error rate

TU/e

End-to-end NN transceiver in optical fiber systems

- Waveform channel

$$\frac{\partial q(z,t)}{\partial z} = -\frac{\alpha}{2}q(z,t) - j\frac{\beta_2}{2}\frac{\partial^2 q(z,t)}{\partial t^2} + j\gamma|q(z,t)|^2 q(z,t)$$

- Nonlinearity and chromatic dispersion
- Transmitter NN transforms messages into **digital waveform** samples
- Received waveform samples decoded by the receiver NN

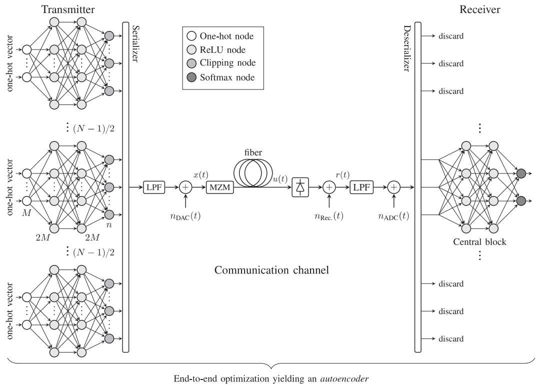

* B. Karanov, M. Chagnon, F. Thouin, T. A. Eriksson, H. Bulow, D. Lavery, P. Bayvel, and L. Schmalen, "End-to-end deep learning of optical fiber communications," Journal of Lightwave Technology, vol. 36, no. 20, pp. 4843–4855, 2018

End-to-end NN transceiver in optical fiber systems

- Transmitter NN transforms messages into **digital waveform** samples
- Received waveform samples decoded by the receiver NN

$$\mathbf{p}_t = f_{\text{Dec.-FFNN}}\left(\mathcal{H}\left\{\ldots, f_{\text{Enc.-FFNN}}\left(\mathbf{1}_{m,t}\right), \ldots\right\}\right)$$

$$\mathcal{L}(\theta) = \ell(\mathbf{1}_{m,t}, \mathbf{p}_t)$$

$$\ell(\mathbf{x},\mathbf{y}) = -\sum_i x_i \log(y_i)$$

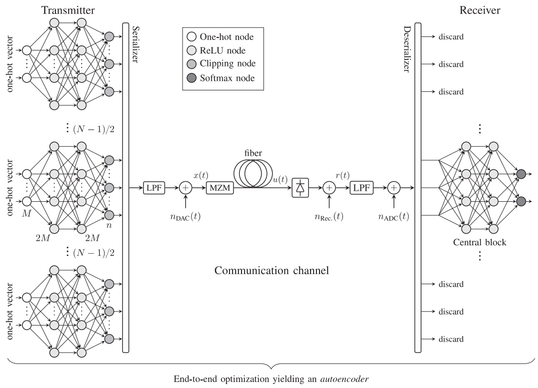

* B. Karanov, M. Chagnon, F. Thouin, T. A. Eriksson, H. Bulow, D. Lavery, P. Bayvel, and L. Schmalen, "End-to-end deep learning of optical fiber communications," Journal of Lightwave Technology, vol. 36, no. 20, pp. 4843–4855, 2018

End-to-end NN transceiver in optical fiber systems

- Transmitter NN transforms messages into **digital waveform** samples
- Received waveform samples decoded by the receiver NN

$$\mathbf{p}_t = f_{\text{Dec.-BRNN}}\left(\mathcal{H}\left\{f_{\text{Enc.-BRNN},t}(\ldots,\mathbf{1}_{m,t},\ldots)\right\}\right)$$

$$\mathcal{L}(\theta) = \ell(\mathbf{1}_{m,t}, \mathbf{p}_t)$$

$$\ell(\mathbf{x},\mathbf{y}) = -\sum_i x_i \log(y_i)$$

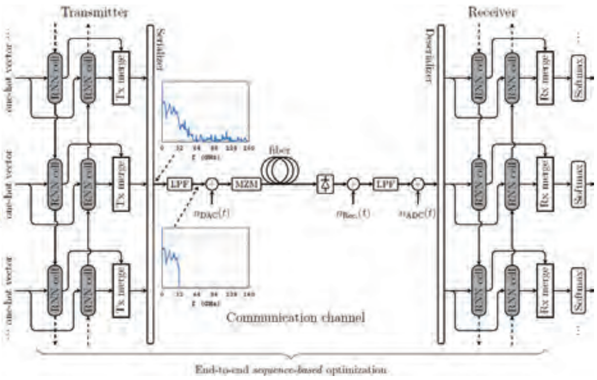

* B. Karanov, D. Lavery, P. Bayvel and L. Schmalen, ``End-to-end optimized transmission over dispersive intensity-modulated channels using bidirectional recurrent neural networks,'' Opt. Express, vol. 27, no. 14, pp. 19650-19663, 2019.

TU/e

Implemented on experimental test-bed

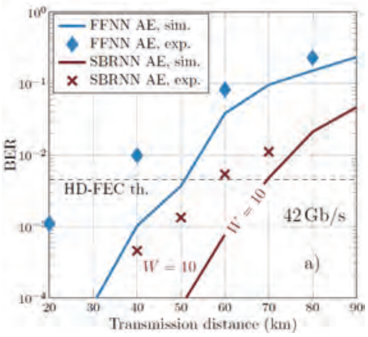

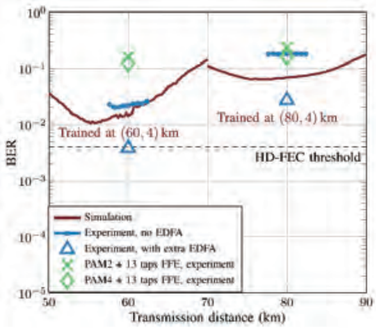

TU/e

Neural network-based receiver

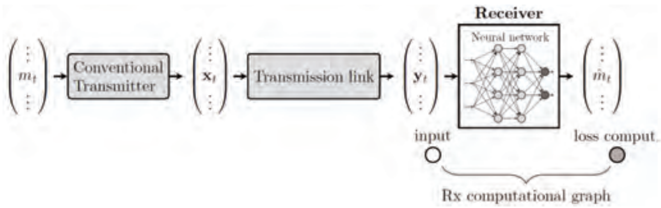

- Conventional transmitter scheme (e.g. PAM with RC filter)
- Can be implemented directly with real-world transmission data
- Labelled training database of received signals and associated messages

$$\mathcal{L}(\theta) = \ell(m_t, f_{\text{RX-FFNN}}((\mathbf{y}_{t-\frac{W-1}{2}}, \ldots, \mathbf{y}_t, \ldots, \mathbf{y}_{t+\frac{W-1}{2}})))$$

Performance

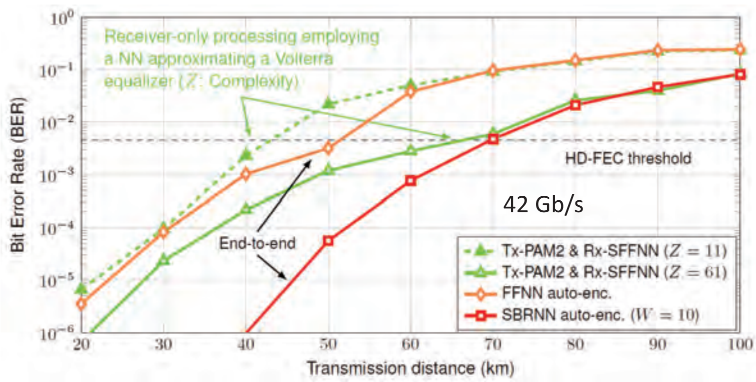

Performance – Symbol detection in linear ISI and AWGN

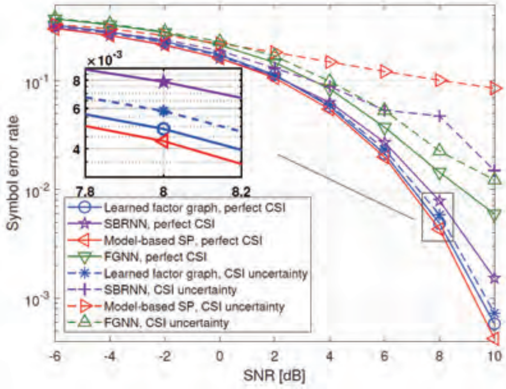

$$y_t = \sum_{l=1}^{L} h_l x_{t-l+1} + z_t$$

* N. Shlezinger, N. Farsad, Y. C. Eldar and A. J. Goldsmith, ``Learned factor graphs for inference from stationary time sequences,'' IEEE Trans. Signal Process., vol. 70, pp. 366-380, 2022.

Neural Network-aided classical systems

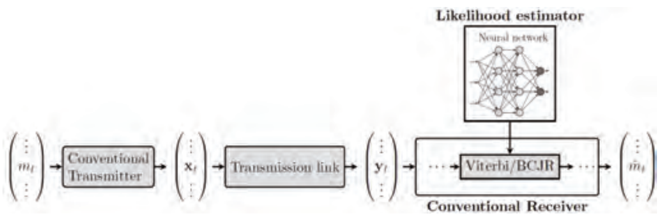

- Data-driven perspective on classical algorithms via NN
- Preserves structure of established optimal algorithms
- Circumvents the need for full CSI

Neural Network-aided classical systems

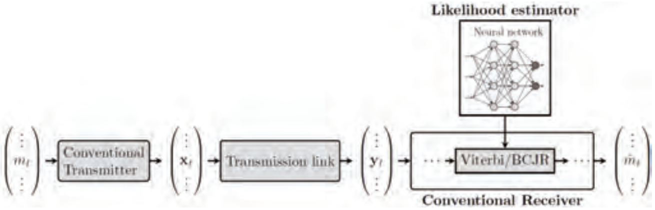

$$\gamma_t(y_t, s_{t-1}, s_t) = p(s_t|s_{t-1})p(y_t|s_t)$$

$$\alpha_t(s_t) = \sum_{s_{t-1}} \alpha_{t-1}(s_{t-1})\gamma_t(y_t, s_{t-1}, s_t)$$

$$\beta_t(s_t) = \sum_{s_{t+1}} \gamma_t(y_{t+1}, s_t, s_{t+1})\beta_{t+1}(s_{t+1})$$

Data-driven symbol detection – linear ISI and impulse noise

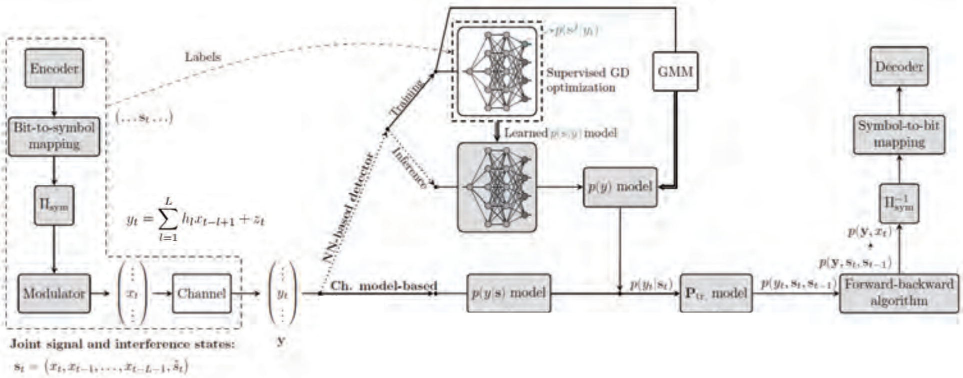

* B. Karanov, C.-H. Chen, Y. Wu, A. Young, W. v. Houtum, ``Data-driven symbol detection for intersymbol interference channels with bursty impulsive noise,'' https://arxiv.org/abs/2405.10814

Performance

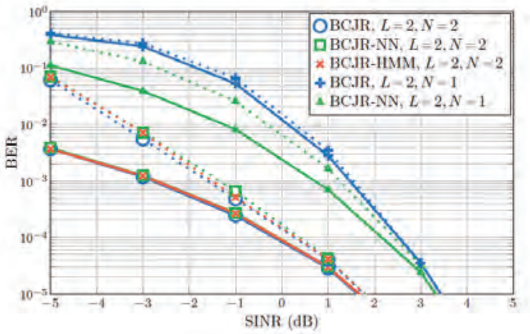

Conclusions

- Neural networks suitable for optical fibre systems where optimal transmitter-receiver pair is unknown or computationally prohibitive to implement
- Data-driven transceiver tailored for communication over the dispersive nonlinear channel
- Reach increase or enhanced data rate compared to state-of-the-art DSP benchmarks

Conclusions

- Neural networks suitable for optical fibre systems where optimal transmitter-receiver pair is unknown or computationally prohibitive to implement
- Data-driven transceiver tailored for communication over the dispersive nonlinear channel
- Reach increase or enhanced data rate compared to state-of-the-art DSP benchmarks
- Integrating NN into classical algorithms can lead to complexity reductions
- Further complexity reduction
- Efficient hardware implementation

16 Neural Networks in Communication Transceivers TU/e

Thank you for your attention!

Neural Networks in Communication Transceivers TU/e

Three-Dimensional Spatial Cell Configuration in Mobile Communications

- Sharing the Same Frequency Band between Ground Cells and Aerial Cells -

Teruya FUJII

SoftBank Corp.

Tokyo Institute of Technology

To make mobile communication systems available even in the sky, a “three-dimensional spatial cell configuration” has been proposed. This configuration uses beamforming technology for base station antennas to spatially divide ground cells and sky cells, allowing the same frequency to be shared between the ground and the sky. In this paper, we first introduce our proposed 2x2 orthogonal polarization MU-MIMO (Multiple-Input Multiple-Output) canceller using orthogonal polarization antennas at the base station to improve communication quality, particularly for sky cells. Next we present the communication quality when applying the proposed 2x2 orthogonal polarization MU-MIMO canceller in a cellular environment composed of multiple cells.

References

[1] T. Fujii, et al, “From 2D Ground Cell Configuration to 3D Space Cell Configuration in Mobile Communication”, IEICE technical report, J. IEICE, Vol.104, No. 7, pp.712-721, 2021-07 (in Japanese).

[2] T. Tsuji, et al, “Frequency sharing between ground and sky cells by applying beamforming and MU-MIMO canceller in mobile communication”, IEICE technical report RCS 2024-11, Apr. 2024-04 (in Japanese).

[3] T. Tsuji, et al, “A study on frequency sharing between ground and sky cells by applying beamforming and orthogonal polarization MU-MIMO canceller for cellular mobile system, IEICE technical report, RCS 2024-94, Jul. 2024 (in Japanese).

Three-Dimensional Spatial Cell Configuration
in Mobile Communications
- Sharing the Same Frequency Band between Ground Cells and Aerial Cells -

2024/09/27
SoftBank Corp.
Tokyo Institute of Technology
Teruya FUJII

1

Aerial Service Area by use of Drone Mobile Communication

•Drone/Flying vehicle need high speed radio communications in sky.
•Construct high speed aerial service areas by use of the existing mobile base stations
(Mobile Communication 3D Cell Configuration)

【Characteristics】
- Use of the same terminal as ground communication
- Use of the same frequency as ground communication

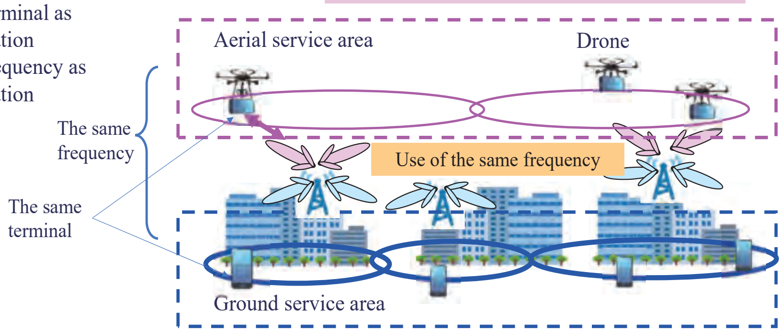

Problems of mobiles and drones by using the same frequency

【Problem】
•Due to a straight sight between drone terminal and base station(BS), there are interferences between them.
•Due to the same frequency use, there are receive signal interferences between drone terminals(DT) and mobile terminals(MT) in a cell.
【Study】
•To solve the problems caused by drone terminal introductions, we need to have interference suppression technologies.

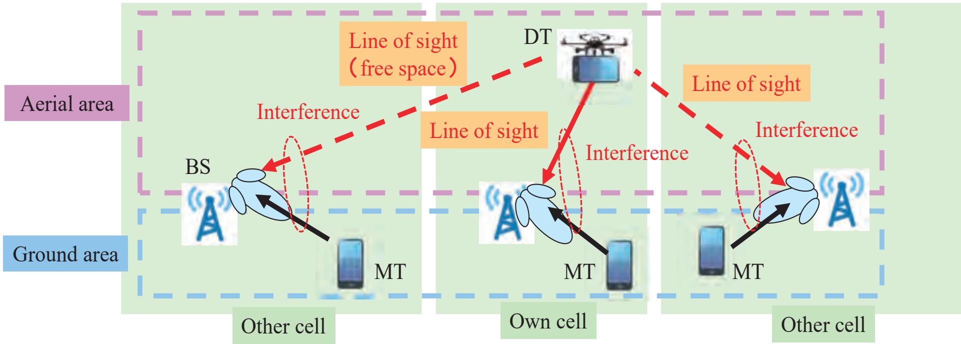

3

Current Studies

- Radio Transmission
  MIMO(Multi-Input Multi-Output) transmission
- Interference Suppression Technologies
  •Base Station： Adaptive Beam-Forming
  •Terminal ： Adaptive Power Control

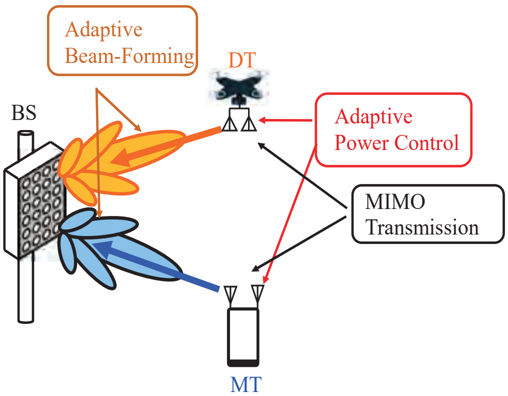

MIMO Transmission

MIMO(Multi-Input Multi-Output) Transmit and Receive Signals

Two different signals are simultaneously transmitted by two antennas of a terminal.
Communication capacity increases two-times by the same frequency.

SIMO (Single-Input Multi-Output)

Communication Capacity: 1

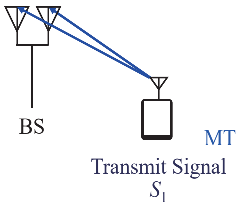

MIMO (Single-Input Multi-Output)

Communication Capacity: 2

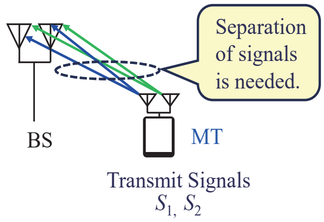

MIMO Signal Separation

Signal separation by singular value decomposition (SVD)

Suppress interferences and orthogonalize signals among antenna by SVD at Propagation path response H.

Propagation path response ↓ ; Singular value (diagonal entries)

$$W_{SVD,R}\ H\ W_{SVD,T} = \begin{bmatrix} \sqrt{\lambda_1} & 0 \\ 0 & \sqrt{\lambda_2} \end{bmatrix} = \tilde{H}$$

$W_{SVD,R}$: MIMO receive weight; $W_{SVD,T}$: MIMO transmit weight

Receive signal Y

$$Y = W_{SVD,R}\ H\ W_{SVD,T}\ S = \begin{bmatrix} \sqrt{\lambda_1} & 0 \\ 0 & \sqrt{\lambda_2} \end{bmatrix} = \begin{bmatrix} \sqrt{\lambda_1} S_1 \\ \sqrt{\lambda_2} S_2 \end{bmatrix}$$

↑ Transmit signal

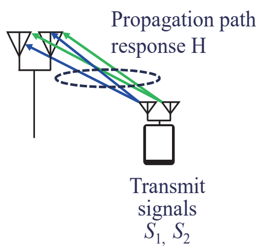

Adaptive Beam Forming

Base station antenna beams toward MT and DT.

- Increase desired signal power
- Suppress interference signal power

} Significantly improve communication quality

Fixed Beam forming

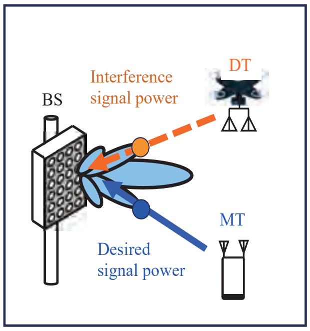

Adaptive Beam forming

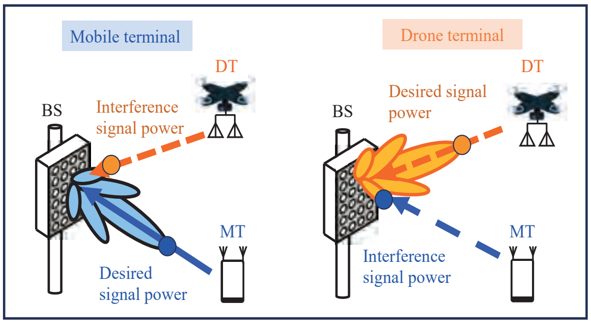

Adaptive Transmit Power Control

Adaptively control transmit powers so that receive signal powers at a base station would not exceed a fixed value Γ[dB].

- Required receive signal powers at a mobile terminal : Γ_M (dB)
- Required receive signal powers at a drone terminal : Γ_D (dB)

Transmit signal power reduction W_P (dB)

- Receive signal power of mobile terminal at a base station E_M (dB)
  $W_P = \max(E_M - \Gamma_M ,0)$ (dB)
- Receive signal power of drone terminal at a base station E_D (dB)
  $W_P = \max(E_D - \Gamma_D ,0)$ (dB)

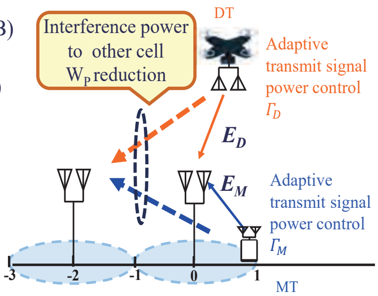

Receive Signal Demodulation

Demodulated receive signal

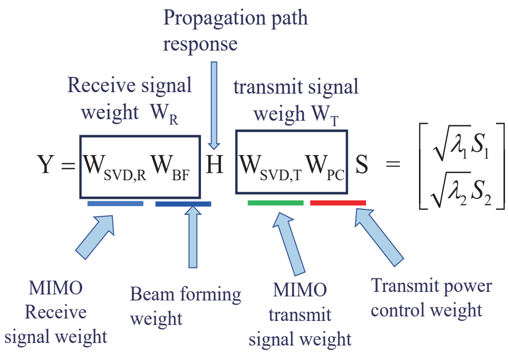

$$Y = W_{SVD,R}\, W_{BF}\, H\, W_{SVD,T}\, W_{PC}\, S = \begin{bmatrix} \sqrt{\lambda_1} S_1 \\ \sqrt{\lambda_2} S_2 \end{bmatrix}$$

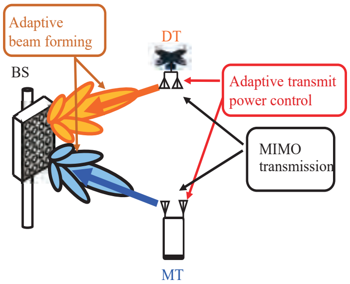

Current Study of System Configuration

Radio Transmission Method

MIMO(Multi-Input Multi-Output) transmission

Interference Suppression Technology

BS： Adaptive beam forming

Terminal ： Adaptive transmit power control (ATPC)

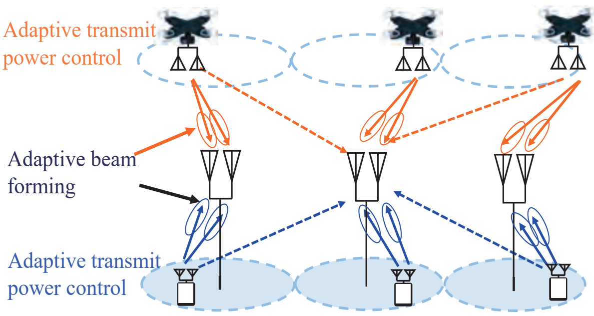

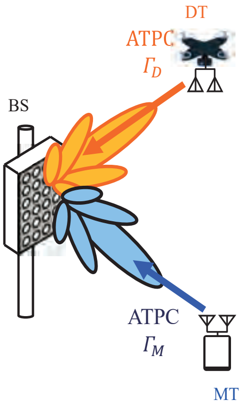

10

Problem of Current Study (I)

When an arrival angle of drone terminal is close to that of mobile terminal, side lobe interference at base station antenna is increased.

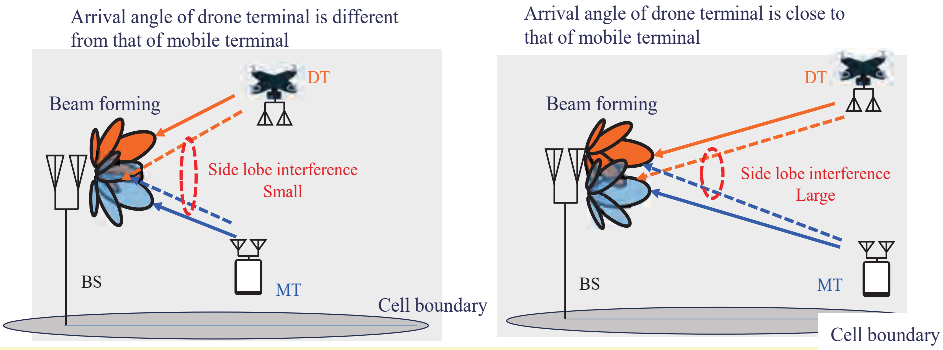

When an arrival angle of signals from drone and mobile terminals to BS is getting close, side lobe interferences of beam forming are not controlled so that communication quality of drone and mobile terminals would be significantly reduced. Impossible for simultaneous use of drone and mobile terminals.

11

Interference Suppression between Drone and Mobile Terminals by Beam Forming

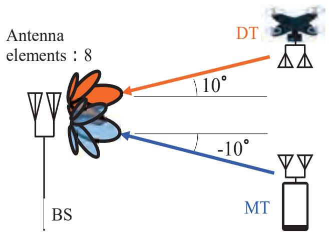

Current Receive Signal Model

$$Y = W_B H W_{PC} S$$

Beam forming Weight

Transmit Power Control Weight

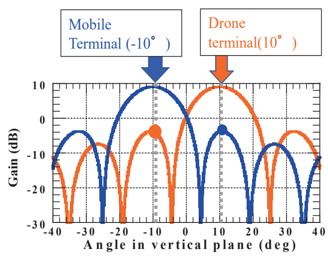

Problem of Current Study (II)

Problem due to MIMO of drone terminal

Two different signals are simultaneously sent by two antennas of a terminal. Communication Capacity increases two-times by the same frequency.

【Condition of two-times communication capacity】

Spatial correlation ρ of base station receive antennas (2 antennas) would be ≒0

Transmit and receive antenna are non-line of sight (Spatial correlation ρ≒0)

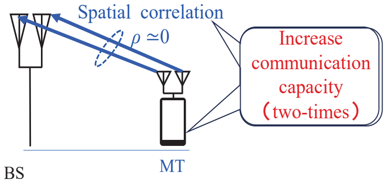

Transmit and receive antenna are line of sight (Spatial correlation ρ≒1)

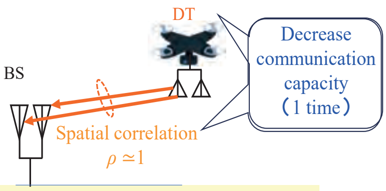

Even with MIMO, the capacity of "drone terminals" does not double due to the impact of spatial correlation between base station antennas.

13

Proposed Interference Suppression between Drone and Mobile terminals (MU-MIMO Canceller)

Current transmit and receive signals model

$$\mathbf{Y} = \mathbf{W}_{BF}\,\mathbf{H}\,\mathbf{W}_{PC}\,\mathbf{S}$$

$\mathbf{W}_{BF}$: Beam forming weight; $\mathbf{W}_{PC}$: Transmit power control weight

Proposed transmit and receive signals model

$$\mathbf{Y} = \mathbf{W}_{BD}\,\mathbf{W}_{BF}\,\mathbf{H}\,\mathbf{W}_{PC}\,\mathbf{S}$$

$\mathbf{W}_{BD}$: Interference Suppression Weight; $\mathbf{W}_{BF}$: Beam forming weight; $\mathbf{W}_{PC}$: Transmit power control weight

Block Diagonalization $\mathbf{W}_{BD}$

- Compute null weight $\mathbf{W}_{BD}$ that makes interference among terminals zero by using block diagonalization.
- Suppress interferences among terminals by superposing null weight $\mathbf{W}_{BD}$ receiving signal $\mathbf{H}\,\mathbf{W}_{PC}$

$$\mathbf{W}_{BD}(\mathbf{W}_{BF}\mathbf{H}\mathbf{W}_{PC}) = \begin{bmatrix} \mathbf{H}_{BD1} & \mathbf{0}_{2\times 2} \\ \mathbf{0}_{2\times 2} & \mathbf{H}_{BD2} \end{bmatrix}$$

Interference suppression weight $\mathbf{W}_{BD}$ is unitary, and does not increase noise.

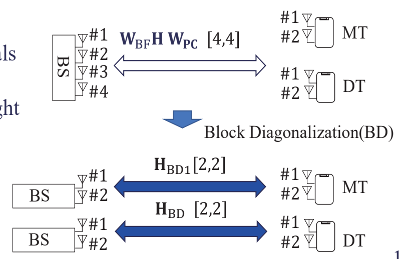

14

Proposed MU-MIMO Canceller

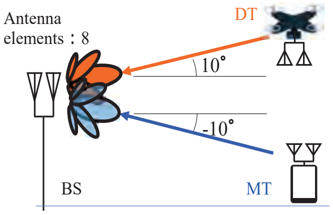

Proposed receive signal model

$$\mathbf{Y} = \mathbf{W_{BD}}\ \mathbf{W_{BF}}\ \mathbf{H}\ \mathbf{W_{PC}}\ \mathbf{S}$$

Interference suppression weight

Beam forming weight

Transmit power control weight

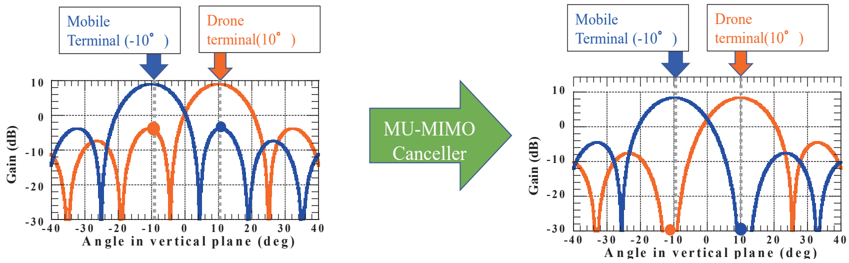

15

Propose Orthogonal Polarization MIMO

Applying 2x2 orthogonal polarization MIMO to reduce spatial correlation caused by line of sight propagation between transmission and reception.

By using orthogonal polarization transmission and reception, the correlation between base station antennas in line of sight propagation can be reduced to approximately $\rho \simeq 0$.

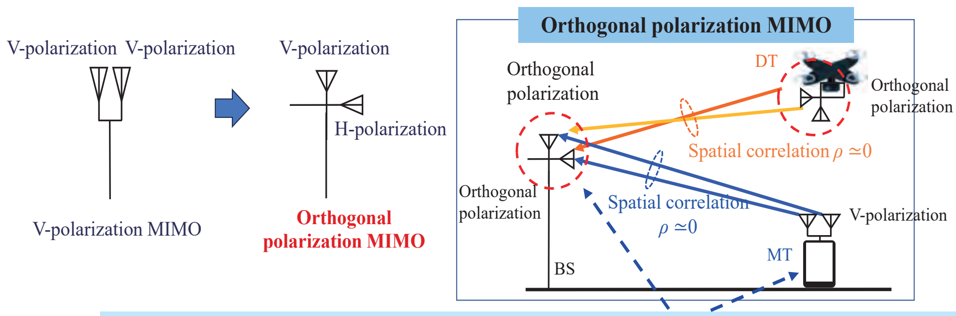

The receive power of the horizontally polarized antennas at the base station (V⇒H) decreases, causing a reduction in the MIMO communication quality of the mobile terminals.

45° Rotated Orthogonal Polarization MIMO

To improve the MIMO communication quality of ground terminals, the orthogonal polarization MIMO antennas at the base station are rotated by 45 degrees.

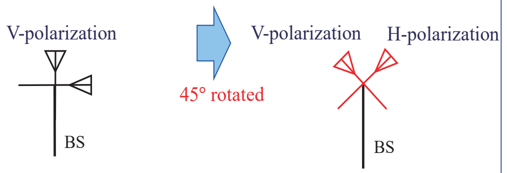

Base station orthogonal polarization MIMO

Base station 45° rotated orthogonal polarization MIMO

45° rotated orthogonal polarization MIMO

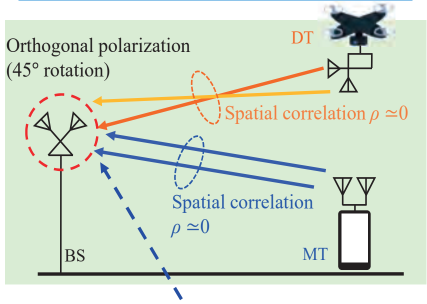

The receive power of the orthogonal polarization antennas at the base station becomes equal and suppressing the reduction in MIMO communication quality of mobile terminals.

45° Rotated Orthogonal Polarization MIMO

Channel response $\mathbf{H}_{X,V}$ of mobile terminal.

$$\mathbf{H}_{X,V} = \begin{bmatrix} h_{VV11} & h_{VV12} \\ h_{HV21} & h_{HV22} \end{bmatrix}$$

V-polarization MIMO

Orthogonal polarization MIMO

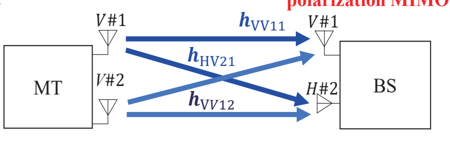

Rotation matrix transformation $\mathbf{W}_{Rotate}$ with a rotation of θ

$\mathbf{W}_{Rotate}\mathbf{H}_{X,V}$

Channel response $\mathbf{H}_{X,X}$ of drone terminal.

$$\mathbf{H}_{X,X} = \begin{bmatrix} h_{VV11} & h_{VH12} \\ h_{HV21} & h_{HH22} \end{bmatrix}$$

Orthogonal polarization MIMO

Orthogonal polarization MIMO

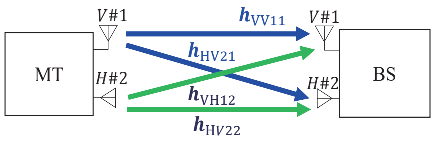

Rotation matrix transformation $\mathbf{W}_{Rotate}$ with a rotation of θ

$\mathbf{W}_{Rotate}\mathbf{H}_{X,X}$

Rotation matrix

$$\mathbf{W}_{Rotate} = \begin{bmatrix} \cos\theta & \sin\theta \\ -\sin\theta & \cos\theta \end{bmatrix} = \frac{1}{\sqrt{2}}\begin{bmatrix} 1 & -1 \\ 1 & 1 \end{bmatrix} \quad (\theta = 45°)$$

Received Signal of 45° Rotated Orthogonal Polarization Beam Forming MIMO Canceller

$$\begin{bmatrix} \tilde{H}_{BD1} & 0 \\ 0 & \tilde{H}_{BD2} \end{bmatrix} S = W_{SVD,R} \, W_{BD} \, W_{BF} \, W_{Rotate} \, H \, W_{SVD,T} \, W_{PC} \, S$$

Rotation matrix

Transmit signals

SVD receive weight

Interference suppression weight

Beam forming weight

SVD Transmit weight

Transmit power control weight

Receive signal of mobile terminal

$$\tilde{H}_{BD1} = \begin{bmatrix} \sqrt{\lambda_{M1}} & 0 \\ 0 & \sqrt{\lambda_{M2}} \end{bmatrix}$$

Receive signal of drone terminal

$$\tilde{H}_{BD2} = \begin{bmatrix} \sqrt{\lambda_{D1}} & 0 \\ 0 & \sqrt{\lambda_{D2}} \end{bmatrix}$$

Orthogonal polarization antennas, adaptive beam forming MU-MIMO cancellers and adaptive transmission power control, can convert each signal of mobile terminals and drone terminals into signals w/o interference.

19

System Evaluation

Evaluate the "Orthogonal Polarization MU-MIMO Canceller," which integrates MU-MIMO cancellers and orthogonal polarization MIMO.

Cell model

-Linear model (Cell radius 1km)

-Height of mobile terminal h_M=0m, Height of drone terminal h_D=100m

-Mobile and drone terminals are uniformly distributed within each cells.

Base station Antenna(orthogonal polarization antenna)

- Height of base station antenna h_b=50m
- Number of elements N_A=8, Element spacing/wavelength=0.7

Transmit power of mobile terminals and drone terminals

- Set the transmission power such that the receive SNR at the cell boundary for mobile terminals is 20 dB.

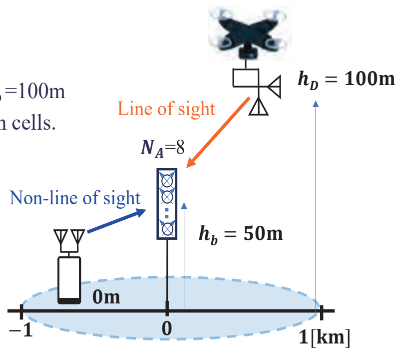

20

Base Station Antenna Configuration

Current System

- Configured with two V-polarization base station antennas sufficiently spaced apart horizontally.
- Number of V-polarized antenna elements: 8 in the vertical direction (N_A =8)

Proposed System

- Configured with a single orthogonally polarized base station antenna.
- Number of Orthogonally polarized antenna elements (45° rotated): 8 in the vertical direction (N_A = 8)

Orthogonal polarization (45° rotated)

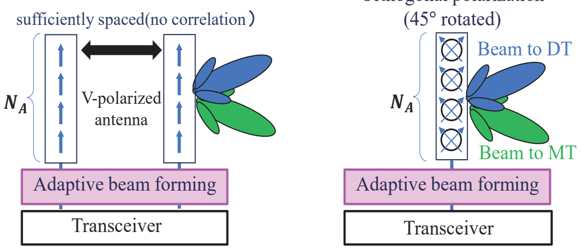

Antenna element directivity

- Assuming a Gaussian function: Half-power beamwidth is 80° .
- Set the relative sidelobe level to a uniform value ($G_s = -20$dB)

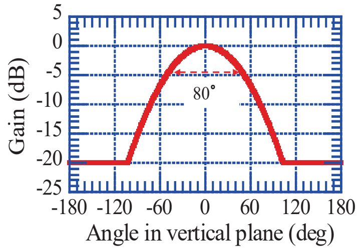

$$G_V(\phi) = G_0 \cdot \max\left[\exp\left(-a_V \phi^2\right), 10^{\frac{SL}{10}}\right]$$

$$a_V = \ln 2/(\Phi/2)^2$$

21

Propagation Model

Variation superimposed with propagation distance and instantaneous fading considering cross-polarization.

Variation due to propagation distance $e(d)$

$$e(d) = Ad^{-\alpha}$$

(α:propagation constant, d:propagation distance , A:constant)

Instantaneous fading $r(t)$

Nakagami-Rice fading

$$r(t) = \frac{K}{\sqrt{|K|^2 + \langle |r_s(t)|^2 \rangle}} + \frac{r_s(t)}{\sqrt{|K|^2 + \langle |r_s(t)|^2 \rangle}}$$

(K: Rice Factor , $r_s(t)$:Rayleigh Fading)

cross-polarization $e_x(t,d)$

$$e_x(t,d) = \left(\frac{r_s(t)}{\sqrt{|K|^2 + \langle |r_s(t)|^2 \rangle}}\right)/\gamma$$

($r_s(t)$: Rayleigh Fading)
(γ:Cross-polarization discrimination(X_{PD}))

Evaluation parameter values

Mobile terminal
- Propagation Constant α_M = -3.5 (Urban propagation)
- Rice Factor K_M=0 (true value)
- Cross-polarization discrimination γ_M = 6dB

Drone terminal
- Propagation Constant α_D = -2 (Free space path loss)
- Rice Factor K_D=20dB
- Cross-polarization discrimination γ_D =15dB

Propagation Model

Mobile terminal

$$\mathrm{H}_{\mathrm{X,V}}(t,d)=\frac{e_M(t,d)}{\sqrt{|K_M|^2+\langle|r_S(t)|^2\rangle}}\begin{bmatrix}K_M+r_{S,1}(t) & K_M+r_{S,2}(t)\\ r_{S,3}(t)/\gamma_M & r_{S,4}(t)/\gamma_M\end{bmatrix}=\frac{e(t,d)}{\sqrt{\langle|r_S(t)|^2\rangle}}\begin{bmatrix}r_{S,1}(t) & r_{S,2}(t)\\ r_{S,3}(t)/\gamma_M & r_{S,4}(t)/\gamma_M\end{bmatrix}$$

Rice Factor K_M=0 (true value)

Cross-polarization discrimination γ_M = 6dB (Urban propagation)

$r_{S,i}(t)$ (i=1〜4) are mutually independent scattered waves (Rayleigh Fading)

Drone terminal

$$\mathrm{H}_{\mathrm{X,X}}(t,d)=\frac{e_D(t,d)}{\sqrt{|K_D|^2+\langle|r_S(t)|^2\rangle}}\begin{bmatrix}K_D+r_{S,1}(t) & r_{S,2}(t)/\gamma_D\\ r_{S,3}(t)/\gamma_D & K_D+r_{S,4}(t)\end{bmatrix}$$

Rice Factor K_D=20dB

Cross-polarization discrimination γ_D = 15dB (Aerial)

$r_{D,i}(t)$ (i=1〜4) are mutually independent scattered waves (Rayleigh Fading)

Propagation Model

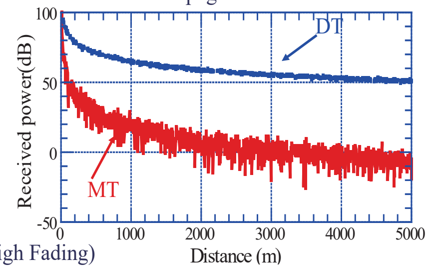

23

Evaluation based on communication capacity

Compare the communication capacity C (Shannon capacity) when MIMO is applied to mobile terminals and drone terminals.

$$C=\log_2(1+SINR_1)+\log_2(1+SINR_2) \quad \text{(bps/Hz)}$$

$$SINR=\frac{\text{Own cell signal power}}{\text{Noise power + Other cell interference signal power}}$$

Communication capacity of mobile terminals C_M

$$\tilde{\mathrm{H}}_{\mathrm{BD1}}=\begin{bmatrix}\sqrt{\lambda_{M1}} & 0\\ 0 & \sqrt{\lambda_{M2}}\end{bmatrix} \Rightarrow C_M=\log_2(1+\lambda_{M1})+\log_2(1+\lambda_{M2}) \quad \text{(bps/Hz)}$$

Communication capacity of drone terminals C_D

$$\tilde{\mathrm{H}}_{\mathrm{BD2}}=\begin{bmatrix}\sqrt{\lambda_{D1}} & 0\\ 0 & \sqrt{\lambda_{D2}}\end{bmatrix} \Rightarrow C_D=\log_2(1+\lambda_{D1})+\log_2(1+\lambda_{D2}) \quad \text{(bps/Hz)}$$

24

Effect of MU-MIMO Canceller (V-polarized MIMO)

・Evaluation in a single cell
・V-polarized MIMO

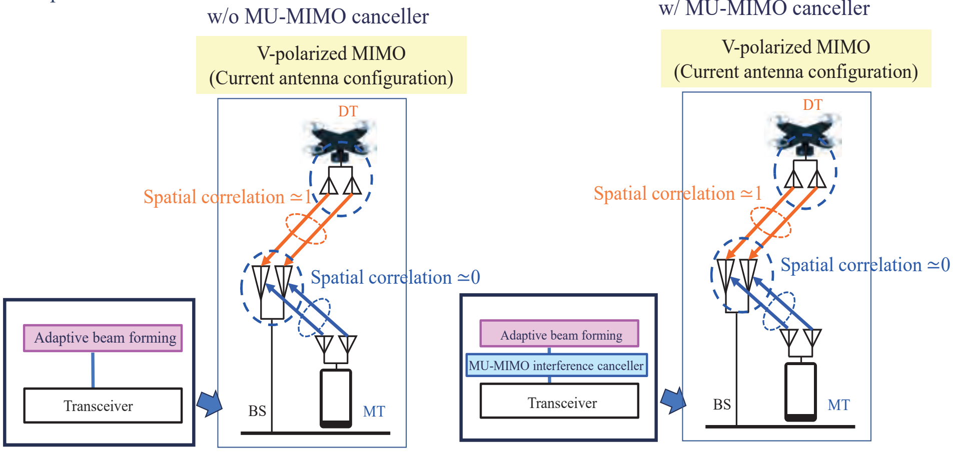

Effect of MU-MIMO Canceller (V-polarized MIMO)

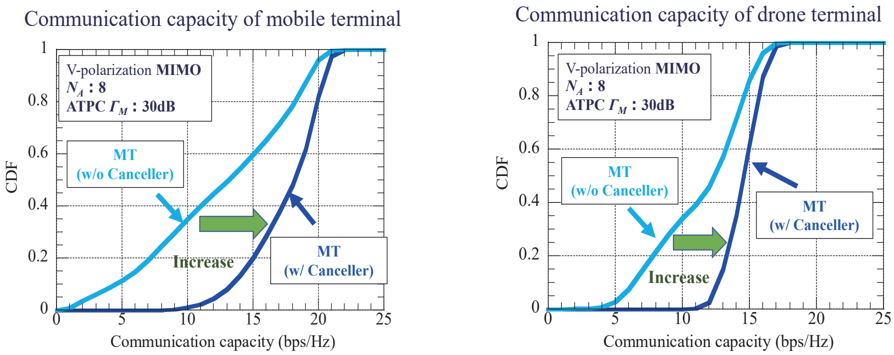

・The communication capacity of both mobile and drone terminals can be significantly improved by using MU-MIMO cancellers.
・The communication capacity of drone terminal is lower than that of mobile terminal.

26

Comparison of V-polarized Antenna and Cross-polarized Antenna at Base Station

- Evaluation in a single cell
- MU-MIMO canceller applied

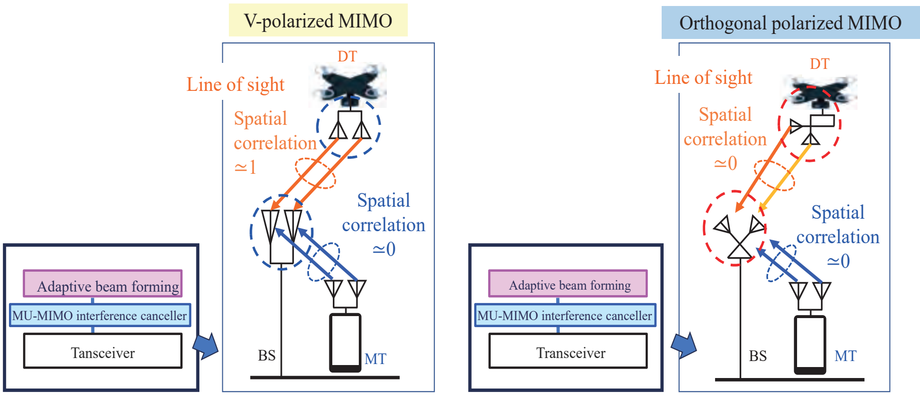

Effect of MU-MIMO Canceller (Orthogonal Polarization MIMO)

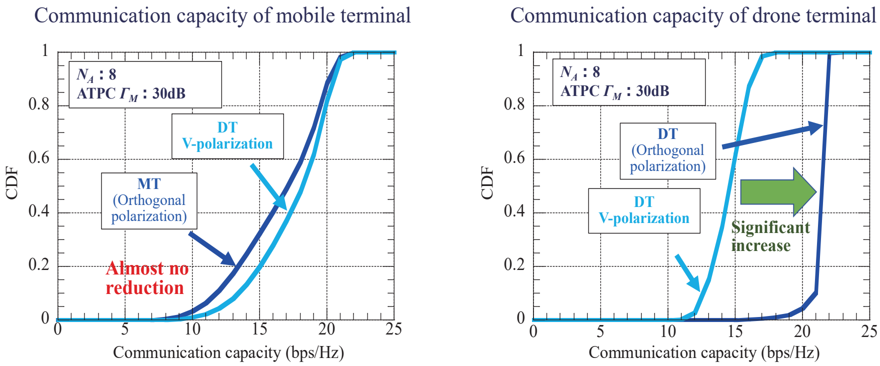

- Mobile terminal capacity is hardly reduced
- Drone terminal capacity is greatly improved compared to V-polarized MIMO

28

Cellular System Evaluation

Cellular System Evaluation

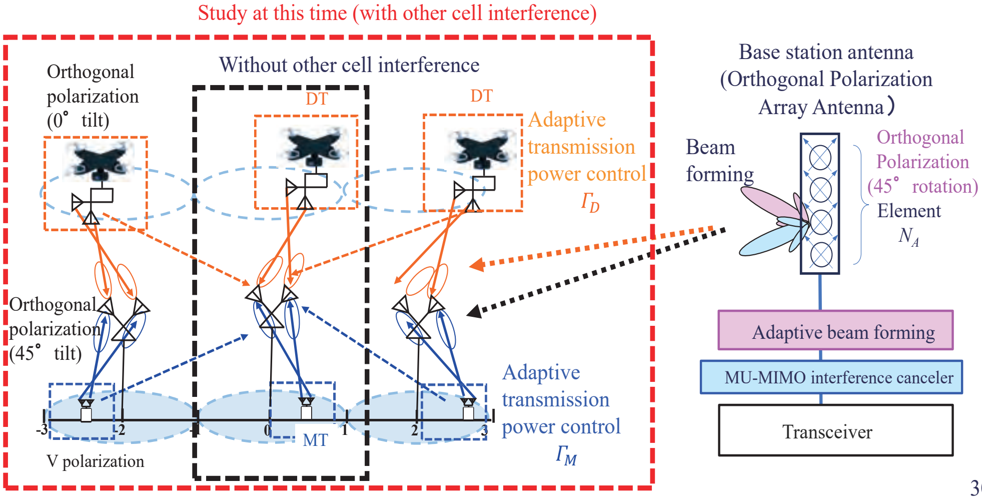

30

Orthogonal Polarization MU-MIMO Canceller

Receive signal Y

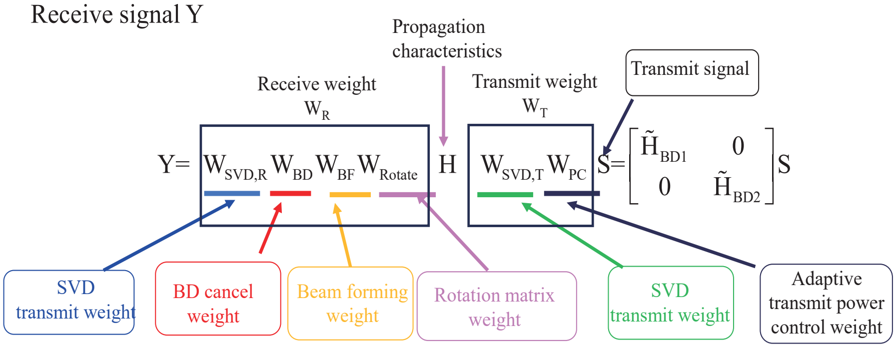

31

Interference Signal

Interference from other cells is generated by the terminals of surrounding base stations. The amount of interference from other cells can be determined by superimposing the transmission weight W_{T1} of the terminals in other cells onto the propagation path H_{01} from other cells and the reception weight W_{R0} of the local base station.

Interference Signal

$$I_{01} = W_{R0} H_{01} W_{T1} S_1$$

Own cell BS receive weight (W_{R0}); Propagation from other cell (H_{01}); Other cell terminal transmit weight (W_{T1}); Other cell signal (S_1)

$$\text{SINR} = \frac{\text{Own cell signal power}}{\text{Noise power} + \text{Other cell interference power}}$$

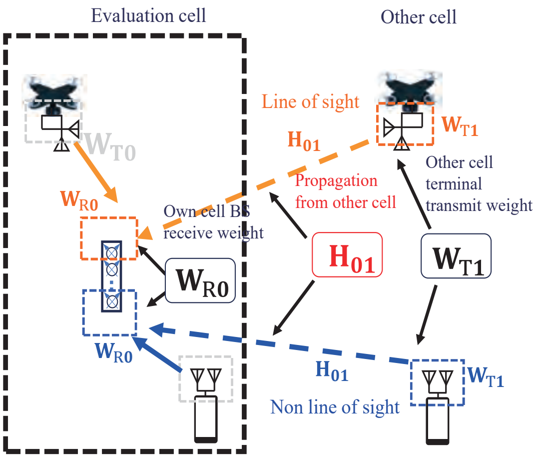

System Configuration

- Cell configuration
  - Radius1km straight line model、3 cells configuration
  - MT height h_M=0m,   DT height h_D=100m
  - MT and DT are equally distributed in cell
  - MT's receive SNR at cell boundary: 20dB
- Base antenna(orthogonal polarization antenna)
  - Base station antenna height h_b=50m
  - Element N_A=16
  - Distance between elements/wave length=0.7
- Transmit power control set value
  - MT Γ_M =25dB (SNR)
  - DT Γ_D =25dB (SNR)

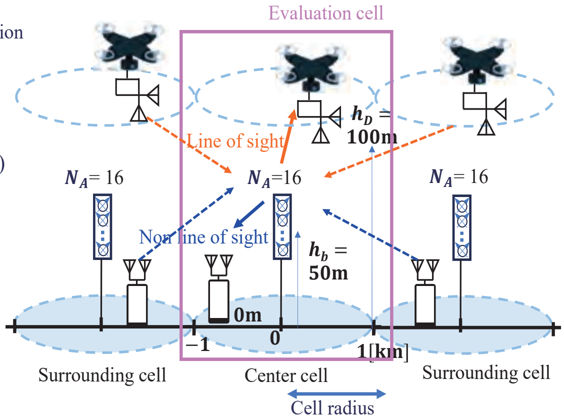

33

Comparison between current and proposed models

Current System (i) (without DT)	Current System(ii) (without DT)	Proposed System (with DT)

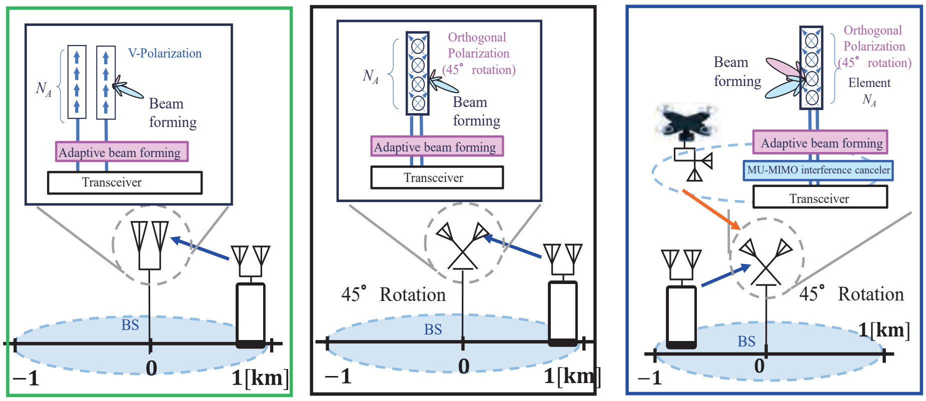

34

Comparison with the Current System

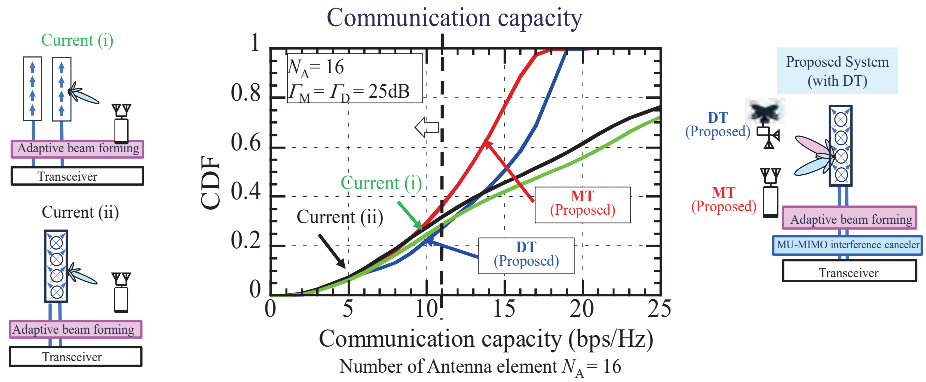

- The proposed system can achieve equal or greater communication capacity for both ground terminals and aerial terminals compared to the current system, which only supports ground terminals, in regions where the communication capacity is 10 bps/Hz or less.
- With the proposed system, it is possible to construct both ground and aerial areas using the same frequency

35

Summary

In the 'Mobile Communication Three-Dimensional Spatial Cell Configuration,' which realizes ground cells and aerial cells using the same frequency, we propose an 'Orthogonal Polarization Beam forming MU-MIMO canceler' that combines the following technologies:

- Adaptive beamforming technology,
- Adaptive transmit power control technology,
- MU-MIMO canceler technology to suppress interference between ground terminals and aerial terminals,
- Orthogonal polarization MIMO technology to improve the MIMO communication quality of aerial terminals.

We investigated the 'Orthogonal Polarization Beamforming MU-MIMO Canceler' considering inter-cell interference. The results clarified that, compared to the current system, which only supports ground terminals, the proposed method enables both MT and DT to achieve equal or greater communication capacity.

The proposed method enables MT and DT to use the same frequency, thereby realizing double the frequency utilization efficiency

36

EOF

MI レクチャーノートシリーズ刊行にあたり

本レクチャーノートシリーズは、文部科学省 21 世紀 COE プログラム「機能数理学の構築と展開」（H15-19 年度）において作成した COE Lecture Notes の続刊であり、文部科学省大学院教育改革支援プログラム「産業界が求める数学博士と新修士養成」（H19-21 年度）および、同グローバル COE プログラム「マス・フォア・インダストリ教育研究拠点」（H20-24 年度）において行われた講義の講義録として出版されてきた。平成 23 年 4 月のマス・フォア・インダストリ研究所（IMI）設立と平成 25 年 4 月の IMI の文部科学省共同利用・共同研究拠点として「産業数学の先進的･基礎的共同研究拠点」の認定を受け、今後、レクチャーノートは、マス・フォア・インダストリに関わる国内外の研究者による講義の講義録、会議録等として出版し、マス・フォア・インダストリの本格的な展開に資するものとする。

2022 年 10 月
マス・フォア・インダストリ研究所
所長　梶原 健司

2024年度採択分　九州大学マス･フォア･インダストリ研究所 共同利用研究集会

情報通信の技術革新のための基礎数理

発　行　2025年 3 月 19 日
編　集　實松　豊 , 大橋　正良 , 長谷川　晃朗 , 篠原　克寿 , 森　慎太郎
発　行　九州大学マス・フォア・インダストリ研究所
九州大学大学院数理学府
〒819-0395 福岡市西区元岡744
九州大学数理・IMI 事務室
TEL 092-802-4402　FAX 092-802-4405
URL https://www.imi.kyushu-u.ac.jp/

印　刷　城島印刷株式会社
〒810-0012 福岡市中央区白金 2 丁目 9 番 6 号
TEL 092-531-7102　FAX 092-524-4411

シリーズ既刊

Issue	Author／Editor	Title	Published
COE Lecture Note	Mitsuhiro T. NAKAO Kazuhiro YOKOYAMA	Computer Assisted Proofs - Numeric and Symbolic Approaches - 199pages	August 22, 2006
COE Lecture Note	M.J.Shai HARAN	Arithmetical Investigations - Representation theory, Orthogonal polynomials and Quantum interpolations- 174pages	August 22, 2006
COE Lecture Note Vol.3	Michal BENES Masato KIMURA Tatsuyuki NAKAKI	Proceedings of Czech-Japanese Seminar in Applied Mathematics 2005 155pages	October 13, 2006
COE Lecture Note Vol.4	宮田　健治	辺要素有限要素法による磁界解析 - 機能数理学特別講義 21pages	May 15, 2007
COE Lecture Note Vol.5	Francois APERY	Univariate Elimination Subresultants - Bezout formula, Laurent series and vanishing conditions - 89pages	September 25, 2007
COE Lecture Note Vol.6	Michal BENES Masato KIMURA Tatsuyuki NAKAKI	Proceedings of Czech-Japanese Seminar in Applied Mathematics 2006 209pages	October 12, 2007
COE Lecture Note Vol.7	若山　正人 中尾　充宏	九州大学産業技術数理研究センター キックオフミーティング 138pages	October 15, 2007
COE Lecture Note Vol.8	Alberto PARMEGGIANI	Introduction to the Spectral Theory of Non-Commutative Harmonic Oscillators 233pages	January 31, 2008
COE Lecture Note Vol.9	Michael I.TRIBELSKY	Introduction to Mathematical modeling 23pages	February 15, 2008
COE Lecture Note Vol.10	Jacques FARAUT	Infinite Dimensional Spherical Analysis 74pages	March 14, 2008
COE Lecture Note Vol.11	Gerrit van DIJK	Gelfand Pairs And Beyond 60pages	August 25, 2008
COE Lecture Note Vol.12	Faculty of Mathematics, Kyushu University	Consortium “MATH for INDUSTRY” First Forum 87pages	September 16, 2008
COE Lecture Note Vol.13	九州大学大学院 数理学研究院	プロシーディング「損保数理に現れる確率モデル」 — 日新火災・九州大学 共同研究2008年11月 研究会 — 82pages	February 6, 2009

シリーズ既刊

Issue	Author／Editor	Title	Published
COE Lecture Note Vol.14	Michal Beneš, Tohru Tsujikawa Shigetoshi Yazaki	Proceedings of Czech-Japanese Seminar in Applied Mathematics 2008 77pages	February 12, 2009
COE Lecture Note Vol.15	Faculty of Mathematics, Kyushu University	International Workshop on Verified Computations and Related Topics 129pages	February 23, 2009
COE Lecture Note Vol.16	Alexander Samokhin	Volume Integral Equation Method in Problems of Mathematical Physics 50pages	February 24, 2009
COE Lecture Note Vol.17	矢嶋　　徹 及川　正行 梶原　健司 辻　　英一 福本　康秀	非線形波動の数理と物理　66pages	February 27, 2009
COE Lecture Note Vol.18	Tim Hoffmann	Discrete Differential Geometry of Curves and Surfaces　75pages	April 21, 2009
COE Lecture Note Vol.19	Ichiro Suzuki	The Pattern Formation Problem for Autonomous Mobile Robots ―Special Lecture in Functional Mathematics―　23pages	April 30, 2009
COE Lecture Note Vol.20	Yasuhide Fukumoto Yasunori Maekawa	Math-for-Industry Tutorial: Spectral theories of non-Hermitian operators and their application　184pages	June 19, 2009
COE Lecture Note Vol.21	Faculty of Mathematics, Kyushu University	Forum "Math-for-Industry" Casimir Force, Casimir Operators and the Riemann Hypothesis 95pages	November 9, 2009
COE Lecture Note Vol.22	Masakazu Suzuki Hoon Hong Hirokazu Anai Chee Yap Yousuke Sato Hiroshi Yoshida	The Joint Conference of ASCM 2009 and MACIS 2009: Asian Symposium on Computer Mathematics Mathematical Aspects of Computer and Information Sciences　436pages	December 14, 2009
COE Lecture Note Vol.23	荒川　恒男 金子　昌信	多重ゼータ値入門　111pages	February 15, 2010
COE Lecture Note Vol.24	Fulton B.Gonzalez	Notes on Integral Geometry and Harmonic Analysis　125pages	March 12, 2010
COE Lecture Note Vol.25	Wayne Rossman	Discrete Constant Mean Curvature Surfaces via Conserved Quantities 130pages	May 31, 2010
COE Lecture Note Vol.26	Mihai Ciucu	Perfect Matchings and Applications　66pages	July 2, 2010

シリーズ既刊

Issue	Author／Editor	Title	Published
COE Lecture Note Vol.27	九州大学大学院 数理学研究院	Forum "Math-for-Industry" and Study Group Workshop Information security, visualization, and inverse problems, on the basis of optimization techniques　100pages	October 21, 2010
COE Lecture Note Vol.28	ANDREAS LANGER	MODULAR FORMS, ELLIPTIC AND MODULAR CURVES LECTURES AT KYUSHU UNIVERSITY 2010　62pages	November 26, 2010
COE Lecture Note Vol.29	木田　雅成 原田　昌晃 横山　俊一	Magma で広がる数学の世界　157pages	December 27, 2010
COE Lecture Note Vol.30	原　　　隆 松井　　卓 廣島　文生	Mathematical Quantum Field Theory and Renormalization Theory 201pages	January 31, 2011
COE Lecture Note Vol.31	若山　正人 福本　康秀 高木　　剛 山本　昌宏	Study Group Workshop 2010 Lecture & Report　128pages	February 8, 2011
COE Lecture Note Vol.32	Institute of Mathematics for Industry, Kyushu University	Forum "Math-for-Industry" 2011 "TSUNAMI-Mathematical Modelling" Using Mathematics for Natural Disaster Prediction, Recovery and Provision for the Future　90pages	September 30, 2011
COE Lecture Note Vol.33	若山　正人 福本　康秀 高木　　剛 山本　昌宏	Study Group Workshop 2011 Lecture & Report　140pages	October 27, 2011
COE Lecture Note Vol.34	Adrian Muntean Vladimír Chalupecký	Homogenization Method and Multiscale Modeling　72pages	October 28, 2011
COE Lecture Note Vol.35	横山　俊一 夫　　紀恵 林　　卓也	計算機代数システムの進展　210pages	November 30, 2011
COE Lecture Note Vol.36	Michal Beneš Masato Kimura Shigetoshi Yazaki	Proceedings of Czech-Japanese Seminar in Applied Mathematics 2010 107pages	January 27, 2012
COE Lecture Note Vol.37	若山　正人 高木　　剛 Kirill Morozov 平岡　裕章 木村　正人 白井　朋之 西井　龍映 栄　伸一郎 穴井　宏和 福本　康秀	平成23年度 数学・数理科学と諸科学・産業との連携研究ワークショップ　拡がっていく数学　～期待される "見えない力" ～ 154pages	February 20, 2012

シリーズ既刊

Issue	Author／Editor	Title	Published
COE Lecture Note Vol.38	Fumio Hiroshima Itaru Sasaki Herbert Spohn Akito Suzuki	Enhanced Binding in Quantum Field Theory　204pages	March 12, 2012
COE Lecture Note Vol.39	Institute of Mathematics for Industry, Kyushu University	Multiscale Mathematics; Hierarchy of collective phenomena and interrelations between hierarchical structures　180pages	March 13, 2012
COE Lecture Note Vol.40	井ノ口順一 太田　泰広 筧　　三郎 梶原　健司 松浦　　望	離散可積分系・離散微分幾何チュートリアル2012　152pages	March 15, 2012
COE Lecture Note Vol.41	Institute of Mathematics for Industry, Kyushu University	Forum “Math-for-Industry” 2012 “Information Recovery and Discovery”　91pages	October 22, 2012
COE Lecture Note Vol.42	佐伯　　修 若山　正人 山本　昌宏	Study Group Workshop 2012 Abstract, Lecture & Report　178pages	November 19, 2012
COE Lecture Note Vol.43	Institute of Mathematics for Industry, Kyushu University	Combinatorics and Numerical Analysis Joint Workshop　103pages	December 27, 2012
COE Lecture Note Vol.44	萩原　　学	モダン符号理論からポストモダン符号理論への展望　107pages	January 30, 2013
COE Lecture Note Vol.45	金山　　寛	Joint Research Workshop of Institute of Mathematics for Industry (IMI), Kyushu University “Propagation of Ultra-large-scale Computation by the Domain-decomposition-method for Industrial Problems (PUCDIP 2012)” 121pages	February 19, 2013
COE Lecture Note Vol.46	西井　龍映 栄　伸一郎 岡田　勘三 落合　啓之 小磯　深幸 斎藤　新悟 白井　朋之	科学・技術の研究課題への数学アプローチ —数学モデリングの基礎と展開—　325pages	February 28, 2013
COE Lecture Note Vol.47	SOO TECK LEE	BRANCHING RULES AND BRANCHING ALGEBRAS FOR THE COMPLEX CLASSICAL GROUPS　40pages	March 8, 2013
COE Lecture Note Vol.48	溝口　佳寛 脇　　隼人 平坂　　貢 谷口　哲至 島袋　　修	博多ワークショップ「組み合わせとその応用」　124pages	March 28, 2013

シリーズ既刊

Issue	Author／Editor	Title	Published
COE Lecture Note Vol.49	照井　　章 小原　功任 濱田　龍義 横山　俊一 穴井　宏和 横田　博史	マス・フォア・インダストリ研究所　共同利用研究集会 II 数式処理研究と産学連携の新たな発展　137pages	August 9, 2013
MI Lecture Note Vol.50	Ken Anjyo Hiroyuki Ochiai Yoshinori Dobashi Yoshihiro Mizoguchi Shizuo Kaji	Symposium MEIS2013: Mathematical Progress in Expressive Image Synthesis　154pages	October 21, 2013
MI Lecture Note Vol.51	Institute of Mathematics for Industry, Kyushu University	Forum “Math-for-Industry” 2013 “The Impact of Applications on Mathematics”　97pages	October 30, 2013
MI Lecture Note Vol.52	佐伯　　修 岡田　勘三 髙木　　剛 若山　正人 山本　昌宏	Study Group Workshop 2013 Abstract, Lecture ＆ Report　142pages	November 15, 2013
MI Lecture Note Vol.53	四方　義啓 櫻井　幸一 安田　貴徳 Xavier Dahan	平成25年度　九州大学マス・フォア・インダストリ研究所 共同利用研究集会　安全・安心社会基盤構築のための代数構造 ～サイバー社会の信頼性確保のための数理学～　158pages	December 26, 2013
MI Lecture Note Vol.54	Takashi Takiguchi Hiroshi Fujiwara	Inverse problems for practice, the present and the future　93pages	January 30, 2014
MI Lecture Note Vol.55	栄　伸一郎 溝口　佳寛 脇　　隼人 渋田　敬史	Study Group Workshop 2013 数学協働プログラム Lecture & Report 98pages	February 10, 2014
MI Lecture Note Vol.56	Yoshihiro Mizoguchi Hayato Waki Takafumi Shibuta Tetsuji Taniguchi Osamu Shimabukuro Makoto Tagami Hirotake Kurihara Shuya Chiba	Hakata Workshop 2014 ~ Discrete Mathematics and its Applications ~　141pages	March 28, 2014
MI Lecture Note Vol.57	Institute of Mathematics for Industry, Kyushu University	Forum “Math-for-Industry” 2014: “Applications + Practical Conceptualization + Mathematics = fruitful Innovation”　93pages	October 23, 2014
MI Lecture Note Vol.58	安生健一 落合啓之	Symposium MEIS2014: Mathematical Progress in Expressive Image Synthesis　135pages	November 12, 2014

シリーズ既刊

Issue	Author／Editor	Title	Published
MI Lecture Note Vol.59	西井　龍映 岡田　勘三 梶原　健司 髙木　　剛 若山　正人 脇　　隼人 山本　昌宏	Study Group Workshop 2014 数学協働プログラム Abstract, Lecture & Report　196pages	November 14, 2014
MI Lecture Note Vol.60	西浦　　博	平成26年度九州大学 IMI 共同利用研究・研究集会（I） 感染症数理モデルの実用化と産業及び政策での活用のための新たな展開　120pages	November 28, 2014
MI Lecture Note Vol.61	溝口　佳寛 Jacques Garrigue 萩原　　学 Reynald Affeldt	研究集会 高信頼な理論と実装のための定理証明および定理証明器 Theorem proving and provers for reliable theory and implementations (TPP2014)　138pages	February 26, 2015
MI Lecture Note Vol.62	白井　朋之	Workshop on "β-transformation and related topics"　59pages	March 10, 2015
MI Lecture Note Vol.63	白井　朋之	Workshop on "Probabilistic models with determinantal structure" 107pages	August 20, 2015
MI Lecture Note Vol.64	落合　啓之 土橋　宜典	Symposium MEIS2015: Mathematical Progress in Expressive Image Synthesis　124pages	September 18, 2015
MI Lecture Note Vol.65	Institute of Mathematics for Industry, Kyushu University	Forum "Math-for-Industry" 2015 "The Role and Importance of Mathematics in Innovation"　74pages	October 23, 2015
MI Lecture Note Vol.66	岡田　勘三 藤澤　克己 白井　朋之 若山　正人 脇　　隼人 Philip Broadbridge 山本　昌宏	Study Group Workshop 2015 Abstract, Lecture & Report 156pages	November 5, 2015
MI Lecture Note Vol.67	Institute of Mathematics for Industry, Kyushu University	IMI-La Trobe Joint Conference "Mathematics for Materials Science and Processing" 66pages	February 5, 2016
MI Lecture Note Vol.68	古庄　英和 小谷　久寿 新甫　洋史	結び目と Grothendieck-Teichmüller 群 116pages	February 22, 2016
MI Lecture Note Vol.69	土橋　宜典 鍛治　静雄	Symposium MEIS2016: Mathematical Progress in Expressive Image Synthesis　82pages	October 24, 2016
MI Lecture Note Vol.70	Institute of Mathematics for Industry, Kyushu University	Forum "Math-for-Industry" 2016 "Agriculture as a metaphor for creativity in all human endeavors" 98pages	November 2, 2016
MI Lecture Note Vol.71	小磯　深幸 二宮　嘉行 山本　昌宏	Study Group Workshop 2016 Abstract, Lecture & Report　143pages	November 21, 2016

シリーズ既刊

Issue	Author／Editor	Title	Published
MI Lecture Note Vol.72	新井　朝雄 小嶋　　泉 廣島　文生	Mathematical quantum field theory and related topics　133pages	January 27, 2017
MI Lecture Note Vol.73	穴田　啓晃 Kirill Morozov 須賀　祐治 奥村　伸也 櫻井　幸一	Secret Sharing for Dependability, Usability and Security of Network Storage and Its Mathematical Modeling　211pages	March 15, 2017
MI Lecture Note Vol.74	QUISPEL, G. Reinout W. BADER, Philipp MCLAREN, David I. TAGAMI, Daisuke	IMI-La Trobe Joint Conference Geometric Numerical Integration and its Applications　71pages	March 31, 2017
MI Lecture Note Vol.75	手塚　　集 田上　大助 山本　昌宏	Study Group Workshop 2017 Abstract, Lecture & Report　118pages	October 20, 2017
MI Lecture Note Vol.76	宇田川誠一	Tzitzéica 方程式の有限間隙解に付随した極小曲面の構成理論 ―Tzitzéica 方程式の楕円関数解を出発点として―　68pages	August 4, 2017
MI Lecture Note Vol.77	松谷　茂樹 佐伯　　修 中川　淳一 田上　大助 上坂　正晃 Pierluigi Cesana 濵田　裕康	平成29年度　九州大学マス・フォア・インダストリ研究所 共同利用研究集会（I） 結晶の界面，転位，構造の数理　148pages	December 20, 2017
MI Lecture Note Vol.78	瀧澤　重志 小林　和博 佐藤憲一郎 斎藤　　努 清水　正明 間瀬　正啓 藤澤　克樹 神山　直之	平成29年度　九州大学マス・フォア・インダストリ研究所 プロジェクト研究　研究集会（I） 防災・避難計画の数理モデルの高度化と社会実装へ向けて 136pages	February 26, 2018
MI Lecture Note Vol.79	神山　直之 畔上　秀幸	平成29年度　AIMaP チュートリアル 最適化理論の基礎と応用　96pages	February 28, 2018
MI Lecture Note Vol.80	Kirill Morozov Hiroaki Anada Yuji Suga	IMI Workshop of the Joint Research Projects Cryptographic Technologies for Securing Network Storage and Their Mathematical Modeling　116pages	March 30, 2018
MI Lecture Note Vol.81	Tsuyoshi Takagi Masato Wakayama Keisuke Tanaka Noboru Kunihiro Kazufumi Kimoto Yasuhiko Ikematsu	IMI Workshop of the Joint Research Projects International Symposium on Mathematics, Quantum Theory, and Cryptography　246pages	September 25, 2019
MI Lecture Note Vol.82	池森　俊文	令和２年度　AIMaP チュートリアル 新型コロナウイルス感染症にかかわる諸問題の数理 145pages	March 22, 2021

シリーズ既刊

Issue	Author／Editor	Title	Published
MI Lecture Note Vol.83	早川健太郎 軸丸　芳揮 横須賀洋平 可香谷　隆 林　　和希 堺　　雄亮	シェル理論・膜理論への微分幾何学からのアプローチと その建築曲面設計への応用　49pages	July 28, 2021
MI Lecture Note Vol.84	Taketoshi Kawabe Yoshihiro Mizoguchi Junichi Kako Masakazu Mukai Yuji Yasui	SICE-JSAE-AIMaP Tutorial Advanced Automotive Control and Mathematics　110pages	December 27, 2021
MI Lecture Note Vol.85	Hiroaki Anada Yasuhiko Ikematsu Koji Nuida Satsuya Ohata Yuntao Wang	IMI Workshop of the Joint Usage Research Projects Exploring Mathematical and Practical Principles of Secure Computation and Secret Sharing　114pages	February 9, 2022
MI Lecture Note Vol.86	濱田　直希 穴井　宏和 梅田　裕平 千葉　一永 佐藤　寛之 能島　裕介 加葉田雄太朗 一木　俊助 早野　健太 佐伯　　修	2020年度採択分　九州大学マス・フォア・インダストリ研究所 共同利用研究集会 進化計算の数理　135pages	February 22, 2022
MI Lecture Note Vol.87	Osamu Saeki, Ho Tu Bao, Shizuo Kaji, Kenji Kajiwara, Nguyen Ha Nam, Ta Hai Tung, Melanie Roberts, Masato Wakayama, Le Minh Ha, Philip Broadbridge	Proceedings of Forum "Math-for-Industry" 2021 -Mathematics for Digital Economy-　122pages	March 28, 2022
MI Lecture Note Vol.88	Daniel PACKWOOD Pierluigi CESANA, Shigenori FUJIKAWA, Yasuhide FUKUMOTO, Petros SOFRONIS, Alex STAYKOV	Perspectives on Artificial Intelligence and Machine Learning in Materials Science, February 4-6, 2022　74pages	November 8, 2022

シリーズ既刊

Issue	Author／Editor	Title	Published
MI Lecture Note Vol.89	松谷　茂樹 落合　啓之 井上　和俊 小磯　深幸 佐伯　　修 白井　朋之 垂水　竜一 内藤　久資 中川　淳一 濱田　裕康 松江　　要 加葉田雄太朗	2022年度採択分 九州大学マス・フォア・インダストリ研究所 共同利用研究集会 材料科学における幾何と代数 III　356pages	December 7, 2022
MI Lecture Note Vol.90	中山　尚子 谷川　拓司 品野　勇治 近藤　正章 石原　　亨 鍛冶　静雄 藤澤　克樹	2022年度採択分 九州大学マス・フォア・インダストリ研究所 共同利用研究集会 データ格付けサービス実現のための数理基盤の構築　58pages	December 12, 2022
MI Lecture Note Vol.91	Katsuki Fujisawa Shizuo Kaji Toru Ishihara Masaaki Kondo Yuji Shinano Takuji Tanigawa Naoko Nakayama	IMI Workshop of the Joint Usage Research Projects Construction of Mathematical Basis for Realizing Data Rating Service 610pages	December 27, 2022
MI Lecture Note Vol.92	丹田　　聡 三宮　　俊 廣島　文生	2022年度採択分　九州大学マス・フォア・インダストリ研究所 共同利用研究集会 時間・量子測定・準古典近似の理論と実験 ～古典論と量子論の境界～　150pages	Janualy 6, 2023
MI Lecture Note Vol.93	Philip Broadbridge Luke Bennetts Melanie Roberts Kenji Kajiwara	Proceedings of Forum “Math-for-Industry” 2022 -Mathematics of Public Health and Sustainability-　170pages	June 19, 2023
MI Lecture Note Vol.94	國廣　　昇 池松　泰彦 伊豆　哲也 穴田　啓晃 縫田　光司	2023年度採択分　九州大学マス・フォア・インダストリ研究所 共同利用研究集会 現代暗号に対する安全性解析・攻撃の数理　260pages	Janualy 11, 2024
MI Lecture Note Vol.96	澤田　茉伊	2023年度採択分　九州大学マス・フォア・インダストリ研究所 共同利用研究集会 デジタル化時代に求められる斜面防災の思考法　70pages	March 18, 2024

シリーズ既刊

Issue	Author／Editor	Title	Published
MI Lecture Note Vol.97	Shariffah Suhaila Syed Jamaludin Zaiton Mat Isa Nur Arina Bazilah Aziz Taufiq Khairi Ahmad Khairuddin Shaymaa M.H.Darwish Ahmad Razin Zainal Abidin Norhaiza Ahmad Zainal Abdul Aziz Hang See Pheng Mohd Ali Khameini Ahmad	International Project Research-Workshop (I) Proceedings of 4th Malaysia Mathematics in Industry Study Group (MMISG2023)　172pages	March 28, 2024
MI Lecture Note Vol.98	中澤　嵩	2024 年度採択分 九州大学マス・フォア・インダストリ研究所 共同利用研究集会 自動車性能の飛躍的向上を目指す Data-Driven 設計　92pages	January 30, 2025
MI Lecture Note Vol.99	Jacques Garrigue	2024 年度採択分 九州大学マス・フォア・インダストリ研究所 共同利用研究集会 コンピュータによる定理証明支援とその応用　308pages	March 17, 2025

Institute of Mathematics for Industry
Kyushu University

九州大学マス･フォア･インダストリ研究所
九州大学大学院 数理学府

〒819-0395 福岡市西区元岡744　TEL 092-802-4402　FAX 092-802-4405
URL https://www.imi.kyushu-u.ac.jp/